

Daniel Bruce Tucker

Effects of Glacial Development on Dam Safety in Norway

Master's thesis in Hydropower Development

Supervisor: Fjóla Guðrún Sigtryggsdóttir

Co-supervisor: Ganesh H. R. Ravindra, Jacob Clement Yde, and Guy Mason

June 2024

Daniel Bruce Tucker

Effects of Glacial Development on Dam Safety in Norway

Master's thesis in Hydropower Development

Supervisor: Fjóla Guðrún Sigtryggsdóttir

Co-supervisor: Ganesh H. R. Ravindra, Jacob Clement Yde, and Guy Mason

June 2024

Norwegian University of Science and Technology

Faculty of Engineering

Department of Civil and Environmental Engineering



Norwegian University of
Science and Technology

Abstract

Dams in Norway, as many others across the world, are susceptible to a multitude of different hazardous glacial mechanisms. These can have serious consequences on downstream communities and populations and must be considered to retain a high level of dam safety practice. They can range in severity and origin, but are possible to assess through a properly applied risk analysis process following their identification.

Although these hazards are numerous, focus is placed on three specific mechanisms; the first bound from climatic conditions with increased precipitation and rapid melt of ice, the second from glacial lake breaching or drainage, and thirdly, calving and icefall processes. Multiple mechanisms can intertwine and lead to dam failure or catastrophic events, most of which have not been considered or researched to great extents within Norway, as compared to other regions. As the climate continues to change, and new hazards are presented at a more frequent rate, these perspectives are needed more than ever.

This paper will employ several empirical and qualitative methods to determine characteristics of various glacial lakes, probabilities leading to dam failure, and eventually outline the assessment procedures for 12 different dam cases investigated across Norway, distributed amongst different glacial systems. The risk analysis method of choice are event trees, which can be developed in both a quantitative and subjective manner without the requirement of immense data. These analyses have their limitations that will be discussed, but as a high-level screening, resulted in the findings of dams characterized by high-risk in all three primary focuses.

Preface

The submittal of this thesis marks the end of studies within the International Master of Science program in Hydropower Development at NTNU. This research-based paper was authored remotely from NTNU's main campus and coordinated through a series of online meetings. Work began in the winter of 2024, and finalized in the summer of 2024. Many of the internal reports and flood calculations necessary to author this thesis were distributed from co-supervisor Ganesh H.R. Ravindra representing Statkraft Energi AS.

Table of Contents

List of Figures	xii
List of Tables.....	xviii
Abbreviations.....	xx
Acknowledgements	1
1 Introduction.....	2
1.1 Scope and objective.....	2
1.2 Selected glaciers and dams.....	3
1.3 Analysis process and methodology.....	3
2 Background	5
2.1 Glacier systems	5
2.1.1 Types of glaciers	5
2.1.2 Mass balance cycle	7
2.1.3 Glacial moraine landforms.....	8
2.1.4 Types of glacial lakes	9
2.1.5 Norwegian glaciers today	12
2.2 Hazardous glacial mechanisms	12
2.2.1 High precipitation and rapid melt	14
2.2.2 Breaching of glacial lakes.....	14
2.2.3 Breaching of ice-dammed glacial lakes	15
2.2.4 Breaching of moraine-dammed glacial lakes.....	15
2.2.5 Calving and icefall	17
2.2.6 Other mechanisms.....	18
2.2.7 Danger and potential damage to dams and reservoirs	19
2.2.8 Worldwide GLOF statistics	19
2.3 Norwegian dam safety.....	21
2.3.1 Dam safety regulations	21
2.3.2 Dam consequence classes	22
2.3.3 Emergency planning	23
2.3.4 Flood design safety	23
2.3.5 Determination of PMF and design flood values	25
2.4 Risk assessment methods	26
2.4.1 Benefits and drawbacks	27
2.4.2 Quantitative methods	27
2.4.3 Qualitative and semi-quantitative methods.....	29
3 Methodology.....	31
3.1 Site selection	31
3.1.1 Initial selection criteria	31

3.1.2	Visual observations and identifications	32
3.2	Other data	33
3.2.1	Catchments and contributing glaciers.....	33
3.2.2	GIS preparation.....	35
3.2.3	Internal reports.....	35
3.3	Glacial lake estimations	35
3.3.1	Lake volume estimation.....	35
3.3.2	Lake depth estimation.....	37
3.3.3	Breach outflow rate estimation.....	38
3.4	Event tree analysis.....	41
3.4.1	Selection of three main hazards.....	41
3.4.2	High precipitation and melt hazard (H1).....	41
3.4.3	Failure from breach of glacial lake (H2)	42
3.4.4	Failure from calving or icefall (H3).....	43
3.4.5	Estimate of reservoir regulation.....	44
3.4.6	Estimate of spillway capacity	45
3.4.7	Estimating the probability of a glacial lake breach	47
3.4.8	Generation and finalization of event trees.....	48
3.4.9	Plotting of risk envelope plots	51
4	Case Studies	53
4.1	Austre Okstindbreen.....	53
4.1.1	Gressvatn	54
4.1.2	Identified hazards.....	55
4.1.3	Other hazards	58
4.2	Jostedalsbreen	59
4.2.1	Styggevatn	62
4.2.2	Tunsbergdalsvatn.....	64
4.2.3	Identified hazards.....	65
4.2.4	Other hazards	68
4.3	Folgefonna	69
4.3.1	Dravladalsvatn	72
4.3.2	Juklavatn	73
4.3.3	Mysevatn	74
4.3.4	Svartadalsvatn.....	75
4.3.5	Identified hazards.....	76
4.3.6	Other hazards	79
4.4	Reinoksfjellet	80
4.4.1	Slæddovagjavre	81
4.4.2	Identified hazards.....	82
4.4.3	Other hazards	83
4.5	Storsteinsfjellbreen.....	83
4.5.1	Norddalen	85
4.5.2	Identified hazards.....	86
4.5.3	Other hazards	87
4.6	Hardangerjøkulen.....	88
4.6.1	Rembesdalsvatn	90
4.6.2	Sysenvatn.....	91
4.6.3	Identified hazards.....	92

4.6.4	Other hazards	95
4.7	Svartisen	96
4.7.1	Storglomvatn.....	97
4.7.2	Identified hazards.....	98
4.7.3	Other hazards	101
4.8	Excluded sites.....	101
4.8.1	Midtre Brevatn and Heimste Brevatn	101
4.8.2	Markjelkevatn	101
4.8.3	Båtsvatn	101
4.8.4	Fossvatn	102
4.8.5	Reinoksdammen.....	102
4.8.6	Kalvatn.....	102
4.8.7	Øvre Glomvatn Hoveddam and Sidedam	102
4.8.8	Ståvatn	102
4.8.9	Langvatn	103
5	Results.....	104
5.1	Rapid melt and high precipitation hazard	104
5.2	Breach of glacial lake hazard	105
5.3	Calving and icefall hazard.....	106
5.4	Glacial lake estimations	107
6	Discussion	108
6.1	Rapid melt and precipitation hazard.....	108
6.1.1	Limitations and drawbacks with H1 analyses.....	109
6.2	Breach of glacial lake hazard	109
6.2.1	Limitations and drawbacks with H2 analyses.....	110
6.3	Calving and icefall hazard.....	111
6.3.1	Limitations and drawbacks with H3 analyses.....	111
6.4	Other limitations.....	112
6.4.1	Timing of reservoir state.....	112
6.4.2	Failure or breach probability.....	112
6.4.3	Recommendations for further study	113
7	Conclusions.....	114
	References	117
	Appendix A.....	125
	Appendix B.....	138
	Appendix C.....	146
	Appendix D.....	148
	Appendix E.....	153

List of Figures

Figure 2.1 Illustration differentiating glacial formations found in nature. Sourced from (National Snow and Ice Data Center, n.d.-a).	6
Figure 2.2 Life cycle of a glacier, showing the ELA, accumulation, and ablation zones. Sourced from (Strandberg et al., 2012).	7
Figure 2.3 Global map indicating the overall shrinkage of glaciers. Sourced from (Dyurgerov & Meier, 2005).	8
Figure 2.4 Depiction of the variations of moraine generated from glaciated regions, sourced from (BBC Bitesize, n.d.).	9
Figure 2.5 Glacial lake types, readapted directly from (Yao et al., 2018).	10
Figure 2.6 Illustrated characteristics of different types of glacial lakes, including erosion (1), moraine-dammed (2), ice-dammed (3), and landslide-dammed (4). Sourced from (Otto, 2019).	10
Figure 2.7 Temperature variations, globally, from the last 2019 years. Sourced from (Hawkins, 2020).	12
Figure 2.8 Illustration adapted from (Richardson & Reynolds, 2000) and (Westoby et al., 2014), outlining different types of GLOF mechanisms: Calving (A), avalanche/ice fall (B), landslide/rockslide (C), dam settlement (D), ice-cored moraine degradation (E), rapid inflow from supra/subglacial lakes (F), and earthquake events (G).	14
Figure 2.9 Potential calving mechanism overtopping a moraine dam, sourced from (Bendle, 2020b).	16
Figure 2.10 Comparison of potential energies with the failing of moraine-dammed lakes and their ice-dammed counterparts, sourced from (Bendle, 2020b).	17
Figure 2.11 Map sourced from (Lützow et al., 2023) indicating the locations and statistics of documented GLOF activity. Q_p is peak outflow, V_0 flood volume, A_b area before, A_a area after.	20
Figure 2.12 Distribution of GLOFs in different regions, sourced from (Lützow et al., 2023).	21
Figure 2.13 Dam safety guidelines issued from NVE, sourced from (Midttømme, 2022).	22
Figure 2.14 PQRUT model structure, sourced from (Chernet et al., 2012).	25
Figure 2.15 Quantitative risk diagram, from (Lacasse, 2022a). Also referred to as “failure envelope.”	29

Figure 2.16 An example of a risk matrix that can plot qualitative assessments based on the probability of an event and its resulting consequence. Sourced from (Lacasse, 2022a).	30
Figure 3.1 Overarching methodology applied to cases for analyzing GLOF hazards and risk.	31
Figure 3.2 An example of the layers visible in Breatlas catalog within Temakart's GIS viewing system, at Svartisen (NVE, n.d.-b).	32
Figure 3.3 Rockslide within mountain cirque, indicating dynamic geology and potential initiator for lake failure near Slæddovagjavre. Photo sourced from NorgeiBilder.no (Norge digitalt, 2024).	33
Figure 3.4 An export from Temakart with Breatlas layer activated, indicating interpolated flow lines beneath Jostredalsbreen glacier extending in all cardinal directions (NVE, n.d.-b).	34
Figure 3.5 Sourced from (Cook & Quincey, 2015). "A conceptual consideration of glacial lake evolution and its impact on volume-area relationships."	37
Figure 3.6 Average discharge (Q) plotted against instantaneous discharges (Q_{max}) from glacial outburst floods in North America, Iceland, and Scandinavia. Figure from (Desloges et al., 1989).	39
Figure 3.7 Flow chart depicting the overall process behind determining a melt-flood failure in a concrete or embankment dam.	42
Figure 3.8 Flow chart depicting the overall process behind determining a moraine or ice-dammed glacial lake breach induced failure in a concrete or embankment dam.	42
Figure 3.9 Flow chart depicting the overall process behind determining a calving event-based failure in a concrete or embankment dam.	43
Figure 3.10 An example of available stage history from Sildre for Dravladalsvatn from 1994 until present. An operative strategy is evident from the similar cyclical formations in the data. Sourced from (NVE, 2024).	45
Figure 3.11 Graphic sourced from (Caetech Llc & Calcdevice.com, n.d.) outlining the parameters for Bazin's 1898 weir flow formula.	46
Figure 3.12 Example format for determining failure probability in an event tree analysis.	50
Figure 4.1 Overview of Austre Okstindbreen glacier, Gressvatn dam, and GL1 and GL2 hazards. DTM data from Høydedata.no (Kartverket, 2024).	53
Figure 4.2 Mass balance for Austre Okstindbreen, 1987-1996, data provided by NVE.	54

Figure 4.3 Aerial photo of Gressvatn dam, showing concrete spillway in use at the north end. 2014 Photo from NorgeiBilder.no (Norge digitalt, 2024).	54
Figure 4.4 Documented ice-dammed glacial lake near Leirskardalen (GL1). After recession of snow and ice, lake appears to be bedrock dammed. Photo from NorgeiBilder.no (Norge digitalt, 2024).	56
Figure 4.5 Identified moraine-dammed glacial lake in Oksskoltbreen glacier (GL2). Photo from NorgeiBilder.no (Norge digitalt, 2024).	58
Figure 4.6 Overview of Jostedalsbreen glacier system, Tunsbergdalsvatn and Styggevatn dams, and GL3 hazard. DTM data from Høydedata.no (Kartverket, 2024).	59
Figure 4.7 Cross section of Stegholtbreen and Austdalsbreen showing subglacial topography and differentiation between Austdalsvatn and Styggevatn (Xu et al., 2015).	60
Figure 4.8 Mass balance for Austdalsbreen, 1988-2022, data provided by NVE.	60
Figure 4.9 Cumulative length change for Tunsbergdalsbreen, 1900-1976, data provided by NVE.	61
Figure 4.10 Map outlining glacial lakes expected to be revealed following the recession of Tunsbergdalsbreen (Bogen et al., 2015).	62
Figure 4.11 Aerial photo of Styggevatn dam, with spillway outlet tunnel visible at western end. Photo from NorgeiBilder.no (Norge digitalt, 2024).	62
Figure 4.12 Aerial photo of Tunsbergdalsvatn dam, with concrete spillway structure at southern end. Photo from NorgeiBilder.no (Norge digitalt, 2024).	64
Figure 4.13 Brimkjelen ice-dammed lake (GL3) location, at unfilled state. Photo from NorgeiBilder.no (Norge digitalt, 2024).	67
Figure 4.14 1m DTM raster showing Brimkjelen area (red boundary) in contact with Tunsbergdalsbreen to the east. A minor depression in the glacier is seen where the river changes direction southward. DTM data sourced from Høydedata.no (Kartverket, 2024).	68
Figure 4.15 Cross section of Austdalsbreen, depicting the recession of the glacier toe from 1986 to the predicted location in 2030 (Laumann & Wold, 1992).	68
Figure 4.16 Overview of Folgefonna glacier system and associated dams. DTM data from Høydedata.no (Kartverket, 2024).	69
Figure 4.17 Cumulative length change for Botnabrea, 1959-2023, data provided by NVE.	70
Figure 4.18 Cumulative length change for Gråfjellsbrea, 1959-2023, data provided by NVE.	71

Figure 4.19 Mass balance for Breidablikkbrea for 2003-2013, data provided by NVE.	71
Figure 4.20 Aerial photo of Dravladalsvatn dam, with spillway structure visible out south end, leading to a flood channel underneath the road. Sourced from NorgeiBilder.no (Norge digitalt, 2024).	72
Figure 4.21 Juklavatn dams and spillway layout. Emergency spillway lies embedded in bedrock gully. Photo sourced from NorgeiBilder.no (Norge digitalt, 2024).	73
Figure 4.22 Aerial photo of the Mysevatn dams, with components lining the western bank. Acc. Dam 2 situated in shadow and difficult to discern. Sourced from NorgeiBilder.no (Norge digitalt, 2024).	74
Figure 4.23 2006 Aerial photo of Svartadalsvatn dam with free-flow concrete spillway visible at the western side. Photo sourced from NorgeiBilder.no (Norge digitalt, 2024).	75
Figure 4.24 Small proglacial lake identified in Midtre Folgefonna for Svartedalsvatn (GL4). Photo sourced from NorgeiBilder.no (Norge digitalt, 2024).	77
Figure 4.25 Location of previous minor flood event for Dravladalsvatn (“Sjoen forsvann pa ei natt,” 2009). Aerial photo sourced from NorgeiBilder.no (Norge digitalt, 2024).	78
Figure 4.26 Series of proglacial lakes extending from the termini of Gråfjellsbrea and Breidablikkbrea, into Mysevatn. Photo sourced from NorgeiBilder.no (Norge digitalt, 2024).	79
Figure 4.27 Overview of Reinoksfjellet glacier system, Slæddovagjavre dam, and GL5 hazard. DTM data from Høydedata.no (Kartverket, 2024).	80
Figure 4.28 Aerial photo of Slæddovagjavre concrete dam, with spillway located in center of crest. Sourced from NorgeiBilder.no (Norge digitalt, 2024).	81
Figure 4.29 Slæddovagjavre proglacial lake identified from glacier 869 in Reinoksfjellet. Photo from NorgeiBilder.no (Norge digitalt, 2024).	82
Figure 4.30 Overview of Storsteinsfjellbreen glacier system, Norddalen dam, and GL6 hazard. DTM data from Høydedata.no (Kartverket, 2024).	83
Figure 4.31 Cumulative length change for Storsteinsfjellbreen, 1960-2023, data provided by NVE.	84
Figure 4.32 Aerial photo of Norddalen embankment dam, with separate concrete spillway visible on north end. Photo sourced from NorgeiBilder.no (Norge digitalt, 2024).	85
Figure 4.33 Small proglacial lake identified extending from a glacier atop Nuorjjo varri mountain, leading to Norddalen. Photo from NorgeiBilder.no (Norge digitalt, 2024).	87

Figure 4.34 Overview of Hardangerjøkulen glacier system, Rembesdalsvatn and Sysenvatn dams, and GL7 hazards. DTM data from Høydedata.no (Kartverket, 2024).	88
Figure 4.35 Mass balance for Rembesdalskåka, 1963-2022, data provided by NVE.....	89
Figure 4.36 Cumulative length change for Rembesdalskåka, 1917-2023, data provided by NVE.....	89
Figure 4.37 Aerial photo of Rembesdalsvatn embankment dam, with separate spillway indicated. Sourced from NorgeiBilder.no (Norge digitalt, 2024).	90
Figure 4.38 Aerial photo of Sysenvatn dam, with spillway outlet indicated on the north end. Active outflow is also visible from the embedded tunnel. Sourced from NorgeiBilder.no (Norge digitalt, 2024).	91
Figure 4.39 Demmevatn (GL7) indicated to the left, extending into the terminus of Rembesdalskåka. Additional proglacial lake identified on right, appearing to be bedrock dammed. Photo sourced from NorgeiBilder.no (Norge digitalt, 2024).	94
Figure 4.40 Proglacial lake identified extending to western margin of glacier 2963 (NVE ID). Timelapse showing significant growth of lake from 2008 (left) to 2019 (right). Photos sourced from NorgeiBilder.no (Norge digitalt, 2024).....	95
Figure 4.41 Overview of Svartisen glacier system, Storglomvatn, and GL8 hazard. DTM data from Høydedata.no (Kartverket, 2024).....	96
Figure 4.42 Aerial photo of Holmvatn dam on the western side of Storglomvatn, which does not feature a spillway structure. Photo sourced from NorgeiBilder.no (Norge digitalt, 2024).	97
Figure 4.43 Aerial photo of Storglomvatn dam on the eastern side of Storglomvatn, with large concrete dam spillway visibly active at northern end. Photo from NorgeiBilder.no (Norge digitalt, 2024).	97
Figure 4.44 Glacial lake Nordvatn (GL8) identified extending from glacier NVE ID 1080, northern margin of Vestre Svartisen. Photo from NorgeiBilder.no (Norge digitalt, 2024).	100
Figure 4.45 Glacial lake emerging from glacier 1083, chosen not to be further assessed due to topographic conditions. Photo sourced from NorgeiBilder.no (Norge digitalt, 2024).	100
Figure 5.1 Risk envelope plot for H1 hazard condition for all applicable dams.....	104
Figure 5.2 Risk envelope plot for H2 hazard condition for all applicable dams.....	105
Figure 5.3 Risk envelope plot for H3 hazard condition for Styggevatn.	106

Figure 0.1 H1 Event tree analysis for Dravladalsvatn dam.....	126
Figure 0.2 H1 Event tree analysis for Gressvatn dam.	127
Figure 0.3 H1 Event tree analysis for Juklavatn dam.....	128
Figure 0.4 H1 Event tree analysis for Mysevatn dam.	129
Figure 0.5 H1 Event tree analysis for Norddalen dam.	130
Figure 0.6 H1 Event tree analysis for Rembesdalsvatn dam.	131
Figure 0.7 H1 Event tree analysis for Slæddovagjavre dam.	132
Figure 0.8 H1 Event tree analysis for Storglomvatn and Holmvatn dams.....	133
Figure 0.9 H1 Event tree analysis for Styggevatn dam.	134
Figure 0.10 H1 Event tree analysis for Svartadalsvatn dam.	135
Figure 0.11 H1 Event tree analysis for Sysenvatn dam.....	136
Figure 0.12 H1 Event tree analysis for Tunsbergdalsvatn dam.....	137
Figure 0.13 H2 Event tree analysis for Gressvatn dam (GL1).....	139
Figure 0.14 H2 Event tree analysis for Gressvatn dam (GL2).....	140
Figure 0.15 H2 Event tree analysis for Tunsbergdalsvatn dam (GL3).....	141
Figure 0.16 H2 Event tree analysis for Slæddovagjavre dam (GL5).....	142
Figure 0.17 H2 Event tree analysis for Norddalen dam (GL6).....	143
Figure 0.18 H2 Event tree analysis for Rembesdalsvatn dam (GL7).....	144
Figure 0.19 H2 Event tree analysis for Storglomvatn and Holmvatn dams (GL8).....	145
Figure 0.20 H3 Event tree analysis for Styggevatn dam.	147

List of Tables

Table 1.1 Original list of dam sites provided from Statkraft for glacial hazard investigation.	4
Table 2.1 Summary of typical glacial related hazards found in nature, non-exhaustive.	13
Table 2.2 Norwegian dam consequence class definitions, adapted from (Midttømme, 2022).....	23
Table 2.3 Flood requirements in Norwegian dam regulations, sourced from (Glad et al., 2022).....	24
Table 2.4 Suggested flood estimation methodologies, translated and adapted from (Glad et al., 2022).....	26
Table 2.5 List of potential quantitative risk assessment methods, directly summarized and adapted from (Lacasse, 2022a).....	28
Table 2.6 List of potential qualitative and semi-quantitative risk assessment methods, directly summarized and adapted from (Lacasse, 2022a).	30
Table 3.1 Average lake depths derived from the study conducted by (Mool et al., n.d.).	38
Table 3.2 Recurrence probability statistics derived from the dataset created by (Lützow & Veh, 2023). Large discrepancies seen from the global and scandinavian contexts.....	48
Table 3.3 Verbal descriptors that can be applied in an event tree analysis. Reformatted from (Lacasse, 2022a).	49
Table 3.4 Applicable hazards determined for selected dam sites in Norway.	51
Table 4.1 Determination of fundamental hazards for Austre Okstindbreen.	55
Table 4.2 Historical GLOF events within Austre Okstindbreen.	57
Table 4.3 Determination of fundamental hazards for selected dams at Jostedalsbreen.	65
Table 4.4 Historical GLOF occurrences within Tunsbergdalsbreen.	66
Table 4.5 Determination of fundamental hazards for selected dams at Folgefonna.	76
Table 4.6 Incoming flood estimates for Folgefonna-area lakes, sourced from provided reports.	77
Table 4.7 Determination of fundamental hazards for selected dams at Reinsokfjellet.	82

Table 4.8	Determination of fundamental hazards for selected dams at Storsteinsfjellbreen.	86
Table 4.9	Determination of fundamental hazards for selected dams at Hardangerjøkulen.	92
Table 4.10	Historical GLOF occurrences within Rembesdalskåka, at Demmevatn.	92
Table 4.11	Determination of fundamental hazards for selected dams at Svartisen.....	98
Table 5.1	Resulting estimations for identified hazardous glacial lakes.	107

Abbreviations

DFV (design value flood)

DTM (digital terrain model)

ELA (equilibrium line altitude)

ETA (event tree analysis)

GLOF (glacial lake outburst flood)

HBV (hydrologiska byråns vattenbalansavdelning)

HEC-RAS (Hydrologic Engineering Center's River Analysis System)

HRV (highest regulated volume)

ICOLD (International Commission on Large Dams)

LRV (lowest regulated volume)

M.W.E. (meters water equivalent)

MASL (meters above sea level)

NVE (Norwegian Water Resources and Energy Directorate)

PMF (probable maximum flood)

PMP (probable maximum precipitation)

RES (radio echo sounding)

RIDM (risk-informed decision making)

USACE (United States Army Corps of Engineers)

Acknowledgements

I would like to extend my most sincere gratitude to my supervisor, Professor Fjóla G. Sigtryggsdóttir and co-supervisors, Ganesh H. R. Ravindra, Jacob Clement Yde, and Guy Mason, for their very helpful guidance and knowledge in this broad thesis topic. I would also like to extend a thank you to Vidar Goldfine, who often joined and contributed to our discussions alongside Ganesh. Their support and availability to meet helped progress the project nicely, and I've appreciated getting to know them a bit better.

My network of great support from family and friends also helped me through this challenging task, whom I very much appreciate. The two years of studies at NTNU were very insightful and enjoyable, and I will always reflect back positively on the great friendships made within the program. My hope is that the program continues to live on and inspire new students each year.

1 Introduction

A significant byproduct of today's changing climate is the increasing hazard in the form of GLOFs (glacial outburst floods) and other glacial-related failures spread amongst the world's glacial formations. These serious events are generated through a multitude of different mechanisms and can appear in many forms that will be outlined and analyzed in relation to their effects and potential risk on several downstream man-made dams in mainland Norway.

1.1 Scope and objective

This paper was found useful to embark upon due to the lack of studies relating to identifying and analyzing these potential risks in Norway particularly, as they are extensively researched in other areas of the world such as Asia, South America, and North America. As Norwegian glaciers continue to melt and recede, as part of the global decline from the end of the Little Ice Age, it is important to assess newly introduced risks that dams can face, whether it be from increasing precipitation patterns, formation of glacial lakes, or the continuing physical alterations to masses of glacial ice (Zhang et al., 2024). Across the world, glacial outburst floods have directly impacted many societies in significant ways, directly responsible for over 12,000 recorded deaths, mostly concentrated in South America and central Asia (Carrivick & Tweed, 2016). Although the impacts of glacial outburst floods have not been seen to these magnitudes in Norway in the past, they still have been responsible for several instances of significant damage to infrastructure, as well as looming as a potential threat in the future for several high-consequence dams situated upstream from populated areas. Norway is one of the many regions that face increasing threats from rapidly expanding net glacial lake area, that can provide fuel for flood hazards (Zhang et al., 2024). Not only are the lakes getting larger, but they are also becoming more numerous. A key factor to a study such as this is that new hazards may appear in only a short few years that may not have been assessed or even observed prior.

Many large dams in Norway (including most featured in this paper) were constructed during a prosperous post-war boom from 1945 to 1990 in the great shift towards sustainable hydroelectric power generation (Jensen et al., 2021). This was a period in which over 400 hydropower plants were constructed, and over 24,000 MW of generation was made available. Although these dams were required to maintain design and safety standards and adhere to regulations set forth by the regulatory body Norwegian Water Resource and Energy Directorate (NVE), they can still be susceptible to failures that may not have been present at the time of their inception. More specifically, they can become targets of hazardous glacial events that can vary in source. This paper attempts to quantify these hazards through assessing probabilities associated with the sequence of events within a glacial-induced failure, and to complete a high-level screening for dams that might require more attention in the future in these regards. The paper will also describe the processes surrounding the origination of these hazardous glacial events, how they interact with a glacial system, and describe the current conditions within dam safety in Norway. The origination and implementation of methods for these purposes will also be discussed in detail, and recognizing some of the shortcomings that may be attributed to them.

1.2 Selected glaciers and dams

In all, 25 dams were selected from Statkraft's vast portfolio that lie in positions either adjacent or below recognized glacial systems, in multiple regions across Norway, shown in Table 1.1. From these, through a screening process later described, 13 were selected as primary "cases" to be analyzed for potential hazards. These primary hazards include (H1) rapid melt and high precipitation, (H2) breach of glacial lake, and (H3) calving and icefall. The origination and procedure in selecting, estimating, and analyzing these hazards will be discussed later in the paper. The cases themselves will be described in detail and provide insight into the basic components of each dam system, as well as address any potential weaknesses or concerns with their function.

1.3 Analysis process and methodology

Although the science for quantifying the risk associated with glacier-related failures are relatively unstandardized, several prominent methods allow one to make generalized judgements on the basis of whether a potential hazardous glacial mechanism is of either little or serious risk to not only the dam itself, but to the population and infrastructure that reside below them. Through the utilization of generated event trees, the risk assessment method of choice for this paper, these judgements can be made, and hazards can be identified as significant or not. As with any screening analysis, many simplifications and assumptions must be made, and these will be discussed throughout. The implementation and dependance on using event trees or other similar risk assessment methods has grown throughout recent years, becoming a more popular method for high-level observations in the respect to risk, probability, and consequences. The advantages and restrictions that these assessments hold will also be touched upon.

Table 1.1 Original list of dam sites provided from Statkraft for glacial hazard investigation.

No.	Dam Name	Dam ID (NVE)	Glacial System	Region	Assessed in Paper?
1	Styggevatn	2666	Jostedalsbreen	Midt	Yes
2	Tunsbergdalsvatn	2816	Jostedalsbreen	Midt	Yes
3	Midre Brevatn	2041	Fresvikbreen	Midt	No
4	Heimste Brevatn	1573	Fresvikbreen	Midt	No
5	Båtsvatn	1215	NA	Nord	No
6	Fossvatn	1385	Veikdalsisen	Nord	No
7	Slæddovagjavre	2488	Reinoksfjellet	Nord	Yes
8	Reinoksvatn	2275	Reinoksfjellet	Nord	No
9	Gressvassvatn	1468	Okstindbreen	Nord	Yes
10	Kalvatn	2273	NA	Nord	No
11	Holmvatn	3618	Svartisen	Nord	Yes
12	Storglomvatn	4361	Svartisen	Nord	Yes
13	Øvre Glomvatn Sidedam	3175	Glombreen	Nord	No
14	Øvre Glomvatn Hoveddam	3183	Glombreen	Nord	No
15	Norrdalen Hoveddam	2178	Storsteinsfjellbreen	Nord	Yes
16	Norrdalen Sperredam	4215	Storsteinsfjellbreen	Nord	Yes
17	Ståvatn	3596	Nupsfonn	Sør	No
18	Rembesdalsvatn	2283	Hardangerjøkulen	Sør	Yes
19	Sysenvatn	2730	Hardangerjøkulen	Sør	Yes
20	Langvatn	1872	Hardangerjøkulen	Sør	Yes
21	Mysevatn	2077	Folgefonna	Sør	Yes
22	Svartadalsvatn	2689	Folgefonna	Sør	Yes
23	Markjelkevatn	6901	Folgefonna	Sør	No
24	Juklavatn	1714	Folgefonna	Sør	Yes
25	Dravladalsvatn	1256	Folgefonna	Sør	Yes

2 Background

To provide context behind the aim of this paper, background information will be provided in this chapter that outline some of the basic components and processes within glaciers, and their potential hazardous mechanisms. Dam safety in Norway and popularized risk assessment methods will also be discussed to familiarize the reader with the methodology later developed in Chapter 3.

2.1 Glacier systems

2.1.1 Types of glaciers

Scientists and academics have classified glaciers in many different methods, but for the purposes of this study, the multiple-order classification nomenclature will be used in this context and summarized from the publication *Glaciers and Glaciation* (Benn & Evans, 2010). These are also distinguished in Figure 2.1.

Ice sheet and ice cap (unconstrained by topography)

- Ice dome
- Ice stream
- Outlet glacier

Glaciers constrained by topography

- Ice field
- Valley glacier
- Transection glacier
- Cirque glacier
- Piedmont lobe
- Niche glacier
- Glacieret
- Ice apron
- Ice fringe

Ice shelves

- Confined ice shelf
- Unconfined ice shelf
- Ice rise

Ice sheet and *ice cap* glaciers are best described as large blankets of ice. They cover immense areas in very remote locations. Unlike other glacier types, they are not significantly influenced by underlying topography near the center region. 50,000 km² is considered the minimum reach for a glacier body to be considered an ice sheet, whereas less would be considered an ice cap (Benn & Evans, 2010). As one might expect, most of the globe's ice sheets are present in Antarctica and Greenland (Hagg, 2022), whereas some of the most prominent ice caps are located in locations such as Svalbard or Iceland. On the outside

fringes of ice sheets and ice caps are *ice streams* and *outlet glaciers*. These are settled in basins and travel at a faster rate than the portions on the interior of ice sheets and ice caps which are known as *ice domes*.

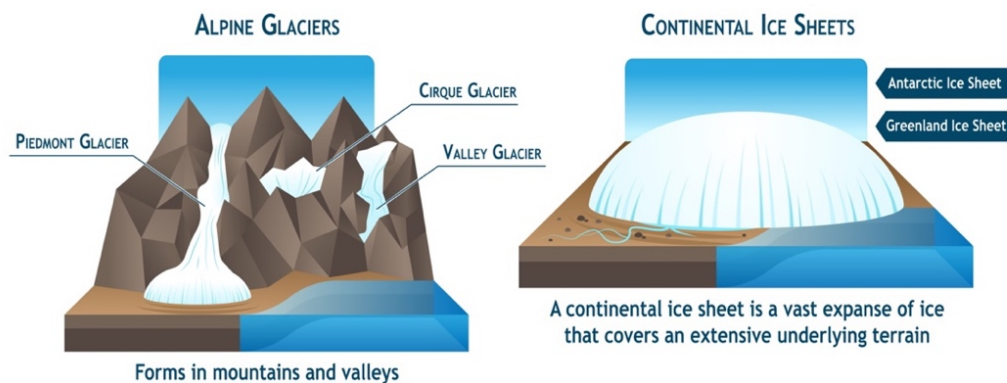


Figure 2.1 Illustration differentiating glacial formations found in nature. Sourced from (National Snow and Ice Data Center, n.d.-a).

The more commonly found types of glaciers (including those in this paper) are typically constrained by topography. *Ice fields* do not have the dome-like feature that ice caps do, and generally form in mild but uneven terrain that are at altitudes conducive for the accumulation of ice. Examples of these can be found in British Columbia and Patagonia, amongst other locations (Benn & Evans, 2010). *Valley glaciers*, as the name suggests, form as valleys when ice is exuded from a cirque or ice field into a valley comprised of strong bedrock. These can appear akin to fluvial formations, or simpler single cut formations. These types of glaciers are heavily influenced by the foundational bedrock in which they lie. *Transection glaciers* are quite complex, in that they branch and flow into different directions. Their structure resembles a web in some ways, and can also form from the conjoining of multiple ice flows into one. These appear in highly dissected mountain terrain. *Cirque glaciers* are very identifiable from their bowl shape. They generally form in depressions in mountains and can be the last remaining glacier structure before complete disappearance (as well as the first to form) (Hagg, 2022). *Piedmont glaciers* are unique in that they can have a significant portion of glacial ice below the equilibrium line. These have an appearance of a viscous flow and can extend into lowland areas following their journey through bedrock troughs. These can also be found in many locations, such as Alaska, Iceland, and the Canadian High Arctic (Benn & Evans, 2010). A commonly identified type of glacier in this study were niche glaciers, glacierets, ice aprons, and ice fringes. These are smaller types of glaciers, which are often remaining fragments of previous formations. *Ice aprons* are characteristic of being quite thin and sticking to the sides of mountains, whereas *ice fringes* differ in that they typically extend from the sea and appear as a small piedmont formation. *Glacierets* originate from avalanche processes or snow drifting, and generally reside in drier terrain and are normally very small in size. Finally, *niche glaciers* are bodies that are controlled by specific features of a mountain or valley side, for example, a niche or rock overhang.

Ice shelves are much more massive formations that are typical to high polar environments. They feature low gradients and suspended glacier tongues (Benn & Evans, 2010). Ice shelves are extensively found in Antarctica and Greenland and will not be as relevant in this paper. They feature very complex movement and flow patterns, and behave similarly to tectonic plates, due to their ability to form ice rises and deep crevasses. These are very impressive

formations that are not as sensitive to climate conditions when compared to other traditional topography-constrained glaciers.

2.1.2 Mass balance cycle

To understand how glaciers form and fluctuate, it is important to first clarify what the mass balance process entails. This involves both *accumulation* and *ablation* phases. Both are highly sensitive to climate and environmental factors, as well as the type of glacier and topography. This overall life cycle is illustrated in Figure 2.2.

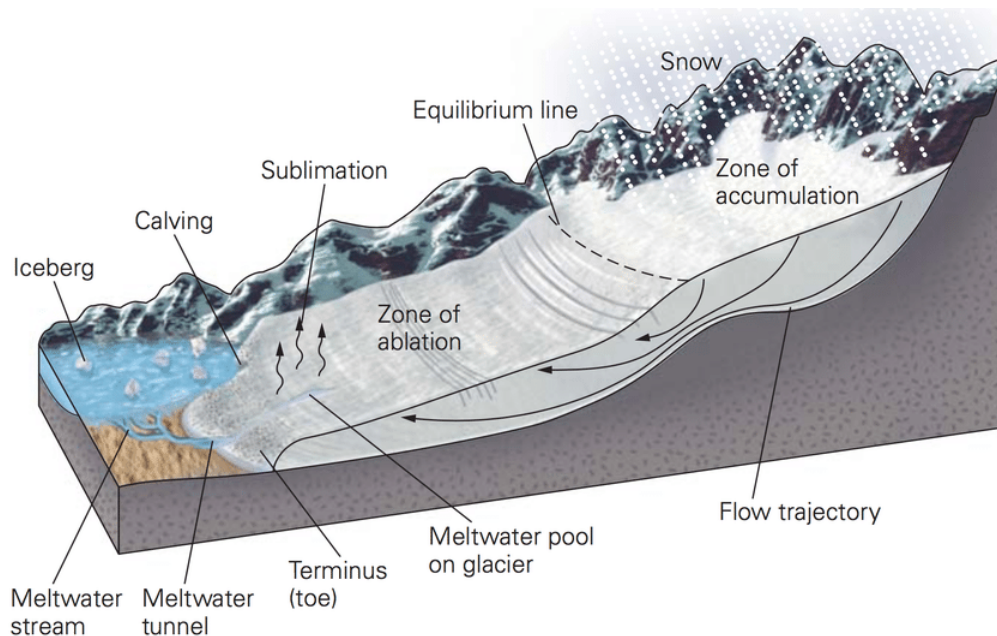


Figure 2.2 Life cycle of a glacier, showing the ELA, accumulation, and ablation zones. Sourced from (Strandberg et al., 2012).

Accumulation occurs when the glacier is being actively “fed” with snow and other precipitation (rain, hail, sleet), which form ice packs that accumulate on the glacier’s surface and can lead to growth of the glacier body. The input of this mass can also be attributed to wind-blown snow, avalanching, and hoar frost (Davies, 2020). This growth will be sustained so long as the glacier does not lose mass in the warmer periods of the year and is typically transported down elevation as a very slow flow in the glacier, due to continuous gravitational forces. The wholistic process of accumulation involves the transition of snow to ice mass through partial melting, refreezing, and eventually fusing. This makes ice cores extracted from glaciers characteristic based on cycles of refreezing through seasons, similar to identifying rings from the center of a tree trunk.

The *ablation* component of the mass balance cycle involves the loss of glacial ice. When the ice mass continues its journey downhill, it will reach lower altitude and henceforth encounter warmer temperatures. It may also encounter a water body or the sea, in which specific mechanisms may occur, such as calving (ice-block chunks separating from the glacial body into the water). Ablation initiates through the mechanisms of avalanching, sublimation, wind dispersion, calving, subaqueous frontal melt, evaporation, and others (Davies, 2020). Land-terminating glaciers and marine-terminating glaciers will undergo different processes at the

terminus. In land-terminating glaciers, the main driver behind ablation processes will be surface melt, due to the higher temperatures at lower elevations. This can cause chain reactions where melt water is produced and carves or drains into the glacier over time, creating englacial channels. When the surface water enters cracks or crevasses, it can pool and form what are known as englacial (within), or subglacial (beneath) lakes. Normally, the melt water will reach the bedrock beneath the glacier and conjoin to form a subglacial stream where it will exit at the toe of a glacier. Marine-terminating glaciers may calve, as previously mentioned, or melt in contact with the water. In some cases, the glacier toe will extend atop the water, suspended by the pressure of the water, and melt from beneath (Davies, 2020). This is difficult to detect without field investigation.

Finally, these two processes intercept at what is known as the *equilibrium line altitude (ELA)*, or the location that defines where the ablation and accumulation phases negate each other. This is recognized at a specific altitude, and can range from year to year, depending on the overall health of the glacier and factors from the climate.

The mass balance is then the net sum of the accumulation and ablation phases. When the accumulation phase outweighs the ablation, the glacier will essentially be growing, or characterized by what can be referred to as a *positive mass balance*. In the reverse situation, the glacier will be shrinking, featuring an overall *negative mass balance*. This can fluctuate through the years and is observed and compared to the previous time periods as a reference point. In most parts of the world, glaciers are experiencing a negative mass balance relationship, due to the effects of warming climates and changes in atmospheric conditions, as shown in Figure 2.3.

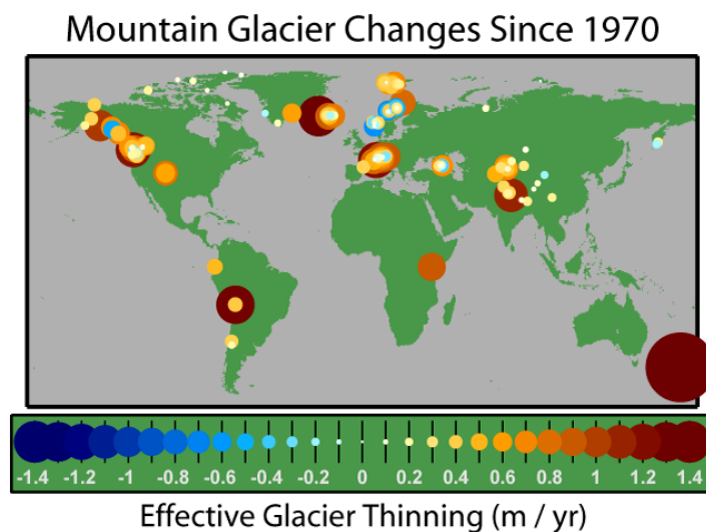


Figure 2.3 Global map indicating the overall shrinkage of glaciers. Sourced from (Dyrugerov & Meier, 2005).

2.1.3 Glacial moraine landforms

Glaciers have a significant impact on the terrain in which they are present. Evidence of these influences can be found at all elevations and can provide insight to some of the glaciological history and future. The most obvious resultant from past glacial activity are carved landscapes- characterized by deep fjords or valleys. Although a glacier's movement will

remove soil and debris from a landscape, the depositional process can leave many of these materials behind, up to several hundred kilometers downslope from the source. These debris can include, but are not limited to, silt, sand, gravel, and boulders, and often generate formations such as moraines, corries, troughs, and drumlins. (Benn & Evans, 2010).

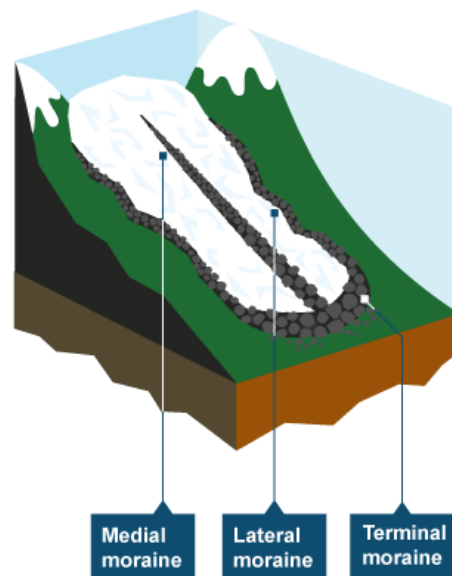


Figure 2.4 Depiction of the variations of moraine generated from glaciated regions, sourced from (BBC Bitesize, n.d.).

A critical formation resulting from glacial retreat are *moraines*. Moraines are heaps of poorly sorted glacial till that were either transported to the glacier terminus (active process) or left behind from a glacier that has receded (passive process) (Bennett, 2001). In some cases, they can also accumulate from a glacial stream at a confluence. The formation of moraines can also be more complex, as a result of “glaciotectonism” and other dynamics in the glacial ice (Bennett, 2001). Moraines can vary in subcategorization as *end moraines*, *lateral moraines*, or *medial moraines*, as shown in Figure 2.4. They often are foundational infrastructure to glacial lakes found in nature and discussed in this paper. As a glacier continues its retreat and produces meltwater, the moraines can entrap the water and form a glacial lake over time.

2.1.4 Types of glacial lakes

As GLOFs are one of the central topics in this paper, it is important to understand and differentiate the different types of glacial lakes that can be found in nature. They can be classified into both primary and secondary types as per (Yao et al., 2018), as shown in Figure 2.5 and Figure 2.6. These naming conventions can indicate the relative position a lake is in respect to the glacier. They can also be used in combination, should a lake exhibit multiple defining characteristics.



Figure 2.5 Glacial lake types, readapted directly from (Yao et al., 2018).

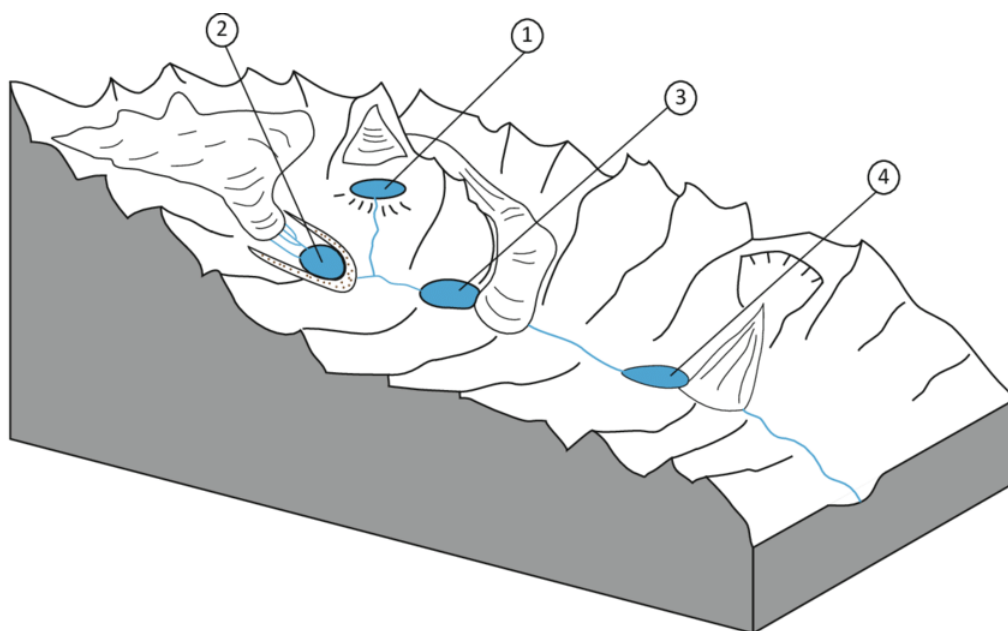


Figure 2.6 Illustrated characteristics of different types of glacial lakes, including erosion (1), moraine-dammed (2), ice-dammed (3), and landslide-dammed (4). Sourced from (Otto, 2019).

Erosion lakes are one of the more commonly observed types, which accumulate in depressions that were originally carved from glacial retreat or movement (Yao et al., 2018). They vary widely in depth and are typically stable throughout the year. Often, these lakes are located far from the original glacier from which the depression was originally generated. *Cirque lakes* are located within a mountain cirque, as the name suggests, which resembles an arm-chair. These are usually smaller and located near the glacier's ELA. *Glacial valley lakes* are present in U-shaped valleys downstream from a glacier and are typically required to have a surface area of 20 km² or greater. It should also be no further than 15 km from the glacier, as to not confuse with tectonic lakes (Yao et al., 2018). As with other water bodies, these still pose risks should a snow or rock avalanche or landslide cause a sudden displacement of water.

Subglacial lakes, as the name suggests, are situated beneath the surface of a glacial body. These can be difficult to detect, as often they are not visible from screenings of photos or aerial data (Yao et al., 2018). To detect such lakes, physical site assessments are typically needed, or by observing the movement of the glacier or exiting waterflow underneath. Drilling cores and radio echo sounding (RES) are popular methods for exploring these formations and have been performed in several glaciers in Norway (Saetrang & Wold, 1986). Both RES and coring have the added benefit of interpolating the underlying bedrock terrain, which is often important in understanding the dynamics of the glacier's movement. One way they can develop is simply from an entrance into the glacier and through a process of melting and channeling. Otherwise, they can originate from within the glaciers themselves when absorbing radiant heat from the earth's core. This creates an oven effect and is hastened by the increased pressure generated by the glacier's overlying ice. The pressure is so great that the melting point of water will decrease, furthering the effect (Palmer et al., 2013).

Contrarily, *supraglacial lakes* are situated atop a glacier body. They are typically bound entirely by the ice and can form near the ablation zone of the glacier (Yao et al., 2018). They are known to last relatively short periods in comparison to other types of glacial lakes because of the dependence on the glacier for maintaining a seal. Supraglacial lakes are very dynamic and can form as a result of combining two or more separate supraglacial lakes, and can also move from location to location. These types of lakes are especially interesting in GLOF studies, as they can be unpredictable and vary between years. They also hold an immense amount of potential energy should a drainage or breach occur.

Moraine-dammed lakes are a very critical type for the focus of this paper. As a glacier retreats, walls of sediment rich barriers are left, which can vary in composition. These are known as lateral moraines and end moraines, depending on how the sediment is oriented in respect to the glacier, seen in Figure 2.4. Depending on which is damming the lake, it then can lead to the classification as either an *end moraine-dammed lake* or a *lateral moraine-dammed lake* (Yao et al., 2018). These sediments, or glacial till as it is sometimes referred to, can behave as a barrier in which a lake can develop over time. These barriers are then filled with precipitation, glacial melt water, and other estuaries (Benn & Evans, 2010). Just as with supraglacial lakes, they can conjoin from separate entities into larger ones. These lakes are also normally synonymous with *proglacial lakes*, or lakes that are formed from water exiting glacial ice into a depression created by the recession of a glacier, from the last ice age. Proglacial lakes normally are in direct contact with the glacier's terminus but can also be in a disconnected nearby downstream location and can be moraine or ice-dammed. Moraine-dammed lakes can be further characterized as ice-cored moraine, in which the core of the natural dam consists of ice and frozen material, remnant from the original glacier that has not yet melted (Lukas, 2011). These can be especially hazardous, as the walls can breach when higher temperatures cause rapid melting within. This ice-laden moraine can also be present at the lake's bottom in some cases. Similar to supraglacial lakes, these tend to be fairly short-lived (Bendle, 2020b). Many factors can have significant influence on the survival of moraine-dammed lakes, which are often seen partially or fully draining in overtopping or piping events. In especially rare instances, glaciers can grow in size, and recover the area that a moraine-dammed lake occupies.

Ice-dammed lakes can take many forms, but most traditionally are bound partially by an ice barrier, normally the glacier itself (Bendle, 2020b). The remaining sides of the lake can be either moraine, bedrock, or virtually any other geological feature. They often form when the side of a glacier is intersected by an existing tributary, after which water begins to pool.

These types of lakes are less susceptible to sudden violent failures associated with GLOFs, but are still important to identify (Lützwow et al., 2023). They are typically smaller in size and can sometimes be short-lived due to the reliance of the glacier for remaining bounded.

2.1.5 Norwegian glaciers today

Glaciers are typically built up over many years and originate from different time periods. In Norway, most are remnants of the Little Ice Age, where glaciers reached their maximum extent around the year 1750 (Fjord Norway, 2024). This is evident from the long-term climate fluctuations seen in Figure 2.7. The young life of these glaciers are attributable to the fact that they are considered temperate glaciers, that are easily influenced by small changes in temperature (USGS, n.d.-b).

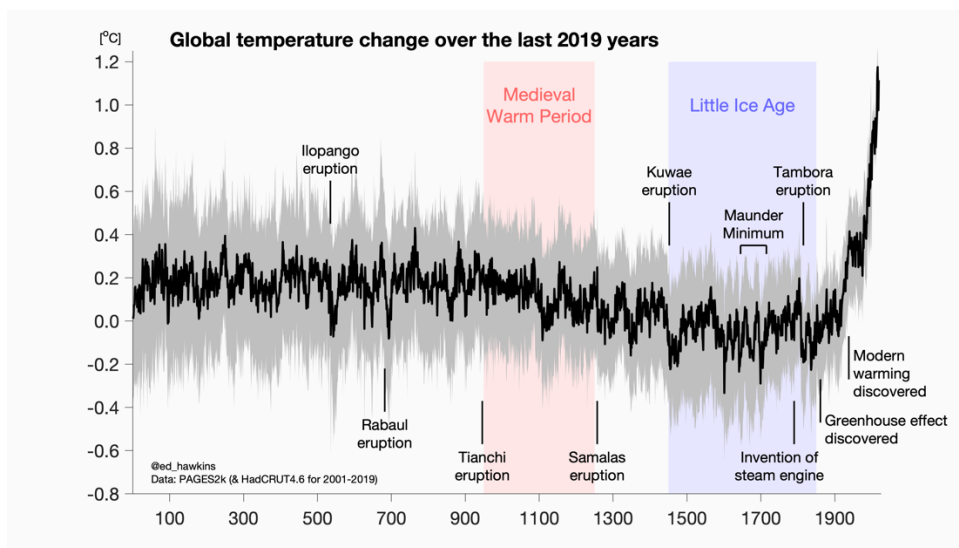


Figure 2.7 Temperature variations, globally, from the last 2019 years. Sourced from (Hawkins, 2020).

In other areas of the world, such as Greenland or Antarctica, glacial ice can be dated back to 100,000-1,000,000 years ago (USGS, n.d.-a). As one can expect, this is characteristic of polar glaciers, that are residing in environments constantly below freezing point (aside from a thin layer of melt at the surface) (National Snow and Ice Data Center, n.d.-b).

One particular event that changed the southeastern Norwegian landscape was the outburst flood from Nedre Glomsjø, which burst following the last Ice Age. This outburst was so enormous, that some estimates reach $1 \times 10^6 \text{ m}^3/\text{s}$ of peak outflow (Høgaas & Longva, 2016). This flood altered the inundated landscape dramatically, leaving behind streamlined bed forms and transporting vast quantities of erosive deposits that are still visible today. Events like these are indicative of how dynamic the end of the last Ice Age was in the realm of glacial mechanisms and changing climate.

2.2 Hazardous glacial mechanisms

The highlighted topic of this paper considers the risk between the interaction of glaciers with man-made dammed lakes, as there are numerous mechanisms responsible for many instances of damage and destruction worldwide. Table 2.1 summarizes the different types of

mechanisms that will be discussed further. Figure 2.8 also illustrates some of these mechanisms. It should be noted that this is not an exhaustive list, as other related environmental factors can lead to triggering one or more of these types of mechanisms.

Table 2.1 Summary of typical glacial related hazards found in nature, non-exhaustive.

Primary Hazard Mode	Secondary Hazard Mode	Brief Description
Rapid ice melt (atmospheric)	High precipitation and rapid melt	Release massive amounts of meltwater due to the interception of precipitation and warmer temperatures- mainly affecting coastal glaciers that are especially sensitive to these temperature fluctuations, such as those in Norway.
Breaching of glacial lake	Moraine-dammed lake failure	Sudden release of stored meltwater from a moraine-dammed lake due to critical failure.
	Subglacial lake failure	Release of stored meltwater from lake positioned atop glacier surface.
	Supraglacial lake failure	Release of stored meltwater from lake positioned beneath glacier mass.
	Englacial lake failure	Release of stored meltwater from lake positioned within glacier mass.
Other mass dynamics	Calving	Sudden detachment of glacial ice from glacier face, in the form of large blocks or chunks.
	Icefall	Avalanche of chunks of ice atop or adjacent to glacier, similar, typically located at portion of glacier moving quickest.
	Avalanche	Rapid release of snow (and if applicable, debris/ice) down a slope.
	Rockfall	Sudden release of rocks and boulders of varying sizes downslope, possibly as a result from external forces enacted by glacial masses.
Other external environmental conditions	Earthquake	Violent seismic events within Earth's tectonic plates can trigger any of above-mentioned mechanisms.
	Volcanic activity	Geothermal processes or volcanic eruptions can trigger any of above-mentioned mechanisms.

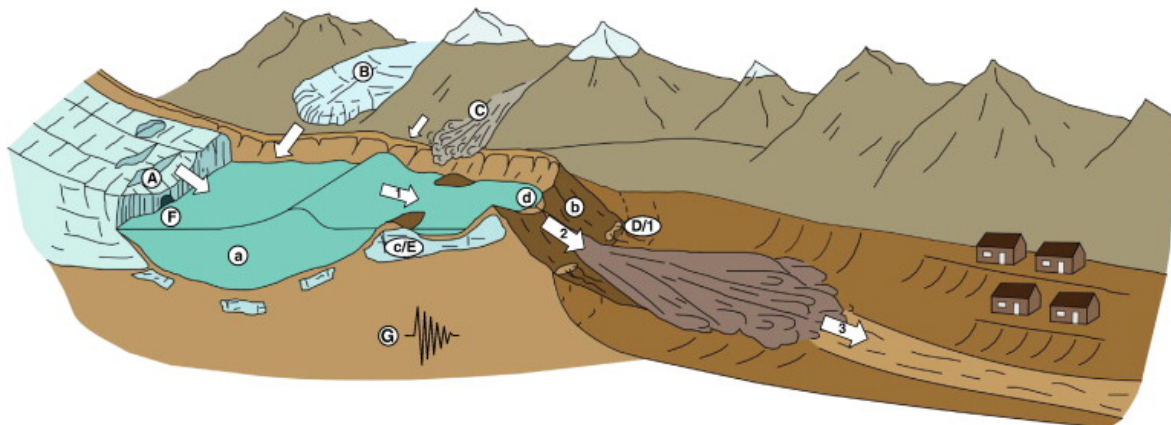


Figure 2.8 Illustration adapted from (Richardson & Reynolds, 2000) and (Westoby et al., 2014), outlining different types of GLOF mechanisms: Calving (A), avalanche/ice fall (B), landslide/rockslide (C), dam settlement (D), ice-cored moraine degradation (E), rapid inflow from supra/subglacial lakes (F), and earthquake events (G).

2.2.1 High precipitation and rapid melt

One of the primary mechanisms that will be observed in this paper are severe precipitation and melt conditions for glaciers. This condition is defined as when glaciers experience rapid melting due to a combination of warmer temperatures and high precipitation rate simultaneously. This can lead to rapid outburst floods from the hastened melting of ice and/or release of stored water within, atop, or below the glacier. An example of climate-induced rapid glacial melt flood generation was reported from Qaanaaq Glacier in northwestern Greenland, in the years 2015 and 2016. In these events, $9.1 \text{ m}^3/\text{s}$ and $19.9 \text{ m}^3/\text{s}$ average flow was released as a result of warm air temperatures and heavy rainfall, leading to the destruction of a critical roadway (Kondo et al., 2021). It should be noted that a flood released from within a glacial (englacial lake) adopts the nomenclature *glacier outburst*. A large factor in determining the severity of this condition is simply the amount of snow or ice that may lie within a lake's catchment. Naturally, in identical climatic and topographical conditions, a catchment with more ice and snow masses present will result in higher flood conditions when compared to one with fewer so. This will be further analyzed and implemented into event tree analyses for applicable cases later in this paper.

2.2.2 Breaching of glacial lakes

The breaching of a glacial lake is a critical risk that will be identified and analyzed for specific cases later in this paper. It concerns the nature of failure of a glacial lake's damming that results in the outflow of (sometimes significant) volumes of melt water in a rapid manner. This mechanism depends on the type of glacial lake, which are defined in 2.1.4. These types of events can vary in duration, but are frequently observed lasting between one hour and a full 24 hours, but in some cases, can last for days. These are considered *GLOFs* (glacial lake outburst floods). GLOFs have the potential to cause significant damage and

endanger the lives of people downstream, so it is important to identify any potential sources and address what level of severity might be expected should one occur.

2.2.3 Breaching of ice-dammed glacial lakes

In the cases of supraglacial lake breaches, they can often drain through cracks underneath the surface, where a void is available, or from a simple breaching through the depression in the ice walls. These failures within the ice are generated through what is known as hydrofractures, initiated by tension in the ice from shifting causing cracks (Woods Hole Oceanographic Institution, 2015).

Ice-dammed lake breaches are alike to supraglacial breaches in that they can propagate through cracks and voids in the ice, and do not typically result in the complete destruction of the dam (Bendle, 2020b). In rare cases, the floods may result in only a temporary failure of the barrier due to ice flotation, which was observed in an instance at Russel Glacier in Greenland (Carrivick et al., 2017). This ice dam flotation phenomenon occurs when water drains from a proglacial lake into a glacier base through open conduits that is situated at a lower elevation, and eventually the hydrostatic pressure overcomes the ice overburden pressure, leading to its rapid draining (Bendle, 2020b). These, along with subglacial drainage events are difficult to predict and model.

Subglacial drainage events are normally governed by the hydraulic potential within the glacier. Similar to mapping the drainage flow net beneath a dam, the water will eventually travel in grid of least resistance, and exit through an open orifice in the glacier or another surface location (Malczyk et al., 2020). Today, most of the models used to predict these flows are based on the condition that the glacier rests atop a bedrock foundation, but this is not always the case (Hart et al., 2022).

Ice-dammed lake drainage events can be repetitive, as generally the dam is not completely destroyed from the event. An example of this phenomenon is well-documented in Hidden Creek Lake, Alaska, USA. At this location outbursts occur for 2-3 days each year as a result of the ice-dam reacting to the seasonal dynamics exhibited by the main glacier (Walder et al., 2006). These can remain cyclical until destruction of the ice dam or death of the glacier itself.

2.2.4 Breaching of moraine-dammed glacial lakes

Moraine dam failures more closely mimic the failure of man-made embankment dams. They occur when the bounding moraine material fails in one way or another, releasing a flood of melt water downstream. These tend to be somewhat frequent in some regions, or even cyclical, and depend on the embankment width, height, compaction, and composition. Generally, moraine dams are more narrow and sharp-crested in shape (J. Clague, 2000). Moraine material itself is composed of unconsolidated, poorly sorted permeable sediment, and can contain bodies of ice. A dam of this composition is even more likely to fail when saturated, as a combination of the weaker material and melting of potential ice (Bendle, 2020b). With that established, some moraine dams are regarded as very strong, should their base be lower, wider, and have an upstream face armored by larger rocks. These may last for thousands of years in the perfect conditions (J. Clague, 2000). Failures in moraine-dam

breaches are initiated by either overtopping or piping within the dam wall. This can be quickened if heavy moraine degradation occurs, which lowers the crest of the dam.

Overtopping events, as shown in Figure 2.9, result from either the entry of too high of a volume of water into the lake (high precipitation or melting), or from displacement waves caused from calving of a glacier, or avalanches or rockfalls (Bendle, 2020b). These displacement waves are also known as *seiche waves* in some literature. These overtopping events can later lead to defections in the crest and cause enlarged incisions in the dam that will continually expand and increase in discharged melt water leading to critical failure.

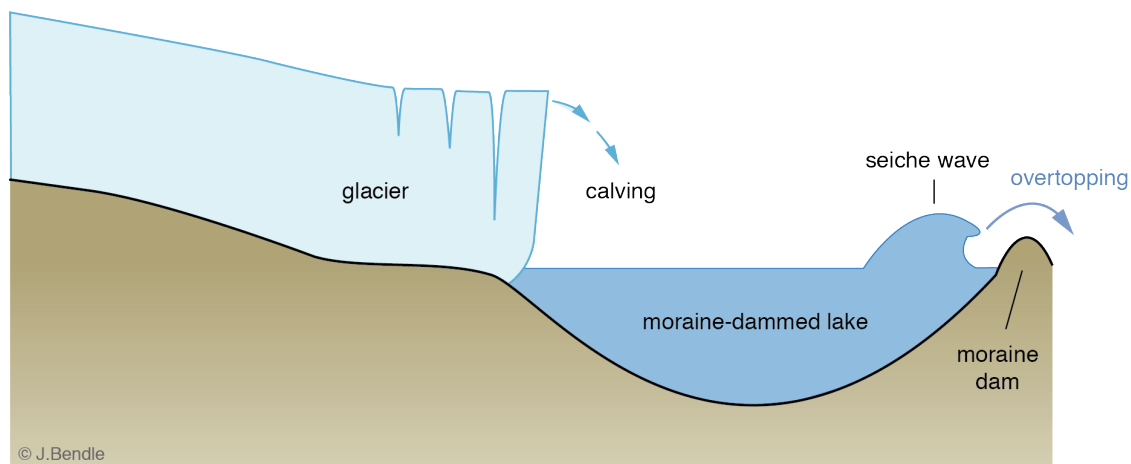


Figure 2.9 Potential calving mechanism overtopping a moraine dam, sourced from (Bendle, 2020b).

Piping and seepage failures on the other hand, are a slower process that may form from transport of melt water through the seepage through the moraine material. It is a less common source of failure when compared to overtopping, and rarely the single triggering mechanism behind a GLOF. It occurs when significant seepage “erodes a hole at the exit, which makes the seepage path short and increases the hydraulic gradient” (Liu et al., 2013). More simply put, the dam fails from within and extends outwards until the dam can no longer contain the water.

When comparing moraine and ice-dam failures, it can be observed that moraine dams tend to release floods more violently, as seen in Figure 2.10. Although this may be the case, they tend to occur less frequently, as moraine dams tend to completely self-destruct when failing (Bendle, 2020b).

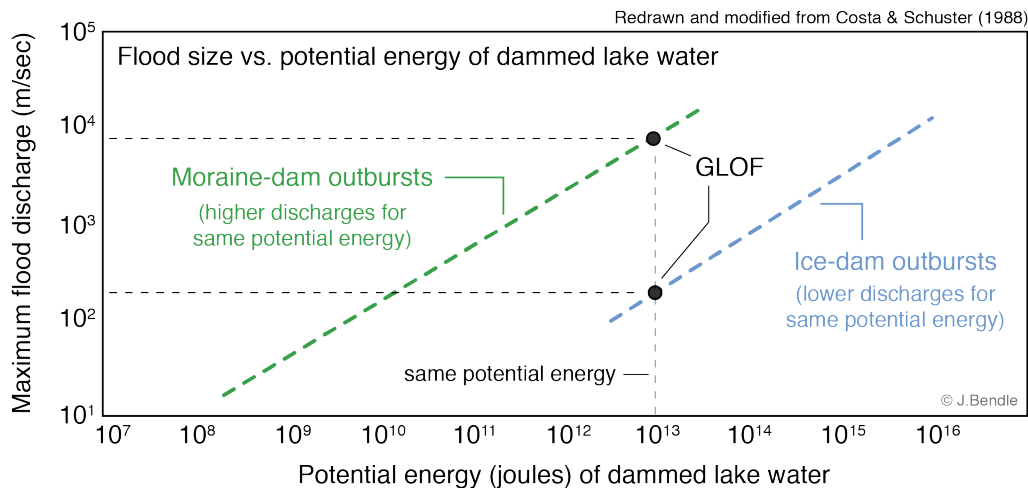


Figure 2.10 Comparison of potential energies with the failing of moraine-dammed lakes and their ice-dammed counterparts, sourced from (Bendle, 2020b).

Significant moraine dam failures are found across the world in a vast variety of mountain ranges, with four exceptional examples in the Cordillera Blanca of Peru between 1938 and 1950 (J. Clague, 2000). The largest event in 1941 resulted in the deaths of more than 6,000 people and the destruction of the city of Huaraz. The largest recorded moraine dam failure can be attributed to the drainage of Laguna del Cerro Largo in Chile, in 1989. In this event, more than $2.29 \times 10^8 \text{ m}^3$ of meltwater was released (Hauser, 1993). These events demonstrate the immense potential threat posed to communities and infrastructure downstream of at-risk moraine dam lakes.

2.2.5 Calving and icefall

The calving of glaciers is a widely studied phenomenon by scientists and researchers. It is the mechanism in which a glacier loses sheets or chunks of ice from the edge of a glacier's face. This can occur when an overhang has been generated from the glacier's creep movement over a water body or lower terrain (when on land, this is considered *dry-calving* (Diolaiuti et al., 2004)). Preexisting strains within the ice in the form of cracks and crevasses provide weak points, allowing breakage once intercepting water or suspending over land. Water that has entered these cracks also play a pivotal role in expanding the cracks to separate the ice into chunks, with the cracks sometimes extending to the glacier bed (Bendle, 2020a). Low basal drag is an important element in the rate and existence of calving as well, where the glacier moves at a faster rate near the terminus due to being nearly suspended or buoyant at the contact of water (Benn et al., 2007; O'Neel et al., 2005). The area with low basal drag is located at the base of the glacier, near the intersection of the water body. When the glacier is essentially stretched as such, it is referred to as longitudinal stretching, and results in significant formation of crevassing (Bendle, 2020a). Calving events can also lead to a sudden widening of an outlet channel within the glacier, which can release destructive floods, like documented in the Perito Moreno Glacier within the southern Patagonia icefield, where calving has been initiated by ongoing outbursts, leading to further violent flood events in the region (Diolaiuti et al., 2004).

Icefall is related to calving in the sense that the glacier is being broken into separate partitions through the stresses acting on the glacial ice. When crevasses form from the dynamic

movement of the glacier at higher altitudes, they can create areas of weakness prone to breaking free and falling. These icefalls can generate potential seiche waves, and lead to the destruction of a dam, such as in an instance in 1985 at Langmoche Glacier in Nepal. In this event, the wave generated by a significant icefall overtopped the Dig Tsho dam and eroded the moraine leading to an outburst (Vuichard & Zimmermann, 1987). Both icefalls and calving are more difficult to model but will be discussed and identified in the cases in this paper. To predict these types of failures, one must observe previous activity of the glacier, and any significant cracks or crevasses along the body of the glacier, as well as have knowledge of the subglacial topography in the area. Icefalls are typically centralized in the region of the glacier that is experiencing the highest rate of movement.

2.2.6 Other mechanisms

Earthquakes are also considered a related hazard when it comes to the relationship between glaciers and lakes. In the right conditions, substantial seismic activity can activate the failure of a natural moraine dam, or initiate landslides, icefalls, or avalanches that can enter a water body and cause a seiche wave, or significant displacement. These are much rarer instances with Norwegian glaciers, as it depends on the locale of the glacier in relation to known epicenters for tectonic activity. In this paper, they will not be analyzed, as this assessment would require significantly more focus on the seismology in the region and insight on the structural geology within the sites. For instance, according to open sources, Jostedalbreen encounters “very few earthquakes,” with only 5.51 occurring on average each year, all very small in magnitude (*Global Earthquake Monitor*, 2024). In some regions, earthquakes are considered to be minor threat, even in environments with many existing opportune GLOF potential threats. In the Tropical Andes, for example, earthquakes were evaluated from 1900-2021, and of the 59 that had occurred, only one had triggered a documented GLOF, leading to the authors’ recommendation to retain earthquake activity at a secondary susceptibility indicator, not a primary when conducting risk assessments in the region (Wood et al., 2024).

Avalanches and rockfalls both result in similar potential damages to lake and dams by potentially routing into glacial lakes and initiating flood events. They can also interact with other mechanisms, such as initiating calving or icefall which then can propagate into the failures mentioned earlier. Avalanches are particularly hazardous in the Indian Himalayas, where a report notes that 36 out of 329 glacial lakes studied are susceptible to avalanche-induced failures (Dubey & Goyal, 2020). In some cases, avalanches and rockfalls can be connected, and lead to an outburst, such as the 2017 outburst of a glacial lake from Langmale glacier. This began with a rockfall which then caused an avalanche that later entered the lake and generated a flood of 1.3×10^6 m³ of meltwater (Byers et al., 2019). Rockfalls and avalanches can also be more difficult to predict, although they can be interpreted from past patterns or visual inspections in the area (evidence of previous rock falls, uneven terrain, or visible cracks in bedrock). NVE provides GIS-based map services that index the steepness of terrain, and in some cases include physical site-assessed risks. Observing these types of data can be helpful in identifying areas of potential risk as a preliminary screening assessment but can be significantly strengthened by field investigations. Additionally, NGU’s (Norges Geologiske Undersøkelse) InSAR data can be detracted from certain areas to identify if there have been any significant ground shifts, which can be a useful detection tool for future landslides and avalanches, as typically these shifts are seen months or years in advance of a major event (Multiconsult, 2022a).

Lastly, an important distinction to make is that of the *jökulhlaup* (also written as *jökulhlaup* in Norwegian). This term is often used interchangeably with GLOFs in literature, however originates from Icelandic events, and is more attributed to the interaction of volcanic activity with the different flooding mechanisms (i.e. causing rapid melting or drainage of glacial lakes, etc.). In July 1999, a volcanic GLOF was documented from Sólheimajökull, Iceland, that initiated an immense flow of nearly $4.4 \times 10^3 \text{ m}^3/\text{s}$ within one hour, as per reconstructive calculations (Russell et al., 2010). Although this is technically not a different subset of mechanism, it is important to recognize that volcanic eruptions and intense geothermal processes can also play a role in hazardous flooding mechanisms outside Norway. These are much more complex to determine risk for and would need a deeper understanding of the local volcanology.

2.2.7 Danger and potential damage to dams and reservoirs

All the aforementioned mechanisms can inflict damage to man-made reservoirs or dams in just a few ways. They primarily fall into the methods in which built dams fail- through overtopping or impact. Most mechanisms result in the significant displacement within the lake or entry of water to the lake, which can cause overtopping should the reservoir not hold adequate volume buffer or exceed the spillway release capacity. In more violent instances, seiche waves can impact the dam wall, and can cause failure if it surpasses the design criteria, as described in relation to moraine dam failures in 2.2.4.

Blockage of a spillway is a significant concern to overall dam safety (Lia, 1998). This is especially prevalent where calving is occurring, or cases where ice is in contact with the lake. Should a spillway be partially or fully blocked, the dam's ability to mitigate overtopping is severely compromised. Dams in this position should have personnel conducting maintenance checks or integrate ice-breaking structures to ensure a failure cannot propagate in this manner. These blockages are not limited to calving, as it is possible for icefalls or landslides to also situate debris afront the spillway.

Glacier hazards can be a mixture of modes, interacting with each other. An example of this is the previously mentioned event described by (Vuichard & Zimmermann, 1987) from moraine dam failure in Nepal. Additional hypothetical conditions could also be an avalanche triggering the destruction of a moraine-dammed lake, sending outflow to the reservoir downstream, or an earthquake causing a supraglacial lake to crack and drain. The transport of large icebergs over dry land within a debris flow that was not previously considered can also be a significant threat. The combinations and iterations can be nearly endless, as so this paper will not attempt to identify all of these. It is important when observing specific sites or in the design or rehabilitation of new dams, that one considers the potential for glacial hazards, individually, or as a product of chain-reactions.

2.2.8 Worldwide GLOF statistics

A very valuable resource was assembled in 2023 by Georg Veh, Natalie Lützwow, and Oliver Korup detailing the locations and characteristics of 3,151 individual GLOFs across the world in 27 different countries (Lützwow et al., 2023; Lützwow & Veh, 2023). These were compiled from events reported in the years 850 to 2022 CE, and can be seen in Figure 2.11. The data can reveal key statistics for the events in different mountain ranges and environments, although these are only from events that were discovered (as many GLOFs can go unnoticed

in reality). They can also be representative in regards to the frequency in which types of lakes tend to fail.

North America had the record of the most documented GLOF failures, at 833 events, whereas 192 were identified in Scandinavia. Luckily, in this dataset, one of the most consistent reported elements with the cases were dam types. A vast majority of the dams were ice-dammed lakes at a glacial margin at 65%, and only 13% were determined to be moraine-dammed. Other dam types included englacial, at 5%, other ice-dam lakes at 8%, and subglacial or bedrock lakes at 4%, with the remainder undetermined. It is interesting to note the disproportionate shares of moraine dam and subglacial lake events. Subglacial lakes are extremely hard to detect failure for, as the drainage may not always be obvious in observable photos or eyewitness accounts and tend to be less violent.

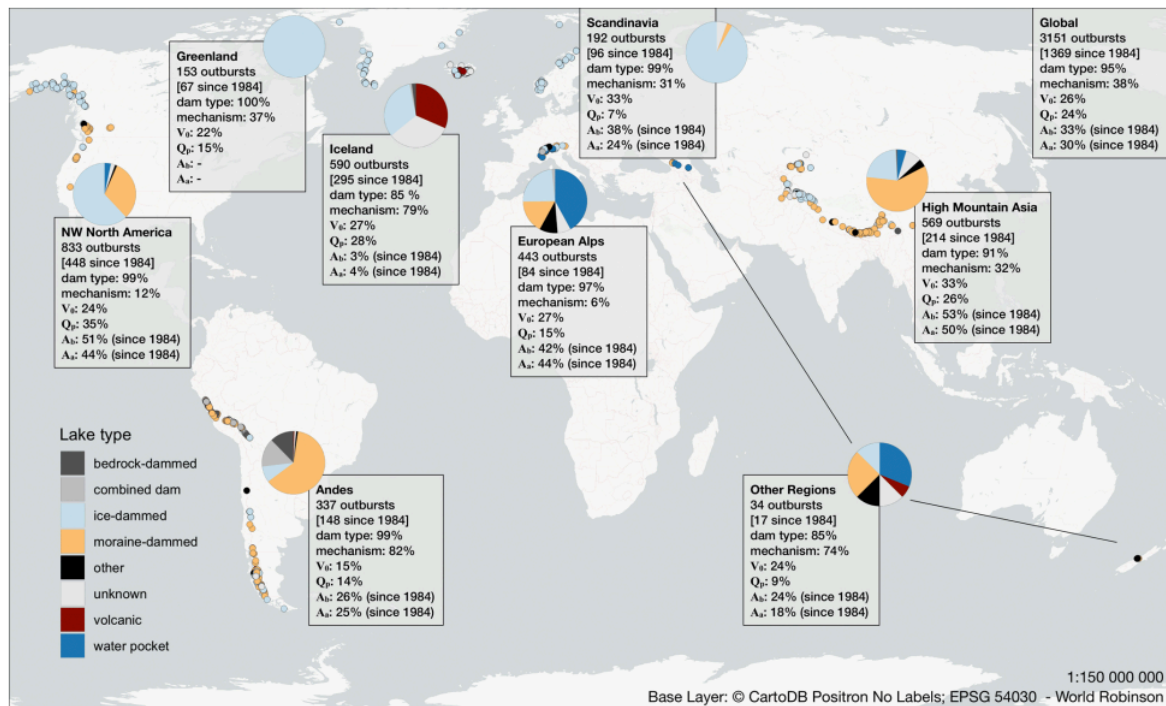


Figure 2.11 Map sourced from (Lützwow et al., 2023) indicating the locations and statistics of documented GLOF activity. Q_p is peak outflow, V_0 flood volume, A_b area before, A_a area after.

An additional interesting metric to observe is the reoccurrence of GLOFs for the same sources. As mentioned before, the potential for moraine-dammed lakes to reoccur are significantly less than ice-dammed, since they are typically destroyed during the event (Bendle, 2020b). High degrees of reoccurrence are then more likely in more glaciated terrain where there are more ice-dam lakes present, which is evident in Figure 2.12.

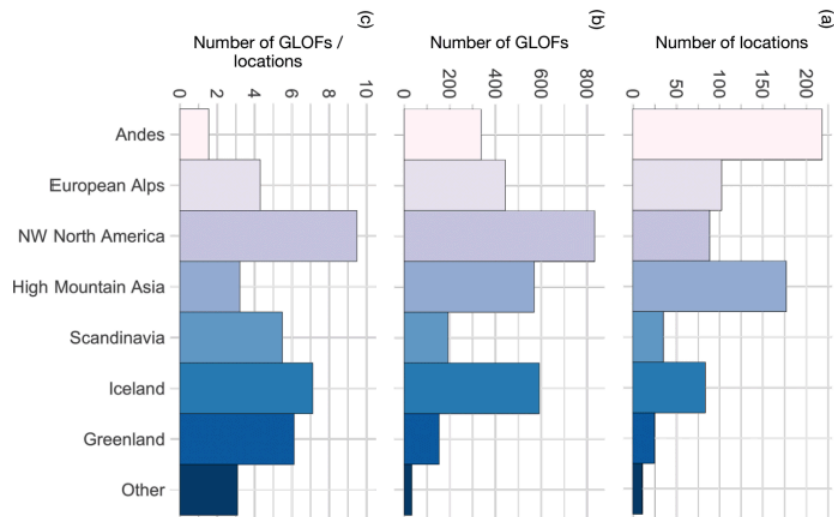


Figure 2.12 Distribution of GLOFs in different regions, sourced from (Lützw et al., 2023).

Scandinavia results show a relatively low ratio of GLOFs per locations, especially when compared to the Andes, where single-event moraine dam lake failures are much more prevalent. This is evident from the data set that shows a great deal of repeating ice-dam failures when compared to moraine dam failures that will be discussed in the context of recurrence intervals in Table 3.2.

2.3 Norwegian dam safety

2.3.1 Dam safety regulations

Dam safety in Norway has been primarily overseen and governed by the Norwegian Water Resources and Energy Administration (NVE), since its inception in 1920, and under its previous iteration, Norwegian Water Administration, in 1909. Their primary objective is to perform supervision “to ensure that dams and other hydraulic structures are not posing a threat to life, property or the environment” (The Water Resources Act § 5). Although the directorate is involved in this regard, it is still the duty of the operator, constructor, and designer of the dams to remain vigilant in fulfilling any of the lawful regulations, guidelines, and requirements. Most of the first dam safety regulations regarding planning and construction of the dams were published in 1981 but were overhauled in revisions in 2001 and 2009. Some of these revisions included the how the dams are to be operated and the all-important classification system, amongst others. Today, there is framework implemented that extend to the safety of appurtenant structures, such as requirements for penstocks and head race tunnels, and regulations for internal control from 2010 and 2012, respectively (Midttømme, 2022). Much of the framework encompasses dam safety aspects. Figure 2.13 outlines some of the dam safety guidelines in current standing from the directorate.



Dam safety guidelines (Norway)

1. Flood estimations (2022)
 2. Reassessment (2018)
 3. Dam surveillance (2019)
 4. Planning and construction (2012)
 5. *Determination of loads**
 6. *Spillways**
 7. *Concrete dams**
 8. Masonry dams (2011)
 9. Embankment dams (2012)
 10. Gates, valves and penstock (2011)
 11. *Dam break hazard analyses**
 12. Classification (2014)
 13. Incident reporting (2014)
 14. Public safety (2015)
- *guidelines to former safety regulation (2001), valid until they are revised

Figure 2.13 Dam safety guidelines issued from NVE, sourced from (Midttømme, 2022).

The organization carries out periodic inspections, tailored to each site's features and classifications. Observations of damage are reported to a chartered engineer if they are discovered. The inspections range from 1-2 times per year, and are function checked to ensure proper order of equipment. More significant inspections usually take place each 5th-7th year, and are more comprehensive in the sense that additional parties are involved, and the consequence class and flood data are reevaluated (Midttømme, 2022). It is critical that during the reassessment inspections that flood, and other calculations are rechecked and that the dam is still adhering to guidelines, and if any changes in the regulations should require rehabilitations.

In order for a dam safety program to be successful it needs to be dynamic, and open to modifications with availability of new safety data, practices, and information gathered for the dam. This requires tedious logging of dam operations, environmental inputs such as the continuous recorded inflow, and a safe but efficient reservoir regulation practice, which can account for expected high precipitation events. GLOFs in particular are unique in that they are not entirely predictable based on the hydrological characteristics or weather data alone and require additional studies understanding these threats.

2.3.2 Dam consequence classes

As mentioned prior, dam consequence classes, summarized in Table 2.2, are a relatively new concept for applying certain regulations in dams across Norway. These were developed to identify the overall consequence as a result of a dam failure, and is helpful when quantifying the risk a dam faces, which is determined from Equation 2.1.

Equation 2.1 Traditional approach to calculating risk

$$\text{Risk} = \text{Probability} * \text{Consequences}$$

The necessity of these classifications arose from a need to have flexible dam safety regulations dependent on direct representative value of the potential failure impacting human lives, the environment, and property. In essence, this allows the dam owners and regulatory agency to utilize a more streamlined consequence-based approach for a particular dam's safety, rather than having the same requirements applied to all dams (Midttømme, 2022).

Table 2.2 Norwegian dam consequence class definitions, adapted from (Midttømme, 2022).

Class Number	Consequences	Criterion
0	Minor	No houses in pathway of breach, minor consequences to society.
1	Small	No houses in pathway of breach, other buildings and infrastructure at risk.
2	Medium	1-20 houses in pathway of breach, or major infrastructure affected (critical to health and safety of community)
3	High	21-150 houses in pathway of breach, major damage to critical infrastructure at risk.
4	Very High	More than 150 houses in pathway of breach.

Simplified methods in estimating a dam’s classification would include calculating breach parameters for a dam to determine the peak flood, and any secondary effects, such as erosion effects downstream. It is also important to identify what areas are at risk of being inundated, either by referring to up-to-date flood zone maps, or modeling a breach using a variety of flood models, including USACE’s popular HEC-RAS.

2.3.3 Emergency planning

In Norwegian dam reports, the emergency preparedness for dams encountering GLOFs are not specifically outlined, instead centered around traditional flooding. Developing plans of action should a dam breach is a critical part of the planning process and are typically required for all dams that pose risk to downstream populations. NVE is an advocate for this practice, and recommend the creation of emergency action plans that include the definitive responsibilities for personnel and organizations, emergency procedures, and accompanied inundation maps to be made available (Midttømme, 2022). Determining the sources of these unfavorable events requires the utilization of a risk analysis method- most commonly an event tree analysis is selected, which will be discussed later. All common possible failures are generally considered, but many emergency plans may not account for niche events, such as those initiated by hazardous glacial mechanisms.

It is also suggested that dams include early warning systems should they encounter potential danger to alert downstream populations in the event of an imminent disaster. These types of warnings can include automatically triggered systems such as sirens, or the implementation of early warning systems that make use of flood forecasting (Midttømme, 2022).

2.3.4 Flood design safety

The aforementioned dam classes have a significant role in the overall design of a dam, in that they can determine the selected design flood and safety check flood for which a dam needs to withstand. As with dams in other countries, the design flood is often a lawful requirement that the design must account for and is represented normally as a return period

(in some cases it is represented as a percentage of the PMF). In Norway, these are represented as “Q” values (flow, in m³/s), with a subscript indicating the return period. For instance, a flow estimated from a 1,000-year flood event would be represented by Q_{1000} . These return events are based on the frequency in which they are calculated to occur. A Q_{1000} event is anticipated to only occur once every 1,000 years. A return period can be interchangeable with the probability of exceedance, by taking the inverse of the return period, and producing a probability of occurrence. For example, a Q_{1000} event hold a 0.1% chance of occurring in any given year.

The *probable maximum flood*, or *PMF*, is an important metric for dam safety in Norway. The PMF is essentially the worst-case scenario that can be deduced from available data regarding extreme precipitation (*PMP*, or *probable maximum precipitation*), snow melt, and transfer from interconnected reservoirs. It is considered the “safety check flood” for higher-risk dams that include the potential to threaten lives. The dams are expected to survive PMFs but may garner some damages. The outflow value that is found is used as a basis of design for outlet modules, such as spillways and flood gates. The most recent of Norwegian dam flood calculation regulations from 2022 (Glad et al., 2022) stipulate the assigning of design flood and safety check flood for the respective dam classes in Table 2.3.

Table 2.3 Flood requirements in Norwegian dam regulations, sourced from (Glad et al., 2022).

Consequence Class	Design Flood	Safety Check Flood	Additional Control
4 and 3	Q_{1000}	PMF	Q_{1000} + hatch failure
2	Q_{1000}	PMF or $1.5*(Q_{1000})$	Q_{1000} + hatch failure
1	Q_{500}	PMF or $1.5*(Q_{500})$	Q_{500} + hatch failure

The “additional control” column is representative of a newer regulation that takes the event that a hatch operation fails during the flood event and remains closed, essentially directing all flow through spillway structures, instead of mitigating some of the release through the outlet control structures (to power stations or other reservoirs). This could also account for a case of clogging, where debris constricts the passageway and prohibits the outflow of water. One may also notice that the consequence class 0 is not displayed. This is due to class 0 dams not needing to adhere to these requirements, as their potential for failure do not have significant impacts on infrastructure, communities, or the environment, and are not held to the stringency that more critical dams are. That being established, the directorate “recommends” that dams in class 0 are still designed for Q_{200} events (Glad et al., 2022).

The flooding events are also assumed under a subset of “unfavorable” conditions, including entrance into the reservoir when at full capacity (HRV). This ensures that should the same event occur at any other period of time of regulation, the reservoir can manage to dampen the flood properly without overtopping or exceeding capacity. Reservoirs that include transfers from other reservoirs must assume the condition of full transfer inflow for the full flood duration, to bolster the worst-case scenario parameters. On the contrary, it must be assumed the any outflow transfer capacities are treated as null in the target reservoir.

A very critical fairly recent update from NVE requirements, key to the studies in this report, are the inclusion of snowmelt in calculations for Q_{500} and Q_{1000} , which were previously not necessitated (SWECO Norge, 2009). In highly glaciated cases such as those in this paper, this change can significantly influence the flood calculations, and thereafter the assessed safety of the existing dams. It is likely that some dams will require modifications to adhere to this newer safety regulation.

2.3.5 Determination of PMF and design flood values

In the past, and as is still practice in some countries, the method for finding PMP was to double the value for the largest peak flow recorded at a dam site (Midttømme, 2002). Nowadays, the methods chosen are a variation of rainfall-drainage models and/or frequency analyses (Glad et al., 2022). These require a certain degree of high-quality, long-term hydrological and climatic data. In frequency analyses (regional analysis, station analysis or a combination), the focused variable is the precipitation itself, and is purely probabilistic in nature. On the other hand, rainfall-drainage models combine the rainfall and runoff relationship into a predictive input-output system, which can be described as deterministic. Both methods retain some benefits and drawbacks, as frequency analyses are often considered too simplified, and not as representative of what a well-calibrated hydrological model may output. In Norway, some examples of flood frequency analysis methods include RFFA-NIFS (Glad et al., 2015) and RFFA-2018 (Engeland et al., 2020).

Hydrological models may need a greater data set to be properly calibrated and can take more time to develop. Some popular choices in Norway include the PQRUT model, which is a simplified rendition of the more advanced HBV model (NVE, 2018).

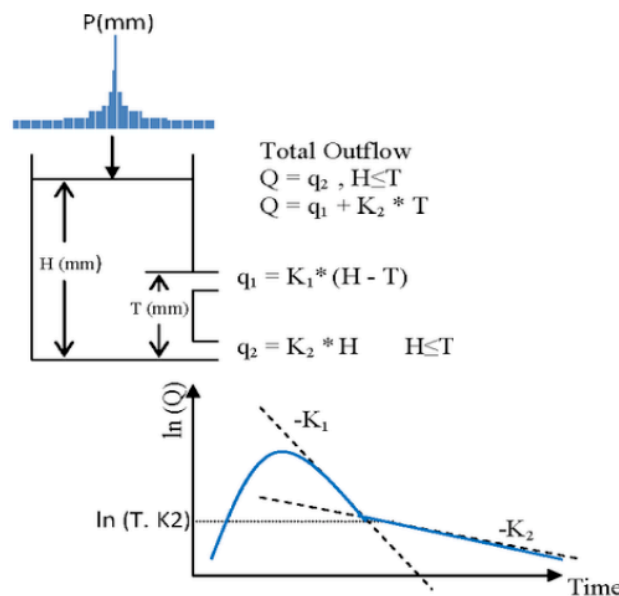


Figure 2.14 PQRUT model structure, sourced from (Chernet et al., 2012).

To properly form the PQRUT model, input precipitation data is needed, as well as catchment characteristics to determine the outflow coefficients (K_1 , K_2) and threshold value (T). It is recommended to have historic flow data from the catchment in order to calibrate the model properly, otherwise NVE has outlined several equations for calculating these.

The recommended approach from NVE to calculating a design flood, or PMF, is based on the catchment size and time resolution. Outlines these recommendations for generating a flood calculation.

Table 2.4 Suggested flood estimation methodologies, translated and adapted from (Glad et al., 2022).

Method	Regional Flood Frequency Analysis		Frequency Analysis	Rainfall-Drainage Models	
	RFFA-NIFS	RFFA-2018		PQRUT	Rational Method
Catchment Area	<60 km ²	All	All	2-800 km ²	<2 km ²
Time Resolution	Culmination	Daily or Culmination	All	Hourly/Daily	Culmination
Q _M	X	X	X		X
Q ₅ -Q ₁₀₀	X	X	X	X	X
Q ₂₀₀	X	X	X	X	X
Q ₅₀₀		X	X	X	X
Q ₁₀₀₀		X	X	X	
PMF				X	

The PMF is typically the most critical figure to compare when assessing dam safety, and in Norway it is suggested to calculate through the PQRUT method (Glad et al., 2022). The formulation of these data are generally recommended to be quality-ensured by a professional hydrologist, and compared with nearby assessments to validate legitimacy. In this paper, available professionally developed estimates for safety check floods and design floods for the case study dams will be discussed.

2.4 Risk assessment methods

Risk assessment is a valuable tool for determining a dam’s susceptibility and subsequent consequence for a particular mechanism of concern. In past years, these types of analyses have become far more commonplace for dam safety practice with implementations in Norway, elsewhere in Europe, North America, and Australia (Donnelly, 2005). In the United States, quantitative risk analyses have been used by federal agencies since the 1990s (France, 2021). These sciences are continuously improving over time and will likely see even further widespread use in other countries.

When assessing a dam’s risk for failure, it can be approached from either a deterministic or a probabilistic method. A deterministic approach identifies whether a facility (dam) can

endure a particular condition or load (GLOF failure mechanisms), without considering the variability introduced from randomness. This approach can underestimate the actual failure risks present (Lacasse, 2022a). On the other hand, a probabilistic method can recognize the uncertainties and by incorporating multiple scenarios, likelihoods and impacts. This can generate a better holistic understanding of the risk for the decision-making processes. These probabilistic methods can lead to what is known as RIDM (risk-informed decision making). Many expert publications, including that of *Handbook Risk assessment and risk management* (Lacasse, 2022b) recommend complementing the two in order to make more informed decisions from calculated factors.

Suitable situations where risk analysis is an appropriate application may be (Lacasse, 2022a):

- High consequence dams (see: *consequence class*)
- Dams with cascading effects
- Dams with significant uncertainties
- Dams with changing behaviors or dynamic external conditions
- Establishment of emergency preparedness plans
- Large-scale dam owner/operators needing to assess which dams require attention most
- Evaluation of needed rehabilitation measures

This list is non-exhaustive and can demonstrate how useful risk analysis can be when properly applied to dam safety practices.

2.4.1 Benefits and drawbacks

Risk assessment provides some valuable benefits, including the ability to systematically review uncertainties and failure modes, and to visualize risk in a more understandable sense, through the implementation of visual aids, such as event trees (Lacasse, 2022a). It also can provide a simpler approach to becoming familiar with multiple risks, and to identify where adjustments can be made to increase the safety of a structure. Depending on the method, they can also be quick to implement and scale across multiple cases simultaneously, allowing high-level overviewing of critical infrastructure, such as dams.

Some drawbacks with risk assessment include the approximation of variables and results. These sometimes do not fully evaluate probabilities to the most extreme accuracy due to some of the judgements that need to be made in the process. In very complex cases, it may also be possible to omit important prerequisites for a failure that was not originally considered. This leads to the largest issue with risk assessments- that they tend to be very focused on a particular chain of events that are calculable, and may exclude sources like human error or organizational factors (Lacasse, 2022a).

2.4.2 Quantitative methods

Risk assessment methods can be further subdivided into quantitative, semi-quantitative, or qualitative. Quantitative methods are the most useful in conducting high-risk assessments, as they provide discrete numerical outcomes to a potential unwanted failure. These types of analyses can also be justified from the previous implementation of a qualitative risk method alerting to higher potential risk (Lacasse, 2022a). It is important to note that these methods

will require more data availability to conduct. Table 2.5 summarizes the potential applicable quantitative risk assessments for the dam safety context.

Table 2.5 List of potential quantitative risk assessment methods, directly summarized and adapted from (Lacasse, 2022a).

Quantitative Method	Brief Description
ETA (event tree analysis)	Simplified method for a what if conditional analysis, following the sequence of events to an unwanted failure or event.
FTA (fault tree analysis)	Similar to the ETA method, however is arranged in a vertical arrangement, and focuses on the causes of an event, rather than the consequences.
Bayesian updating	Moderately advanced method for updating estimates with the use of new information.
FOSM (first-order second-moment)	Advanced method for calculating the effects associated with the uncertainty of a failure.
MC (Monte Carlo) simulations	Advanced method for analyzing outcomes via high repetition of analysis with random values.
BN (Bayesian network)	Advanced method represented in graphical form resembling ETA.
RSM (response surface method)	Very advanced method for calculating the probabilities using complex calculations with polynomial.
FORM/SORM (1st/2nd order reliability method)	Very advanced method for problems with an explicit formulation.
Stress testing	Most advanced method, for complete analysis for events with low probability and high consequences, reserved for extreme events.

For the purposes of this paper, the primary risk method selected for assessing the safety of dams regarding glacial mechanisms in Norway will be event tree analysis (ETA). This is due to the method best suiting the different sequences of events that can lead to the outcome of a dam failure, and remains the more simplistic model for revealing a higher-level understanding of the present risks. This process is later described in more detail within 3.4. An example of a visual aid for quantitative methodology is the risk diagram presented in Figure 2.15. This can help identify whether a risk is determined as either acceptable or unacceptable, based on its probability and the number of potential fatalities. This graphic is commonplace in the dam safety field.

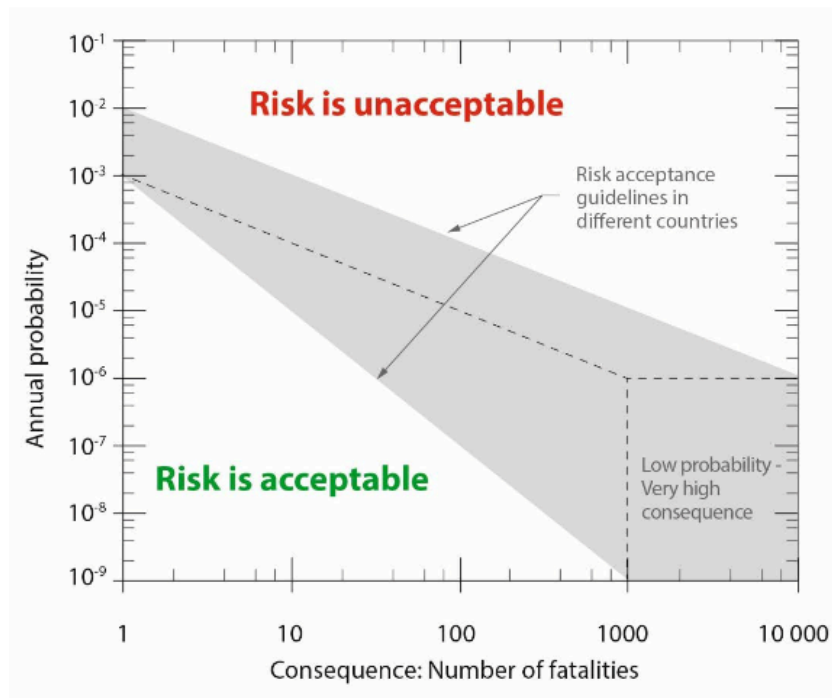


Figure 2.15 Quantitative risk diagram, from (Lacasse, 2022a). Also referred to as “failure envelope.”

2.4.3 Qualitative and semi-quantitative methods

Qualitative methods are more subjective in nature, and can allow the ranking of risks or judgements that aren't normally included in quantitative methods (Altenbach, 1995). They have their advantages, especially in situations where there is not a significant amount of data available for analysis. These are typically less difficult to conduct, and are better suited to low-risk applications, or as screening processes for further assessments with quantitative applications.

There are a large variety of different qualitative and semi-quantitative methods that are outlined in Table 2.6 (Lacasse, 2022a). These will not be applied in this context, however, they can be implemented into other cases relating to dam safety.

Table 2.6 List of potential qualitative and semi-quantitative risk assessment methods, directly summarized and adapted from (Lacasse, 2022a).

Qualitative and Semi-Quantitative Methods	Brief Description
Risk matrix	Simplified method for initial estimates. Can help determine if a more comprehensive assessment is needed.
LCI (life cycle analysis)	Simplified method specializing in showing potential threats, primarily gauged to financial/environmental analysis.
Bowtie analysis	Moderately advanced method for risk management and determining if more assessments are needed.
DSMM (dam safety maturity index)	Moderately advanced method for evaluating a company's risk management practices.
OM (observational method)	Simplified method for identifying potential worst-case scenarios.
Failure mode analysis, FEMA, FMECA and PFMA	Moderately advanced method for identifying all failure modes in all types of dams and safety conditions.

An example of an illustrative qualitative method visual aid could be that of Figure 2.16. This can take a relationship from the hazard category's probability and its relative consequence and develop a plot that indicates whether a risk is acceptable or not, and if measures are needed to either mitigate the risk or limit the exposure to it.

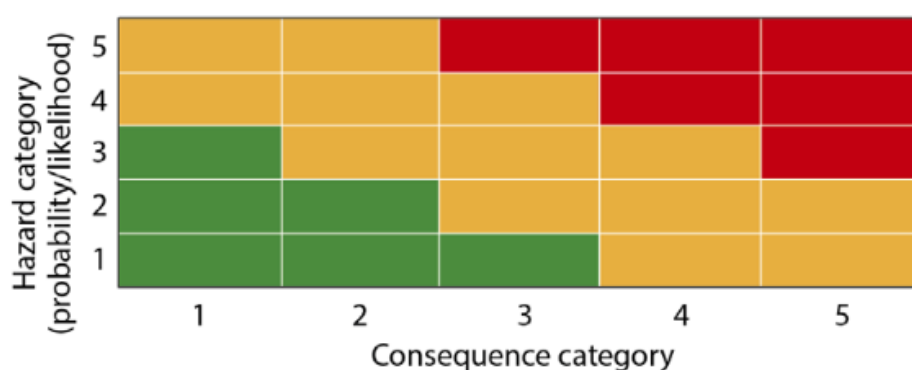


Figure 2.16 An example of a risk matrix that can plot qualitative assessments based on the probability of an event and its resulting consequence. Sourced from (Lacasse, 2022a).

3 Methodology

Within this chapter, the steps taken in determining the apparent risk in Norwegian dams are defined, through the formulation of event trees and application of various empirical methods. The origination of the three primary hazards and a description of how they are assessed are also discussed in detail. Figure 3.1 provides a condensed summary of these steps and the thought process behind their inception.

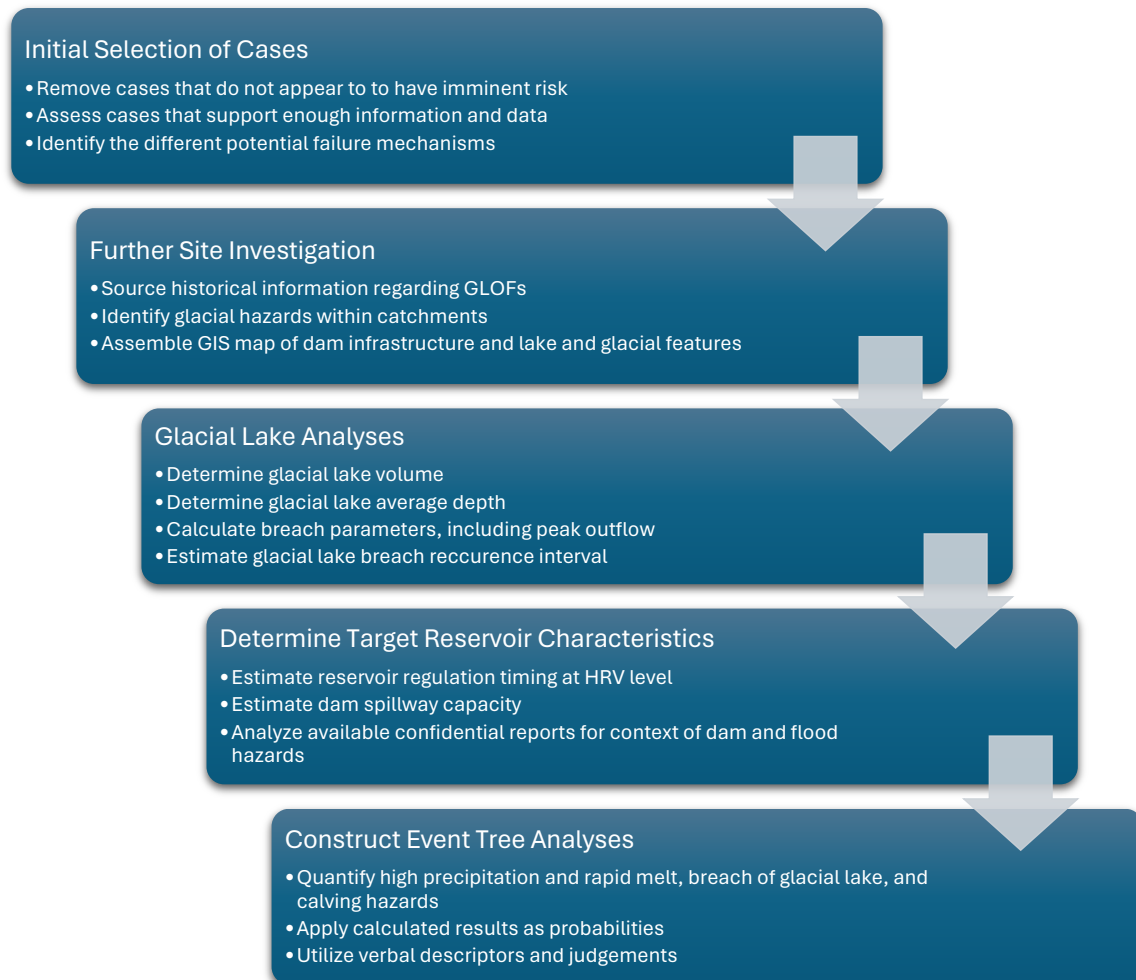


Figure 3.1 Overarching methodology applied to cases for analyzing GLOF hazards and risk.

3.1 Site selection

3.1.1 Initial selection criteria

The first step for the aim of this paper was to identify all provided at-risk lakes from Statkraft, in Table 1.1, and determine which should be selected as sites to further analyze using the event tree analysis method. This process was aided by several discussions with professionals in the dam and dam safety fields, as well as from glacial sciences.

An overarching criterion for these sites was the availability of data. With the lack of certain information, making assertions becomes incredibly challenging and in many cases infeasible, as the variables become too great and can compound into extremely misrepresentative conclusions. History of previously reported GLOF incidents, availability of reservoir regulation history, and status of glacier monitoring data from NVE were all very important data sources that were checked in this process. One particularly useful tool was NVE's Breatlas (NVE, n.d.-a). Breatlas is a database myriad of glacial data features that are presented within a GIS viewer (Figure 3.2), including details and locations of previous GLOFs, glacial monitoring data such as ice thickness, recession, and mass balance, as well as formed proglacial lakes, and more. This resource is unique, in that most nations do not compile and maintain a database regarding these types of data and require an individual to source it independently. Aside from Breatlas, further research was conducted to pinpoint if any other glacial lake mechanisms have been observed and/or recorded. Scholarly sources were very crucial for understanding some of the features of both the glaciers and the lakes, as many studies have already been conducted in the past in several of these locations by other researchers.

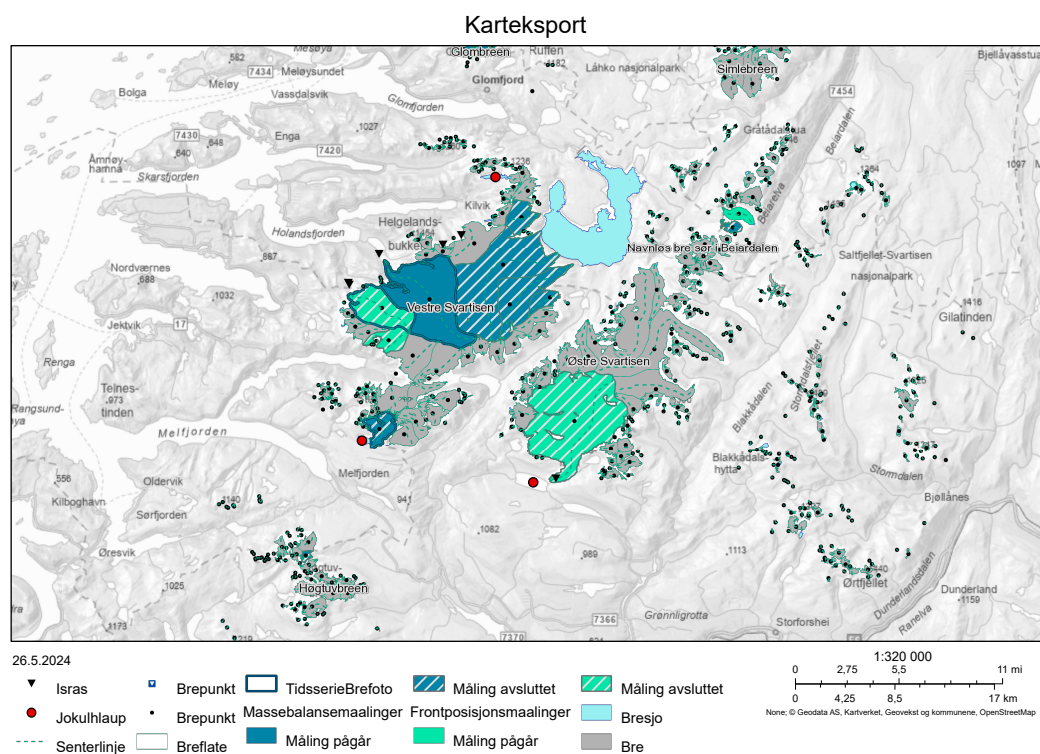


Figure 3.2 An example of the layers visible in Breatlas catalog within Temakart's GIS viewing system, at Svartisen (NVE, n.d.-b).

3.1.2 Visual observations and identifications

Following this process, it was then necessary to conduct a visual assessment of the sites themselves and understand what influence the glaciers could have upon the lakes in question. Special attention was placed on the size and locations of glacial lakes and glacial ice in respect to the reservoirs. This dismissed several cases, as discussed later, and helped narrow down further which sites would be most critical to further evaluate. In several of the initial

sites, there was simply a very small volume of fragmented glacial ice, or ice that was located at a far distance, and not of risk to the lake (even under rapid melt conditions). Another aspect was observing if there were any signs of previous mechanisms, such as recent rockfalls/landslides, or glacial lake drainage. These are usually visible in aerial photos, with evidence of striated soil and rocks, as in Figure 3.3.

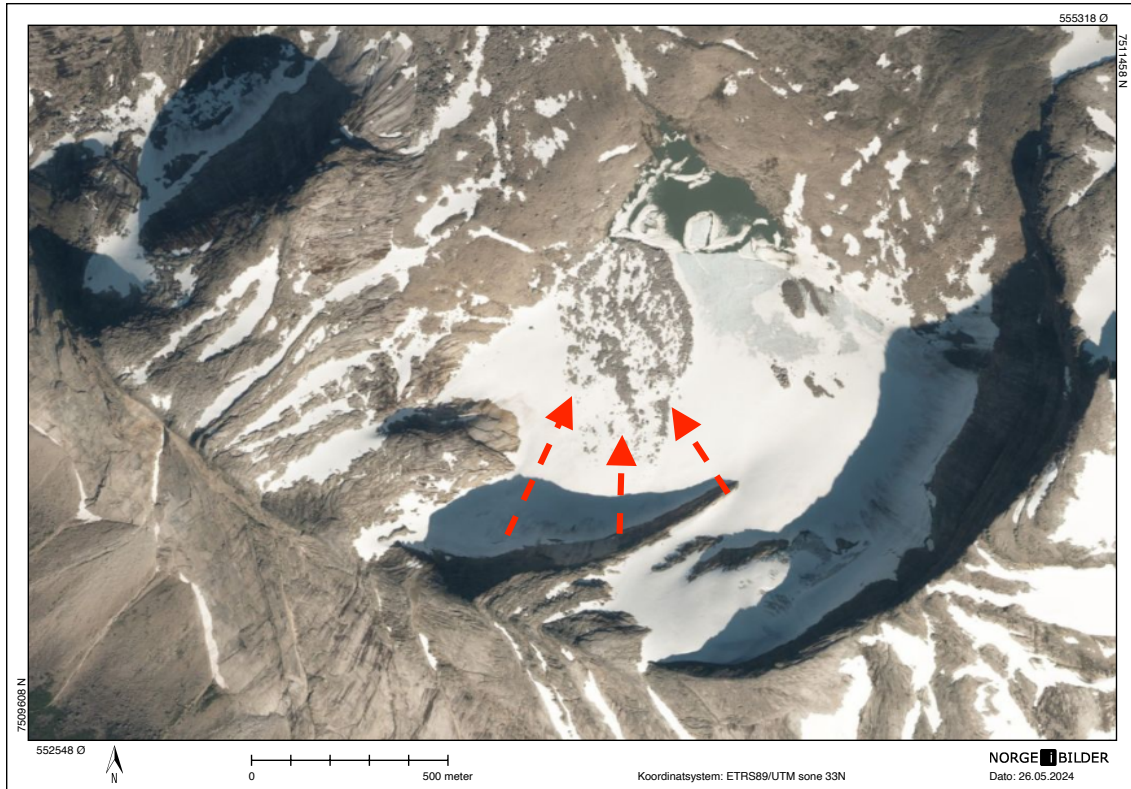


Figure 3.3 Rockslide within mountain cirque, indicating dynamic geology and potential initiator for lake failure near Slæddovagjavre. Photo sourced from NorgeiBilder.no (Norge digitalt, 2024).

Finally, as the last part of the screening process, it was important to check any present glacial lakes located within the lake's catchment, and to determine if they posed potential danger. Only ice-dammed or moraine-dammed lakes are of significant interest, as general erosion bedrock-lined lakes are quite stable and do not experience rapid drainage events typically. If the glacial lakes appear too small in footprint, they were considered as not a threat to the reservoirs and disregarded for further analysis. This is a significant generalization, as to ensure the lake volume is not substantial would require site measurements to develop bathymetric data (submerged topography). The methods used in estimating the glacial lake volumes, and the drawbacks associated with these are discussed later. The excluded sites in this paper are discussed in more detail with justifications in 4.8.

3.2 Other data

3.2.1 Catchments and contributing glaciers

To understand what glaciers were contributing to the lakes in this study, catchments were needed generated and overlaid into a GIS interface. A useful tool for this purpose is NVE's

NEVINA (Nedbørfllet-Vannføring-INdeks-Analyse) service (Geodata AS et al., n.d.). Through interpolation of topography and other registered features in regions (such as recognized rivers), an output of a catchment delineation can be made that identifies boundaries for which a target location receives its water. This is not a perfect system, and occasionally there can be errors that need manual correction. In detail-critical studies, it is recommended to take further investigations into the delineation of a catchment. For the purposes of this paper, the NEVINA tool was found to be very practical when observing such a number of cases. Once the catchments were generated, they could then be overlaid and viewed with the current registry of recognized and identified glacier bodies in Breatlas (NVE, n.d.-a) to identify which contribute to the lakes.

An important note is that the glaciers embedded within a catchment may not contribute meltwater to the lake. With subglacial drainage systems as sporadic as they are, outlets to these glaciers can sometimes deviate into other directions entirely. This is very difficult to identify via aerial photographs, so this simplification was made. Additionally, it is entirely possible (and likely) that glaciers outside these catchments also contribute to the target lake, so this should be considered. Just as the drainage systems can deviate water away from lakes, they may also deviate towards them. Catchment generations are limited to being based on surface topography found from DTM data, which do not incorporate subglacial topography. Fortunately, most larger glaciers in Norway do have identified internal flow lines indicating the flow in which meltwater is directed, as shown in Figure 3.4.

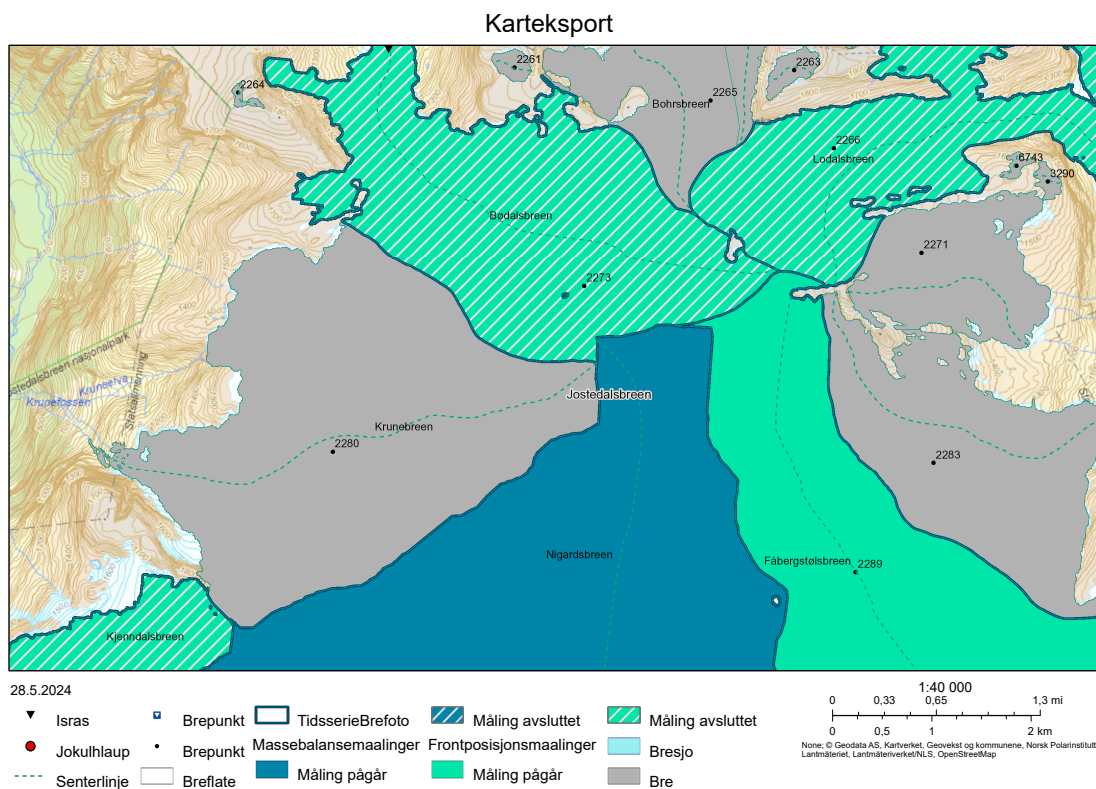


Figure 3.4 An export from Temakart with Breatlas layer activated, indicating interpolated flow lines beneath Jostredalsbreen glacier extending in all cardinal directions (NVE, n.d.-b).

3.2.2 GIS preparation

To best visualize all the applicable sites in this paper, QGIS (open-source GIS program) was utilized to compound all DTM raster files, dams, lakes, catchments, transfer tunnels, glaciers, and glacial lakes into a single locale. The DTM raster files were sourced from Høydedata.no (Kartverket, 2024) at a resolution of 1m and 10m, to provide more details of the terrain for visual aid. The other attributes were available as exported shapefiles from Temakart, utilizing both the Breatlas and Vannkraft (hydropower) layers (NVE, n.d.-b).

Having a conglomerate of this data presented in one map aids in the understanding of how the glaciers may contribute to the target lakes, and how the glacial lakes are embedded within the terrain or glaciers.

3.2.3 Internal reports

A critical reference to the information behind the history of the dams and lakes are the reports that were shared from Statkraft AS. These documents outline key information necessary to conducting the event tree analysis, such as calculated flood parameters, dam dimensions and layout, as well as any identified past issues. None of these data are available to the public domain and would make an external assessment as such significantly more inconclusive. The reports typically took the form of reassessments, a practice that is described previously in 2.3.

3.3 Glacial lake estimations

3.3.1 Lake volume estimation

To find the volume of these lakes to later assess for their outburst potential, a method was necessary to be utilized where the only input was the lake surface area, measured from aerial photos. This is the only definitive parameter that might be found in an initial screening study with the limitations on available data. Many scientists and researchers have been investigating this type of relationship for estimating lake volumes, as there is a vast array of available empirical formulas that have been developed. These relationships may be characteristic of certain mountain ranges from where they were derived, or from across the globe. Some of the more popular formulations are discussed and compared in the publication *Estimating the volume of Alpine glacial lakes* (Cook & Quincey, 2015). In this study, three well-known equations from (Huggel et al., 2002), (Evans, 1986), and (O'Connor et al., 2001), were applied and gauged for accuracy in a series of additional available lake studies that have had bathymetric studies conducted (an established volume).

Equation 3.1 Relationship developed by (O'Connor et al., 2001) derived from moraine-dammed lakes in the Central Oregon Cascade Range.

$$V = 3.114A + 0.0001685A^2$$

Equation 3.2 Relationship developed by (Huggel et al., 2002) derived from a variety of ice-dammed, moraine-dammed, and thermokarst lakes worldwide.

$$V = 0.104A^{1.42}$$

Equation 3.3 Relationship developed by the Canadian Inland Water Directorate, cited from (Evans, 1986). Exclusively based on relationships from ice-dammed lakes.

$$V = 0.035A^{1.5}$$

Of the three equations applied, it was found that both (Huggel et al., 2002) and (Evans, 1986) appear to estimate the lake volume to a reliable degree, whereas the relationship derived by (O'Connor et al., 2001) only managed to represent “unusually deep” glacial lakes correctly. As a result of this, Cook and Quincey redeveloped both the (Huggel et al., 2002) and (Evans, 1986) formulas to incorporate the additional lakes involved in the study (with many repeated from the original studies). Because Huggel’s formula was originally derived from both moraine and ice-dammed glacial lakes, Cook and Quincey’s evolution of this formula will be utilized for the glacial lakes in this paper.

Equation 3.4 introduces this evolved formula.

Equation 3.4 Relationship developed by (Cook & Quincey, 2015) as a result of 45 lakes of varying charactersitics. Includes 15 lakes originally involved in the studies of (Huggel et al., 2002).

$$V = 0.1697A^{1.3778}$$

This formula results in a relatively good degree of correlation r^2 value of 0.74. Here, V is measured in m^3 , and A is measured in m^2 . Taking in consideration the original study’s vastly different types of lakes (bedrock, ice, and moraine-dammed) and their locations spread across Tibet, Canada, Russia, Norway, and elsewhere, this is an acceptable margin of accuracy for purposes of application in this paper. The formula is also considered by (Zhang et al., 2024), amongst others, to have an applicable global implementation. One of the biggest challenges associated with developing an empirical relationship that can be applied to most glacial lake types is the vastly different basin proportions, as shown in Figure 3.5.






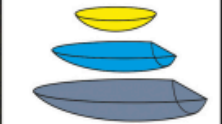
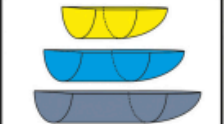


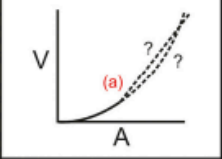
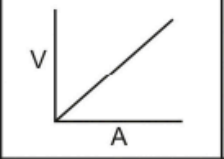
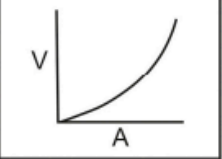
	Supraglacial ponds	Supraglacial lake	Moraine-dammed lake	Ice-dammed lake
a				
b	Belvedere Lake, Italian Alps	Ngozumpa Tsho, Nepal	Tasman Lake, New Zealand	Kyagar Glacier, Pakistan
c	Kääb et al., 2003	Thompson et al., 2012	Dykes et al., 2011	Haemmig et al., 2014
d	Expand mainly via marginal melt so tend to be shallow but large areal extent	Expand rapidly via calving once fetch > ~80 m. Multiple calving faces may exist	Expand mainly via calving at glacier terminus. Bottom melting may be minimal	Deep, long, and narrow in areas of high relief. Ice-cliff may dam downstream end
e				
f				
g	Area and volume increase approximately linearly	Relationship may become linear after onset of calving (a)	Area and volume increase approximately linearly	Areal increase is initially dominant but becomes less so as basin fills

Figure 3.5 Sourced from (Cook & Quincey, 2015). "A conceptual consideration of glacial lake evolution and its impact on volume-area relationships."

After applying Equation 3.4 to the identified glacial lakes, the only additional parameter needed to estimate breach characteristics was the estimated lake depth, discussed in 3.3.2.

3.3.2 Lake depth estimation

To determine the maximum breach outflow, the final parameter required was the breach depth. In a worst-case scenario, a piping or overtopping-induced breach will essentially drain an entire lake's volume. With this established, the final breach depth can be considered interchangeable with the lake's estimated average depth altogether. Just as with the hurdle to calculating the lake volume, the lake depth would also require bathymetric data to reliably pinpoint actual values.

With the volume of the lakes already estimated, and surface area known, one method could entail deriving the average depth from these two values, as was implemented in *Sino-Nepalese Investigation of Glacier Lake Outburst Floods in the Himalayas* (Zhongguo ke xue yuan. Lanzhou bing chuan dong tu yan jiu suo et al., 1988). This would in effect preserve the initial volumetric estimation made without compounding additional potential errors into a breach analysis by using different empirical formulations for the lake's depth. Huggel's average depth estimation does just this, as evident in Equation 3.5.

Equation 3.5 Relationship developed by (Huggel et al., 2002) to determine a lake's mean depth from the measured surface area.

$$D = 0.104A^{0.42}$$

In order to best represent the lake’s estimated depth, and to follow the same derivation as the lake volume estimate, the readapted formula from (Cook & Quincey, 2015) is used for the cases in this paper (Equation 3.6), where D is represented in m, and A is input as m^2 .

Equation 3.6 Formula derived by (Cook & Quincey, 2015) to determine a lake's average depth from its surface area.

$$D = 0.1697A^{0.3778}$$

This was found to have a r^2 value of 0.57 in Cook and Quincey’s study, which is a relatively low correlation, but a significant improvement over the previous r^2 of 0.38 in Huggel’s initial study (Cook & Quincey, 2015). To validate the calculated estimated average depths for the glacial lakes in this study, they were compared directly to the findings from a large collection of glacial lakes in a study within the Hindu Kush Himalayan Region Bhutan (Mool et al., n.d.). In Mool’s study, the following average depths were estimated based on the types of lakes identified in Table 3.1.

Table 3.1 Average lake depths derived from the study conducted by (Mool et al., n.d.).

Lake Type	Average Depth (m)
Cirque lake	10
Moraine lake	30
Trough valley lake	25
Blocking lake and glacier erosion lake	40
Lateral moraine lakes	20

3.3.3 Breach outflow rate estimation

Ideally, with cases that have documented outbursts, the historical flow data from a nearby gauging station would be the most useful resource in determining the peak inflow a lake experiences from a nearby glacial lake outburst. As some cases in this paper are not as fortunate, a method is needed to calculate the potential maximum breach outflow. This value will help assess whether the flow can theoretically overwhelm the spillway structure or flood protection that is preventing overtopping.

Dam breach estimations vary widely in accuracy and methodology. These range from “simple parametric equations to complex multi-dimensional erosion models” (Morris et al., 2018). For the purposes here, simple parametric models will be applied to determine the breach characteristics exhibited by both ice-dammed and moraine-dammed glacial lakes. These models are suitable for higher-level investigative studies and require only the input of simple estimated lake and dam parameters. They are also quick to apply, but may introduce some significant estimation errors (Morris et al., 2018). Moraine-dammed and ice-dammed lakes drain very differently, invalidating the approach of applying the same formulation to each. The mechanisms behind these drainages are discussed in the prior chapter. For the

purposes of quantifying the potential outflow rate, two different methods are applied to each case.

For ice-dammed lakes, the method discussed by (Desloges et al., 1989) is utilized, which is an evolution of the empirical formulation created by (Ferguson, 1986). Ferguson originally quantified the trend initially observed by (J. J. Clague & Mathews, 1973) who found that the lake volume drainage is an explanatory variable, seen in Figure 3.6 and Equation 3.7.

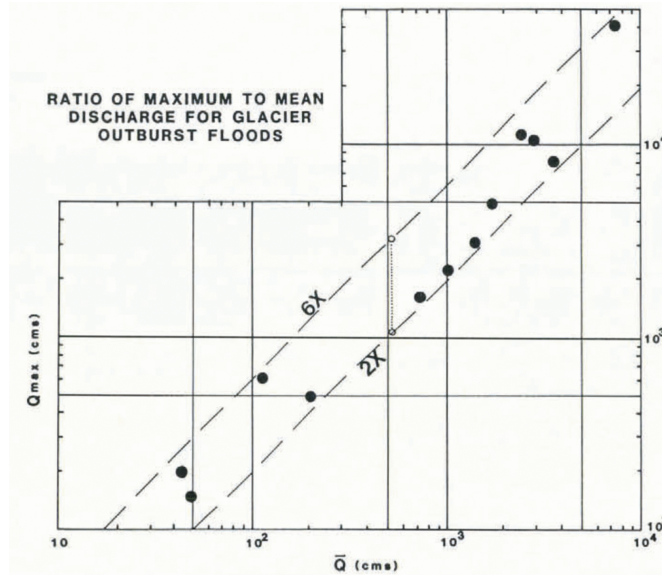


Figure 3.6 Average discharge (\bar{Q}) plotted against instantaneous discharges (Q_{max}) from glacial outburst floods in North America, Iceland, and Scandinavia. Figure from (Desloges et al., 1989).

Equation 3.7 Original formulation from (Ferguson, 1986) to quantify the maximum breach flow from an ice-dammed glacial lake, based on numerous outburst studies.

$$Q_{max} = 113V^{0.64}$$

Because the log-log formulation was derived from least-squares analysis and reflects the geometric mean instead of the arithmetic mean, it could underestimate the peak discharge in some cases by up to 38% (Desloges et al., 1989). Once this was applied with a correction factor and readjusted to remove bias, it led to Equation 3.8, which is the chosen formulation for identified ice-dammed lakes in this paper. V is measured in $1 \times 10^6 \text{ m}^3$ and Q_{max} reflects m^3/s .

Equation 3.8 Revised formulation by (Desloges et al., 1989) to estimate maximum breach outflow from a glacial lake.

$$Q_{max} = 179V^{0.64}$$

Although this results in a discrete value, Desloges notes that the cases in the study in North America, Iceland, and Scandinavia can vary between 2 and 6 times the mean discharge of the glacial lake. This in effect generates a very significant range of potential outflow peaks for the glacial lakes and should be considered. For the purposes of this paper, only the values generated from Equation 3.8 are utilized in the event tree analyses, to prevent introducing

too many combinations and uncertainties. As ice-dam lakes can drain in vastly different periods of time, ranging from hours to weeks, an average flow assumption cannot be made.

To estimate the maximum outflow for a moraine-dam breach, the popular formulas developed by (Froehlich, 2016) from a series of regressive analyses are implemented (Equation 3.9). These equations are an evolution of a series of previous formulas developed by Froehlich in 1995 and 2008, with the continuous addition of new data. Alternatively, one can use the parametric formula developed by (Capart, 2013) that is also popular in these types of studies, but requires many more parameters that could be misestimated.

Equation 3.9 Relationship derived by (Froehlich, 2016) to determine a (moraine) lake's estimated peak outflow from breach characteristics.

$$Q_p = 0.0175k_0k_h \sqrt{\frac{gv_w h_w h_b^2}{\bar{w}}}$$

Where,

$$k_0 = 1.85 \text{ (overtopping failure)}$$

or

$$k_0 = 1.0 \text{ (piping failure)}$$

And,

$$k_h = 1 \text{ (if } h_b < 6.1)$$

or

$$k_h = \left(\frac{h_b}{6.1}\right)^{1/8} \text{ (if } h_b > 6.1)$$

Froehlich's formula results in a peak outflow Q_p (m^3/s) that can be then used to compare with the spillway or floodway capacity for each of the cases. In this formula, g is representative of the acceleration of gravity (9.81 m/s^2), v_w is the reservoir's volume at the time of failure (m^3), h_w is the height of water above breach bottom (m), and \bar{w} is the average embankment width (m). In this assessment, to once again consider the worst-case scenario (full drainage condition), v_w is assumed to be the full estimated lake volume, and h_w is equal to the calculated average lake depth from Equation 3.6. Realistically, a breach does not always extend to the base of a lake, but without other information, this assumption has to be made. To find the average embankment width, a measuring tool is applied to aerial photos of the likely breach location of the glacial lakes (usually where streams are emerging from the embankment) between the lake surface and the extent of the apparent moraine. There is the possibility of introducing many errors with this approach, as the embankment can vary widely, and are sometimes difficult to distinguish from aerial photos alone. To complete a more confident assessment, it is recommended to perform field measurements of these attributes.

The resulting peak outflows indicate wide variation between overtopping and piping failures. This is indicative of the more sudden nature attributable to overtopping failures.

It should be noted that these processes are heavily inferred and can introduce many errors that can compound. As with any critical assessment, it is highly recommended to complete more in-depth studies into the individual sites, and to perform comprehensive field data-collection. These combined methods are only used as a screening tool to identify significant potential from lake drainages.

3.4 Event tree analysis

3.4.1 Selection of three main hazards

Among the numerous glacial hazard mechanisms outlined in Table 2.1, a focus was needed on a several few that posed high consequence and were quantifiable in an event tree analysis. Early on, it was decided to primarily focus on the high precipitation and rapid melt (H1), breach of glacial lake (H2), and calving or icefall (H3) hazards for further study. These hazards are largely identifiable in aerial photo inspections and can be applicable across Norway. In other cases, the data collection needed to evaluate hazards do not fit the scope of this paper and require extensive further analysis. This could include the earthquake, rockfall, and avalanche mechanisms that demand significant field investigations or specialty expertise to diagnose.

For the breach of glacial lake hazard, the scope is limited to identifiable glacial lakes in the vicinity of the glacial system and respective reservoirs. This excludes the lakes that are not possible to identify from this level of study, such as englacial lakes or subglacial lakes that are not visible, nor documented. To fully assess any embedded or underlying lakes within glaciers, physical site assessments are needed to ensure they are properly identified and analyzed for risk.

3.4.2 High precipitation and melt hazard (H1)

One of the most destructive and sensitive hazards are rapid snow and ice melt within catchments. In some cases, a minute change in temperature can activate large melting mechanisms and result in a large flood, as a result of significant alteration in the energy balance (Sicart et al., 2008). This is particularly applicable for temperate glaciers, such as most of the glaciers existing in continental Norway (USGS, n.d.-b). Additionally, the continuous onset of climate change has been linked to increasing GLOF events, both in quantity and magnitude (Harrison et al., 2018). In this context, this will be quantitatively expressed with existing professional flood assessments. These are typically found in the form of return period floods, or PMFs, as discussed in 2.3.5. As these are intensive to calculate, and depend often on climatic conditions and topographic layout, it was chosen to use the latest available flood estimates enclosed within reassessment reports for the dams. These estimations include the rapid snow and glacial melt in the flood peak flow rate based on expected climatic conditions presently, and in the future. The practice to include the snow and ice melt condition is a relatively new guideline for Norwegian flood estimations. This change was made in the 2011 rendition of the NVE *Retningslinjer for flomberegninger (Guidelines for flood calculations)* (Midttømme & Pettersson, 2011), where the authors note

the “topic that has been added since the previous edition of these guidelines is a new section on the calculation of snowmelt.” The current version *Veileder for flomberegninger (Guide for flood calculations)* (Glad et al., 2022) was released in 2022, entails further information for incorporating the snow melt regime into rainfall-runoff models.

To determine the potential outcome for a failure in a dam from this hazard, the format in Figure 3.7 was developed following discussions with dam and glacial experts, and followed for all applicable cases in concrete and embankment dams.

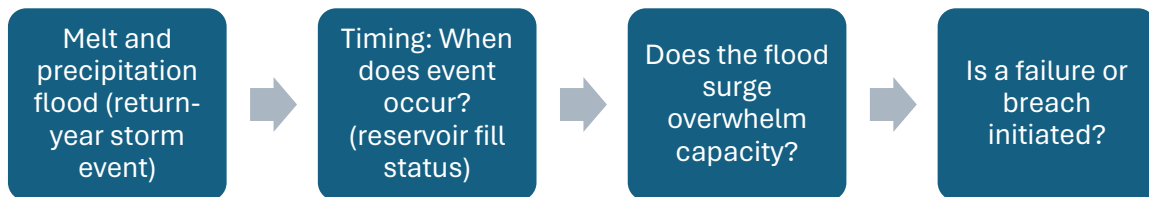


Figure 3.7 Flow chart depicting the overall process behind determining a melt-flood failure in a concrete or embankment dam.

This process was implemented into the event trees to develop a probability of failure for each case. It was critical not to introduce too many steps, as not only does it lead to more uncertain calls of judgement but can also artificially reduce the overall probability of a failure occurring.

The timing step was necessary to determine whether the lake was in a vulnerable position to be breached. In most cases, if the lake is not at or within a close margin of the HRV, it is expected that it will most likely be able to endure the flood through buffering from available capacity. This step is also founded on the fact that when professional computations for floods for dams are carried out, they also assume the worst condition where the dam is at HRV level (Haugsrud et al., 2022). The probability estimation for reservoir regulation will be discussed later in 3.4.5.

3.4.3 Failure from breach of glacial lake (H2)

To form the basis on the probability of dam failure from an associated glacial lake breach required the implementation of recurrence interval statistics. The method used in estimating these recurrence intervals are discussed later in 3.4.7. This generates an initial probability to later progress to further steps in the event tree analysis shown in Figure 3.8.

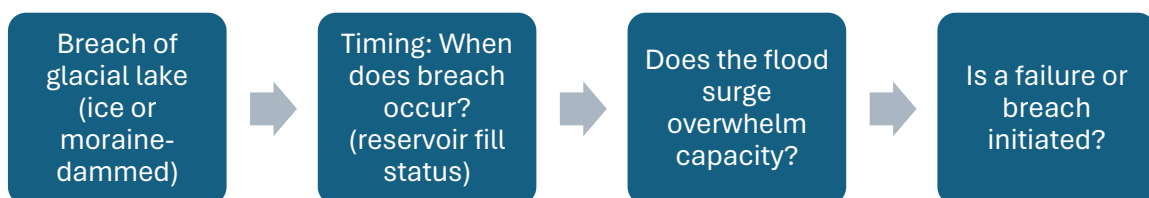


Figure 3.8 Flow chart depicting the overall process behind determining a moraine or ice-dammed glacial lake breach induced failure in a concrete or embankment dam.

A significant compromise taken in this method is the lack of a routing model, where flow is dampened by topography and surface material as it travels downstream. These event trees utilize the breach estimations discussed in 3.3.3, which only predict the peak outflow at the breach location itself, not what is entering the affected reservoir. This can lead to the inference that the actual peak flow will likely be significantly less, depending on the environment and breach route. In more comprehensive (and time-consuming) analyses, it is recommended to perform these breach simulations and routing in either combined or separate processes in multi-dimensional erosional models and flow transport models. Popular semi-physical models could include that of USACE’s HEC-RAS, and more advanced physically based models might be modelled in EMBREA, DL Breach and WinDAM (Morris et al., 2018). These can introduce temporal variables for breach flow (generating hydrographs for better breach characterization), and more accurately replicate the natural flow of floodwater through complex terrain.

Lastly, the final assumption made in this series is the full drainage of the glacial lake, and full delivery to the affected reservoir. It is entirely plausible that in some cases, a flood flow may disperse into different directions altogether or only partially into the reservoir. Realistically, additional iterations of event trees could be generated for lower or partial breaches, but in this context only the worst case is assumed to provide a high-level assessment for potential risk.

This hazard assessment does not introduce the possibility of failure generated from a seiche wave that can be initiated by the sudden failure of a glacial lake and directed at a dam. Because this requires a significantly more in-depth analysis of the actual flood propagation and fluid mechanics, it is not included in this assessment, but should still be observed as a potential failure mechanism in these cases.

3.4.4 Failure from calving or icefall (H3)

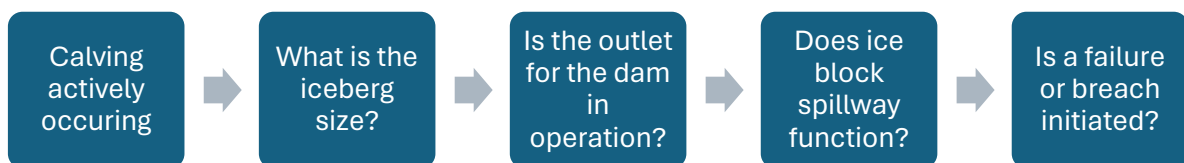


Figure 3.9 Flow chart depicting the overall process behind determining a calving event-based failure in a concrete or embankment dam.

The determination of calving and ice fall as a mechanism incurring failure is largely a subjective matter, as evident in Figure 3.9. Calving is an ongoing process identified only at Tunsbergdalsbreen, but there is no data to support measurements in the size of the exuded icebergs in the lake. This leaves the potential for failure to be inferred from features of the dams, such as ice breakers at inlet structures, or reinforced protection at spillways. One method for quantifying this was taking the measurements of iceberg diameters visible in the lakes from multiple years in aerial photos. These then can be compared to the structure of the spillway and outlet, to identify if any vulnerabilities are apparent. Most dams in Norway are very well protected from ice blockage, as the dams are built to a standard that expects significant ice load from the winter seasons (Sigtryggsdóttir, 2022).

It was then considered that the icebergs do not pose significant risk when lying stagnant away from the spillway structure. This is why the step for reservoir outlet operation was included in the event tree analysis. When the outlet is in operation, a draft is created in the reservoir that initiates a current for the water to travel to the outlet, which can attract floating ice, reducing the likelihood for clogging at the spillway. In 2019, hydropower contribution totalled 93.4% (Holstad, 2020) in Norwegian electricity, so this is incorporated into the node as an inferred operative time.

A significant mechanism not included in this hazard analysis is the potential for the generation of a seiche wave and impact to the dam, just as with the H1 hazard. This type of assessment would require knowledge or statistical probability on the size of the iceberg to calve, and remains too unpredictable to include in this context.

3.4.5 Estimate of reservoir regulation

Determining the reservoir level state is a critical prerequisite for the potential of breaching of a dam, as discussed in 3.4.2. To generate a probability, the decision was made to use available data from NVE's Sildre hydrological resource (NVE, 2024). This resource gives access to numerous hydrological stations across Norway, with historical data pertaining to flow rate (in streams and waterways), as well as volume and stage status in lakes, as seen in Figure 3.10. Fortunately, for this study, most of the cases had an active gauging station with plentiful data, with the exception of Norddalen. In the case of Norddalen, the reservoir fill status was estimated to be "at or around" HRV level for approximately 90% of the time by dam operators at the site.

Firstly, the data was extracted in the form of daily measured reservoir stage values. An arbitrary range of 30 cm below the registered HRV for each dam was selected as a threshold for when the reservoirs can be considered at "max capacity" (HRV). The days without data (either unreported or malfunction with the gauge) were excluded, and the remaining days were filtered under this condition. Sildre appears to make available 20 years of historical data, so most of the stations dated back to 1994, resulting in over 10,000 days of data. The days that met the criteria of 30 cm or closer to HRV were then formulated into a frequency from the total number of daily measurements.

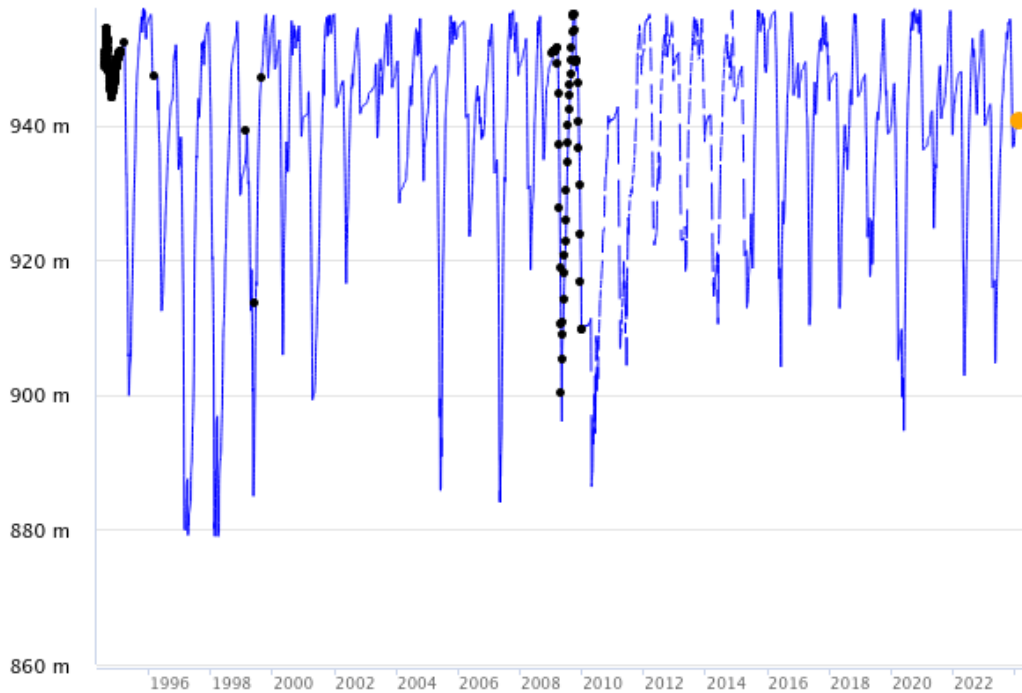


Figure 3.10 An example of available stage history from Sildre for Dravladalsvatn from 1994 until present. An operative strategy is evident from the similar cyclical formations in the data. Sourced from (NVE, 2024).

A simplification made in this process is utilizing daily averaged stage data. In most cases, this data is available in hourly or semi-hourly increments, but it was decided unnecessary to include in such an extensive time span and would result in insignificant differences in the calculated frequency.

Additionally, a significant simplification was not considering the operation scheme with the reservoirs and considering the seasonal melt and rain periods. The most likely period in which the rapid melt and precipitation hazard (H1) occurs is in the spring floods, when snowmelt is generally at its peak in Norway (Krøgli et al., 2018). This is variable for the different sites and would need to be pinpointed individually through analysis of more climatic data. Typically, reservoir operators account for anticipated yearly melt floods, and maintain the lake at a lower level in these periods. Therefore, this probability is likely lower than what is represented in the frequency analysis for this assessment. In the H2 hazard, this frequency is more adept at representing the actual reservoir fill status indication, as these hazards can occur throughout the year.

3.4.6 Estimate of spillway capacity

When assessing in event trees, an important characteristic from the dam is the discrete spillway capacity. This would give good indication as to whether the dam is overwhelmed by a certain flood size, such as those created by H1 or H2. In the provided reports, spillway capacity isn't normally expressed, therefore simplified calculations were necessary based on some of the physical parameters of the spillway structures. The highly popular method developed by Henri Bazin from 1898 for weirs was selected for this purpose. In the two

variations of Bazin’s formula, only the rectangular spillway application is applied, as there are no dams in this study that utilize a triangular spillway structure.

Equation 3.10 Bazin's 1898 weir flow rate formula for a rectangular spillway.

$$Q = m_0 * b * h * (2gh)^{0.5}$$

Where,

$$m_0 = \left(0.405 + \frac{0.0027}{h} - 0.03 * \frac{B - b}{B} \right) * \left(1 + 0.55 * \left(\frac{b^2}{B^2} \right) * \left(\frac{h}{H + P} \right) \right)$$

In the case of this formulation, the variables are representative of both the physical characteristics of both the flow, and the weir. The output, Q , results in the peak estimated outflow in m^3/s . All other measurements are in m. Figure 3.11 indicates these input parameters for Equation 3.10.

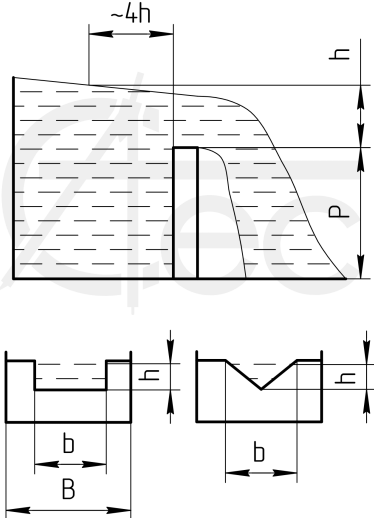


Figure 3.11 Graphic sourced from (Caetech Llc & Calcdevice.com, n.d.) outlining the parameters for Bazin’s 1898 weir flow formula.

As with all other approximations, this is subject to accuracy based on the assumed parameters. For the fluid height, h , the distance between the HRV (where the spillway thresholds are typically set) and the dam’s registered crest elevation is used. There are some cases where the spillway is arranged differently than this and are individually discussed. P , or the weir’s height, is typically outlined within reports, however in situations where they are not explicitly noted, are assumed as the distance between the elevations of HRV and LRV for the dam.

These approximations can lead to significantly skewed accuracies, due to the amount of inferring involved, however this is only purposed for a very high-level understanding of the capacities. The floods are still compared with the hydrologists’ flood assessments for the expected lake level rise in the outlined return floods, which will commonly be expressed as x -meters above or below HRV. This provides additional reassurance for the reasonings made within the event tree analyses.

3.4.7 Estimating the probability of a glacial lake breach

For the initiating event in the H2 hazard (the actual breaching of the lake), it is incredibly challenging to introduce a prediction on when, or even if, a dam is expected to breach. There are immense variables that can intertwine and lead to a breach, including virtually any of the mechanisms discussed in 2.2.

In several cases, such as those with Austre Okstindbreen and Tunsbergdalsbreen, recorded previous GLOF events can be used to develop a statistical recurrence interval which then can be implemented into an event tree analysis. In some other cases, global statistics are utilized to assess the possibility of a dam breach. In a sense, this evaluates GLOFs in the same realm as earthquakes or return floods, as they are typically described in the context of recurrence intervals. This approach has significant limitations, as it relies solely on statistics and categorization as either a moraine or ice-dammed lake, and does not consider the physical characteristics, such as instability of the moraine. In fact, it may be the most unpredictable factor in the event tree analyses. To better determine the instability of an identified glacial lake, more information is needed from field-level assessments, detailing the condition of the lake and the surrounding geophysical features. To find the recurrence variable for any of these applications, the approach was followed from Equation 3.11.

Equation 3.11 Basic formulation to determine a GLOF breach probability.

$$\text{Recurrence Probability} = \frac{\text{Number of GLOF breach events at singular location}}{(\text{Present year (2024)} - \text{First reported year})}$$

For the majority of cases that do not have specific GLOF history, the dataset from (Lützow & Veh, 2023) was extracted and adjusted to reveal individual global/Scandinavian datasets for only moraine and ice-dammed lake drainage events. The requirement was for these events to have a reported year associated with them. With this organized, the final step was to isolate each of the unique GLOF sites and determine the number of events that had occurred at each of these unique locations. These could now be analyzed for recurrence intervals individually, and later averaged together. It was decided with such an immense range of recurrence values, that the median of the dataset was to be used, in order to avoid bias from outliers in the results. The following recurrence probabilities were then determined in Table 3.2.

Table 3.2 Recurrence probability statistics derived from the dataset created by (Lützow & Veh, 2023). Large discrepancies seen from the global and scandinavian contexts.

Location	Dam Type	No. Unique Locations	Average Recurrence Probability	Median Recurrence Probability
Global (incl. Scandinavia)	Moraine-dammed	168	5%	3%
	Ice-dammed	190	16%	6%
Scandinavia	Moraine-dammed	1	3%	3%
	Ice-dammed	30	19%	12%

One can observe that for the Scandinavian region, only one moraine-dam lake is registered in this database, however, it is supported by the global median of 3% probability. Therefore, this is applied to all the moraine-dam failure event trees. Contrarily, in the case of the ice-dammed lakes identified, the Scandinavian median probability was twice what was found for global cases. Because the data available for the Scandinavian cases most likely better represents the climatic and topographic conditions, the median of 12% is used in ice-dam failure event trees for cases that do not have documented GLOF history. The number of individual cases (30) are leaning slightly towards the lower end, but would likely be enough to base this upon.

A simplification made in obtaining all the recurrence variables was that the first year of a GLOF recording was treated as the first event to occur whatsoever. This isn't completely realistic, as GLOFs occur without detection commonly, and far beyond record-keeping capabilities. Additionally, this treats all events in the database as complete dam failures, for which these event trees are assessing. Much of the data from (Lützow & Veh, 2023) are events that do not result in complete drainages or failures. This is all to be kept in consideration when observing the potential probability of a moraine or ice-dam failure in this paper.

3.4.8 Generation and finalization of event trees

The process for determining the probabilities for the event trees is largely a reiterative process, that requires judgements to be made through the usage of probabilities originating from statistical data, calculations, or verbal descriptors. The event trees applied here rely often on the proper usage of verbal descriptors, shown in Table 3.3. These are applied subjectively and are normally assigned by someone who has experience in the related area.

Table 3.3 Verbal descriptors that can be applied in an event tree analysis. Reformatted from (Lacasse, 2022a).

Probability	Verbal Description
0.001 (~0.0-0.005)	Virtually impossible, <i>known physical conditions or process that can be described and specified with almost complete confidence</i>
0.01 (0.005-0.02)	Very unlikely, <i>although the possibility cannot be ruled out on the basis of physical or other reasons</i>
0.10 (0.02-0.33)	Unlikely, <i>but it could happen</i>
0.50 (0.33-0.66)	As likely as not, <i>with no reason to believe that one possibility is more or less likely than the other</i>
0.90 (0.66-0.98)	Likely, <i>but it may not happen</i>
0.99 (0.98-0.995)	Very likely, <i>but not completely certain</i>
0.999 (0.995~1.0)	Virtually certain, <i>known physical conditions or process that can be described and specified with almost complete confidence</i>

Once applying the verbal descriptor, the rationale is expressed as a note within the tree. Verbal descriptors can have a significant influence on the final probability outcome, so it is key to include multiple participants with knowledge in the subject to properly assess the viability of a probability. In most settings, these discussions will take place in an “event tree workshop” where the participants can adjust or reformat branches of a tree, as it is intended to be a cooperative process.

After deducing all the probabilities for each branch in the event tree, a final probability for failure is calculating by summing the compounded probabilities for each branch that leads to the final target failure (branches that lead directly to a STOP condition are not included in the calculation). This overall process is shown in Figure 3.12.

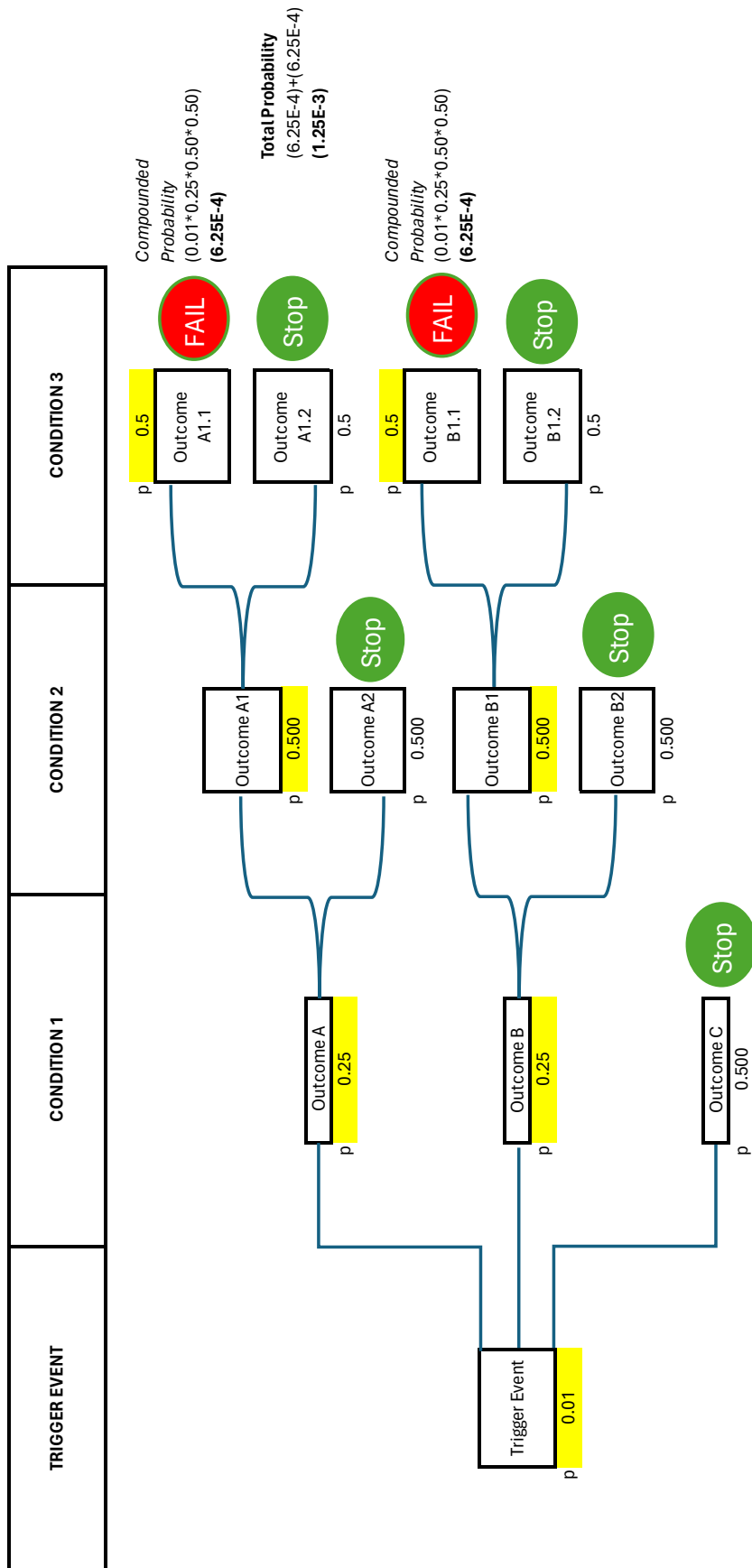


Figure 3.12 Example format for determining failure probability in an event tree analysis.

In Table 3.4, the complete list of overall assessments determined for and applied to each case are outlines. This list will be repeated individually for each location in Chapter 4.

Table 3.4 Applicable hazards determined for selected dam sites in Norway.

Overall Application of Primary Risks			
Dam	H1 (rapid melt and precip.)	H2 (breach of glacial lake)	H3 (icefall or calving)
Gressvatn	Applicable	Documented hazard	Low concern
Styggevatn	Applicable	Low concern	Applicable
Tunsbergdalsvatn	Applicable	Documented hazard	Low concern
Dravladalsvatn	Applicable	Minor hazard, low concern	Low concern
Juklavatn	Applicable	Low concern	Minor hazard, low concern
Mysevatn	Applicable	Low concern	Low concern
Svartadalsvatn	Applicable	Low concern	Low concern
Slæddovagjavre	Applicable	Applicable	Low concern
Norddalen	Applicable	Applicable	Low concern
Rembesdalsvatn	Applicable	Documented hazard	Low concern
Sysenvatn	Applicable	Low concern	Low concern
Storglomvatn (Holmvatn and Storglomvatn dams)	Applicable	Documented hazard	Minor hazard, low concern

3.4.9 Plotting of risk envelope plots

The final step in presenting the determined failure probabilities were to plot into the failure envelope diagram discussed earlier and shown in Figure 2.15. This required the knowledge of the number of potential fatalities as a result of a significant dam breach. To do so, several assumptions were made, in lieu of the traditional method of surveying each inundation extent and finding the registered populations. This latter is far more intensive regarding analysis and data collection.

In these simplifications, the dam consequence classifications discussed in Table 2.2 are applied to the number of average residents per household in Norway. This figure was found to be 2.11 people per household in 2023 (SSB, 2023). There is a significant limitation with the classification system in that it does not pinpoint exactly how many houses are located

within an inundation zone, but for the purposes of this paper, they are estimated on the high end (i.e. class 3 dams are estimated to have 316.5 fatalities from 150 households). In the case of consequence class 4, there is no range, so the simplification of 300 households (633 people) are made. In reality, this can vary widely, and would benefit greatly from detailed population surveys.

4 Case Studies

To divulge into the details within each selected dam and their respective glacial system, the case studies are presented in this chapter. Here, the basic layout of the dams and their hydropower systems will be discussed, as well as the properties found in the glaciers upstream. At the end of this text, excluded sites originally proposed will also be briefly described.

4.1 Austre Okstindbreen

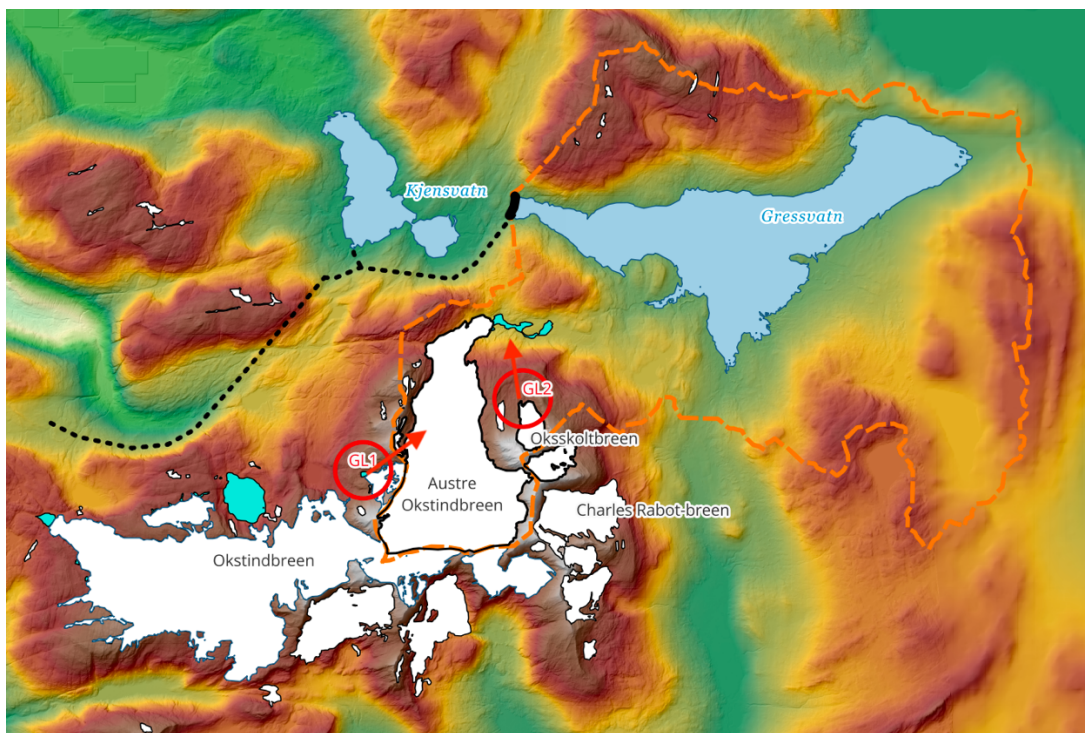


Figure 4.1 Overview of Austre Okstindbreen glacier, Gressvatn dam, and GL1 and GL2 hazards. DTM data from Høydedata.no (Kartverket, 2024).

Austre Okstindbreen is a valley glacier situated within Okstindbreen in the Hemnes municipality, Nordland. Seen in Figure 4.1, it is sandwiched between the Oksskolten and Okstinden peaks and terminates to the north into a small proglacial lake *Bretjøna*. In 2014, Austre Okstindbreen was estimated to span approximately 13.1 km², however this figure should be expected to be significantly less in present day. In a 2022 report by NVE, the glacier's front was reported to have receded approximately 35 meters that year and 320 meters in the 10 years prior, making it one of the fastest shrinking glaciers in Norway (*Breane fortset å smelte tilbake i 2022 - NVE, 2022*), although the mass balance between 1987-1996 in Figure 4.2 surprisingly indicates a positive trend. Oksskoltbreen, on the other hand, is a very small 0.63 km² cirque glacier, situated adjacent to the Oksskolten peak. It contributes a small amount of meltwater into *Bretjøna*, but will not be of particular interest, aside from a small glacial lake identified within that is discussed in 4.1.2.

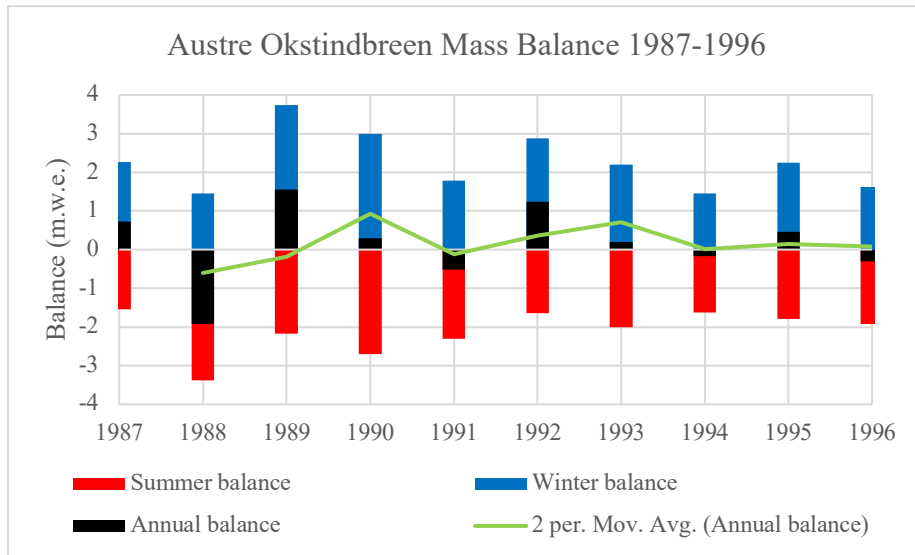


Figure 4.2 Mass balance for Austre Okstindbreen, 1987-1996, data provided by NVE.

Okstindbreen ice cap (approximately 46 km² in coverage), the parent glacier of Austre Okstindbreen and Oksskoltbreen, is comprised of 19 individual glaciers (Bakke et al., 2010). For the purposes here, only Austre Okstindbreen will be of focus, as the others are either too small to have a significant influence on the water bodies of interest (Gressvatn and Kjennsvatn), or do not drain to them at all.

4.1.1 Gressvatn

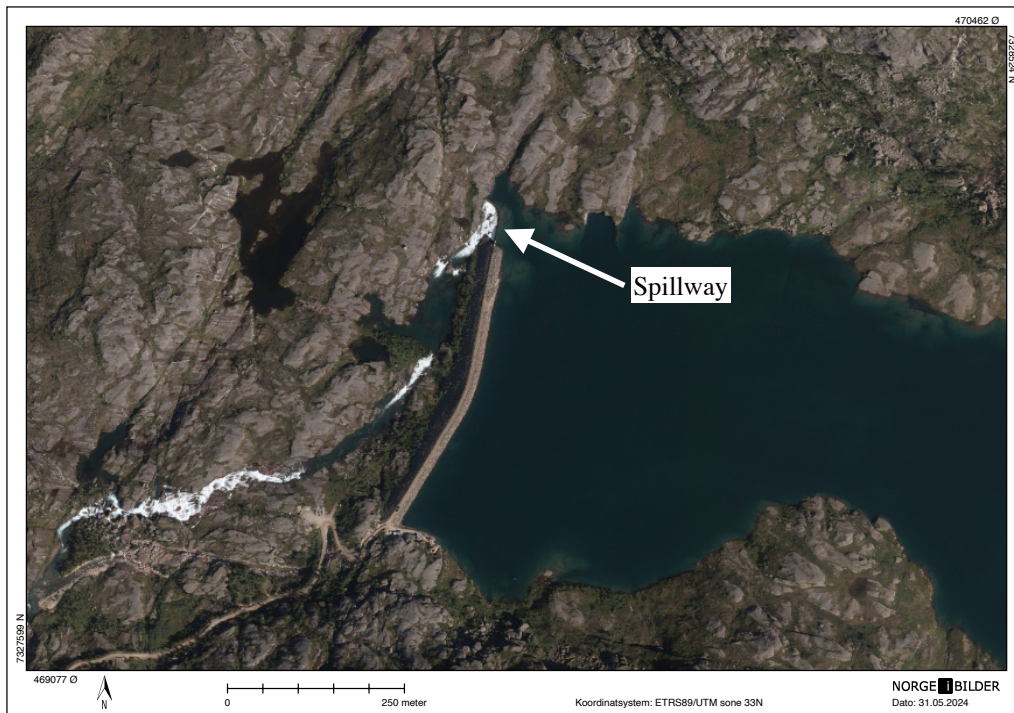


Figure 4.3 Aerial photo of Gressvatn dam, showing concrete spillway in use at the north end. 2014 Photo from NorgeiBilder.no (Norge digitalt, 2024).

Gressvatn and Kjennsvatn are lakes that lie directly below Austre Okstindbreen. Located in Hemnes municipality, Nordland, Gressvatn contains $3.14 \times 10^8 \text{ m}^3$ of capacity and has a HRV of 598 MASL and LRV of 582 MASL. Its surface area can span up to 22.6 km^2 . Both lakes have continuously received meltwater from the glacial system, and these distributions of flow have changed over time. In present day, meltwater exits the toe of the glacier into Gressvatn (Bakke et al., 2010). Previously, the flow would primarily enter Kjennsvatn, estimated to be applicable prior to 1980 (Knudsen & Theakstone, 1988). The two lakes provide input to the Statkraft Energi-owned 12 MW Kjennsvatn power plant. The more critical of the two is Gressvatn, with a rock-filled moraine-cored dam complemented by an adjacent integrated and uncontrolled, 74 m long, 6 m tall concrete gravity dam spillway, founded on bedrock, shown in Figure 4.3. Its crest elevation is noted as 603 MASL, providing 5 m of freeboard and 1 m of reinforcement from waves, however the sealed core only extends to 599.5 MASL (SWECO Norge, 2017). The embankment maximum height is approximately 23 m and spans 445 m long. This class 3 dam also features an internal hatch for emergency draining of the reservoir, with a maximum capacity of $76 \text{ m}^3/\text{s}$ that leads to an external watercourse. The spillway capacity is not reported directly, however from calculations, is estimated to accommodate up to approximately $1,000 \text{ m}^3/\text{s}$ of continuous flow, and initiates when water level reaches HRV. At the calculated PMF of $781 \text{ m}^3/\text{s}$, the dam still retains 3.5 m of freeboard. Then the very important question arises: *is this dam entirely protected from a glacial melting event?* There is a significant likelihood that initial planning of the dam at Gressvatn didn't incorporate the potential variable flow from Austre Okstindbreen at the time, since the dam was constructed in 1969 when the meltwater was being directed elsewhere. The dam did undergo rehabilitation efforts from 1968 to 1969, but it is unclear as to what this entailed. To be conservative, assuming this change in glacier melt inflow wasn't accounted for, this could make the dam susceptible to overtopping events in the scenario where the spillway capacity is overwhelmed.

4.1.2 Identified hazards

Table 4.1 Determination of fundamental hazards for Austre Okstindbreen.

Austre Okstindbreen Hazard Matrix			
Dam	H1 (rapid melt and precip.)	H2 (breach of glacial lake)	H3 (icefall or calving)
Gressvatn	Applicable	Documented hazard	Low concern

One particular feature of Austre Okstindbreen that should be investigated further is the ice-dammed lake on the western side of the glacier, located in Leirskardalen (Figure 4.4). This lake appears insignificant in size, however, has played a direct role in most of the observed GLOF events in Table 4.2. Its estimated volume change was used to calculate the 1976 outburst flood ($3.4 \times 10^5 \text{ m}^3$) (Knudsen & Theakstone, 1988). The same publication notes intense storm events, changes in ablation conditions, and development of drainage systems as potential contributors to the repeated drainage events. Although the inlet of this lake into the glacier was last observed in 1988, it can be inferred that this lake still leeches water through Austre Okstindbreen. With that established, the westward bank is noted as lower than the eastward, so in the event of an overflowing event, the water would be delivered

eastward away from Gressvatn. It was concluded that the lake still will be the source of further outbursts from Austre Okstindbreen in the future.

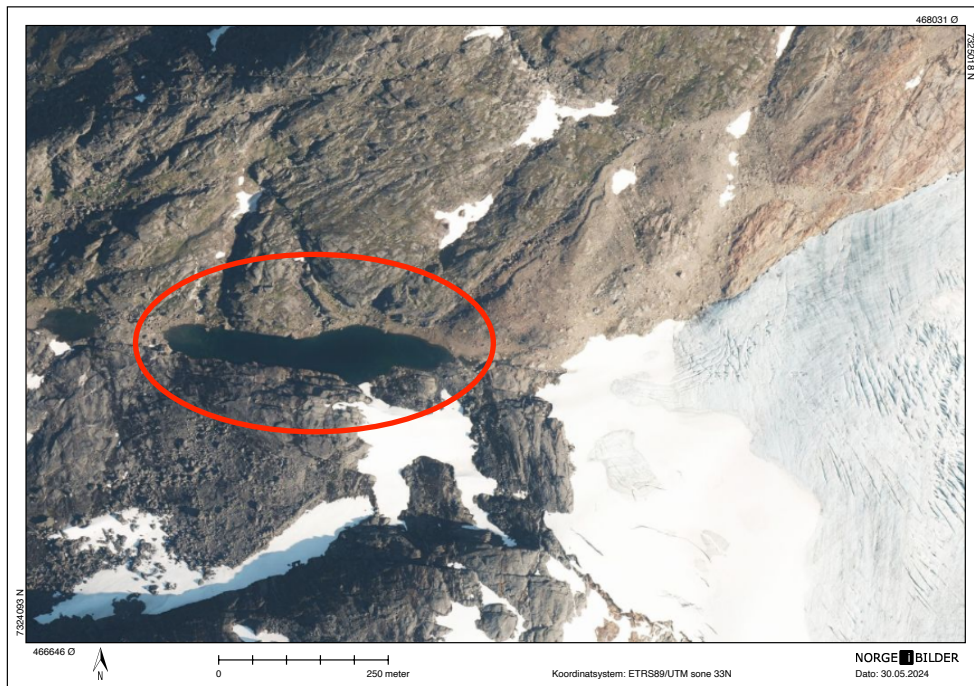


Figure 4.4 Documented ice-dammed glacial lake near Leirskardalen (GL1). After recession of snow and ice, lake appears to be bedrock dammed. Photo from NorgeiBilder.no (Norge digitalt, 2024).

One dataset that makes this system especially interesting are the recorded GLOF events at Leirskardalen. Officially, 10 events have been observed between the periods of 1976 and 1987, occurring cyclically each summer (with exceptions for two winter events). These were found in result of a series of 12 individual annual studies in the 1970s and 1980s and are summarized in Table 4.2.

Table 4.2 Historical GLOF events within Austre Okstindbreen.

Date	Outburst Volume (1x10⁶ m³)	Details of Event
31/07/1976	0.34	Lake drained during low snow melt, potentially from low water pressure in glacier's drainage system (Theakstone, 1978).10.6.2024 13:15:00
08/05/1977	Unkown	8-hour drainage of small northwest lake after period of heavy rainfall. Water burst upwards through glacier and into Kjennsvatn. Caused extensive damage to roadway and changes to terrain through deposition and scouring. Almost all flow was directed to Kjennsvatn (Theakstone, 1978).
01/08/1978	Unkown	No details available (Knudsen & Theakstone, 1988).
30/6/1979	Unkown	Early summer occurrence, contributed from winter snow cover melt (Knudsen & Theakstone, 1988).
01/08/1979	Unkown	Lake drained in combination with melt of winter's snow cover (Knudsen & Theakstone, 1988).
19/7/1982	Unkown	Lake drained in response to major storm event. Potentially initiated by July 17th's subglacial drainage collapse (Knudsen & Theakstone, 1988).
29/7/1984	0.36	Similar to 1977 occurrence, upwards water burst from glacier interior, after period of heavy rainfall. First to be witnessed in person. Only a small portion of this event was directed to Kjennsvatn. Highly documented. 6-7 hour discharge event (Knudsen & Theakstone, 1988).
01/07/1985	Unkown	Early summer occurrence, contributed from winter snow cover melt (Knudsen & Theakstone, 1988).
01/07/1986	Unkown	Early summer occurrence, contributed from winter snow cover melt (Knudsen & Theakstone, 1988).
16/7/1987	Unkown	Lake partially drained in response to successive high air temperatures and rapid ablation (Knudsen & Theakstone, 1988).

Furthermore, another lake identified in aerial photos off the northern tip of Oksskoltbreen (unnamed) and appears to lie in a loose moraine sediment indentation. In aerial photographs (Figure 4.5), there appears to be a drainage line leading northeast directly into the basin supplying Gressvatn, so can be inferred it would enter the lake upon a rapid release from failure. Upon further inspection, the lake is estimated to contain approximately $9.99 \times 10^4 \text{ m}^3$.

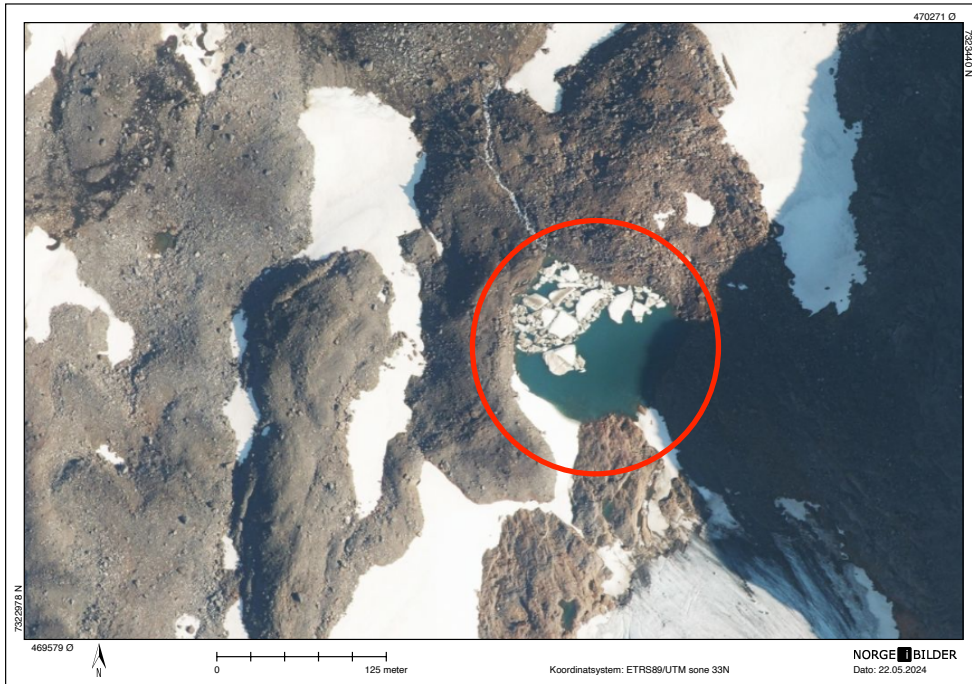


Figure 4.5 Identified moraine-dammed glacial lake in Oksskoltbreen glacier (GL2). Photo from NorgeiBilder.no (Norge digitalt, 2024).

An additional concern is the rapid melt and high precipitation condition. This is analyzed to have a potential impact of 781 m³/s for a PMF event, or 574 m³/s for a 1,000-year storm event (SWECO Norge, 2017). These estimates are greatly influenced by snow and ice melt within Gressvatn's natural topographical catchment, which has been calculated to be 10.8% glaciated.

4.1.3 Other hazards

As Gressvatn is not a proglacial lake, the risks of ice falls or ice calving is extremely unlikely to cause a direct concern. Although the surrounding terrain appears to be steep, the material is likely bedrock from visual inspection, negating problematic landslides or rockfalls. It would be wise to identify subglacial topography, as there are likely some extensive melt channels below the glaciers surface transporting the meltwater towards the outlet to Bretjønna.

4.2 Jostedalsbreen

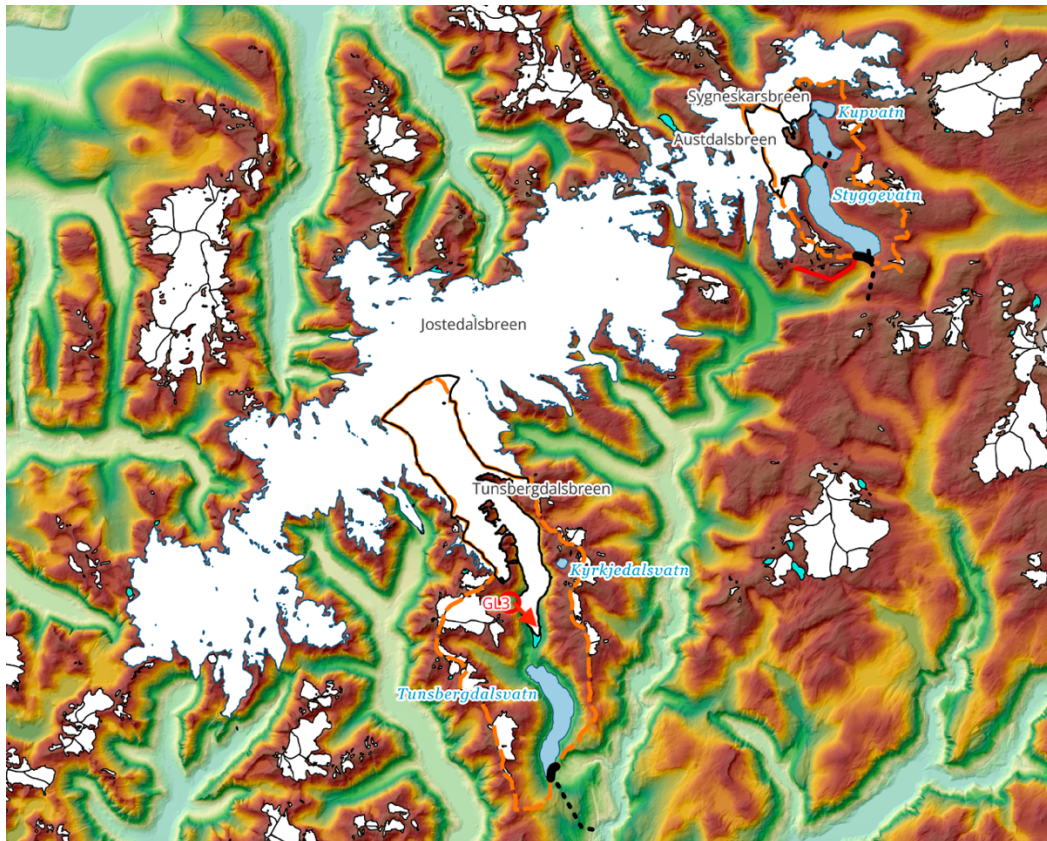


Figure 4.6 Overview of Jostedalsbreen glacier system, Tunsbergdalsvatn and Styggevatn dams, and GL3 hazard. DTM data from Høydedata.no (Kartverket, 2024).

Jostedalsbreen is a glacier widely known to be the largest in the European mainland. It reaches just beyond 100 km long and 15 km wide, and lies along the border between Nordfjord and inner Sogn, seen in Figure 4.6. The glacier is not a remnant of the little ice age, and is likely composed of ice no older than 1,000-2,000 years (Askheim, 2023). It is comprised of many smaller glaciers, and when combined, reaches beyond 458 km² in footprint size. The site has been of special interest to many scientists and researchers with a long history of documented size reduction and direct indicator of changing climate. Jostedalsbreen is also one of the few glaciers in Norway that have undergone radio echo-sounding measurements to determine more accurate figures for ice thickness and subglacial topography (Saetrang & Wold, 1986). In this context, particular attention will be directed to the glaciers Austdalsbreen (shown in cross section view in Figure 4.7) and Tunsbergdalsbreen within the Jostedal system, which are the glaciers primarily responsible for supplying meltwater to Styggevatn and Tunsbergdalsvatn, respectively.

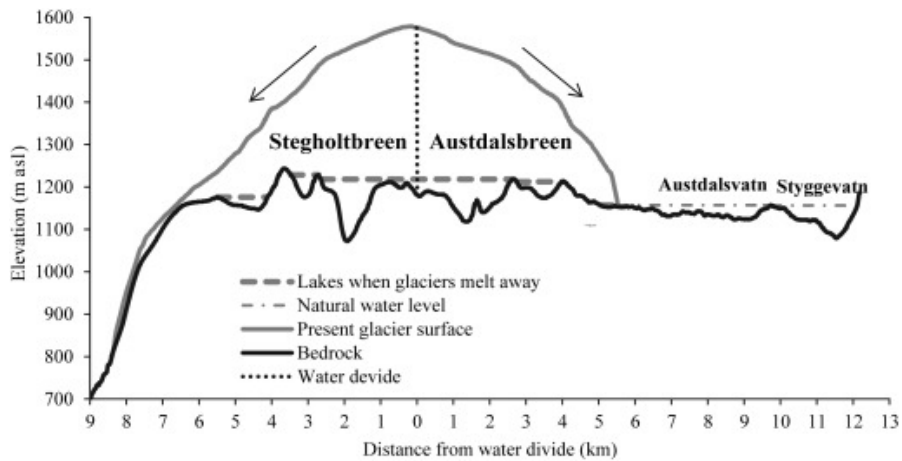


Figure 4.7 Cross section of Stegholtbreen and Austdalsbreen showing subglacial topography and differentiation between Austdalsvatn and Styggevatn (Xu et al., 2015).

Located in the northeastern reach of Jostedalbreen, Austdalsbreen is a valley glacier of approximately 10.1 km² in size, with active mass balance measurements from NVE since 1988 to 2022 (Figure 4.8). The mass balance data has indicated that the average winter gains (+) 2.2 and summer losses (-) 2.7 m.w.e. (meters water equivalent), a relationship bolstered by its continued recession (*Austdalsbreen - NVE*, 2009). Both before and after Styggevatn was regulated, the glacier had continuously calved in small amounts into the lake, accounting for 5-10% of loss in the summer balancing. Currently, the glacier is still in direct contact with the lake. Large research efforts have been conducted in accordance with the associated hydropower system (Jostedal hydropower, operated by Statkraft Energi AS).

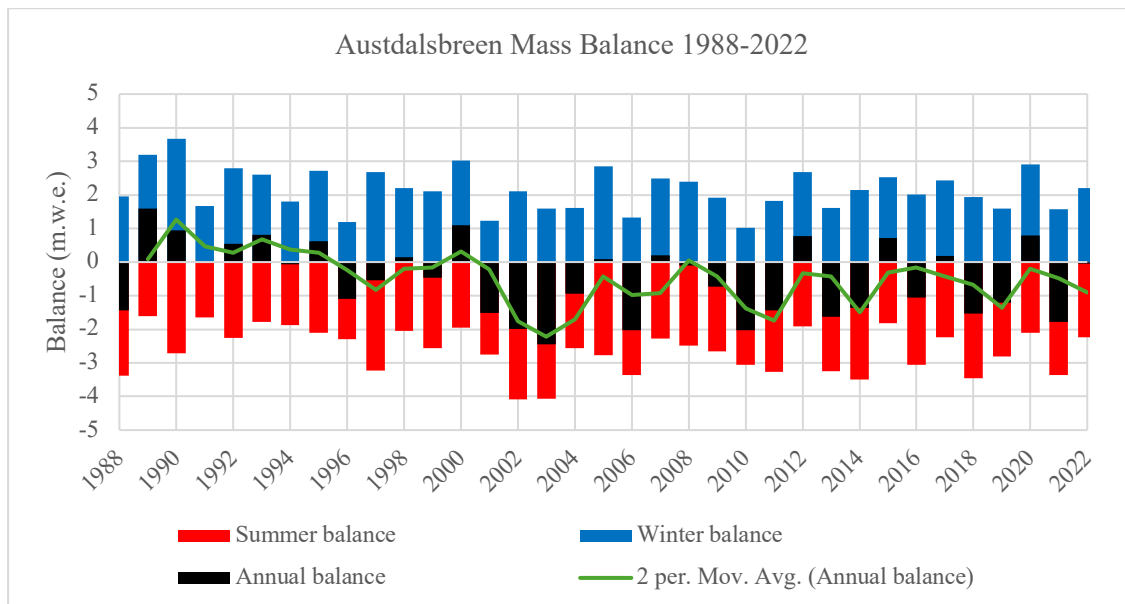


Figure 4.8 Mass balance for Austdalsbreen, 1988-2022, data provided by NVE.

It has been observed that the velocity of the glacier front at Austdalsbreen increases rapidly when the water level is high in Styggevatn. This is due to the decreased friction from the increased water pressure beneath the glacier. Many of the relationships for this glacier have been conducted through the implementation of measuring sticks and traditional surveying, as well as visual observations.

Tunsbergdalsbreen is a massively long valley glacier approximately 46.23 km² in coverage area. In the past, it had contact with Tunsberdalsvatn, however has receded to present day upwards in the mountain valley at a very rapid pace. There are length change measurements available from NVE from 1900 until 1976, indicating its significant shrinkage (Figure 4.9). There are also mass balance estimates from the years 1966-1972 available.

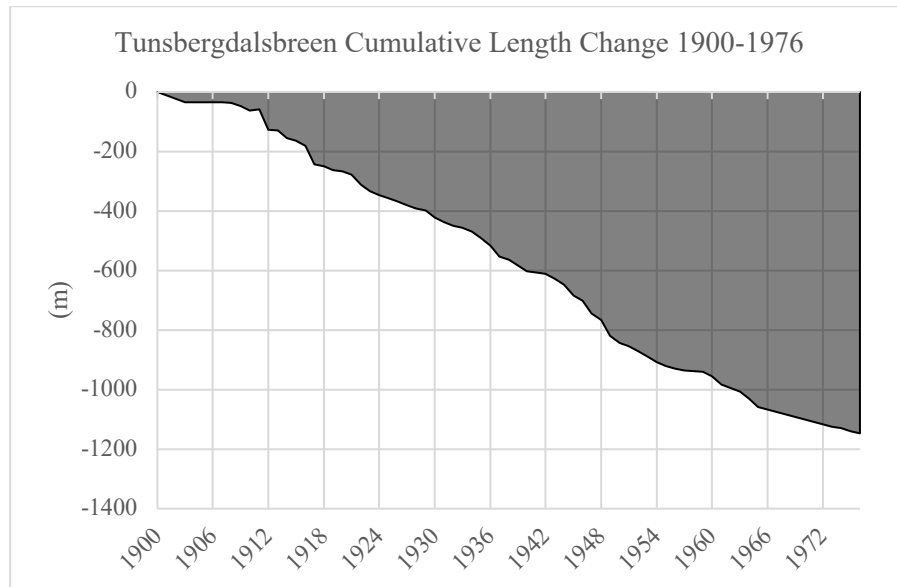


Figure 4.9 Cumulative length change for Tunsbergdalsbreen, 1900-1976, data provided by NVE.

The glacier has also been often studied by different scientists in the context of its rapid change in size, as well as the exposed glacial-dammed lake generated at its terminus. This lake became exposed in the 1990s and was estimated to be approximately 500 m long and 9 m deep (Bogen et al., 2015). Tunsbergdalsbreen recession has been so rapid, that some experts predict that this lake will be completely revealed by 2050. Figure 4.10 shows the expected lake distribution once the glacier has melted entirely, based on the subglacial topography. Additionally, particular attention has been placed on *Brimkjelen*, an ice-dammed lake bounded by Tunsbergdalsbreen, located at the western margin (Howarth, 1968). This water body had several drainage events that will be later discussed and was last seen in 1999.

Styggevatn has become synonymous with Austdalsvatn, the lake originally situated below Austdalsbreen, as shown in Figure 4.7, after the lake became regulated when the dam began construction in 1987 for the 290 MW Jostedal hydropower plant (owned and operated by Statkraft Energi, AS). Styggevatn is situated just below and in contact with Austdalsbreen, in Luster municipality, Vestland. It is from Austdalsbreen that it receives most of the inflow, within its 41.4 km² catchment. There are also 4 stream intakes directing water from Vetledøya. The lake has an approximate capacity of 3.52x10⁸ m³, with an LRV of 1110 MASL and HRV of 1200 MASL. The dam's crest elevation is noted at an elevation of 1206 MASL, providing 6 m of freeboard, however the core is designed to extend to just 1203 MASL (Multiconsult, 2023). The lake receives inflow transfer from Kupvatn, a somewhat similarly sized reservoir situated just northeast. Styggevatn dam, shown in Figure 4.3, is considered class 4, making it even more integral to investigate for potential risks from local glacial activity. Following the construction of its approximately 890 m long, 52 m high infill dam with sealed asphalt core, the lake rose 40 meters, which had a significant effect on the terminus of Austdalsbreen (Laumann & Wold, 1992). This led to hastened retreat for several years until stabilization. Although the velocity near the glacier front had increased, the calving events into the lake did not rise in correlation due to air temperature fluctuations during those years.

In lieu of a traditional integrated crest spillway, the Styggevatn dam utilizes a combined outlet shaft with concrete thresholds which transfer water to a drainage channel (Multiconsult, 2023). The entrance to this floodway is located at the western end of the dam, visible in Figure 4.11. The newer flood threshold and shaft were additions to the original design and were constructed and installed in 2014, just adjacent to the older one, which is situated at a lower elevation. The flood dampening was significantly increased for PMF flooding, as it was found to be unsuitable prior to this upgrade. The capacity for the new shaft is rated at 235 m³/s, with an initiating spillway threshold elevation of 1201 MASL, and a crest length of 40.2 m. The older shaft held a capacity of 125 m³/s, initiated at HRV elevation, and had a crest length of 38.2 m. According to provided calculations, when in conjunction, the outlets alone have a capacity for keeping water level below the top of the core for flows up to approximately 350 m³/s (Multiconsult, 2021). This value is very high and was likely designed so in relation to the high consequence class.

The dam features concrete ice breakers with snow cover to protect from both snow and ice clogging. Although ice blockages have been identified in the tunnel in the past, it has been noted that issue is not of great concern, as the water temperature from the lake can melt through the blockage in the flooding seasons in summer and autumn (Multiconsult, 2023). These ice breakers are located just in front of the outlet spillway and “reduce risk” of floating ice or icebergs from blockage of the channel (Multiconsult, 2023).

4.2.2 Tunsbergdalsvatn

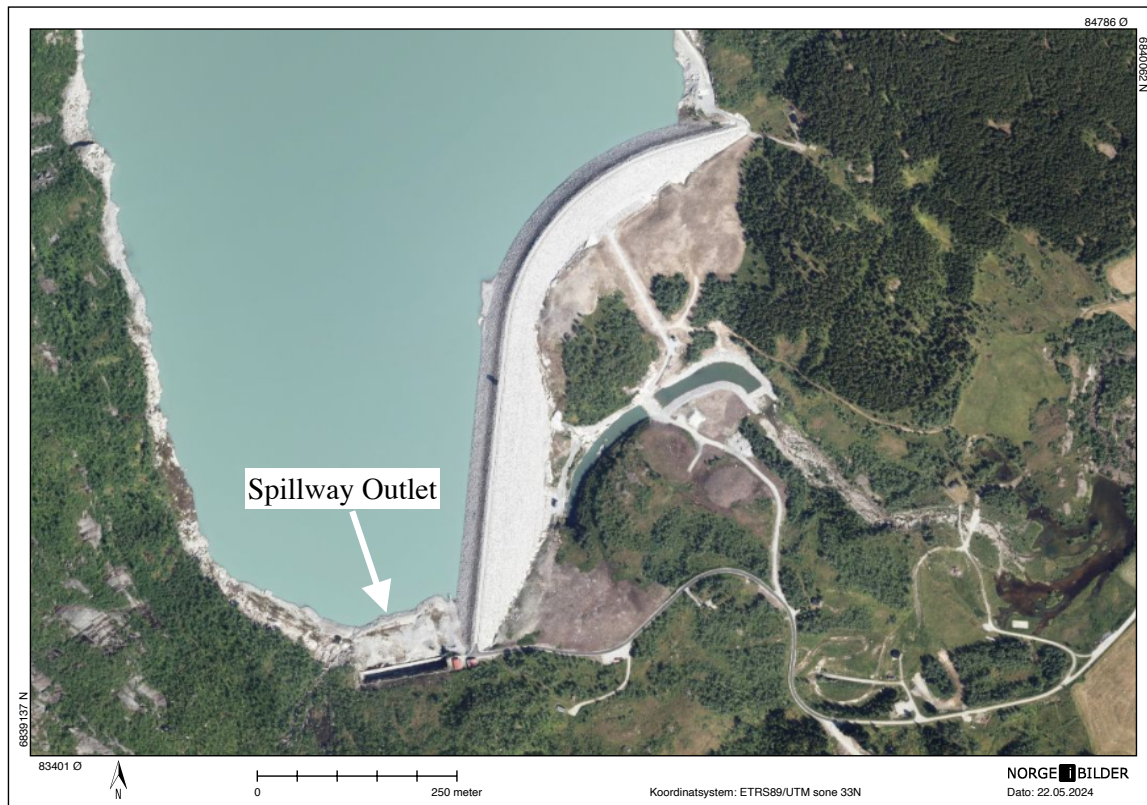


Figure 4.12 Aerial photo of Tunsbergdalsvatn dam, with concrete spillway structure at southern end. Photo from NorgeiBilder.no (Norge digitalt, 2024).

Tunsbergdalsvatn is a massive regulated glacial-fed lake with a capacity of approximately $1.78 \times 10^8 \text{ m}^3$ located in Luster municipality, Vestland. It is located just downstream of Tunsbergdalsbreen glacier, one of its primary water sources. In the past, this glacier had direct contact with the lake (Andreassen et al., 2023). The dam was constructed in 1978 to supply Statkraft's 125 MW Leirdøla power plant. The lake has a LRV of 440 MASL and HRV of 478 MASL, with the dam's crest elevation at 484 MASL (6 m of freeboard) (Multiconsult, 2022a). The sealed core reaches 481 MASL. Its catchment size spans approximately 137 km^2 , with a significant portion falling under glaciated terrain (42.7 km^2). The class 4 fill dam with central sealed core spans approximately 870 meters in length and is 43 meters at its highest. It also features a separated 100 m long, approximately 4 m tall concrete spillway at the southern end of the reservoir that leads into a collection channel and tunnel. There is a 4 m^2 emergency outlet hatch near the center of the lake that can also be used to divert floodwater at 440.2 MASL, if necessary (up to $80 \text{ m}^3/\text{s}$). Additionally, the intake leading to the power plant is located centrally in the dam, into a 145 m long bypass tunnel. Just prior to its construction in 1976, a study presented to the International Congress on Large Dams (ICOLD) revealed that the lake was subject particularly to risks from avalanches (wave generation) and glacial lake floods in particular (Lied et al., 1976). Tunsbergdalsvatn receives a great deal of glacial meltwater from several smaller glaciers, with Tunsbergdalsbreen as one of the larger contributors.

In 2017, rehabilitation efforts were completed at Tunsbergdalsvatn dam that renewed and improved the downstream slope, spillway, and dam crest. The total spillway capacity is

suggested to endure greater than the estimated PMF flood (642 m³/s) (Multiconsult, 2022a). This capacity is very overbuilt and has much to do with the generous freeboard and physical footprint of the lake (7.73 km²). This could also be the case as the original PMF flood estimates were originally estimated as much more when the dam was originally constructed. Fortunately, the dam has been noted in Multiconsult’s report to adequately handle the inflow of potential GLOFs (including the case of Brimkjelen mentioned later) (Multiconsult, 2022a).

4.2.3 Identified hazards

Table 4.3 Determination of fundamental hazards for selected dams at Jostedalsbreen.

Jostedalsbreen Hazard Matrix			
Dam	H1 (rapid melt and precip.)	H2 (breach of glacial lake)	H3 (icefall or calving)
Styggevatn	Applicable	Low concern	Applicable
Tunsbergdalsvatn	Applicable	Documented hazard	Low concern

The rapid melt and precipitation events are important to study for both Styggevatn and Tunsbergdalsvatn, as the lakes’ position adjacent to the glacier masses make them susceptible to potential flood surges and subsequent overtopping. Styggevatn is estimated to have a glaciated catchment of 27.9%, whereas Tunsbergdalsvatn receives 42.7%. A PMF of 452 m³/s and 1,000-year storm event of 362 m³/s was found for Styggevatn (Multiconsult, 2021), whereas a PMF of 642 m³/s and a 1,000-year storm event of 400 m³/s is estimated for Tunsbergdalsvatn (Multiconsult, 2022a).

Although there are no recorded official GLOF events at Austdalsbreen, GLOF activity has been observed in the nearby Stigaholt glacier, as recent as 2017 (Kjøllmoen et al., 2019), which were confirmed with aerial historical photos. With that being acknowledged, there are no identified ice-dammed lakes identifiable within Austdalsbreen, eliminating the need for a glacial lake breach hazard analysis for it in this paper. The potential existence of obscured subglacial lakes is very possible in this glacier.

As previously noted, the identification of a glacial lake breach as a potential hazard for Tunsbergdalsvatn dam is already acknowledged in literary sources before its construction. Furthermore, a number of GLOF events have been observed from Tunsbergdalsbreen itself. The events listed in Table 4.4 are documented in various studies.

Table 4.4 Historical GLOF occurrences within Tunsbergdalsbreen.

Date	Outburst Volume (x10⁶ m³)	Details of Event
07/1896	Unknown	Flooding evident in successive summers (July months). Believed to have originated from Brimkjelen. Outburst volume noted as less than the 1900 occurrence (Mottershead & Collin, 1976).
07/1897	Unknown	
07/1898	Unknown	
07/1899	Unknown	
06/08/1900	2	A flood of larger magnitude than previous from Brimkjelen. It was after this flood that the glacial lake volume was estimated around 2x10 ⁶ m ³ (Liestøl, 1956).
23/08/1903	Unknown	Noted to be very similar to occurrence in 1900 just 3 years prior. Sourced from Brimkjelen (Liestøl, 1956).
14/08/1926	15-30	A much more significant flood than previously observed events. Bridge spanning Leirdøla stream was destroyed in the event. Differing estimations on drainage volume, as interpreted by different individuals. Sourced from Brimkjelen (Liestøl, 1956).
21/06/1970	5.7	Flood recorded via hydrograph in Leirdalen, however could not be confirmed that it had originated from Brimkjelen. This was inferred, as no other source would have this impact on the gauge (Mottershead & Collin, 1976).
11/08/1973	Unknown	Site visit confirmed the past presence of one lake at Brimkjelen and current presence of a new one, as well as ongoing drainage (Mottershead & Collin, 1976).
01/1999	Unknown	Lake observed to be empty once more once observations were resumed in 1997 (Kjøllmoen & Norges vassdrags- og energidirektorat., 2000).

Because of the nature and well documented history of Brimkjelen lake, it is considered as a direct potential mechanism for future GLOF activity in an event tree analysis. It should be noted that the last significant flood from this location was in 1926, however the possibility for the lake to refill and repeat failure is still a potential phenomenon. The likelihood of this occurring is continuing to decrease, as the retreat of Tunsbergdalsbreen has significantly shrunk the potential volume and storage of such a lake. The lake was last reported to have contained water visible outside the glacier prior to 1999's minor flood event.

Another lake in the vicinity of Tunsberdalsbreen is Kykedalsvatn, bordering the eastern margin of Tunsbergdalsbreen. Upon further screening inspection, it was found that the

erosion lake is bordered by solid bedrock, which is not prone to moraine breach or progressive piping failures, so it is discounted from being a potential hazard in this paper.

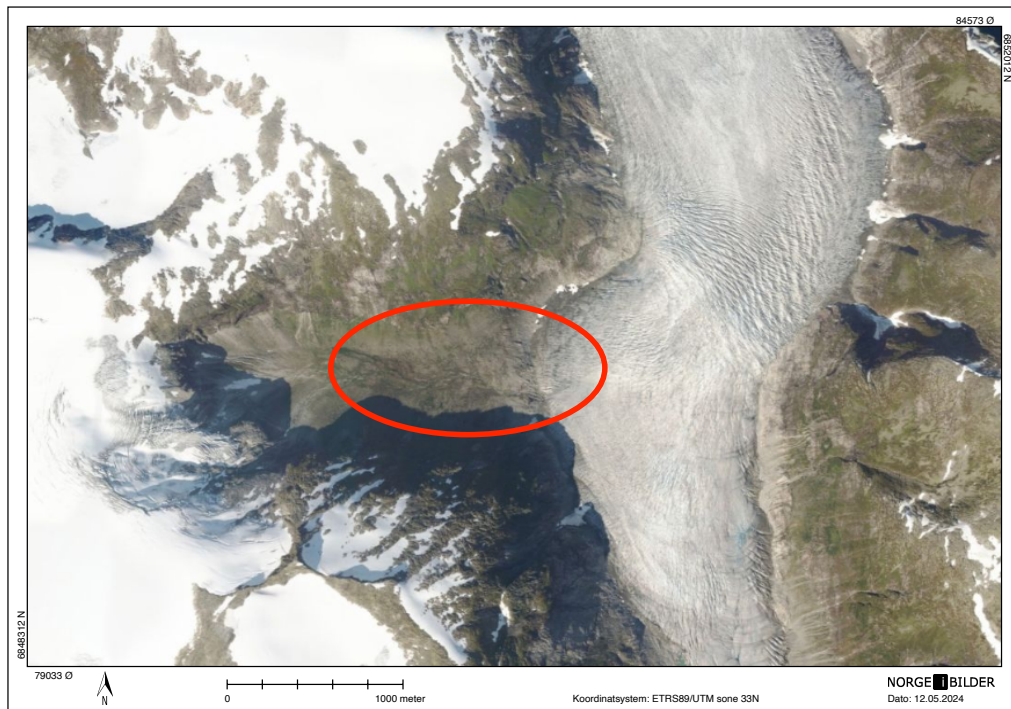


Figure 4.13 Brimkjelen ice-dammed lake (GL3) location, at unfilled state. Photo from NorgeiBilder.no (Norge digitalt, 2024).

To assess in an event tree analysis, an estimate for the volume of the ice-dammed lake is needed. In this case, the last estimated outflow volume of the lake will be taken ($5.7 \times 10^6 \text{ m}^3$). This is a very crude estimate, as this figure originated from a 1973 event prior to significant shrinkage of the glacier. Today, the storage, if to occur again, would likely be significantly less. Current DTM data sourced from Høydedata.no (Kartverket, 2024) shown in Figure 4.14 indicates that the glacier may no longer be able to dam water from the east due to its shrinkage. Also, the mapped direction of the riverway from the east is seen travelling adjacent to the glacier towards the south, rather than ponding or leading directly underneath the ice. Reports state the unlikelihood of this lake reforming or draining once more, and even if were the case, that Styggevatn had enough capacity to buffer the resulting flood (Multiconsult, 2023).

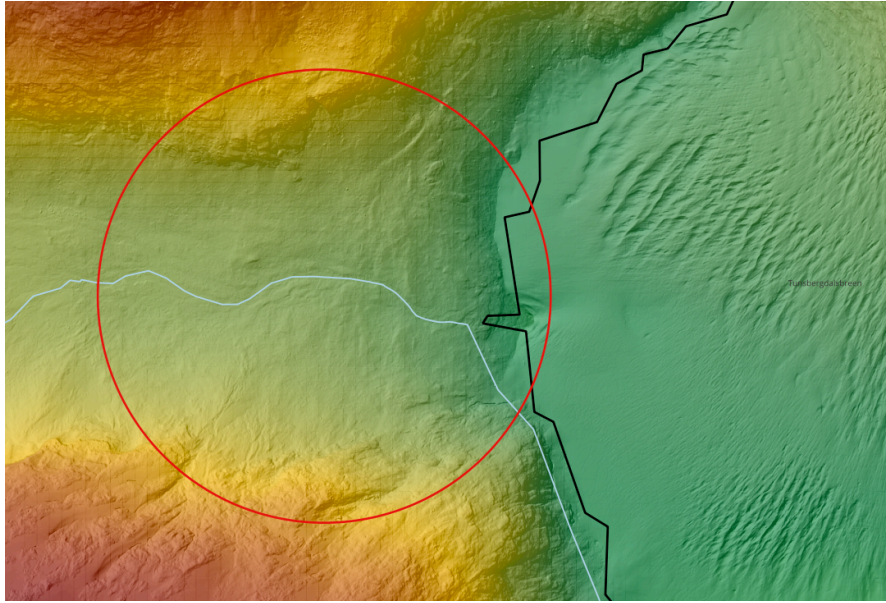


Figure 4.14 1m DTM raster showing Brimkjelen area (red boundary) in contact with Tunsbergdalsbreen to the east. A minor depression in the glacier is seen where the river changes direction southward. DTM data sourced from Høydedata.no (Kartverket, 2024).

Styggevatn’s direct contact with the glacier terminus leads to the decision that an analysis of risk for icefall or glacier calving is necessary regarding potential overtopping- from blockage of the spillway. This assessment is also recommended due to the number of eyewitness reports indicating the increased continuous calving occurring into the lake (*Austdalsbreen - NVE*, 2009; Bakke et al., 2010). Figure 4.15 shows the visibly receding front as a result of calving and general glacier ablation. The spillway blockage failure condition is especially unlikely due to the dam’s inclusion of robust ice-breaker mechanisms. It has been noted in reports that icebergs have never been identified near or colliding with the spillway, via installed live cameras (Multiconsult, 2023).

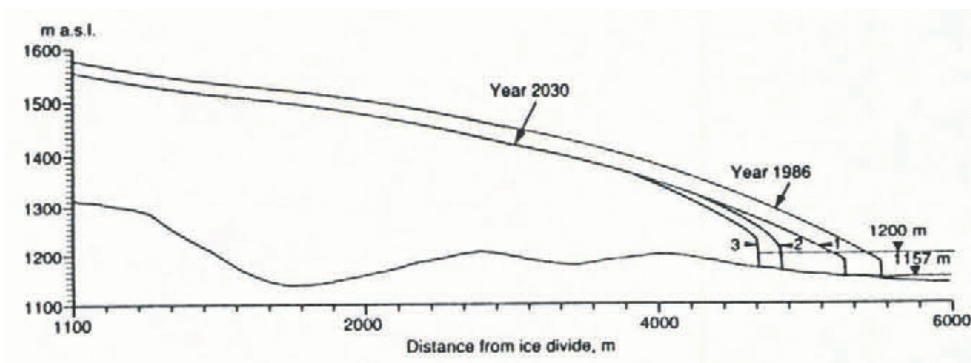


Figure 4.15 Cross section of Austdalsbreen, depicting the recession of the glacier toe from 1986 to the predicted location in 2030 (Laumann & Wold, 1992).

4.2.4 Other hazards

Additional hazards faced by both lakes are potential rockfalls and landslides, as they are situated in terrain with very steep slopes, and cannot be ruled out, as per comments from (Multiconsult, 2022a). Because both Tunsbergdalsvatn and Styggevatn are situated in what

is essentially a bowl of mountain peaks, they are especially susceptible to avalanche risk. These mechanisms should not be discounted, however for the purposes of this paper, it must be left at further recommendation of study to those with higher knowledge and experience in these types of geological studies.

4.3 Folgefonna

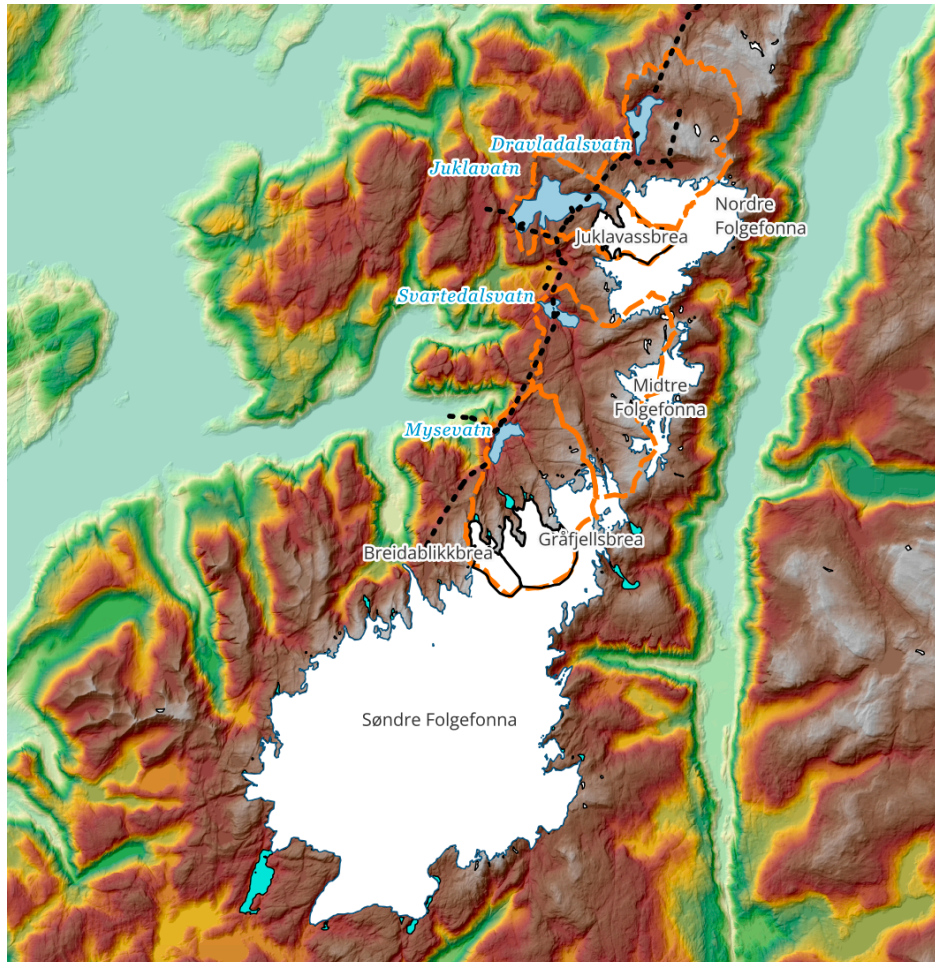


Figure 4.16 Overview of Folgefonna glacier system and associated dams. DTM data from Høydedata.no (Kartverket, 2024).

Folgefonna is a massive ice cap glacial system located in southwest Norway in Vestland. It is comprised of three different ice caps- Nordfonna (north), Midtfonna (middle), and Sørfonna (south), and is the Norway's third largest glacier. Interestingly enough, the region was not designated a national park until 2005. The three primary regions of glacial ice, and many other smaller locales, are estimated to span approximately 207 km² in size when combined, and feature ice thicknesses up to nearly 400 meters (*Om nasjonalparken*, n.d.). NVE estimates that Nordfonna is 23.9 km², Sørfonna at 153.79 km², and Midtfonna at 8.01 km². Folgefonna, just as with Jostedalssbreen, is a maritime glacier that is sustained by snow generated from humid and mild southwesterly winds from the North Atlantic ocean (Imhof et al., 2012). It is also extremely sensitive to changing climate conditions and is heavily dependent on the winter season for accumulation. NVE has monitoring data for many of the

glaciers within Folgefonna, with respect to length change and mass change. Presently, only Botnabrea is actively measured regarding the glaciers in focus in this paper.

In Nordfonna, glaciers Juklavassbrea and Botnabrea are of most interest, due to them being the primary source of glacier melt to Juklavatn and Markjelkevatn, respectively. Botnabrea also contributes a small portion of melt to Svartadalsvatn. Botnabrea is an approximately 4.26 km² glacier with ongoing length change measurements by NVE since 1996. It is rapidly declining in size, as shown in Figure 4.17.

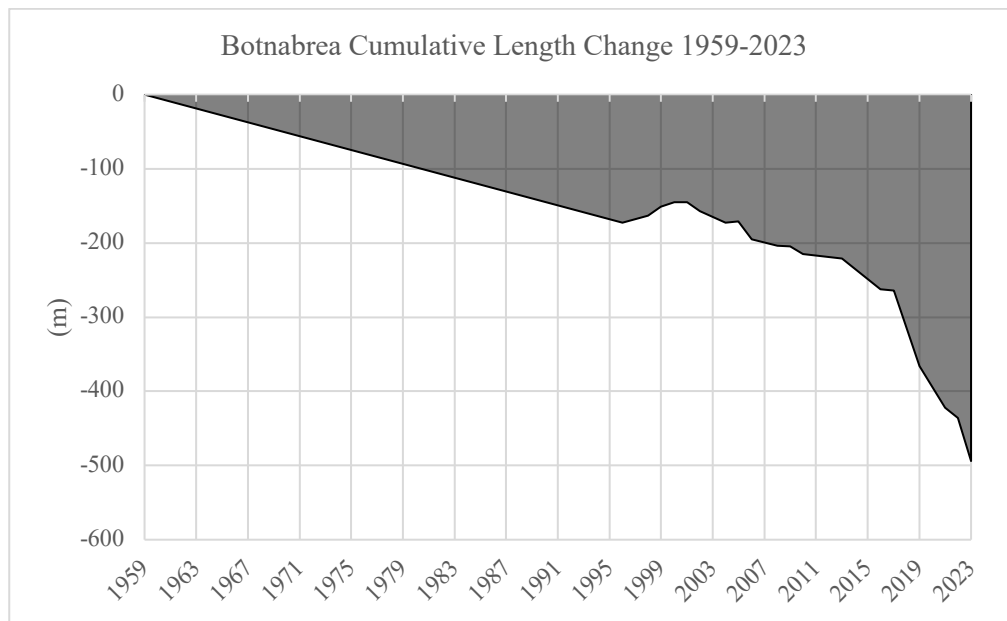


Figure 4.17 Cumulative length change for Botnabrea, 1959-2023, data provided by NVE.

The rapid thinning of Botnabrea is of large concern to downstream catchments, as melt floods can result from minute changes in temperature during warmer periods (Sicart et al., 2008).

Midtfonna is the primary source of melt water for Svartadalsvatn. It is also losing mass at an exceedingly fast rate, nearly 50% of its size from 1860 (Robson, 2012). At current, it is estimated to span approximately 8 km² and leads melt water in all cardinal directions. In February 1849, it was responsible for a documented GLOF event where a moraine-dammed lake burst, sending large quantities of snow, water, and debris towards the eastern side of Folgefonna, which later terminated in the Hardangerfjord. This event injured several people downstream of the glacier, and the total volume or flow was not determined. 94 years later on the same date, the same lake underwent the same catastrophe, destroying a school. After this event, a tunnel was constructed and embedded to ensure safety for future events (Kolltveit, 1962). On the western side of the glacier mass, no GLOFs have been recorded from Midtfonna. Additionally, no further ice-dammed lakes can be identified at this time with aerial photos.

In Sørfonna, both Gråfjellsbrea and Breidablikkbrea are sources of meltwater to Mysevatn, amongst several other unnamed glaciers in the region. Gråfjellsbrea does not have any recorded GLOF history, however, does have several glacial lakes extending from the outlet fingers at the base of the glacier. Length change data has been collected from 1959-2023 by

the directorate, as shown in Figure 4.18. In this figure, a significantly faster rate of length shortening can be observed from 1996 onwards. These were performed with DTM data, as well as staking and depth probing (Kjøllmoen, 2016).

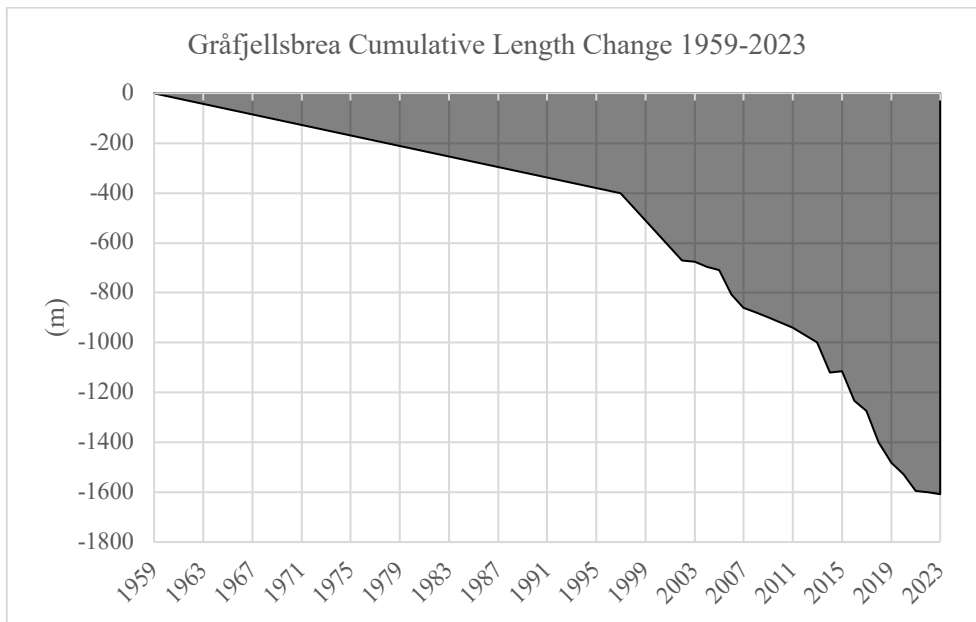


Figure 4.18 Cumulative length change for Gråfjellsbrea, 1959-2023, data provided by NVE.

Breidablikkbrea is not well documented in literature, but does have mass balance and length change measurements from 1963 to present, nonconsecutively. The years between 2003 2013 are shown in Figure 4.19. This shows a continuous annual moving average of net loss mass balance. It currently spans approximately 2.99 km², and also features some glacial lakes extended from the terminus. There are no recorded GLOF events for Breidablikkbrea.

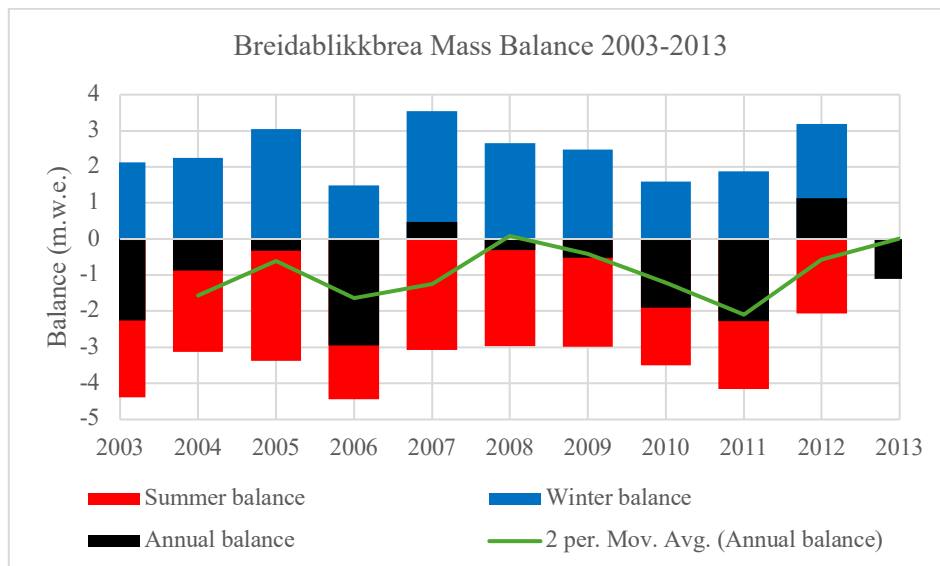


Figure 4.19 Mass balance for Breidablikkbrea for 2003-2013, data provided by NVE.

4.3.1 Dravladalsvatn



Figure 4.20 Aerial photo of Dravladalsvatn dam, with spillway structure visible out south end, leading to a flood channel underneath the road. Sourced from NorgeiBilder.no (Norge digitalt, 2024).

Dravladalsvatn is a 5.8×10^7 m³ capacity reservoir located in Ullensvang municipality, Vestland, near the northeastern flank of Folgefonna glacier. Its catchment size reaches just 27.25 km², but can be supplemented with inflow from Kvanngrovatn, Skarvabotn, and Juklavatn lakes. The dam was originally constructed between 1971 and 1972, and provides flow to the 40 MW Jukla pumped-storage hydropower plant, owned and operated between Statkraft Energi AS (85.06%) and Skagerak Energi AS (14.94%). It also contributes to the Mauranger power plant network (same owning distribution) connecting most of the western Folgefonna reservoirs, capable of 250 MW production. This Mauranger power station is unique in that it is Norway's first to utilize melt water from beneath a glacier (Bondhusbreen glacier) (Statkraft AS, n.d.). The dam has a HRV of 957 MASL and a LRV of 880 MASL, giving a very large 77 m of operating freeboard. The crest is noted to lie at 959 MASL, resulting in 2 m of freeboard from HRV (NGI, 2016). The consequence class 3 embankment dam is rock-filled, with a sealed internal moraine core, extending 340 m long and 29 m tall, and situated at 961.5 MASL. Dravladalsvatn dam consists of a concrete overflow threshold

spillway configuration that is 25 m long and 3 m tall, and begins functioning at HRV elevation.

According to reports (NGI, 2016), a series of significant rehabilitation constructions took place between the years 1997 and 2012. This included a new dam toe (expanding drainage capacity), leakage measurement system, downstream slope protection (which can aid in protection from overtopping), in addition to new crown protection and spillway threshold. Then in 2005, the dam was further upgraded by improving the upstream slope to hinder ice load damage. Further upgrades in 2010 and 2011 furthered some of the instrumentation capabilities, increased drainage capacity, and further improved upstream slope protection once more.

4.3.2 Juklavatn

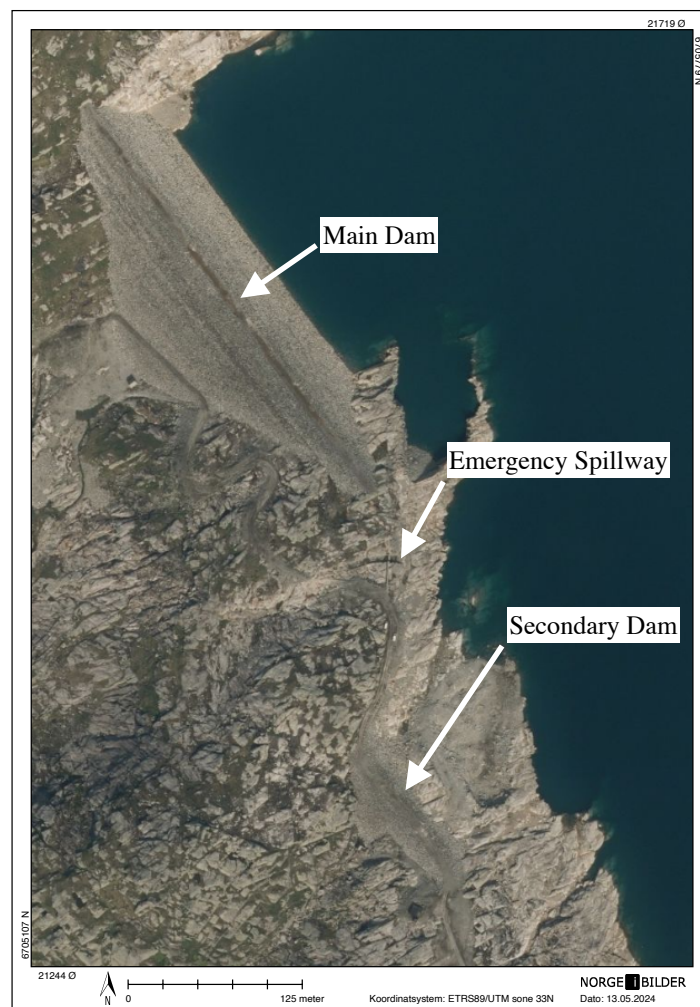


Figure 4.21 Juklavatn dams and spillway layout. Emergency spillway lies embedded in bedrock gully. Photo sourced from NorgeBilder.no (Norge digitalt, 2024).

Juklavatn is a large $2.36 \times 10^8 \text{ m}^3$ capacity reservoir also situated in Ullensvang municipality, Vestland. The class 3 dam was originally constructed in 1974, just after Dravladalsvatn dam, and is situated above Svartadalsvatn, with an HRV of 1060 MASL and LRV of 950 MASL. Juklavatn supplies water directly to Svartedalsvatn, as part of the Mauranger power plant

system (Statkraft Energi and Skagerak Energi-owned) but can also receive water back via pumping. The dam crest is situated at approximately 1064 MASL, providing 4 m of freeboard (SWECO Norge, 2011). The dam's emergency spillway is configured as a linear concrete dam founded on bedrock, measuring 15 m long and has an initiating flow elevation just above HRV, at 1061 MASL, and directs flow into a deep cut channel. It has been noted that due to the lack of vegetation in the area, and the design of the spillway crest, that clogging is not of concern (SWECO Norge, 2011). From aerial photos, the dam is estimated to span 340 m in length, and from Norgeskart.no (Kartverket, n.d.) 50 m in height was estimated.

4.3.3 Mysevatn

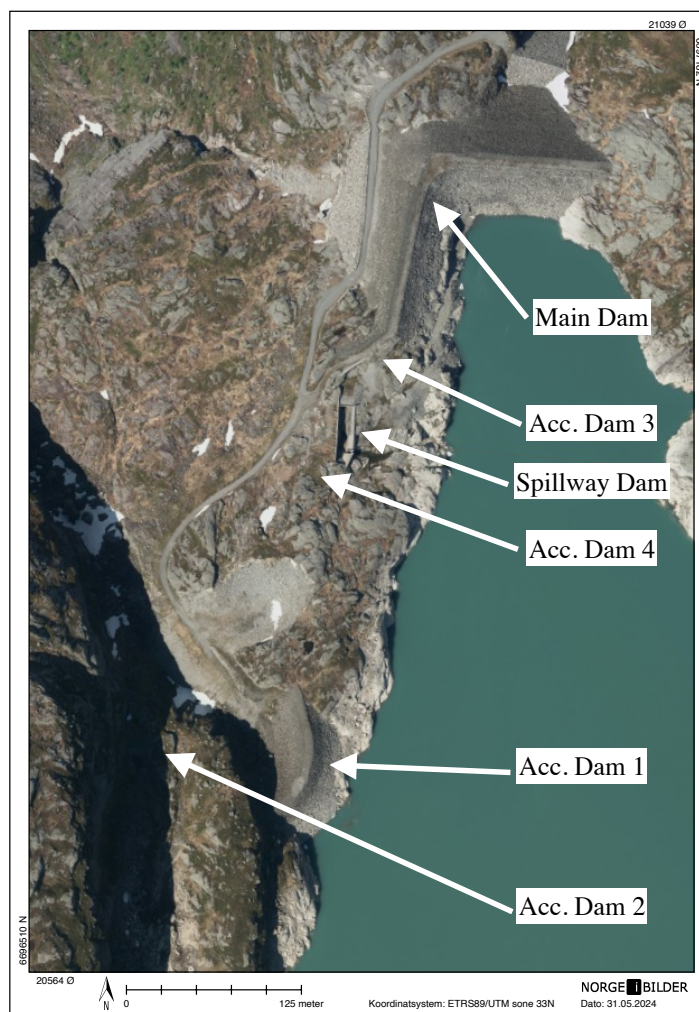


Figure 4.22 Aerial photo of the Mysevatn dams, with components lining the western bank. Acc. Dam 2 situated in shadow and difficult to discern. Sourced from NorgeiBilder.no (Norge digitalt, 2024).

Mysevatn is a $3.9 \times 10^7 \text{ m}^3$ reservoir located just east of Midtre Folgefonna in Kvinnherad municipality, Vestland. Compared to the other cases at Folgefonna, it has a relatively small footprint at 1 km^2 . It is regulated between the elevations of 775 MASL (LRV) and 855 MASL (HRV). Built in 1973, the main rock-fill dam, situated in a right-angle, is founded on bedrock, with central sealed moraine core, and spans 250 m in length, and a height of 58 m. The crest width is 8 m and is at elevation 859 MASL, providing 4 m of freeboard,

however the core has been noted to extend to 857 MASL. It is considered to be in consequence class 2. The reservoir is connected to the Mauranger power plant system as with the other dams in this study within Folgefonna (see prior for additional details). The overall layout of the reservoir is complex- with its main moraine dam, supplemented by 3 separate secondary dams towards the south. One of the secondary dams is identified of having a height of 24 m and length of 130 m, whereas the remaining two are quite small (4 m tall and 18 m long, and 3 m tall, 29 m long, respectively) (Multiconsult, 2022b). Additionally, there is a purposed concrete gravity threshold dam with a height of 4 m and length of 31 m. The overflow threshold is noted to initiate at HRV elevation. These components are identified in Figure 4.22. Mysevavn receives water both from its 32.6 km² catchment, and from transfer from Svartadalsvatn and Bondhusbreen.

According to reports, the main dam has had a history of leaks, specifically when first filled in 1974. These leaks varied in intensity over the years, and led to the decision to carry out extensive improvement work in 1977 (Multiconsult, 2022b). During this year, the downstream backfill was expanded, modifications to the core, and a series of injection-resolved the problems. From 2004-2005 there was additional work carried out the entailed implementing additional leakage detection infrastructure, as well as plastered slope protection.

4.3.4 Svartadalsvatn

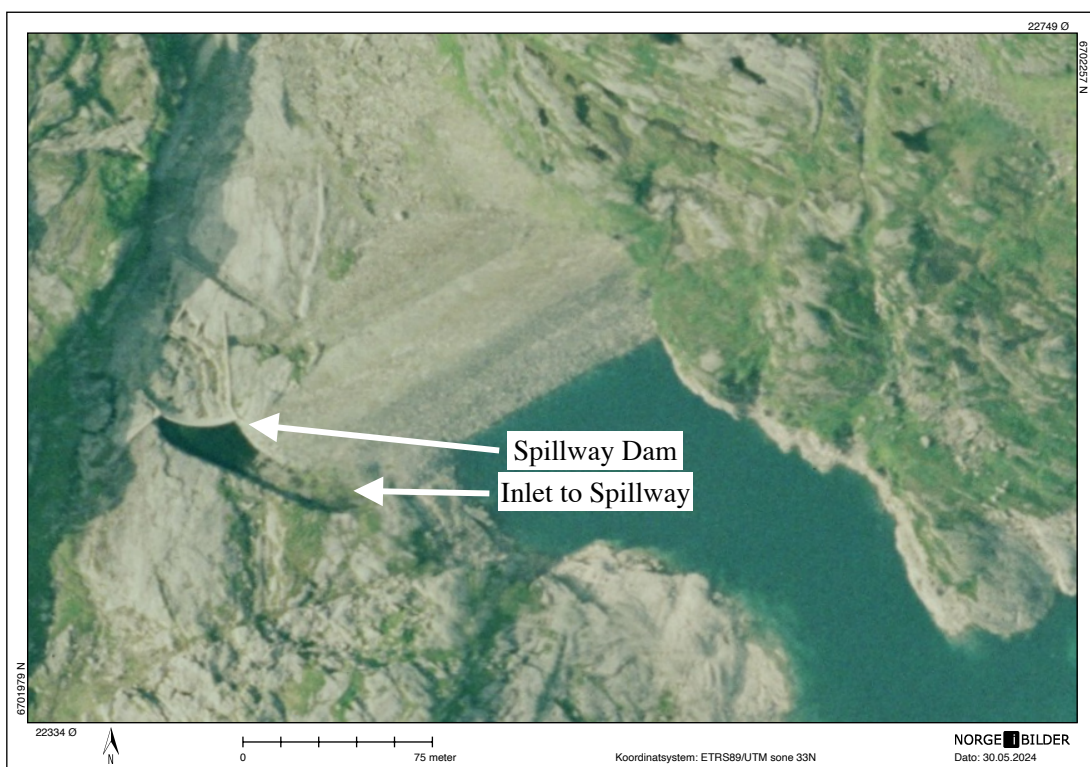


Figure 4.23 2006 Aerial photo of Svartadalsvatn dam with free-flow concrete spillway visible at the western side. Photo sourced from NorgeiBilder.no (Norge digitalt, 2024).

Svartadalsvatn (also referred to as *Svartedalsvatn*) is a 3.1×10^7 m³ reservoir constructed in 1974 falling under consequence classification 2, with a catchment size of 21.8 km² located in Kvinnherad municipality, Vestland. Interestingly, this classification is from a reevaluated

assessment, as it had previously fallen under classification 3 before 2012 (SWECO Norge, 2018). When the reservoir was first filled in 1974, it had many issues with significant leakage and underwent several iterative repairs, which repeated cyclically for years as the regulation level increased. It now features a HRV of 860 MASL and a LRV of 780 MASL, making it a very flexible dam regarding regulation (with the core extending to 862 MASL). The dam crest is situated at 864 MASL (4 m of freeboard) and is approximately 160 m in overall length. At its greatest extent, the rock-filled embankment with sealed moraine core measures 39 m tall. The dam features a curved concrete gravity dam spillway located at the south-most part of the site. This spillway is purposed for free overflow, and is 32 m long, and 3 m high. Svartadalsvatn receives inflow both from the glaciated areas in the catchment, as well as transfer from the Blådalsvatn reservoir. Svartadalsvatn can direct water into Mysevatn, where the Mauranger power station receives its inflow (SWECO Norge, 2018). It is also part of both the Mauranger and Jukla (pumped) power plants, owned and operated by Statkraft Energi AS and Skagerak Energi AS, as previously described for other Folgefonna reservoirs.

Within the lake are two intakes, situated at 790 and 780 MASL, that supply the hydropower plants. The overflow spillway at the south end will be of main focus, at it is responsible for mitigating a flood should a surge occur, and features additional concrete guidewalls just downstream. In 2017, this spillway was proposed to be expanded, as part of a series of other improvements to account for updated significantly larger flood values greater than when constructed, and to also consider future climate surcharge (SWECO Norge, 2018). This expansion was to include an additional 10 m of crest length by widening the passageway. It is unclear whether or not this change has been implemented yet. There is a possibility this change has been implemented, as aerial photos from 2019 show the dam mostly drained, with the spillway appearing to be in construction. As per reports, the spillway is reportedly theoretically limited to a capacity of 250 m³/s before causing inundation to the dam’s core.

4.3.5 Identified hazards

Table 4.5 Determination of fundamental hazards for selected dams at Folgefonna.

Folgefonna Hazard Matrix			
Dam	H1 (rapid melt and precip.)	H2 (breach of glacial lake)	H3 (icefall or calving)
Dravladalsvatn	Applicable	Minor hazard, low concern	Low concern
Juklavatn	Applicable	Low concern	Minor hazard, low concern
Mysevatn	Applicable	Low concern	Low concern
Svartadalsvatn	Applicable	Low concern	Low concern

As all of the specified lakes in Folgefonna retain high glacierated catchements (Dravladalsvatn 21.5%, Juklavatn 34%, Svartadalsvatn 23.2%, and Mysevatn undetermined), it is decided that they all apply for the H1 hazard condition, and are further

analyzed in event tree analyses. They also report high flood estimates from reports, with peak flows shown in Table 4.6.

Table 4.6 Incoming flood estimates for Folgefonna-area lakes, sourced from provided reports.

Dam	Q ₁₀₀₀ (m ³ /s)	PMF (m ³ /s)
Dravladalsvatn (NGI, 2016)	70	123.2
Juklavatn (SWECO Norge, 2011)	141.7	204.9
Mysevatn (Multiconsult, 2022b)	212	303
Svartadalsvatn (SWECO Norge, 2018)	142.1	204.9

As for H2 (breach of glacial lake), only one could be identified within the upper extent of the glaciers, within the catchment for Svartedalsvatn, shown in Figure 4.24. This lake is extremely small, and appears to be a small proglacial pocket exiting from Midtre Folgefonna to the north. It appears to be solidly bound by bedrock, and can either drain back into the glacier to the south, or exit into a valley to the north where dampened by other glacial valley lakes. In any case, its volume was estimated to be 3.9×10^4 m³, and was determined as not a candidate for further analysis, as it is simply too negligible in size.



Figure 4.24 Small proglacial lake identified in Midtre Folgefonna for Svartedalsvatn (GL4). Photo sourced from NorgeiBilder.no (Norge digitalt, 2024).

An identified previous GLOF outburst was located in Nordre Folgefonna in 2009, where an estimated 1.2×10^4 m³ of water was released during the evening near a ski center (“Sjoen forsvann pa ei natt,” 2009). This would have ended up draining to Dravladalsvatn, however was decided as not an imminent issue or addressable hazard, as the volume was simply too

small to be of concern. Its outlet location is shown in Figure 4.25. In summary, there are no applicable glacial lakes for analyses for the applicable lakes in Folgefonna.



Figure 4.25 Location of previous minor flood event for Dravladalsvatn (“Sjoen forsvann pa ei natt,” 2009). Aerial photo sourced from NorgeiBilder.no (Norge digitalt, 2024).

Following further visual assessments, the observation of several proglacial lakes extending from the termini of Gråfjellsbrea and Breidablikkbrea were made. These lakes are a result of the receding glacier front, and are dammed by bedrock. It was concluded that these lakes in particular were not of critical risk to the underlying dam, Mysevatn. As Søndre Folgefonna continues to recede, these lake will continue to grow in size until extinction of the glacier. These finger lakes can be clearly seen in Figure 4.26.

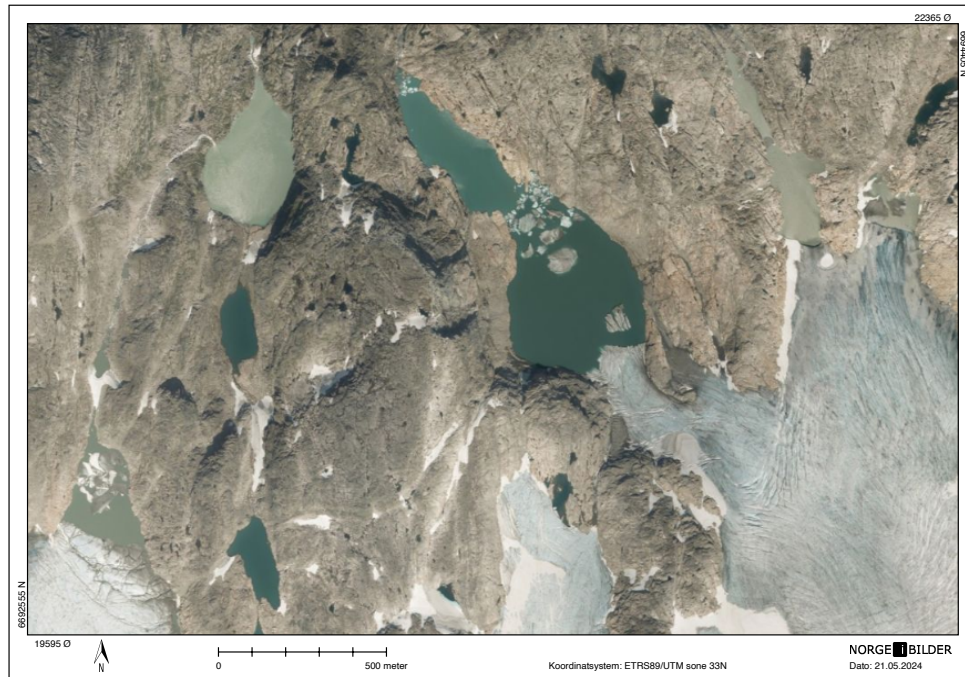


Figure 4.26 Series of proglacial lakes extending from the termini of Gråfjellsbrea and Breidablikkbrea, into Mysevatn. Photo sourced from NorgeiBilder.no (Norge digitalt, 2024).

Ice fall is a potential issue faced by Juklavatn, with the Juklavassbrea terminus present just 65 m from the lake boundary. As Juklavassbrea continues to recede, this will likely become less of a problematic condition, as the lake, at full extent, does not come into direct contact with the glacier, and the distance between it and the calved icebergs will only become larger. No documented cases or events are present for Juklavatn in this case. Because the icefall hazard is not calculable from visual observations (no aerial photos show active icebergs present in the lake of any available year), it will not be included in an event tree analysis, but should still be recognized as a viable hazard. More data and information is needed in this regard.

4.3.6 Other hazards

The only other recognized hazards for Folgefonna reservoirs are the potential for rockfalls and avalanches. There don't appear to be loose soils present in the region (only hardened bedrock), but the lakes are positioned in locations with heightened peaks susceptible to sudden avalanche. These would have to be further analyzed in a separate study with more available information and understanding.

Another additional hazard is lack of subglacial topography. With unknown potential subglacial lakes, an assessment may be needed for a potential breach that can't be identified visually. There are no records of such events, reducing its likelihood, but should still be contended as a viable hazard.

4.4 Reinoksfjellet

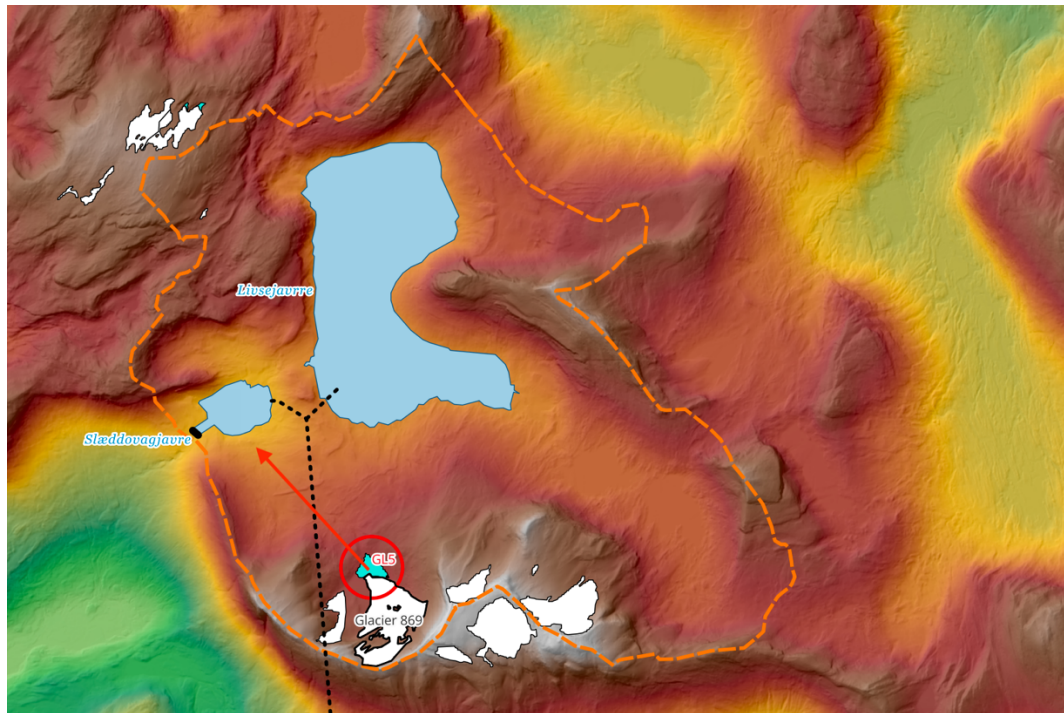


Figure 4.27 Overview of Reinoksfjellet glacier system, Slæddovagjavre dam, and GL5 hazard. DTM data from Høydedata.no (Kartverket, 2024).

Located at in Hamarøy municipality, Nordland, Reinoksfjellet (also referred to as *Hierggevarre*) is a remote mountain peak reaching 1472 MASL, covered by several smaller, unnamed glaciers. These glaciers direct meltwater into Reinoksvatn to the south and Livsejav'ri and Slæddovagjavre to the north. NVE recognizes 7 individual glacial formations with numerical identifications, ranging in size from 0.01 km² to 0.58 km². It is evident that these glaciers are remnants of a once much larger body of ice that has shrunk considerably. Glacier 869, a small cirque glacier, is of particular interest, as it now features an exposed proglacial lake near its outlet. This will be observed further for its influence on Slæddovagjavre reservoir later. The other glaciers in this location appear to also be of cirque-type, or as small ice aprons. It can be assumed that if climatic conditions continue, the glaciers will likely become extinct in this region in the near future. As remote and small-scaled as this region is, there is no available literature regarding the glaciers or mountain peaks, however the site is located just around 9 km northeast from Veikdalsisen, a 2.67 km² glacier with geophysical features similar features.

4.4.1 Slæddovagjavre

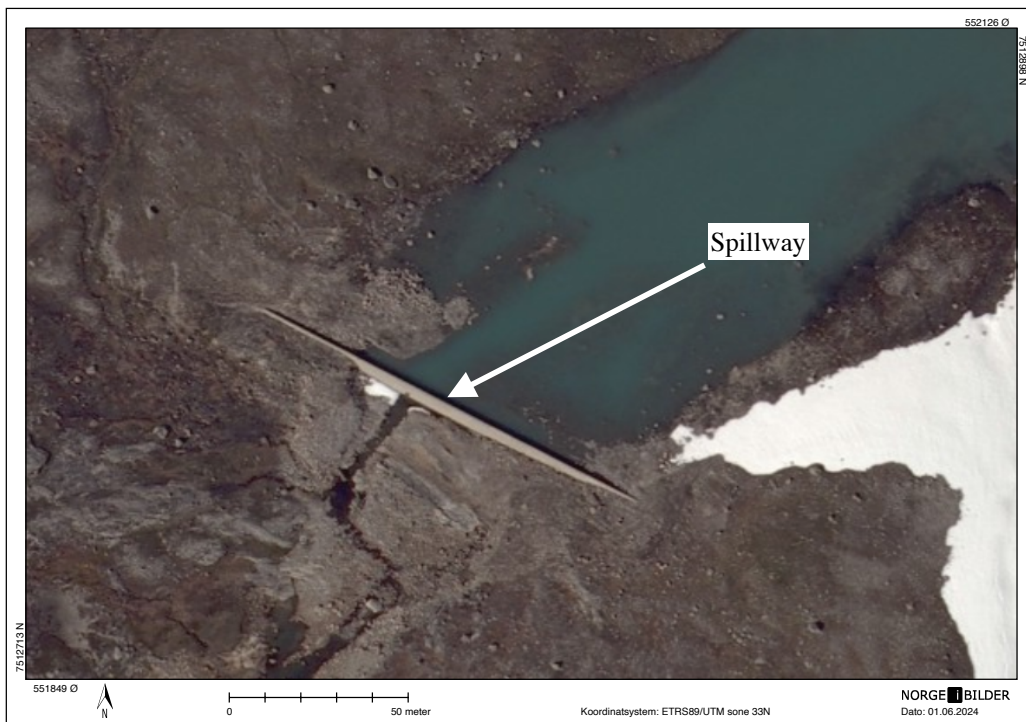


Figure 4.28 Aerial photo of Slæddovagjavre concrete dam, with spillway located in center of crest. Sourced from NorgeiBilder.no (Norge digitalt, 2024).

Slæddovagjavre (spelled in variations of *Slæddovagjavrre*, *Slæddovagjav'ri*) is a 2×10^6 m³ reservoir built in 1987, with a short 5 m tall gravity dam located in Hamarøy municipality, Nordland. The catchment size for the lake is estimated at 41.95 km² whereas the lake spans just 0.49 km². It is considered a consequence class level 1 dam, in large part due to the remoteness, and is part of the Kobbelv power plant, operated and owned by Statkraft Energi AS, with a potential generating capacity of 2x150 MW (SWECO Norge, 2009). Its operating HRV is noted as 652.5 MASL and LRV at 650.5 MASL. The dam is founded entirely on solid bedrock, and is approximately 135 m long, and 0.5 m thick. It features a singular bottom release flow hatch. The dam's crest is situated at 653 MASL (0.5 m of freeboard from HRV). The spillway is inset in the crest by 1.1 m and begins to initiate flow at 651.9 MASL.

An interesting note is how susceptible the dam is to overtopping. As it is in consequence class 1, this is not of significant priority, however the recommendation is made to enlarge the dam to increase its potential buffering capacity. In its current state, Slæddovagjavre dam is capable of only managing below the design flood (Q_{500}) of 88 m³/s flow before overtopping. At this flow rate, consultants estimate that the dam is still overtopped by 0.10

m. This of course is an alarming note, as a Q_{500} event is a small event when compared to other dams dimensioned to Q_{1000} , however, the dam is solidly founded on bedrock.

4.4.2 Identified hazards

Table 4.7 Determination of fundamental hazards for selected dams at Reinsokfjellet.

Reinoksfjellet Hazard Matrix			
Dam	H1 (rapid melt and precip.)	H2 (breach of glacial lake)	H3 (icefall or calving)
Slæddovagjavre	Applicable	Applicable	Low concern

As indicated by Figure 4.29, there is a significant moraine-dammed glacial lake extending from the outlet of the cirque glacier identified as 869 by NVE ID. This glacier, although small, has been generating a lake pocketed by what appears to be weak moraine material within the mountain cirque. When observing aerial photos from different years, it is evident that the lake is growing at a significant pace. Using the selected estimation method discussed in 3.3.1, it was found to have a potential volume in the realm of $1.50 \times 10^6 \text{ m}^3$. If completely released, it would almost certainly overwhelm the under-dimensioned dam at Slæddovagjavre lake.

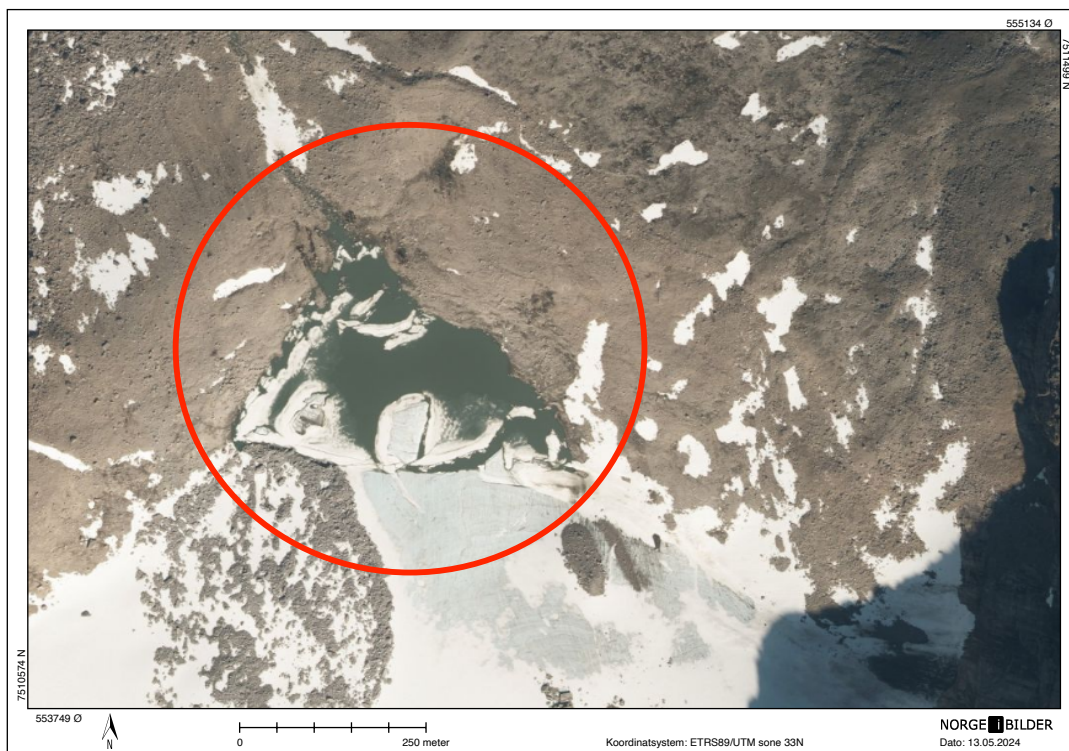


Figure 4.29 Slæddovagjavre proglacial lake identified from glacier 869 in Reinoksfjellet. Photo from NorgeBilder.no (Norge digitalt, 2024).

In photos, the lake appears to be draining through the loser material to the north, into the watershed that leads to Slæddovagjavre. An additional possibility is that in its sudden release, it could also transport high volumes of debris and glacial ice, worsening the flood condition with potential landslide or ice blockage. As discussed in 3.1.2, this specific case also has what appears to be early signs of rockfall or landslides surrounding the site. This is further indication of the dynamics of the geology in the area.

As with other reservoirs in this study, Slæddovagjavre is also assessed for the H1 condition. Although its catchment is noted as just 5.7% glaciated, and has design floods of Q_{500} (88 m^3/s) and PMF (133 m^3/s) exceeding the spillway capacity, as previously mentioned. These will be further analyzed in event trees for this case.

4.4.3 Other hazards

The only other concerning attribute for Slæddovagjavre is the steep cliff face located just northwest of the dam. This could be a potential location for avalanche or rockslide, however the danger is minimal, as the topography is not of great heights. The other surround areas are more gentle in slope, and do not appear to be of risk to the dam. The lake is fairly isolated, but may be influenced by potential overflow from Livsejavvre lake, just to its eastern side. This is likely also negligible, as the two are separated by a small peak, and both lakes have the ability to also divert water southward to the much larger reservoir, Fossvatn.

4.5 Storsteinsfjellbreen

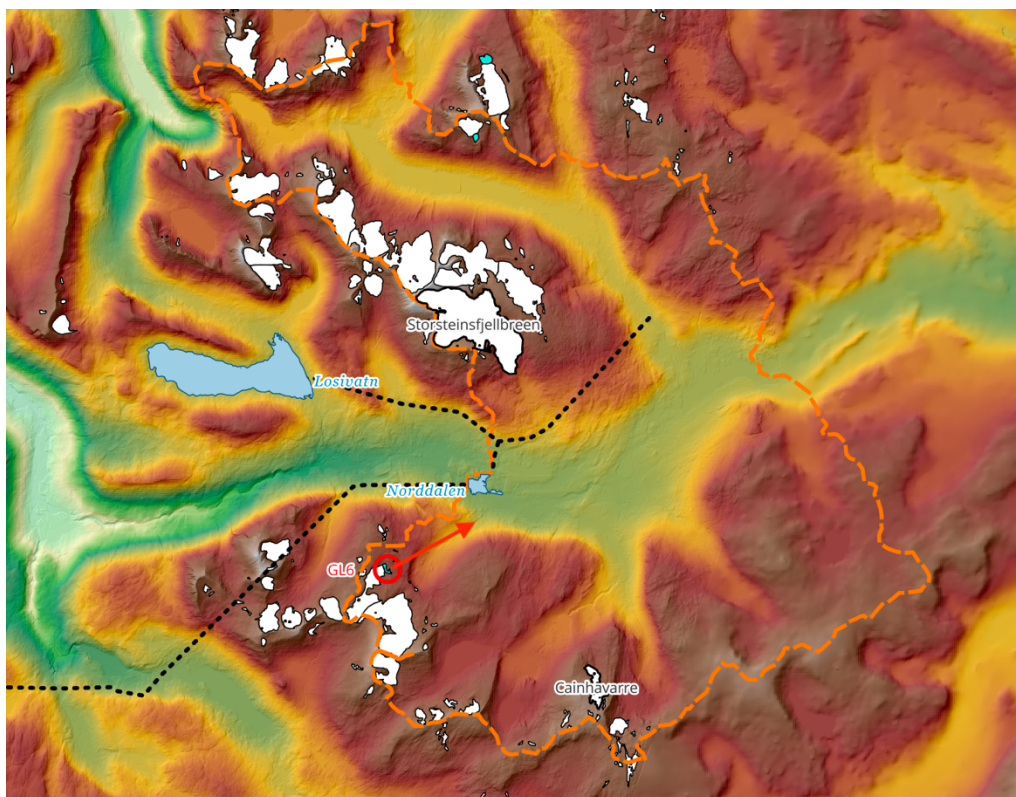


Figure 4.30 Overview of Storsteinsfjellbreen glacier system, Norddalen dam, and GL6 hazard. DTM data from Høydedata.no (Kartverket, 2024).

Storsteinsfjellbreen is one of the largest contributing glaciers to the Norddalen reservoir. Located 3.6 km away in Narvik municipality, Nordland, Storsteinsfjellbreen is a 5.17 km² valley glacier situated on and surrounding Storsteinsfjellet peak, reaching 1893 MASL (Kartverket, n.d.). A surprising finding from a series of mass balance studies conducted in the 1960s to 1990s was that although Storsteinsfjellbreen showed 60 m of drop at the tongue, the portion near the equilibrium line showed an increase of 20 m (Kjøllmoen & Østrem, 1997). The cumulative length change measurements from the directorate for Storsteinsfjellbreen are shown in Figure 4.31. These data collection studies were originally conducted as preparation for the construction of Norddalen and other hydropower projects in the region. Kjøllmoen and Østrem also note the overall mass loss from Storsteinsfjellbreen from 1960 to 1993 was approximated as 1.68×10^7 m³ of water.

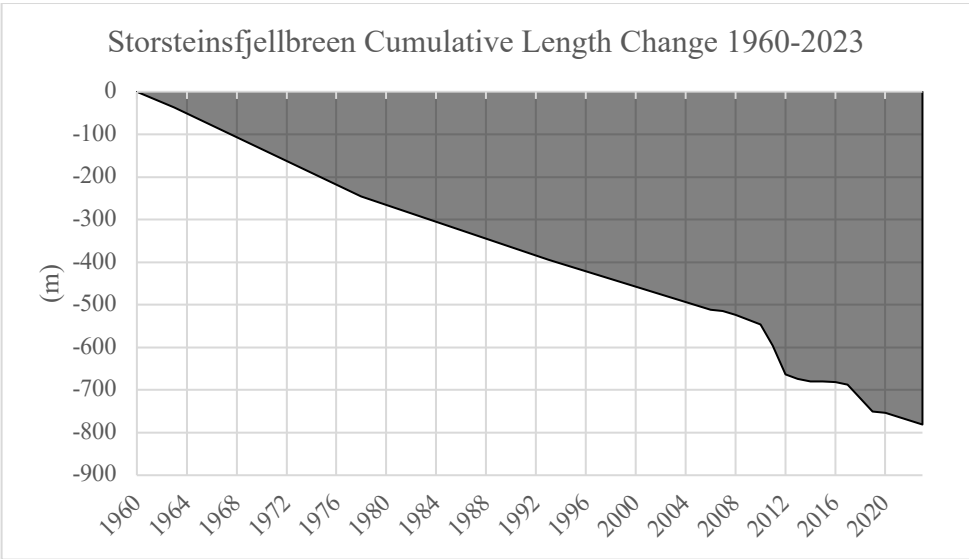


Figure 4.31 Cumulative length change for Storsteinsfjellbreen, 1960-2023, data provided by NVE.

Also contributing to Norddalen is the Cainhavarre glacier, measuring at only 0.45 km². This valley glacier is located 6.8 km southwest within a series of smaller fragmented glacierets near the Swedish border also in Narvik municipality. It currently hangs from the northeastern face of Rivgovarri peak (1582 MASL (*Huippuja*, n.d.)) as a remnant from a previous ice cap. There is a limited dataset for mass balance for Cainhavarre from 1965-1968. It is unclear why these observations were initially taken, but they also may have been conducted for upcoming hydropower projects.

Although these glaciers discussed appear to be very small, there are dozens of other small unnamed glacierets in the region, as seen in Figure 4.30 that do not have additional information.

4.5.1 Norddalen

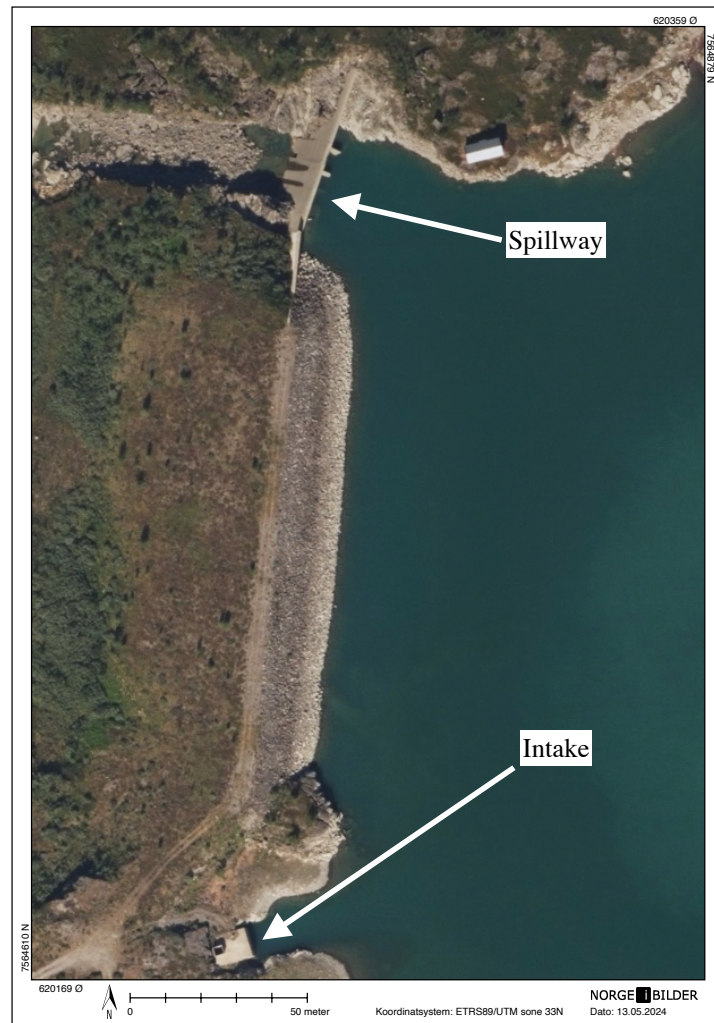


Figure 4.32 Aerial photo of Norddalen embankment dam, with separate concrete spillway visible on north end. Photo sourced from NorgeiBilder.no (Norge digitalt, 2024).

Norrdalen is a reservoir built in 1974 that is located in Narvik municipality, Nordland, which features a main moraine-cored rock-filled dam, as well as a separated concrete spillway structure. The dam is placed under consequence classification 2, and is responsible for transferring flow to the 313 MW Skjomen power plant, owned and operated by Statkraft Energi AS. The lake transfers flow to the Ipto reservoir further south and is connected to the transfer tunnel pulling water from the Lossivatn reservoir lying at the northwest, and the stream intake at Sælkajokka, northeast. Norrdalen dam includes an outflow sliding hatch near the base of the embankment that can be deployed in events of heavy inflow. The crest of this dam is measured at 16 m tall, and 145 m long, whereas the spillway dam is approximately 11 m tall and has a length of 18 m, that initiates at HRV elevation. The regulation of the dam is set between a HRV of 641 MASL and a LRV of 636 MASL. At the northern end of Norrdalen, there is also a check dam composed of rock-fill that measures 55 m long and 6.5 m tall.

The lake is very unique to this study in regards to the enormous catchment area (281 km²) in respect to the lake size (0.36 km²), and its original designed purpose- to capture extreme

floods from rapid snow melt or “breakage of snow dams” (potentially a reference to GLOFs) (SWECO Norge, 2023). Perhaps this is why the dam features a very high freeboard of 5 m (top of crest is 646 MASL). This location is however a double-edged sword, as it has been noted that the current design floods overtop the concrete dam. This does not yet affect the main dam, however. It should be noted that the filter extends the entirety of the dam height to the crest elevation. To add to the danger, the dam does not currently have any sort of protective armoring at the crest (SWECO Norge, 2023), meaning a sizeable flood or seiche wave could initiate cutting into the embankment.

The separate concrete spillway dam fails to regulate the standard design flood rated at 336 m³/s and is overtopped by 0.22 m. As concerning as this is, this does not lead to overtopping of the embankment dam, which won’t occur until the PMF is greatly exceeded (which is estimated as 1,012 m³/s).

4.5.2 Identified hazards

Table 4.8 Determination of fundamental hazards for selected dams at Storsteinsfjellbreen.

Storsteinsfjellbreen Hazard Matrix			
Dam	H1 (rapid melt and precip.)	H2 (breach of glacial lake)	H3 (icefall or calving)
Norddalen	Applicable	Applicable	Low concern

As Norddalen has a significantly large catchment area of 281 km², it is worthwhile investigating a potential H1 hazard, as it is estimated to be 8.5% glaciated, and could generate a significant amount of meltwater to a reservoir that is relatively small in comparison. With design floods rated at Q₁₀₀₀ of 336 m³/s and PMF of 1,012 m³/s (SWECO Norge, 2023), this secured the potential hazard to be assessed in an event tree analysis following. To alleviate this concern, there was the note in reports that the lake was knowingly designed to capture GLOF floods, so its susceptible position was recognized upon the planning of the dam and was most likely properly accounted for.

Glacial lake hazards are not very evident in this case, aside from a small proglacial lake found at the outlet of glacier 687 (NVE ID). This is a small valley glacier of just 0.9 km², however the lake was further analyzed for properties. It is visible at the end of the glacier terminus in Figure 4.33.

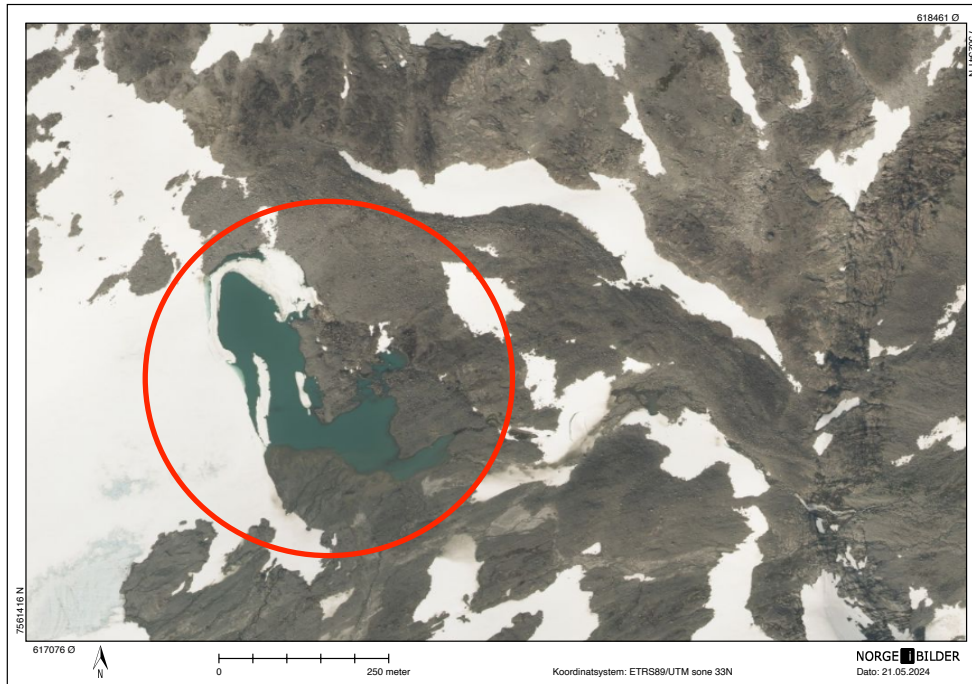


Figure 4.33 Small proglacial lake identified extending from a glacier atop Nuorjjo varri mountain, leading to Norddalen. Photo from NorgeBilder.no (Norge digitalt, 2024).

After applying the calculations referred to in 3.3.1, it was found to have a potential volume of approximately $6.23 \times 10^5 \text{ m}^3$. This is a very small value, and likely not of significant concern to Norddalen, however it is still assessed in an event tree later. If the lake were to breach completely, it would still need to travel nearly 4.4 km to enter the reservoir. At this travel distance, it has likely been dampened significantly. The lake appears to be moraine-dammed, and is situated atop a significant cliff that leads into a basin. The cliff face appears to also be made of slightly weaker material, and could experience a paired landslide in the event of drainage.

4.5.3 Other hazards

Other very small glacial lakes were identified even further to the southeast, however these were not assessed further, as they likely contained even lower volumes of meltwater, and would need to travel much further distances, making them not an applicable threat. Norddalen is very well protected in a broad valley from the types of hazards such as landslides, avalanches, or rockfalls. Calving is also clearly not an issue faced by this reservoir. The closest steeper slope would be Cahppesjunni peak, located just under 1 km away, however it is very small and likely not an issue to the reservoir. The largest potential hazard is a possibly unidentified subglacial lake beneath Storsteinsfjellbreen. This glacier is quite significant, and unless a subglacial topographic map can be generated, may contain pocket of meltwater with dangerous potential that should be recognized.

4.6 Hardangerjøkulen

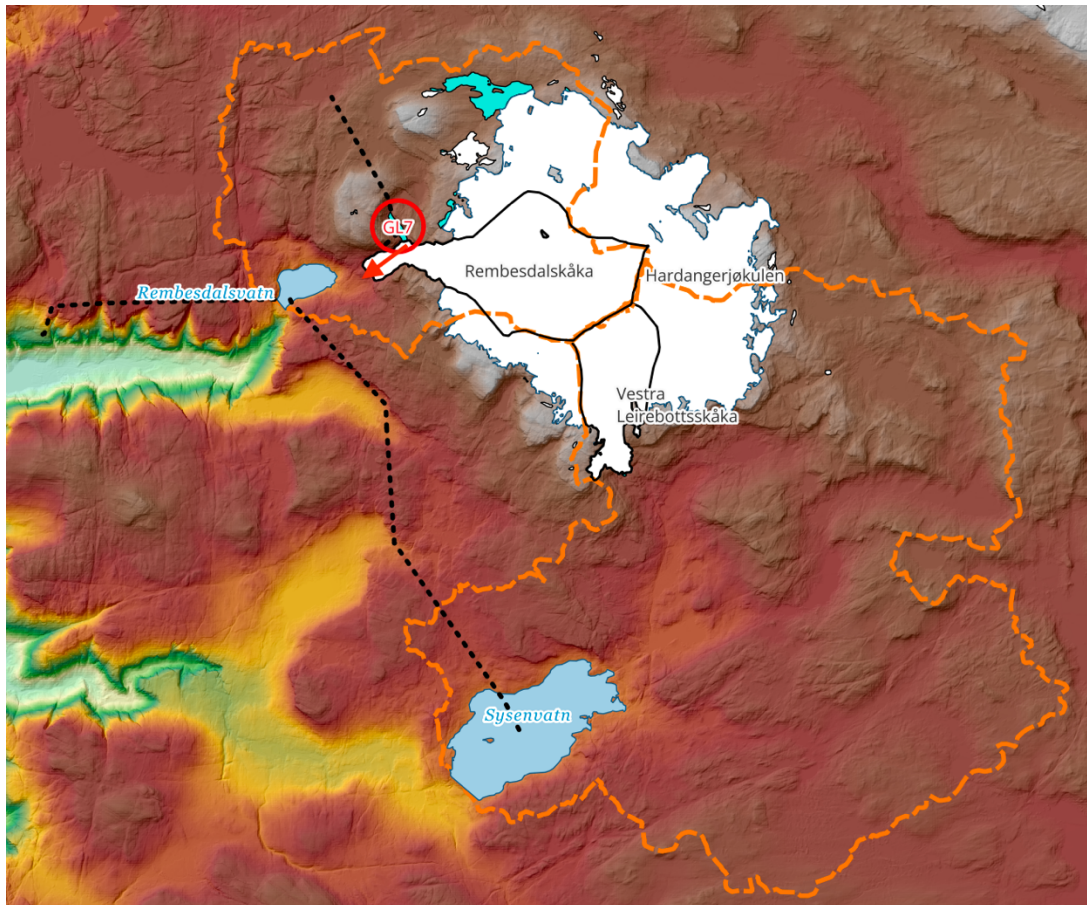


Figure 4.34 Overview of Hardangerjøkulen glacier system, Rembesdalsvatn and Sysenvatn dams, and GL7 hazards. DTM data from Høydedata.no (Kartverket, 2024).

Hardangerjøkulen is a well-known ice cap glacier located in Vøringfoss and Finse municipalities, Hordaland. It spans across 64 km² and is the main contributor to both Rembesdalsvatn and Sysenvatn, discussed later. Hardangerjøkulen is also a popular study case for scientists regarding climate change and its effects on glacial dynamics. One study (Giesen & Oerlemans, 2010) made the prediction that the entire glacier may potentially disappear by year 2100, so long as there is a linear temperature increase of 3° from 1961-1990 to 2071-2100. This is correlated to the estimate that predicts the ELA will be above the upper margins of the glacier by the 2080s (Nesje, 2023).

Within Hardangerjøkulen, there a number of smaller divided glaciers. To the west, Rembesdalskåka is a 17 km² valley glacier primarily feeding Rembesdalsvatn. It has available ongoing mass balance data from NVE starting in 1963, as shown in Figure 4.35, and length changes in Figure 4.36. One may notice the interesting variation seen in the late 1980s to 1990s, where there was several years of trending positive mass balance. This is also reflected in the length change history, where Rembesdalskåka actually grew in length over the course of several years following the positive mass balance trend.

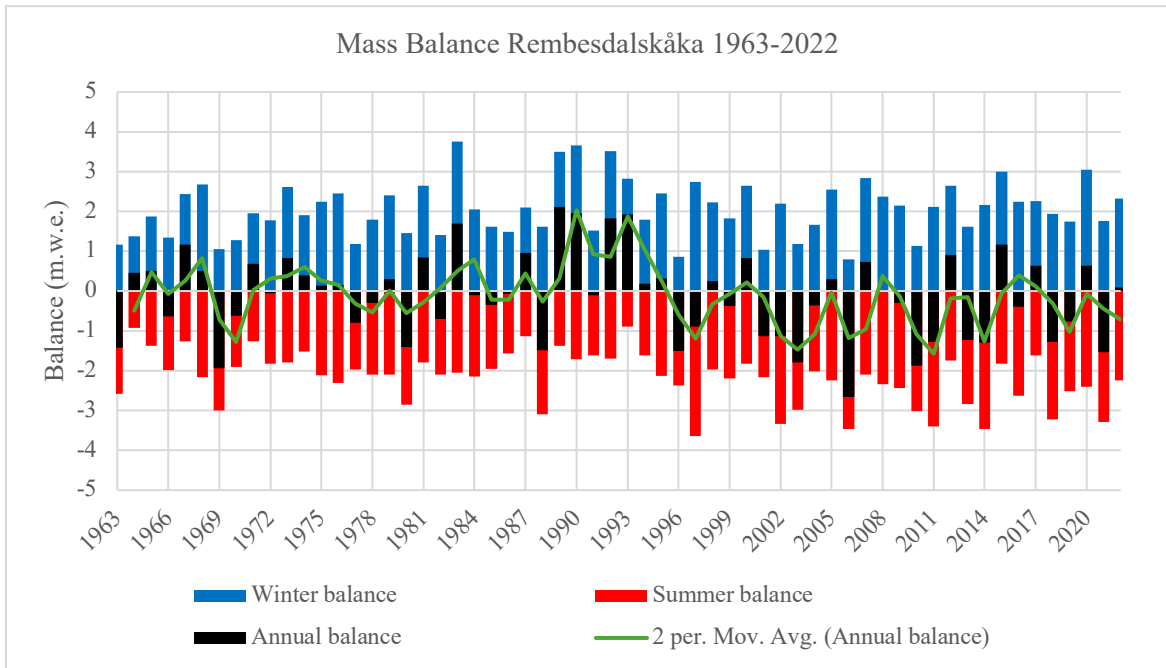


Figure 4.35 Mass balance for Rembesdalskåka, 1963-2022, data provided by NVE.

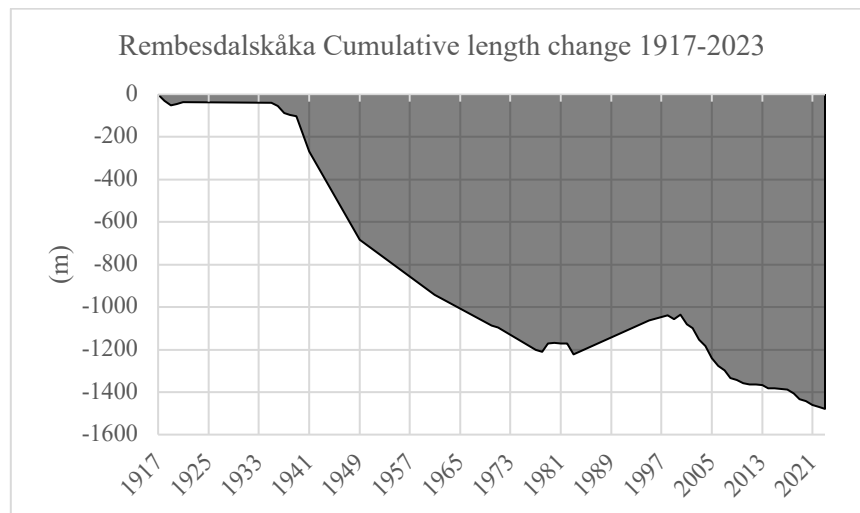


Figure 4.36 Cumulative length change for Rembesdalskåka, 1917-2023, data provided by NVE.

One particularly interesting feature of Rembesdalskåka is the ice-dammed glacial lake extending north from near the terminus. It has a well-documented history of GLOF drainage events into Rembesdalsvatn that are later discussed in detail.

On the eastern margin, lie the Vestra Leirebottskåka and Torsteinsfonna glaciers, 7.55 km² and 1.1 km², respectively. They provide meltwater through a series of erosion lakes and other reservoirs eventually leading to Sysenvatn at the south. These glaciers do not have any mass balance data and are flanked by unnamed glaciers within Hardangerjøkulen of similar size.

4.6.1 Rembesdalsvatn

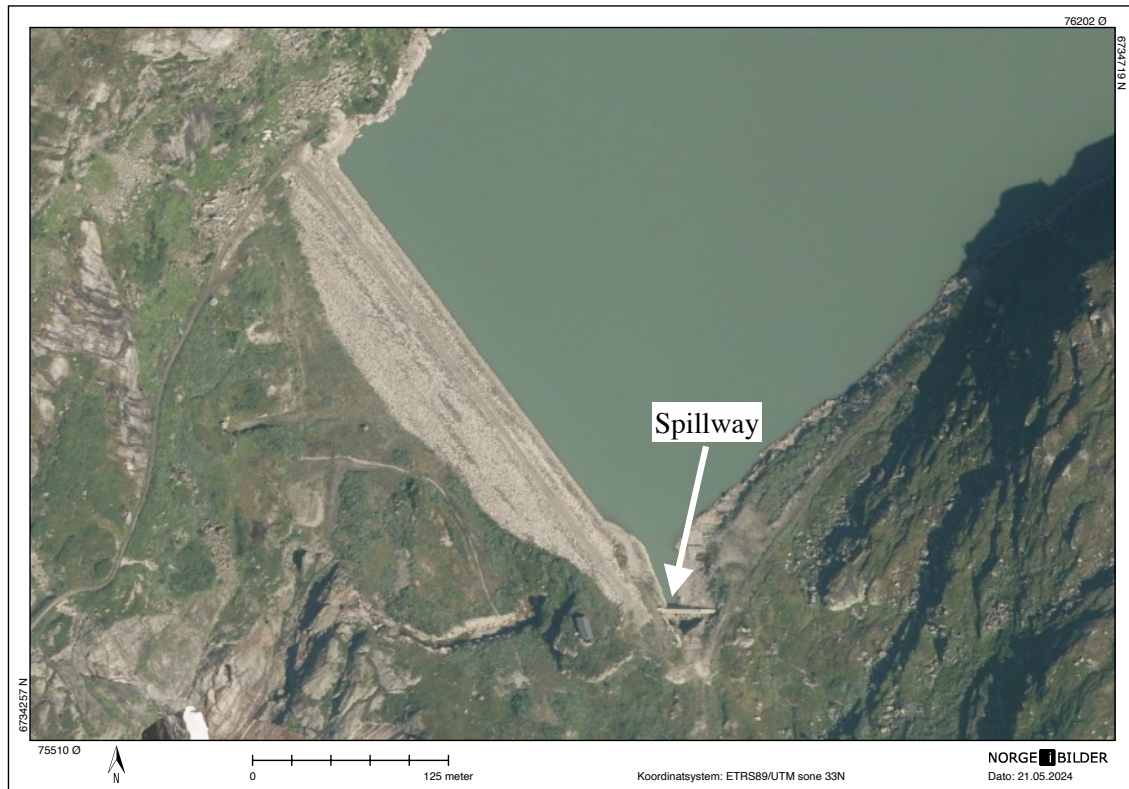


Figure 4.37 Aerial photo of Rembesdalsvatn embankment dam, with separate spillway indicated. Sourced from NorgeBilder.no (Norge digitalt, 2024).

Located in remote Eidfjord municipality, Vestland, Rembesdalsvatn is a regulated reservoir serving the 1,120 MW Sima power station owned and operated between Statkraft Energi AS (65%), Eviny AS (26.25%), and SKL AS (8.75%). It has approximately 3.9×10^7 m³ in capacity at HRV (905 MASL). The LRV is noted as 860 MASL, and the crest is situated at 910.5 MASL (5.5 m of freeboard) (Norconsult, 2019). Rembesdalsvatn receives inflow from its highly glaciated catchment, as well as from a transfer tunnel via Sysenvatn from the south. The dam is rock filled with a sealed moraine core extending to 908.5 MASL and was built in the period of 1976-1980. The dam is regarded as consequence class 3, and measures 385 m long and 43 m tall at its greatest extent. Fortunately, Rembesdalsvatn dam is constructed on a base entirely composed of bedrock.

The concrete spillway is detached from the dam, shown at the southern end in Figure 4.37, and measures at 23.5 m long at an average of 5.5 m tall. It is configured in a plate-style, sandwiched between two taller weirs (extending to 906 and 908.2 MASL, respectively), with an outlet directing the flow into a chute later directed into a tunnel. It initiates overflow when the water level reaches HRV elevation and can activate explosive measures should there be an emergency where rapid lowering is necessary. In 1998, there were a number of different improvements implemented, including a rehabilitation of the spillway structure by increasing its length, as well as widening the outlet flood tunnel from 24 to 29 m². A concerning finding is that the estimated PMF flood results in complete overtopping of the dam, as a result of limitations with the outlet flood tunnel. The recommendation was to expand its capacity by 100-150 m³/s to mitigate this (Norconsult, 2019).

4.6.2 Sysenvatn

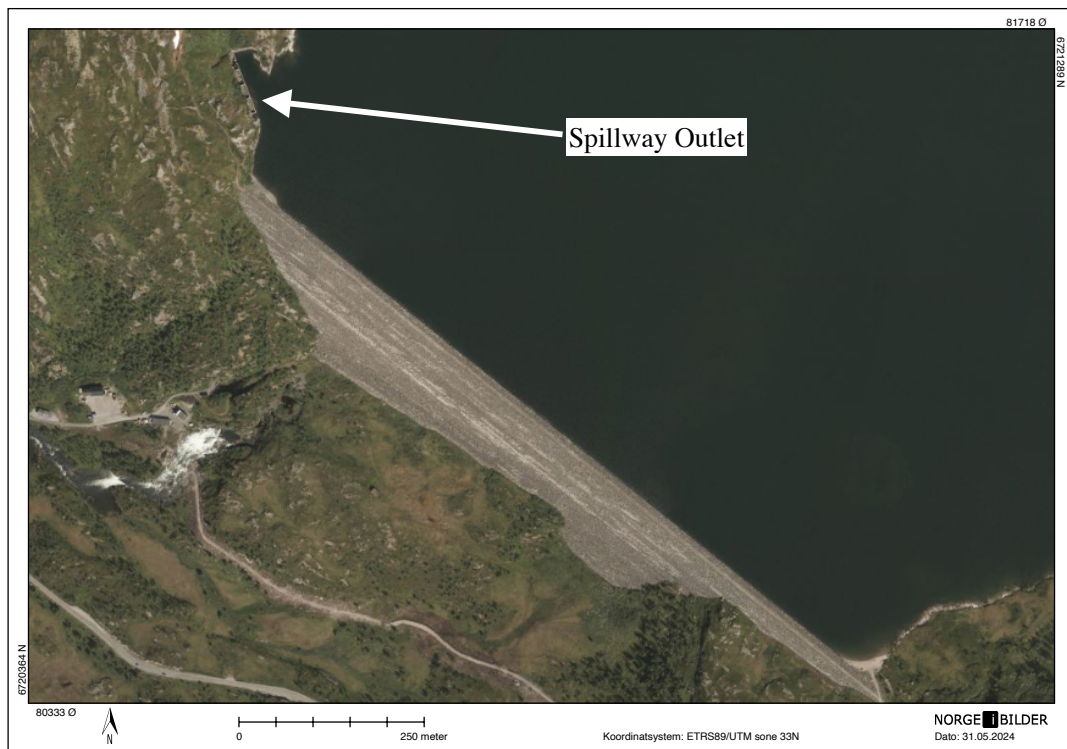


Figure 4.38 Aerial photo of Sysenvatn dam, with spillway outlet indicated on the north end. Active outflow is also visible from the embedded tunnel. Sourced from NorgeiBilder.no (Norge digitalt, 2024).

Sysenvatn is a 10.47 km² lake located south of Handangerjøkulen in Eidfjord municipality, Vestland. The lake's capacity is reported as 4.00x10⁸ m³ at HRV (940 MASL). The LRV is specified at 874 MASL, and the crest of the class 4 dam lies at 945 MASL (providing 5 m of freeboard) (Norconsult, 2020). This 1,160 m long, 81 m tall rockfill dam, founded on bedrock, directs water to the Sima power plant system, through Rembesdalsvatn. Inflow is generated from the massive 211.4 km² catchment, and intakes further south at Bjoreia/Tinnhølen. There is an outlet that can also be directed to the Lero watercourse, to the south. The dam was constructed between 1975 and 1980 by NGI on a solid bedrock foundation, and features a sealed moraine core extending to 942.3 MASL. The separate spillway exists at the north side of the dam, indicated in Figure 4.38. This spillway arranged in 4 canal sections that drop into a 335 m long collection tunnel and is equipped with an explosive field for emergency use. It has been noted in reports that the dam does not adequately divert flood flows from design. Another deficiency was the low 5 m of freeboard, which is less than the required 6 m in regulation.

4.6.3 Identified hazards

Table 4.9 Determination of fundamental hazards for selected dams at Hardangerjøkulen.

Hardangerjøkulen Hazard Matrix			
Dam	H1 (rapid melt and precip.)	H2 (breach of glacial lake)	H3 (icefall or calving)
Rembesdalsvatn	Applicable	Documented hazard	Low concern
Sysenvatn	Applicable	Low concern	Low concern

Rembesdalsvatn and Sysenvatn lie in highly glaciated catchments, 36.6%, and 9.3%, respectively. They are significantly influenced by both the western and southern margins of Hardangerjøkulen and are assessed for H1 for this reason. According to reports, Rembesdalsvatn's design floods are 318.1 m³/s for Q₁₀₀₀ and 592.2 m³/s for PMF (Norconsult, 2019), whereas Sysenvatn's are 425.4 m³/s for Q₁₀₀₀ and 666.5 m³/s for PMF (Norconsult, 2020).

For glacial breach condition, H2, Rembesdalsvatn is a well-suited candidate for encountering potentially dangerous lake drainages from the aforementioned glacial lake identified in some literature as *Demmevatn*, located on the northern margin of the terminus (Snorrason et al., 2002). This lake has significant history of outbursts, summarized in Table 4.10.

Table 4.10 Historical GLOF occurrences within Rembesdalskåka, at Demmevatn.

Date	Outburst Volume (x10 ⁶ m ³)	Details of Event
1736	Unkown	Only "flood damage" reported (Jackson & Ragulina, 2014). Earliest known flooding events at Demmevatn.
1813	Unkown	
1842	Unkown	
17/09/1861	Unkown	Significant flood damage reported, including two bridges (Liestøl, 1956).
20/08/1893	35	Estimated to have drained in the span of 24 hours. Reached an average flow rate of approximately 400 m ³ /s. One of the most significant floods on record for Demmevatn (Liestøl, 1956).
17/08/1897	Unkown	Demmevatn noted to have rose above the surface of Rembesdalskåka, draining over the glacier, and then proceeding to melt into the ice and form a crack that reached the base of the glacier in the span of 26 days, in which the lake proceeded to drain (Liestøl, 1956).

10/08/1937	11.5	Significant flood determined to have lasted around 3.5 hours. Estimated outflow average was 900 m ³ /s and had been found to drain through a tunnel below Demmevatn (Liestøl, 1956).
23/08/1938	10	Flood started before new drainage tunnel was completed, and took place through a tunnel at the bottom of Demmevatn (Liestøl, 1956).
25/08/2014	1.9	Flood duration of 3 hours, had occurred in the evening of the 25th and discovered the next day (Jackson & Ragulina, 2014).
25/01/2016	1.44	Demmevatn noticed empty on January 30th, whereas it was originally confirmed filled on January 24th (Kjøllmoen et al., 2017).
06/09/2016	1.87	Sudden increase in Rembesdalvatn noticed, and lasted for a total four hours (Kjøllmoen et al., 2017).
27/10/2017	1.85	Drainage discovered by Statkraft when Demmevatn was reported once more emptied. Rembesdalvatn had reportedly rose by 1.87 m in less than 24 hours. Undiscovered for nearly a month. Outflow had increased from 5 m ³ /s to 40 m ³ /s following the drainage (Kjøllmoen et al., 2018).
10/08/2018	Unkown	Unkown volume drained, however the event was reported by local that had noticed that Demmevatn had released, likely from overnight (Kjøllmoen et al., 2019).
24/08/2019	1.8	Only discovered during a noticeable rise in Rembesdalvatn. The lake allowed release flow of 170 m ³ /s for 3 hours (Kjøllmoen et al., 2020).
06/09/2020	2.3	Flood released in 5-6 hours, the second largest recorded since 1938. Initiated in the morning until afternoon hours (Kjøllmoen et al., 2021).
13/07/2021	2	Flood determined to be approximately 1.5-2.0x10 ⁶ m ³ in the span of 3-4 hours (Kjøllmoen et al., 2022).
30/08/2022	2.2	An outflow was recorded by Statkraft during the evening in 11 hours (Kjøllmoen et al., 2023).
22/06/2023	1	An outflow was recorded by Statkraft during the evening, released in just 6 hours (NVE, n.d.-a).

As evident by the nature and activity of Demmevatn (shown in Figure 4.39), it is safe to assume this ice-dammed lake will continue to drain in the future and will be directly assessed in an event tree analysis. Although the floods have become significantly more dampened when compared to events recorded in the 20th century with the inclusion of a drainage tunnel, they are still important to observe for potential impacts that may occur to Rembesdalvatn. An independent study financed by Statkraft estimated that the lake will continue to flood, however in much more modest values, unless blockage of the rock tunnels were to occur (Snorrason et al., 2002).

Aside from this lake, to the north and northwest margins of Hardangerjøkulen, there are several exposed proglacial lakes of significant size (may be supraglacial- difficult to

discern). Without subglacial topography available, it is unclear whether these drain back into the glacier for certain, or remain stagnant. The large bedrock-dammed glacial lake to the northwest from glacier 2962 appears to drain into the lakes to the west and does not appear to be dangerous or susceptible to GLOF events, from visual inspection, and is excluded from this assessment. This is also the case for the smaller supraglacial lake to the west, shown in Figure 4.39, from glacier 2963. Also shown in Figure 4.40, it appears to be growing at a significant pace. It is also unclear whether this drains back into the glacier, however there is an identified stream exiting to the southwest into Rembesdalskåka. Upon inspection of the surrounding topography, it was determined as likely bedrock dammed in a basin below the glacier, which is not a rapid drainage hazard, therefore chosen to be excluded from further analysis.

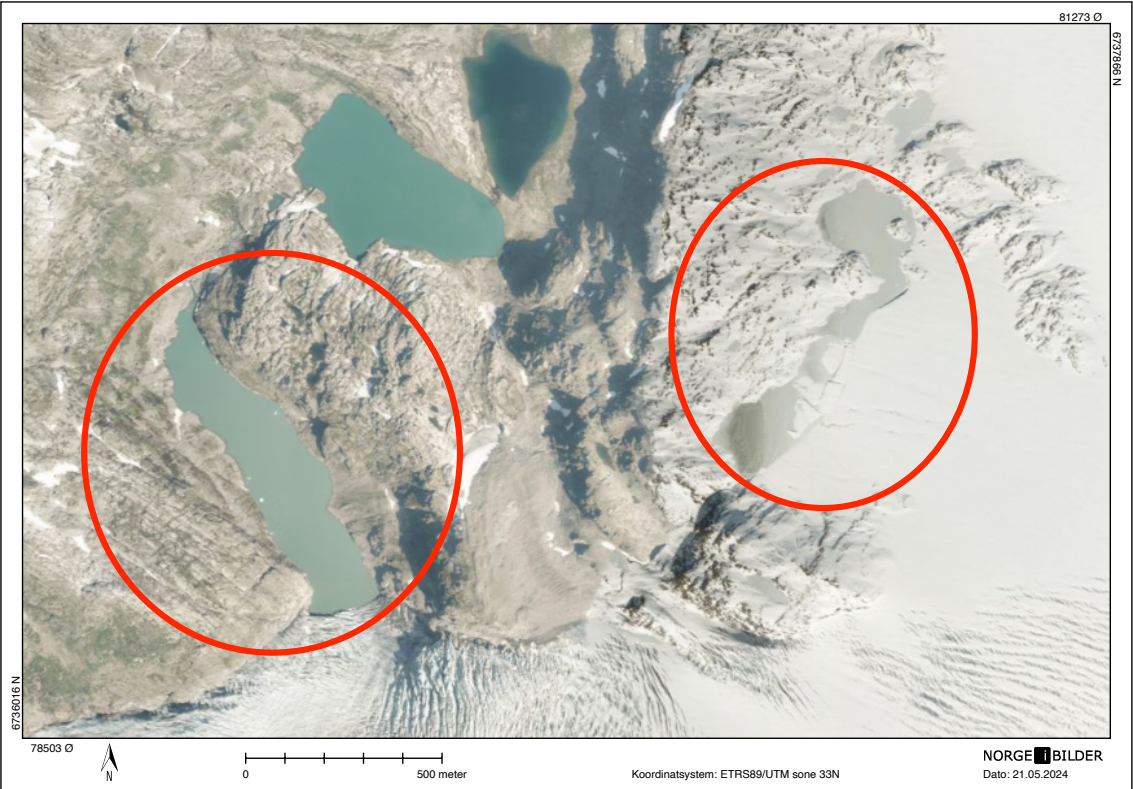


Figure 4.39 Demmevatn (GL7) indicated to the left, extending into the terminus of Rembesdalskåka. Additional proglacial lake identified on right, appearing to be bedrock dammed. Photo sourced from NorgeiBilder.no (Norge digitalt, 2024).

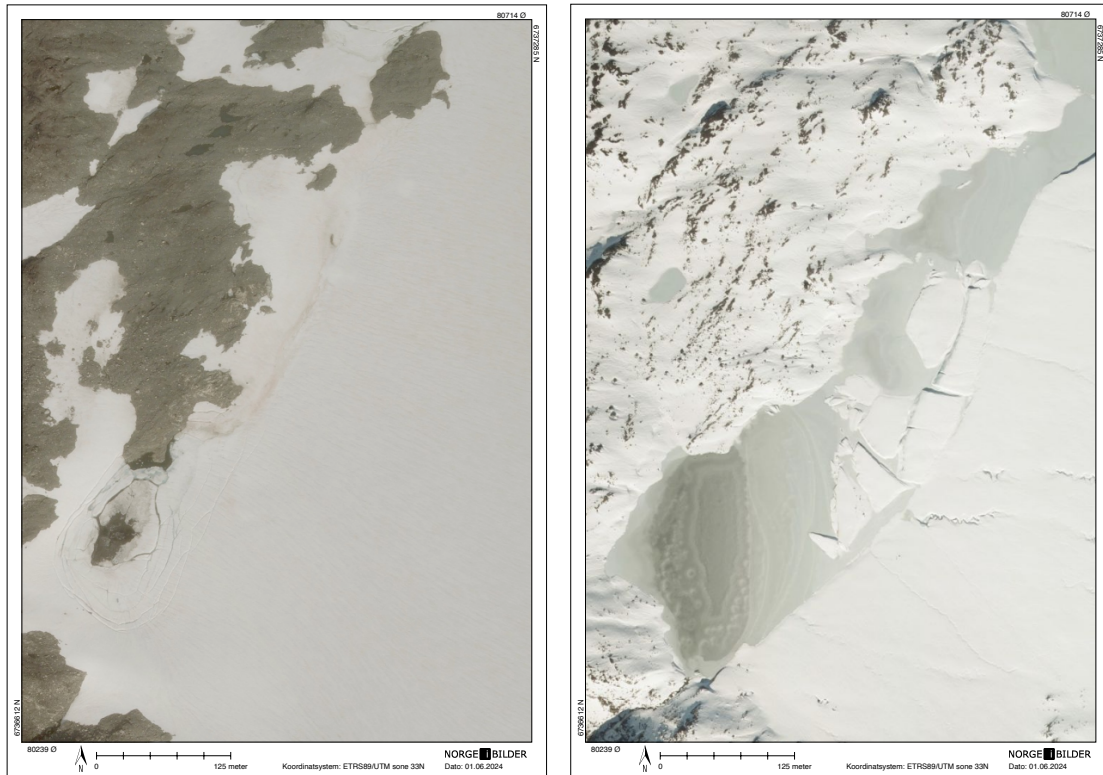


Figure 4.40 Proglacial lake identified extending to western margin of glacier 2963 (NVE ID). Timelapse showing significant growth of lake from 2008 (left) to 2019 (right). Photos sourced from NorgeiBilder.no (Norge digitalt, 2024).

4.6.4 Other hazards

In past years, Rembesdalskåka would have had contact with Rembesdalsvatn, but as it no longer does, the condition of calving is not of concern. In regards to hazards such as avalanche, rockfall, or landslide, neither Rembesdalsvatn nor Sysenvatn are in a geographical position for these to be of real concern. Of course, they should be further assessed, but from visual assessment, they lie in flat plains in far proximity from steeper cliffs.

With a large enough GLOF from a glacial lake, Rembesdalsvatn could be at some level of danger for iceberg entry, should the flood be powerful enough to transport partitions of Rembesdalskåka downstream. This is a highly unlikely scenario due to the distance this would need to travel.

4.7 Svartisen

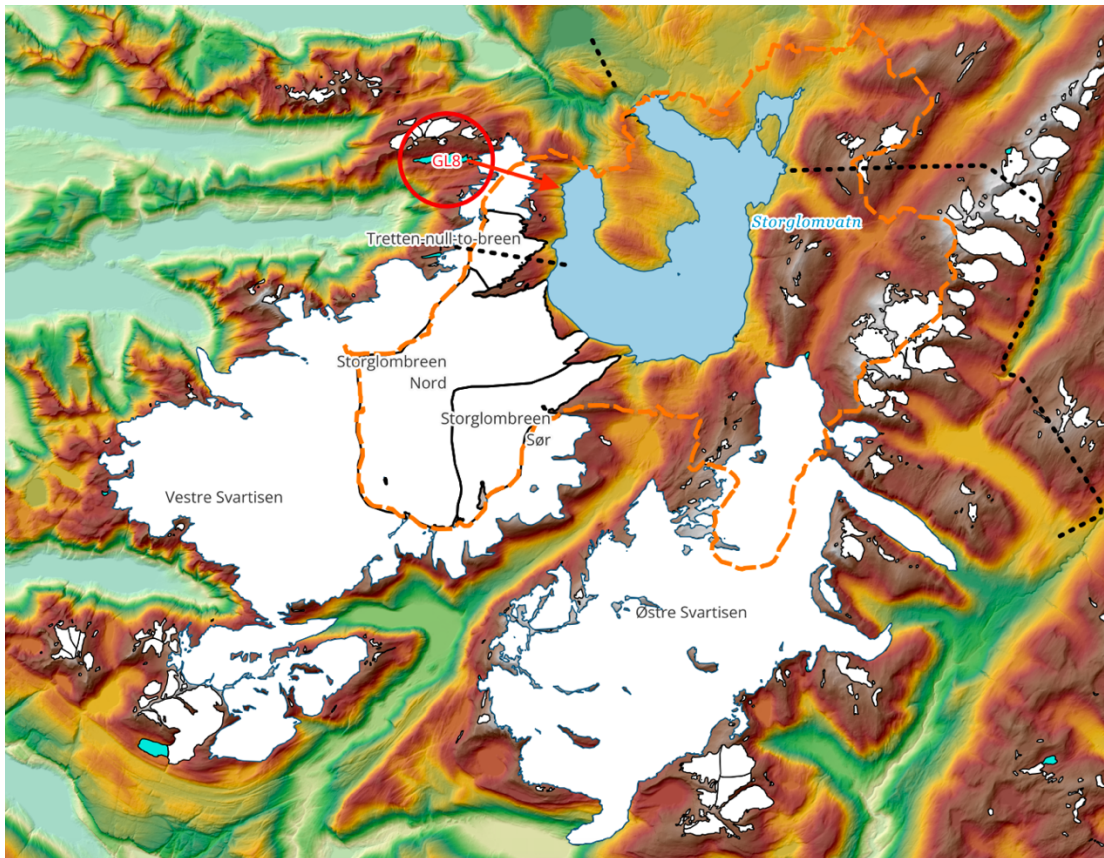


Figure 4.41 Overview of Svartisen glacier system, Storglomvatn, and GL8 hazard. DTM data from Høydedata.no (Kartverket, 2024).

Svartisen is a massive ice cap glacier complex in Nordland consisting of both Vestre Svartisen (190.22 km²) and Østre Svartisen (125.1 km²). These glaciers are separated by the Vesterdalen valley, one of the concentrated collection basins for meltwater. Vestre Svartisen alone is one of the largest in Norway, second only to Jostedalsbreen, whereas Østre Svartisen is the fourth-largest (Liestøl & Thorsnæs, 2024). As it is located in such close proximity to the Atlantic ocean, there is a significant differentiation in annual precipitation, with the western side receiving on average 2,000 mm/year, where the drier eastern side receives approximately 1,000 mm/year (Benham & Dowdeswell, n.d.). This resulted in Vestre Svartisen actually experiencing periods of advancing front positions in the past, whereas Østre Svartisen experienced recession in the same years.

Within Vestre Svartisen, particular interest is on Storglombreen Nord (40.54 km²), Storglombreen Sør (15.3 km²), and Tretten-null-to-breen (5.03 km²), as these named glaciers directly contribute to Storglomvatn lake. Although they have mass balance data from the 1980s and 2000s from NVE, the data collection was very inconsistent, and isn't particularly useful when attempting to identify trends.

4.7.1 Storglomvatn

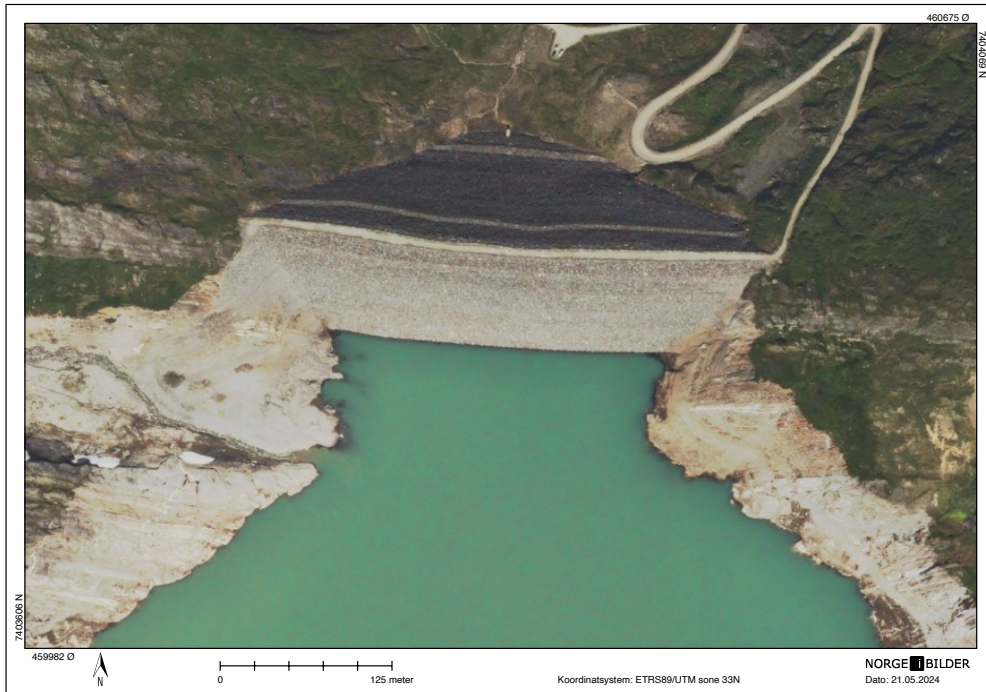


Figure 4.42 Aerial photo of Holmvatn dam on the western side of Storglomvatn, which does not feature a spillway structure. Photo sourced from NorgeiBilder.no (Norge digitalt, 2024).



Figure 4.43 Aerial photo of Storglomvatn dam on the eastern side of Storglomvatn, with large concrete dam spillway visibly active at northern end. Photo from NorgeiBilder.no (Norge digitalt, 2024).

Located in Meløy municipality, Nordland, Storglomvatn (also referred to as *Stårglomvatn*) is an enormous 3.51×10^9 m³ reservoir, located within the Svartisen glacial system. The reservoir is dammed in two ends, one being Storglomvatn, and the other being Holmvassdammen, both labeled as consequence class 3. The lake was originally dammed from an older concrete slab dam, also under the name Storglomvatn dam (NVE, 2015). The older was built in 1942 and is now located well within the current reservoir body after decommissioning. Storglomvatn has a regulated HRV of 585 MASL and a LRV of 460 MASL, indicating an enormous variability in storage capacities. To date, it is Norway's most usable reservoir volume that can be regulated (NVE, 2015). Both current dams hold a crest height of 591 MASL, resulting in 3.4 m of freeboard. The lake supplies flow to the 600 MW Svartisen power plant, owned and operated both by Statkraft Energi AS (70%) and Nordland Fylksekommune (30%). This power plant was originally installed with 350 MW, which was enough to power approximately 80,000 homes, and was Norway's largest at the time (Benham & Dowdeswell, n.d.; Statkraft, n.d.). The lake receives flow directly from the 251 km² catchment area, as well as the potential from 50 different stream intakes across the region, with a combined 70 km long tunnel system, that can also be sent directly to the power station (Multiconsult, 2016).

The new Storglomvatn dam was constructed in 1997, at a height of 128 m (the world's highest at the time of build), and a vast length of 825 m. It is a rock-fill dam founded on bedrock, with a central seal of asphalt concrete and is registered as consequence class level 3. Its seal reaches an elevation of 587.6 MASL. The spillway structure is a separate massive concrete dam, with a length of 75 m and a height reaching 6.7 m. It is constructed in three slabs, with a threshold at HRV. For additional security, there is also an emergency spillway with a tap run and upper hatch that can activate 7 m below HRV, if necessary. Holmvatn dam mirrors a lot of the same characteristics as Storglomvatn dam. It was also constructed in 1997, is a fill dam with central seal of asphalt core and is determined to be consequence class 3. Its seal also reaches 586.6 MASL. However, this dam is 60 m tall and 380 m wide, making it noticeably smaller in comparison. In available documentation, it does not appear as though Holmvatn dam consists of a spillway structure, as this is already sufficed by the spillway associated with Storglomvatn dam.

4.7.2 Identified hazards

Table 4.11 Determination of fundamental hazards for selected dams at Svartisen.

Svartisen Hazard Matrix			
Dam	H1 (rapid melt and precip.)	H2 (breach of glacial lake)	H3 (icefall or calving)
Storglomvatn (Holmvatn and Storglomvatn dams)	Applicable	Documented hazard	Minor hazard, low concern

As both Holmvatn and Storglomvatn dams are connected to the same reservoir, the hazards discussed will be applicable to both of these dams.

Firstly, regarding the H1 condition of rapid melt and high precipitation. It was decided, just as with other dams in this study, that it is an applicable condition due to the highly glaciated catchment, which in this case is 37.6% of a total catchment of 251 km². Additionally, according to calculations, the design floods of 1,047 m³/s for a 1,000-year event and 1,882 m³/s for a PMF justify the need additional assessment in an event tree analysis (Multiconsult, 2016).

Storglomvatn is no longer in contact with the termini of Storglombreen nord and Storglombreen sør, observed from aerial photos from 2019, so the potential for calving (H3) is not applicable in this case. Breakage of ice into the lake (as ice fall) could be of concern, should be recognized as a viable hazard, however cannot be assessed, as no data is available to analyze. It does appear that these termini from Storglombreen (nord and sør) appear to be lying on flatter terrain, so if breakage were to occur, it would be gentle. The last time calving had been reported officially were in NVE investigative reports over 20 years ago (Kjøllmoen, 2001).

One of the larger concerns affecting Storglomvatn is the lake breach failure, H2, from an identified ice-dammed lake at the far northern margin of Vestre Svartisen, named *Nordvatn*, shown in Figure 4.44. This lake is estimated to contain approximately 2.92x10⁷ m³ of meltwater in calculations, however NVE researchers note it may only be 8x10⁶ m³ (Guldbjørnsen, 2017). This discrepancy is likely due to an overestimated lake depth. To remain consistent and conservative in analysis, the larger estimation will be used as a potential threat in event tree analysis. Although its drainage characteristics aren't known, a recorded event from August of 1971 indicates that the lake had drained, and resulted in a significant flood (NVE, n.d.-a). Since this time, the lake has grown continuously due to the recession of the glacier's terminus and continues to be a potential threat. In its current state, it drains slowly via a small outlet to its south, leading into the town of Kilvik. This town is reportedly concerned of the hazardous lake, should it drain eastward instead in the case of a GLOF event, and have requested an early warning system be put in place (Guldbjørnsen, 2017). NVE representatives have reportedly anticipated taking measures in order to reduce the hazard in a 2017 interview, such as potentially lowering the lake level, but it is unclear if any action has yet been taken following the investigation.

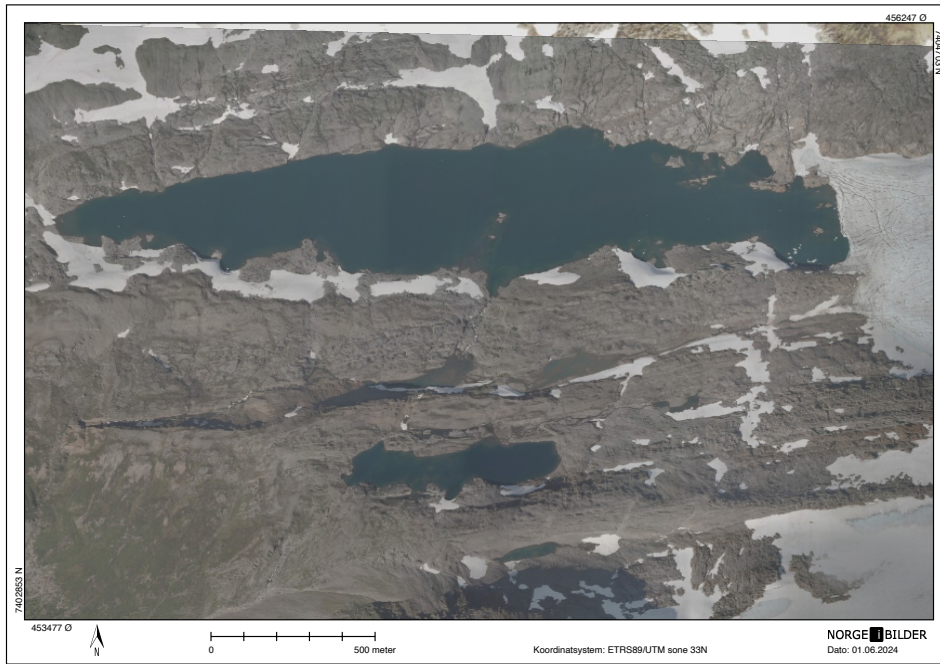


Figure 4.44 Glacial lake Nordvatn (GL8) identified extending from glacier NVE ID 1080, northern margin of Vestre Svartisen. Photo from NorgeiBilder.no (Norge digitalt, 2024).

An additional ice-dammed lake was identified further south extending from glacier NVE ID 1083, shown in Figure 4.45. This lake, however, appears to not be of threat to Storglomvatn, as there is evidence of drainage to the east, and appears to be situated in a region of the topography where flow eastwards into the glacier is highly unlikely. It was confident enough to determine that this lake was not of significant issue, and not pursued for further assessment in this paper.

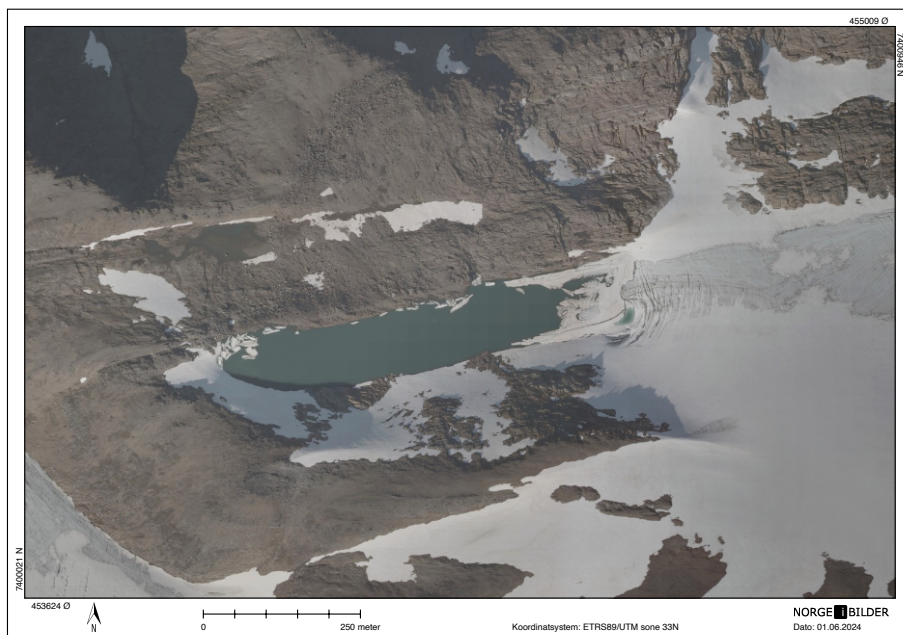


Figure 4.45 Glacial lake emerging from glacier 1083, chosen not to be further assessed due to topographic conditions. Photo sourced from NorgeiBilder.no (Norge digitalt, 2024).

4.7.3 Other hazards

Due to the position of Storglomvatn essentially surrounded by glaciated terrain to the south and western directions, it is absolutely a candidate for potential avalanche hazards. This could also apply to rockfalls, as the slope is quite steep on the western side of the lake. Landslide may be less of a concern, as the material in the areas appears to mostly consist of bedrock, void of most looser appearing soils. Subglacial drainage could also be a potential threat that is not known, as the extent and location of Vestre and Østre Svartisen is critical to the lake. Unless subglacial topography is generated, the possibility of the hazard cannot be ruled out.

4.8 Excluded sites

After the initial screening process outlined in 3.1, the following cases were chosen to be excluded from further analysis, based on a variety of conditions.

4.8.1 Midtre Brevatn and Heimste Brevatn

Located near the Fresvik glacier system in Vik, Vestland, Heimste Brevatn and Midtre Brevatn are two concrete dam structures retaining the reservoirs Øvra Brevatn and Hestastodvatn, in series. In initial screening, it was decided that although there appear to be significant meltwater input from Fresvikbreen to the northeast, that dams appear to be very rigidly designed, and would require a significant flood to cause any type of failure. In the case where these were composed of rockfill, they would cause more reason for concern. For these reasons, and the lack of any documented GLOF history, were chosen to be dismissed from further study.

4.8.2 Markjelkevatn

Located between Juklavatn and Svartadalsvatn, which are discussed in this report, Markjelkevatn receives inflow from the Nordre Folgefonna glacier system. It has been excluded from this study due to the unavailability in data regarding the dam and flood calculations. Without this information, the analyses are not feasible. It is recommended as a potential study site nonetheless, as it could be susceptible to rapid melt conditions.

4.8.3 Båtsvatn

Located in Narvik, Nordland, Båtsvatn is a very large 1.73×10^8 m³ reservoir with a significant embankment dam at the northern end. Although the dam is of embankment type, and more susceptible to failure from overtopping, it was decided to be excluded from the paper, due to very small amount of glaciation in the catchment (calculated at 0.7%). Surrounding Båtsvatn are very small glacierets and remnant of past glaciers that are not of imminent danger.

4.8.4 Fossvatn

Fossvatn is a $3.78 \times 10^8 \text{ m}^3$ regulated reservoir in the Veikdalsisen glacier system, in Hamarøy municipality, Nordland. This large lake appears to only receive a small portion of inflow from glacier melt from Veikdalsisen due to the arrangement in topography (only eastern face). This is relatively small contribution, but when combined with the very strong concrete dam that appears to be deeply inset into the bedrock, eliminates this dam from further study in the context of these analyses. The lake was identified to potentially be at risk for avalanche or rockslides, as it is located down slope of very steep terrain in multiple directions.

4.8.5 Reinoksdammen

Although adjacent to the Slæddovagjavre dam discussed elsewhere in this paper, Reinoksdammen, in Hamarøy municipality, Nordland, was determined to be removed from further analysis in the screening phases. This regulated reservoir does not appear to receive a great deal of meltwater in the catchment, and is constructed of a very rigid concrete dam at the western end. Because the dam appears to be very structurally integral, and lacks any surrounding identifiable glacial lakes, it furthers the confidence that the dam and lake are well-protected.

4.8.6 Kalvatn

Kalvatn is a very large $7.06 \times 10^8 \text{ m}^3$ reservoir located in Rana municipality, Nordland, that has also been excluded from this study. The dam located at the western end of the lake is a significant embankment structure. Although the lake is comparatively large to others in this study, it does not receive any glacial contribution within its catchment. This led to the decision not to be pursued for further analysis in this paper.

4.8.7 Øvre Glomvatn Hoveddam and Sidedam

Øvre Glomvatn main and secondary dams are located on the south end of Øvre Glomvatn, a remote $2.23 \times 10^7 \text{ m}^3$ glacial fed lake in Meløy, Nordland. The lake is located downslope from the Glombreen glacial system, just adjacent to the northwest. Although the glacier is of fairly significant size (3.7 km^2) and does have an identifiable small proglacial lake extending from one of the outlets (which appears to be bedrock dammed), it has been determined to likely not be of danger to the lake or its dams. Both Øvre Hoveddam and Sidedam are rigid concrete dams situated in bedrock, allowing ample strength to sustain even overtopping events, if they were to occur. It should be noted that the lake also does not have any available information from NVE Sildre, furthering the decision to omit from this study.

4.8.8 Ståvatn

Located downslope of the Nupsfonn glacial system, in Vinje municipality, Telemark, Ståvatn is a $4.8 \times 10^7 \text{ m}^3$ regulated reservoir with a robust buttress concrete dam located at the southern end. The lake is situated at a far distance away from Nupsfonn (approximately 4.8 km), and only has a 2.4% glaciated catchment. Due to these factors in combination, as well as the visual assessment that there don't appear to be any other obvious hazards, it was chosen to be excluded from this study. The one exception that does warrant the recommendation for

further study is the glacial lake within Nupsfonn that has a large documented GLOF from 2019, where $1.0 \times 10^7 \text{ m}^3$ was determined to be drained (Kjøllmoen et al., 2020). Although this may be the case, Ståvatn is located a great distance from this flood, and would likely be protected through diminished intensity from buffer and routing through a series of other glacial lakes between the source and Ståvatn.

4.8.9 Langvatn

Langvatn is a $1.6 \times 10^8 \text{ m}^3$ reservoir located in Ulvik municipality, Vestland. It is located west of Hardangerjøkulen and is bound by a series of 4 embankment dams, to its east and west. Although this lake and its dams are significant, it was found to not lie in the direct catchment of Hardangerjøkulen, or the glacierets present southwest at Onen peak, once delineating the catchment. Because the overall contribution of glaciers are so small, and don't appear to be any hazardous glacial lakes or ice fall hazards, it is dismissed for further analysis in this paper.

5 Results

The following chapter will present results from event tree analyses performed for the applicable dam sites for all three conditions, H1 (rapid melt and high precipitation), H2 (breach of glacial lake), and H3 (calving or icefall). These results can be further inspected within the even trees themselves, presented in Appendices A, B, and C.

Additionally, the parameters estimated for the glacial lakes and their breach properties will be summarized, with calculations available in Appendix D.

5.1 Rapid melt and high precipitation hazard

In Figure 5.1, the results from the rapid melt and high precipitation are illustrated. The methods in calculating the annual probability and number of fatalities are discussed in 3.4.2 and 3.4.9, respectively.

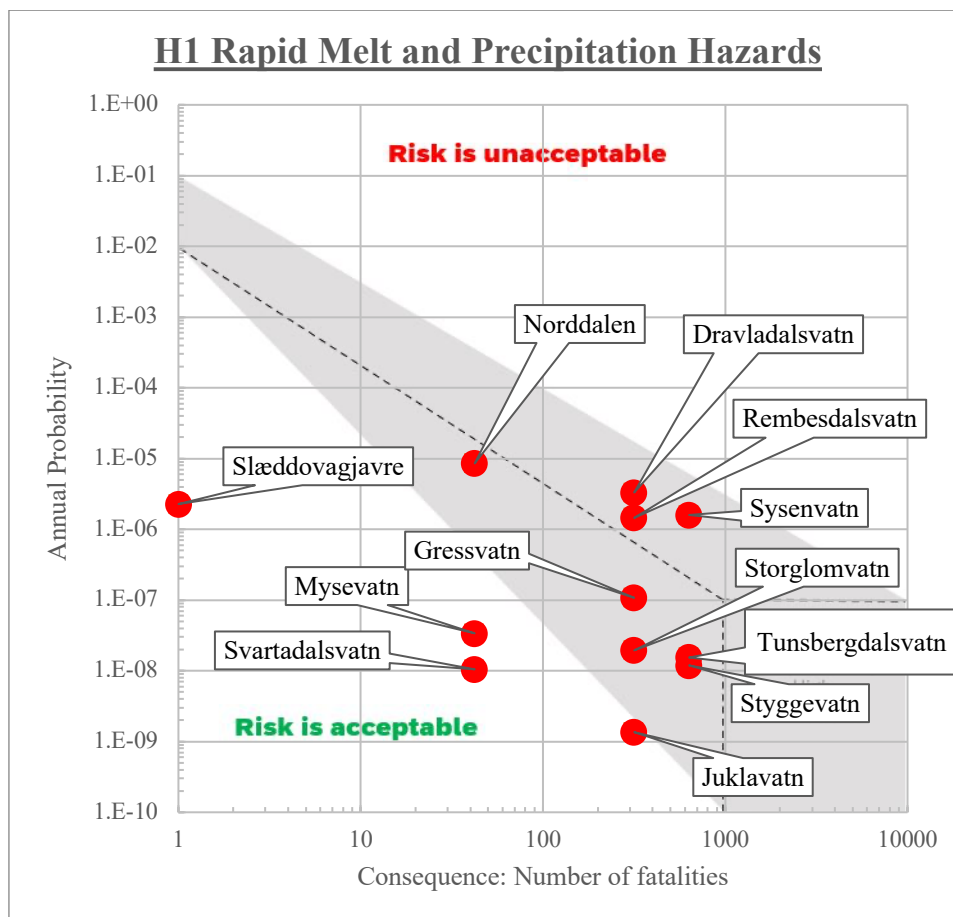


Figure 5.1 Risk envelope plot for H1 hazard condition for all applicable dams.

It is clearly evident that there are a wide range in probabilities from the different selected dams, all as a result of their different hydrological conditions, topography, and assessed risk from their design. Probabilities range from 1.36×10^{-9} (Juklavatn) to 8.55×10^{-6} (Norrdalen). As the envelope is used to indicate, a high risk is observed from Dravladalsvatn,

Rembesdalsvatn, and Sysenvatn. Other dams, such as Slæddovagjavre, Mysevatn, and Svartadalsvatn appear to remain very safe for their respective consequence class, and do not warrant much extra attention in regards to further analysis. Other dams within the grayed envelope nearing the differentiation line between acceptable and unacceptable risk (dashed line) are very sensitive to becoming more of a concern if there are slight adjustments in either the probability or potential consequence (fatalities). The class 4 dams Styggevatn and Tunsbergdalsvatn would need special attention and assurance that the estimation of population and households are in fact representative, as they were assumed, as per discussion in 3.4.9. Should the number of households be higher than this, the dams would then be shifted into the zone of “low probability, very high consequence.”

5.2 Breach of glacial lake hazard

Figure 5.2 illustrates the resulting risk envelope plot from identified glacial lake hazards endangering select dams. As mentioned prior, the method in which the plot was generated can be found in 3.4.3 and 3.4.9.

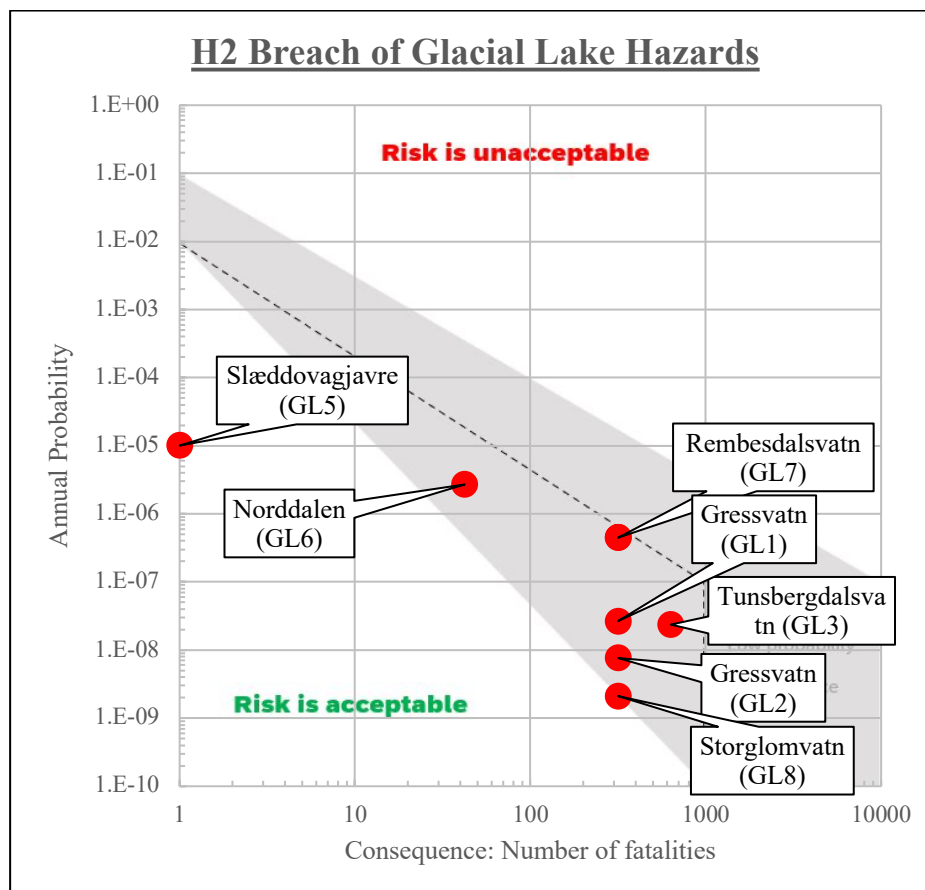


Figure 5.2 Risk envelope plot for H2 hazard condition for all applicable dams.

Fortunately, it appears as though the estimated hazards from identified glacial lakes do not cross the dashed boundary into a “unacceptable risk” criteria. That being said, GL7, affecting Rembesdalsvatn, seems to come close to this threshold. Just as with the H1 results, the class 4 dam in this plot (Tunsbergdalsvatn) is subject to moving further to the left or right on the consequence scale, based on the actual population present. With the assumption, it remains

as an acceptable risk, but should the potential fatalities exceed 1,000, it also puts the dam into the zone of “low probability, very high risk.” It is surprising to see these hazards mainly situated within the grayed zone of the envelope (with the exception of Slæddovagjavre), as was not the case in H1.

5.3 Calving and icefall hazard

Within Figure 5.3, the results from the event tree completed for Styggevatn’s H2 condition are plotted. This was the culmination from methods introduced in 3.4.4.

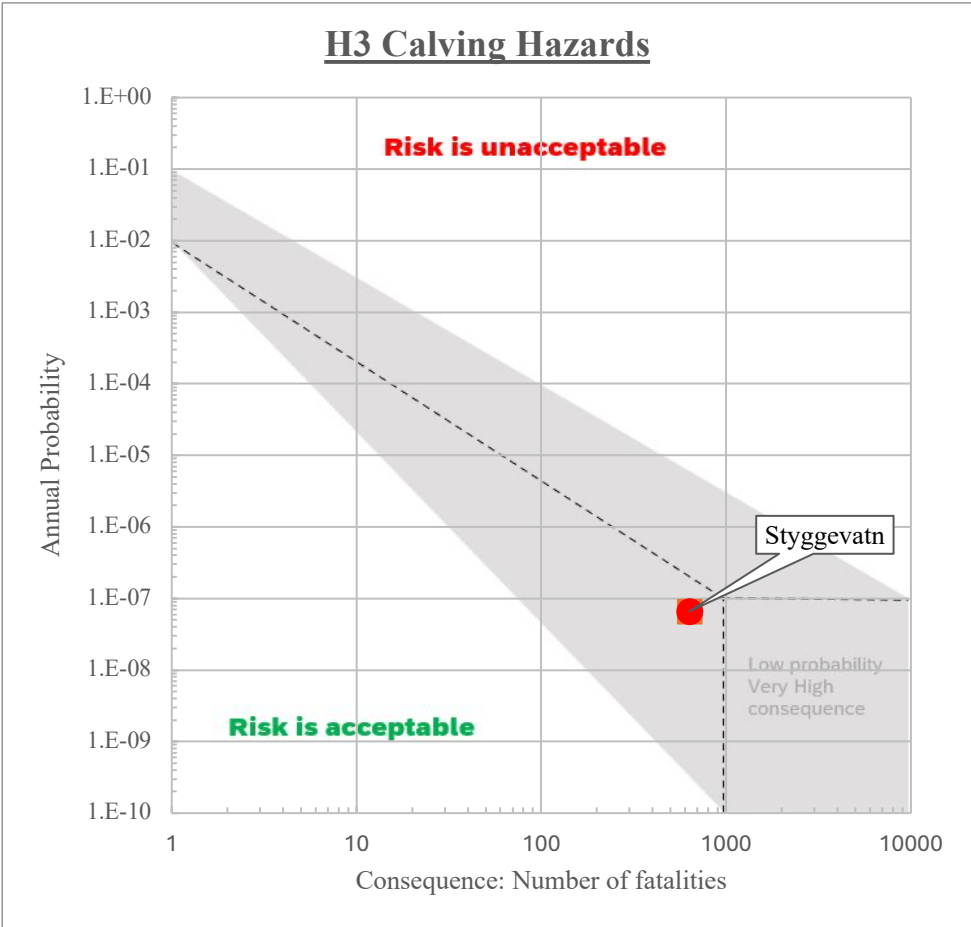


Figure 5.3 Risk envelope plot for H3 hazard condition for Styggevatn.

As this was a very limited assessment, with only Styggevatn applicable for predictable calving conditions, it is still interesting to observe the closeness the hazard is plotted to unacceptable risk threshold. The methods in assessing this risk may be simplified and unproven, however this indicates that the risk should perhaps be observed a bit closer in further studies. As the dam owners had anticipated this risk, the implementation of ice breakers at Styggevatn likely kept the threshold for unacceptable risk from being surpassed using the methodology in this paper.

5.4 Glacial lake estimations

In Table 5.1, the results for the estimated parameters of identified glacial lakes are outlined. These utilize the methods presented throughout Chapter 3, and are subject to large degrees of uncertainty.

Table 5.1 Resulting estimations for identified hazardous glacial lakes.

Lake ID	Lake Type	Coordinates	Lake Surface Area	Lake Volume	Maximum Breach Outflow Rate*
			(m ²)	(m ³)	(m ³ /s)
GL1	Ice-dammed	66.0396°N, 14.2731°E	25,000	350,000	91.4
GL2	Moraine-dammed	66.0280°N, 14.3384°E	15,410	99,916	97.4
GL3	Ice-dammed	61.5548°N, 7.1148°E	Unknown	5,700,000	545.3
GL4**	Ice-dammed	60.1675°N, 6.4761°E	7,808	39,158	Not estimated
GL5	Moraine-dammed	67.7095°N, 16.2817°E	110,000	1,498,693	776.6
GL6	Moraine-dammed	68.1457°N, 17.8279°E	58,404	626,450	243.0
GL7	Ice-dammed	60.5423°N, 7.3197°E	150,000	1,820,000	262.4
GL8	Ice-dammed	66.7527°N, 13.9803°E	950,000	29,227,349	677.4

*Only overtopping breach flow estimations for moraine-dammed lakes used in the right-most column.

**GL4 is determined to be too small to include in further analyses.

Although the lakes have large variations in footprint and volume, it was found that the average identified lake volume was 4,920,195 m³ (largely influenced by GL5 and GL8). Other parameters, such as the smaller seepage failure peak flow rate for moraine-dammed lakes not shown in Table 5.1, are disclosed in Appendix D. The actual lake volume and area would likely need field-verified and further investigated from bathymetric surveys to pinpoint actual values. It is also important to note that these estimations can also vary widely based on the timing of measurement, as they can fluctuate from the input of snow and ice melt, as well as any evaporation or seepage occurring in severe cases.

6 Discussion

In this chapter, the three primary hazards are discussed, in relation to the generated results in event tree analyses, as well as their respective limitations and simplifications. At the end of the chapter, recommendations for further study are made.

6.1 Rapid melt and precipitation hazard

Within the plotted results in Figure 5.1, it is apparent that many dam dams lie within range, or close to, the grayed portion of the risk envelope. In the event tree analysis process, the largest influencer to the end results for this hazard was both the question of whether the flood surge overwhelmed spillway capacity, and if this caused a failure or breach. These were largely subjective categories, that relied heavily on the use of verbal descriptors. Due to this, the resulting probability can be altered quite drastically only from differing interpretations in these steps. Dams that indicated a much safer level (further from crest elevation) from flood calculations resulted in a safer figure in the hazard analysis, as their probability for overwhelmed spillway was significantly lower. This can be seen in the event trees for Slæddovagjavre, which saw a nearly certain overwhelming of spillway in either flood condition, versus a dam such as Styggevatn, which saw a near impossible probability of overwhelming from even a PMF flood.

The division between concrete and embankment dams is also important to observe, as they react much differently to floods in respect to a safety context. Concrete dams are notably much more secure from surviving overtopping events (which is why many were excluded in the original filtering of sites discussed in 3.1.1). When combining the two last steps of the H1 event trees, this can cause an almost leveling effect, where a concrete dam (such as Slæddovagjavre) may have a very high probability of spillway exceedance, but extremely low probability for dam failure from this mechanism. In the reverse, an embankment dam may see an exceptionally small chance for spillway exceedance, but much higher probability failure probability in the event where the spillway is overwhelmed.

In the case of Norddalen, which had the highest probability of failure for this hazard, the factor most responsible for the output was the reservoir regulation step. At 90% probability for full reservoir status, this had a large impact on the final resulting risk. All other dams in this study saw much lower percentages, normally less than 5%. Should Norddalen operate at a lower level more often, it would've placed it within the range of the other dams in this study regarding potential failure probability.

Although the methods in determining the values are slightly unconventional, the recommendation is to further pursue the higher risk dams seen in this paper seen from the H1 hazard, such as Dravladalsvatn, Rembesdalsvatn and Sysenvatn. These rank highly on the risk envelope plot, and even if the accuracy for probability of failure is misrepresented, lie in a high consequence class that warrants additional investigation to ensure high population areas aren't subjected to unnecessary risk.

6.1.1 Limitations and drawbacks with H1 analyses

There can be several sources of error associated with the assessing of the first hazard, rapid melt and high precipitation. They can stem into the methodology and how they are quantified in the event tree analyses.

All the event trees utilize either a Q_{1000} or Q_{500} (in the case of Slæddovagjavre) flood condition, with the upper branch representing a condition larger than Q_{1000} that could be in the realm of a PMF flood, but not for certain. To more accurately quantify this condition, it would be recommended to gather enough hydrological data for each site and conduct a hydrological analysis to determine the Q_{10000} values in most cases, as they would be more definitive for the purposes of estimating probabilities (as an associated return event rather than ambiguous PMF recurrence).

One of the largest constraints with this assessment is the lack of routing, or modelling of the temporal aspect of an inflow flood, where a hydrograph is utilized to represent the peaks and plateaus of a flood. This could have a significant effect in how the dam manages the flood, and whether the spillway system is capable at mitigating it. Because this would require extensive analysis and modelling, the simplification was made to only utilize the peak value from flood calculations and use this as the “worst-case scenario” which is useful as a higher-level overview but may not represent accurately how the dam would actually react in the situation.

Future scenarios incorporating climate change through increased precipitation would also be helpful to be included. In the coming years, most parts of Norway will experience increased frequency and quantities of precipitation, which would have a significant effect on the future flood calculation estimates (Konstali & Sorteberg, 2022). Another constructive addition could be the outlining of the actual contribution from the glacial and snow melt included in the flood calculations to be outlined. As they are assessed in this paper, they are a combined value with precipitation, and the snow melt partition isn't discretely expressed. This could give a helpful insight to the numerical trend behind the volume of floods and how they are predicted in a region or compared to other regions. A popular approach for this is the degree-day model, which remains a very simplified method with its own drawbacks and may not best represent the actual melting conditions within a catchment.

6.2 Breach of glacial lake hazard

The breaching of glacial lakes is one of the most critical to assess due to the unpredictable nature and potential lack of consideration into dam design. The plotting of the assessed risks in Figure 5.2 show a relatively high risk for nearly all identified glacial lakes. Interestingly, most of the identified lakes applicable for the analyses were associated with dams of consequence class 3 or higher, except for Norddalen and Slæddovagjavre.

Most lakes were found to be quite small, and not of significant risk to the downstream reservoirs. As an example, this was the case for Gressvatn, who's ice-dammed lake (GL1) only resulted in a miniscule $97 \text{ m}^3/\text{s}$ estimated breach flood, which was significantly below the estimated $1,000 \text{ m}^3/\text{s}$ spillway capacity threshold. With these types of events, the only potential possibility for inducing failure is the clogging of outflow facilities, or with the transport of significant debris as a component of the resulting flood. Nonetheless, the lakes

are important to identify and keep in observation, should they grow or shrink in size in the future. The growing trend found in these studies were the shrinkage of ice-dammed lakes. The extensive history and studies for the GL1, GL3, and GL7 lakes demonstrate that the floods have become smaller in magnitude, simply as a result of hastened ablation of glacial ice, exacerbated by increased climate temperatures and leading to smaller dams, or regions that can no longer be dammed by ice whatsoever (in the case of Tunsbergdalsvatn, GL3).

Due to the higher consequence class and risk estimation, it is recommended to pursue GLOF lake GL7 (Rembesdalsvatn) further. Although there is much activity with NVE's ongoing assessments of the ice-dammed lake Demmevatn, more studies can be conducted regarding the risk presented by the lake. An interesting hypothetical would be to further explore the possibility and consequences associated with the collapse or failure of the rock tunnel that currently aids in the drainage of this lake, and how Rembesdalsvatn would be affected should another outburst occur without the aid of this drainage tunnel.

Another recommendation is to further pursue investigation into the rapidly enlarging proglacial moraine-dammed lake at Slæddovagjavre (GL5). When inspecting visually, the lake appears to be the most dynamic in regard to how fast it has been growing, as well as its status of having neither any GLOF history, nor any other studies conducted that could be found. Its source glacier is declining rapidly in size, which will continue to feed the lake for years to come until it has become extinct. Being what appears to be a moraine-dammed lake, it is susceptible to more violent drainage failures than its ice-dammed counterparts, and could have a significant effect downstream, regardless of its low consequence classification.

6.2.1 Limitations and drawbacks with H2 analyses

The method in this paper heavily weighs on the breach characteristics from the identified glacial lakes. Therefore, alterations to this can have a significant influence on the calculated probability of dam failure. Because these values were derived from observations from aerial photos, there are potential mistakes that can originate at this stage, more specifically, the dams' embankment widths for moraine-dammed lakes. This can be a difficult parameter to discern, and in aerial photos it is not entirely obvious. Small changes in this can lead to larger changes to the peak outflow and other characteristics associated with a breach. Compound this variation with the inaccuracies characteristic with using empirical methods, and the resulting estimations may be severely compromised in accuracy. To make more certain estimations of breach outflows, the implementation of a more complex model, such as those mentioned in 3.4.3, would be recommended. This could be built from site-collected measurements and are most suited for focus on only one or few locations, as the development of these models can be resource and time-intensive.

In the case of ice-dammed lakes, the breaching characteristics are even more unsure, as the drainage process with these are extremely complex. In high-level assessments, it is unfortunately not possible to further pinpoint how an ice-dammed lake may drain other than using empirically based methods, as used in this paper. These empirical methods are largely based on how other observed ice-dammed lakes drain, as discussed in 3.3.3. There are limitations with this approach, as ice-dammed lakes can drain in a number of different ways, and are very much unique events, especially if there are no recorded events associated with them, as is the case with GL8 in particular. Ice-dammed lakes that drain periodically due to seasonal shifting of glacial ice, as was recorded in Demmevatn (GL7) and Brimkjelen (GL3),

are more predictable, as they result in floods that retain somewhat similar characteristics in both flood peak and volume.

Impacted by the same simplification made with H1, the lack of routing and a temporal component within the data can also have a large impact on the results generated from the event tree analyses for this hazard. If one were to pair an appropriate breach model with an advanced inundation model, such as HEC-RAS, the result would provide a much more confident resultant for risk assessment. The current method of using only the estimated peak breach outflow at the breach location is not realistic for determining the actual response at the reservoir itself, as the flood flow will be significantly buffered through travel down slope. For the purposes of this assessment, the empirical formulations provide a good generalization for understanding around what risk can be found for each glacial lakes' breaching. High-risk lakes can be investigated further for more comprehensive assessments to ensure there aren't looming failures in the horizon for the affected reservoirs.

6.3 Calving and icefall hazard

In the case of Styggevatn, calving is a constantly ongoing mechanism that has been occurring over the years since the reservoir's original creation. This is monitored on an ongoing basis and is likely of little concern due to the facility's ability to remotely manage and identify hazardous icebergs arriving to the dam. At an estimated annual probability of 6.60×10^{-8} , the likelihood for failure is very minimal, however is still important to observe as a potential hazard as Austdalsbreen continues its recession and shrinkage. As Styggevatn is considered a class 4 dam, the resultant of a potential failure would be very severe for the larger populations and infrastructure downstream. The hazard would likely be much more critical if Styggevatn had not included the ice breaking structures near the outlet of the dam as described within reports.

6.3.1 Limitations and drawbacks with H3 analyses

Determining calving and ice fall hazards is incredibly challenging process and requires a robust method to quantify the risks associated from them. As discussed, calving can generate dangerous forces through seiche waves, creating enough displacement in the lake to cause overtopping, or from generating blockages at the spillways. All of these are complex to diagnose and requires a full understanding of when the glacier will calve, how long it will take the iceberg to travel to the spillway, and how long the iceberg is expected to survive. Additionally, the shape and size of these icebergs would need to at least be predictable, which would likely require on-site measurements and analyses due to the complex and dynamic nature behind the calving process. Small environmental factors can also have a significant influence on these analyses, from the wind pattern, current, and temperature within the lake, to the atmospheric conditions in a year, and its effect on the lifecycle of the glaciers within the region. These are all very dynamic processes and can vary widely from year to year, making it nearly infeasible to calculate in a probabilistic context.

The method itself for obtaining the probability of failure is also very subjective and has not been proven outside of this paper. This could mean the results may not fully represent what can be found realistically, as calving mechanisms aren't generally assessed in these types of assessments.

The condition for iceberg size isn't necessarily the only route in which the calved ice can incur blockage and overtopping to a dam- smaller pieces of ice can conjoin and also create blockage hazards should the dam not be suitably designed. On the contrary, icebergs that are large enough to block the spillway aren't necessarily a hazard in themselves. Most of the fractured ice remains near the terminus location until they have fully melted, as observed in aerial photos over the years.

An additional avenue that could expand this hazard assessment would be the inclusion of a seiche wave analysis. This isn't included in this paper, due to the extensive analyses and data required but is still a very important mechanism to assess that is documented in other cases. Seiche waves are perhaps more destructive to naturally formed moraine-dammed glacial lakes than man-made embankment dams, as expressed earlier in GLOF hazards, but could have a detrimental impact to the integrity of the dam, should the wave be large enough to overtop the crest by a large enough margin. Some cases, such as that with Storglomvatn, have potential hazards from hanging glaciers, that can fracture in weakness zones within the glacier and fall from great heights into reservoirs, generating severe waves. These are particularly hazardous, however the assessment required to find the probability in these risks are even further fetched and must be conducted with more data and observations.

6.4 Other limitations

6.4.1 Timing of reservoir state

Determining the reservoir fill state was a prerequisite step in determining whether or not any of the hazards inflict potential damage to the dam in the first place. This is a difficult metric to identify, as each dam is undergoing individual regulation schemes and schedules that are tailored to the seasonal conditions present in the environment. These schedules on their own would directly affect the probability for when a hazard occurs. For example, in the season in which melting is most prevalent (spring, in most regions), dam operators generally lower the reservoir ahead of time in anticipation, which would result in a lower probability than is estimated in the event trees, which take the regulation averaged over a year.

Regardless, the introduction of a timing step is needed for the H1 and H2 hazards, as the lakes in this paper are significant in capacity and would need to be full to encounter a failure. Should the lakes be smaller in volume (in the realm of less than $1 \times 10^6 \text{ m}^3$), this step would likely not be necessary, as the introduction of a large glacial lake breach or melting hazard would likely overwhelm lakes at this size no matter the water level at the time.

6.4.2 Failure or breach probability

Another significant drawback from these assessments is the lack of quantified breach calculations in the final step of the event tree analyses. This step is applied with a verbal descriptor for all cases and is a "call of judgement" based on the results of the previous steps. Should this be altered from different perspectives, it would have a significant influence on the final probability of failure for the hazards.

To better assess this hazard, a detailed dam failure analysis paired with the flood inundation and reservoir routing would be optimal. This would require significantly more data and

resources to complete and wouldn't be appropriate for a large screening assessment as such. For embankment dams, the application of overtopping failure calculations would be best, whereas overturning and sliding analyses for concrete dams would be the most appropriate. Although the application of verbal descriptors is significantly subjective, they still can be assigned based on the features of the dam, and how they characteristically respond to floods. As discussed in 6.1, a concrete dam will be much less susceptible to failure (and applied with a much lower probability in the assessment) than an embankment dam from overtopping events.

6.4.3 Recommendations for further study

Regardless of these limitations and simplifications, the assessing of this risk as a “worst-case scenario” in event tree analyses provides a useful insight into potentially investigating some select cases further. This really is the intention behind event trees, as they can be notably subjective, as especially seen in this paper, and are generally purposed for screening analyses for later, more quantitative-based assessments.

For future studies, a recommendation is to perhaps select only one or few dams to evaluate in a more comprehensive manner. It would also be suggested to focus on a single hazard, such as glacial lake breach. With the implementation of more intensive methods, a more secure recommendation can be made regarding the risk present within a glacier-reservoir system. Additionally, an interesting metric to observe would be the inclusion of a sensitivity analysis, where adjustments can be made with an event tree analysis to identify the confidence range in estimates and quantify the amount of uncertainty in an assessment.

The inclusion of early warning systems would also have a dramatic impact on the safety of dams in relation to GLOF hazards, as they can prevent the downstream populations of an incoming breach that is detectable via implementation of monitoring equipment downstream of glaciers or glacial lakes. This is susceptible to its own set of potential failures, but would significantly increase the safety without needing enormous overhauls to the designs of dams or glacial lake features within the pathways of these hazards. A notable example of this would be the scenario the town of Kilvik faces, just downstream from GL8 (Nordvatn), within Storglombreen. As discussed in 4.7.2, the implementation of a proper early warning system for the drainage of Nordvatn would significantly increase the safety of the residents and would not require much additional actions to be taken with the lake itself. An example of proper mitigations being applied to lower risk is seen at Demmevatn lake, within Rembesdalskåka. The construction and implementation of a rock tunnel significantly lowers the risk from the ice-dammed lake by reducing the flood sizes, even though they still regularly occur.

7 Conclusions

In Norway, it is found that glacial hazards are ever present, and pose a considerable quantifiable risk to the safety of both concrete and embankment dams. Although the probabilities are shown as on the lower spectrum of possibility, they are still critical to identify and monitor as glaciers recede, and the landscape continues to change with the climate. Norway is fortunate to have a great abundance of resources and data available to assess these types of risks, as many other countries that are similarly or more susceptible to them do not have this available. The country also benefits widely from what were found to be very soundly designed and built dams and reservoirs that are well protected from flood events induced from glacial hazards, or traditional climatic processes.

Throughout the construction and inception of the tailored event trees, it was found that there does not exist one uniform method or procedure for analyzing the risks posed by hazardous glacial mechanisms, as they are unique in nature, and can differ widely based on the region, glacier, and dam. This allows a fantastic opportunity for molding and alteration based on known factors, and implementing the knowledge from different scientific fields, such as hydrology, glaciology, structural engineering, and flow mechanics, amongst many more.

The methodology utilized in this paper makes a number of simplifications and assumptions and can leave room for more comprehensive analyses in the future. Fortunately, in most of cases (aside from glacial calving) there exist proven, more descriptive methods for determining confident values for further assessment purposes. As discussed, these would be best applied to one or few cases of concern and done so with extensive data extracted from field investigations and including the perspectives of specialists from various fields.

Following the assessments of the 12 applicable cases, it was found that particular attention should be placed on dams that are lacking capacity to buffer from flood events incurred by rapid melting and high precipitation (H1), breaching of glacial lakes (H2), and calving and icefall incidents (H3). In the context of the H1 hazard, it is recommended to further inspect the protection of Norddalen dam in Narvik, Dravladalsvatn, in Ullensvang, and Rembesdalsvatn and Sysenvatn, in Eidfjord. These range within a small margin of annual failure probabilities estimated from 1.45×10^{-6} to 8.54×10^{-6} . With the exception of Norddalen, these are higher consequence dams, that should be rigorously examined to ensure a dam failure from one of these glacial hazards do not occur, or that a proper warning system can be implemented. Regarding the H2 hazard, it's recommended that attention be placed on further investigating the undocumented moraine-dammed lakes that were identified, such as GL5 at Slæddovagjavre, GL6 at Norddalen, and GL2 at Gressvatn. Although these are lower in the risk envelope of Figure 5.2, and have lower probabilities than some ice-dammed lakes such as GL7 at Rembesdalsvatn, they remain much more unpredictable regarding timing of failure, and can be much more catastrophic if drained instantaneously. Fortunately, in this paper, several of the identified ice-dammed lakes have a good amount of documented history and can be, to some degree, anticipated by dam owners. Glacial lakes stand out as the most critical of the three main hazard types discussed in this paper, as they are directly responsible for the most damage and cause of fatalities worldwide. They also provide the opportunity to assess more directly, as the climatic conditions behind the H1 hazard are largely based on hypothetical calculated events that do not have a physical presence like a standing glacial

lake does. The H3 hazard for calving ice is a very difficult metric to quantify, and although it is recommended to follow up on Styggevatn's ongoing calving process, further development for the methodology in assessing a dam's susceptibility for this mechanism is needed. The limitation lies in the unpredictability and vast number of variables that are present in the calving and ice fall mechanisms. Not only are they challenging to predict, but also require ongoing observations and significant amounts of available data to more accurately assess.

Although these three hazards were selected as the primary focuses within this paper, other glacial hazards not analyzed, such as avalanches, landslides, subglacial lakes, and others have an opportunity to be diagnosed and analyzed within Norway. They may be more challenging to quantify and identify, but are still present as potential risks with the ability to endanger communities and lives.

References

- Altenbach, T. J. (1995, February 13). *A comparison of Risk Assessment Techniques from Qualitative to Quantitative*. <https://www.osti.gov/servlets/purl/67753>.
- Andreassen, L. M., Robson, B. A., Sjursen, K. H., Elvehøy, H., Kjølmoen, B., & Carrivick, J. L. (2023). Spatio-temporal variability in geometry and geodetic mass balance of Jostedalbreen ice cap, Norway. *Annals of Glaciology*, 64(90), 26–43. <https://doi.org/10.1017/aog.2023.70>
- Askheim, S. (2023). Jostedalbreen. In *Store norske leksikon*. <https://snl.no/Jostedalbreen>
- Austdalsbreen—NVE*. (2009, February 10). <https://www.nve.no/vann-og-vassdrag/vannets-kretsloep/bre/bremaalinger/massebalansemaalinger/austdalsbreen/>
- Bakke, J., Dahl, S. O., Paasche, Ø., Riis Simonsen, J., Kvisvik, B., Bakke, K., & Nesje, A. (2010). A complete record of Holocene glacier variability at Austre Okstindbreen, northern Norway: An integrated approach. *Quaternary Science Reviews*, 29(9), 1246–1262. <https://doi.org/10.1016/j.quascirev.2010.02.012>
- BBC Bitesize. (n.d.). *Landscapes of glacial deposition—Glaciated landscapes—Higher Geography Revision*. BBC Bitesize. Retrieved May 18, 2024, from <https://www.bbc.co.uk/bitesize/guides/z9wx3k7/revision/3>
- Bendle, J. (2020a, July 27). Calving of freshwater glaciers. *AntarcticGlaciers.Org*. <https://www.antarcticglaciers.org/glacier-processes/glacial-lakes/calving-of-freshwater-glaciers/>
- Bendle, J. (2020b, August 27). Glacial Lake Outburst Floods. *AntarcticGlaciers.Org*. <https://www.antarcticglaciers.org/glacier-processes/glacial-lakes/glacial-lake-outburst-floods/>
- Benham, T., & Dowdeswell, J. (n.d.). *Svartisen*. Scott Polar Research Institute. Retrieved June 3, 2024, from <https://www.spri.cam.ac.uk/research/projects/integral/svartisen/>
- Benn, D. I., & Evans, D. J. A. (2010). *Glaciers & glaciation* (2nd ed). Hodder education.
- Benn, D. I., Warren, C. R., & Mottram, R. H. (2007). Calving processes and the dynamics of calving glaciers. *Earth Science Reviews*, 82(3–4), 143–179. <https://doi.org/10.1016/j.earscirev.2007.02.002>
- Bennett, M. R. (2001). The morphology, structural evolution and significance of push moraines. *Earth-Science Reviews*, 53(3), 197–236. [https://doi.org/10.1016/S0012-8252\(00\)00039-8](https://doi.org/10.1016/S0012-8252(00)00039-8)
- Bogen, J., Xu, M., & Kennie, P. (2015). The impact of pro-glacial lakes on downstream sediment delivery in Norway. *Earth Surface Processes and Landforms*, 40(7), 942–952. <https://doi.org/10.1002/esp.3669>
- Breane fortset å smelte tilbake i 2022—NVE*. (2022, December 1). <https://www.nve.no/vann-og-vassdrag/vannets-kretsloep/bre/brenyheter/breane-fortset-aa-smelte-tilbake-i-2022/>
- Byers, A. C., Rounce, D. R., Shugar, D. H., Lala, J. M., Byers, E. A., & Regmi, D. (2019). A rockfall-induced glacial lake outburst flood, Upper Barun Valley, Nepal. *Landslides*, 16(3), 533–549. <https://doi.org/10.1007/s10346-018-1079-9>
- Caetech Llc & Calcdevice.com. (n.d.). *Weir Spillway | Online Calculator*. Retrieved May 29, 2024, from <https://calcdevice.com/weir-spillway-id239.html>

- Capart, H. (2013). Analytical solutions for gradual dam breaching and downstream river flooding. *Water Resources Research*, 49(4), 1968–1987.
- Carrivick, J. L., & Tweed, F. S. (2016). A global assessment of the societal impacts of glacier outburst floods. *Global and Planetary Change*, 144, 1–16. <https://doi.org/10.1016/j.gloplacha.2016.07.001>
- Carrivick, J. L., Tweed, F. S., Ng, F., Quincey, D. J., Mallalieu, J., Ingeman-Nielsen, T., Mikkelsen, A. B., Palmer, S. J., Yde, J. C., Homer, R., Russell, A. J., & Hubbard, A. (2017). Ice-Dammed Lake Drainage Evolution at Russell Glacier, West Greenland. *Frontiers in Earth Science*, 5. <https://doi.org/10.3389/feart.2017.00100>
- Chernet, H., Alfredsen, K., & Midttømme, G. H. (2012). Assessment of Changes in Design Flood Due to Climate Change for Sysen Dam in Norway. *ICOLD*.
- Clague, J. (2000). A review of catastrophic drainage of moraine-dammed lakes in British Columbia. *Quaternary Science Reviews*, 19(17–18), 1763–1783. [https://doi.org/10.1016/S0277-3791\(00\)00090-1](https://doi.org/10.1016/S0277-3791(00)00090-1)
- Clague, J. J., & Mathews, W. H. (1973). The magnitude of jökulhlaups. *Journal of Glaciology*, 12(66), 501–504.
- Cook, S. J., & Quincey, D. J. (2015). Estimating the volume of Alpine glacial lakes. *Earth Surface Dynamics*, 3(4), 559–575. <https://doi.org/10.5194/esurf-3-559-2015>
- Davies, B. (2020, June 22). Glacier accumulation and ablation. *AntarcticGlaciers.Org*. <https://www.antarcticglaciers.org/glacier-processes/mass-balance/glacier-accumulation-and-ablation/>
- Desloges, J. R., Jones, D. P., & Ricker, K. E. (1989). Estimates of Peak Discharge from the Drainage of Ice-Dammed Ape Lake, British Columbia, Canada. *Journal of Glaciology*, 35(121), 349–354. <https://doi.org/10.3189/S0022143000009278>
- Diolaiuti, G., Smiraglia, C., Vassena, G., & Motta, M. (2004). Dry calving processes at the ice cliff of Strandline Glacier northern Victoria Land, Antarctica. *Annals of Glaciology*, 39, 201–208. <https://doi.org/10.3189/172756404781813880>
- Donnelly, C. R. (2005). *ASSESSING THE SAFETY AND SECURITY OF DAMS*. <https://doi.org/10.13140/2.1.3736.7362>
- Dubey, S., & Goyal, M. K. (2020). Glacial Lake Outburst Flood Hazard, Downstream Impact, and Risk Over the Indian Himalayas. *Water Resources Research*, 56(4), e2019WR026533. <https://doi.org/10.1029/2019WR026533>
- Dyurgerov, & Meier. (2005). *Global Trend of Glacier Melting or Growing and its Impact on Heavy Storms*. ResearchGate. https://www.researchgate.net/figure/The-graph-on-the-right-of-average-annual-rate-of-thinning-since-1970-for-the-173_fig2_308303328
- Engeland, K., Glad, P. A., Hamududu, B. H., Li, H., Reitan, T., & Stenius, S. (2020). *Lokal og regional flomfrekvensanalyse* (10/2020). NVE.
- Evans, S. (1986). *Landslide Damming in the Cordillera of Western Canada*. <https://www.semanticscholar.org/paper/Landslide-Damming-in-the-Cordillera-of-Western-Evans/87b0b33827b1ef7831a20aa7040dc22332cde6a3>
- Ferguson, R. (1986). River loads underestimated by rating curves. *Water Resources Research*, 22(1), 74–76.
- Fjord Norway. (2024, January 30). *What is a glacier?* <https://fjordnorway.com/en/inspiration/what-is-a-glacier>
- France, J. W. (2021). *Risk Analysis Is Fundamentalley Changing the Landscape of Dam Safety in trhe United States*. National Dam Safety Program Technical Seminar.
- Froehlich, D. (2016). Empirical model of embankment dam breaching. *River Flow 2016*, 1821–1826. <https://doi.org/10.1201/9781315644479-285>

- Geodata AS, Kartverket, Geovekst og kommunene, OpenStreetMap, & NVE. (n.d.). *NEVINA*. Retrieved May 27, 2024, from <https://nevina.nve.no/>
- Giesen, R. H., & Oerlemans, J. (2010). Response of the ice cap Hardangerjøkulen in southern Norway to the 20th and 21st century climates. *The Cryosphere*, 4(2), 191–213. <https://doi.org/10.5194/tc-4-191-2010>
- Glad, P. A., Reitan, T., & Stenius, S. (2015). *Nasjonalt formelverk for flomberegning i små nedbørfelt* (13–2015). NIFS.
- Glad, P. A., Stenius, S., Leine, A.-L. Ø., Væringstad, T., Holmqvist, E., Dahl, M.-P. J., & Trondsen, E. (2022). *Veileder for flomberegninger* (Guide 1/2022). NVE.
- Global Earthquake Monitor*. (2024, May 9). [Open Source]. AllQuakes. <https://allquakes.com/earthquake-monitor.html>
- Guldbjørnsen, Y. B. (2017, January 26). *Frykter flom*. kulingen.no. <https://www.kulingen.no/nyheter/i/kErLbj/frykter-flom>
- Hagg, W. (2022). Glacier Types and Distribution. In W. Hagg (Ed.), *Glaciology and Glacial Geomorphology* (pp. 61–71). Springer. https://doi.org/10.1007/978-3-662-64714-1_5
- Harrison, S., Kargel, J. S., Huggel, C., Reynolds, J., Shugar, D. H., Betts, R. A., Emmer, A., Glasser, N., Haritashya, U. K., Klimeš, J., Reinhardt, L., Schaub, Y., Wiltshire, A., Regmi, D., & Vilímek, V. (2018). Climate change and the global pattern of moraine-dammed glacial lake outburst floods. *The Cryosphere*, 12(4), 1195–1209. <https://doi.org/10.5194/tc-12-1195-2018>
- Hart, J. K., Young, D. S., Baurley, N. R., Robson, B. A., & Martinez, K. (2022). The seasonal evolution of subglacial drainage pathways beneath a soft-bedded glacier. *Communications Earth & Environment*, 3(1), 1–13. <https://doi.org/10.1038/s43247-022-00484-9>
- Haugsrud, H., Midttømme, G. H., Straume, K. M., & Marchand, W.-D. (2022). *Flomberegninger for dammer* (Veileder til damsikkerhetsforskriften 2/2022). NVE.
- Hauser, A. (1993). *Remociones en mas en Chile* (Issue 45). Servicio Nacional de Geología y Minería.
- Hawkins, E. (2020, January 30). *2019 years*. Climate Lab Book. <https://www.climate-lab-book.ac.uk/2020/2019-years/#:~:text=The%20data%20show%20that%20the,'pre%2Dindustrial'%20level>.
- Høgaas, F., & Longva, O. (2016). Mega deposits and erosive features related to the glacial lake Nedre Glomsjø outburst flood, southeastern Norway. *Quaternary Science Reviews*, 151, 273–291. <https://doi.org/10.1016/j.quascirev.2016.09.015>
- Holstad, M. (2020, January 30). *All time high wind power generation in Norway*. Statistisk Sentralbyrå. <https://www.ssb.no/en/energi-og-industri/artikler-og-publikasjoner/all-time-high-wind-power-generation-in-norway>
- Howarth, P. J. (1968). A Supraglacial Extension of an Ice-Dammed Lake, Tunsbergdalsbreen, Norway. *Journal of Glaciology*, 7(51), 413–419. <https://doi.org/10.3189/S002214300002061X>
- Huggel, C., Kääb, A., Haeberli, W., Teyssie, P., & Paul, F. (2002). Remote sensing based assessment of hazards from glacier lake outbursts: A case study in the Swiss Alps. *Canadian Geotechnical Journal*, 39(2), 316–330. <https://doi.org/10.1139/t01-099>
- Huippuja. (n.d.). Retrieved June 1, 2024, from <https://www.tunturivaellus.fi/huippuja.php>
- Imhof, P., Nesje, A., & Nussbaumer, S. U. (2012). Climate and glacier fluctuations at Jostedalbreen and Folgefonna, southwestern Norway and in the western Alps from the ‘Little Ice Age’ until the present: The influence of the North Atlantic Oscillation. *The Holocene*, 22(2), 235–247. <https://doi.org/10.1177/0959683611414935>

- Jackson, M., & Ragulina, G. (2014). *Inventory of glacier-related hazardous events in Norway* (83/2014). NVE.
https://publikasjoner.nve.no/rapport/2014/rapport2014_83.pdf
- Jensen, T., Stensby, K. E., Vognild, I., & Brittain, J. (2021). *Norway's hydroelectric development 1945-1990* (28/2021). NVE.
- Kartverket. (n.d.). *Norgeskart*. Retrieved April 30, 2023, from <https://norgeskart.no/>
- Kartverket. (2024). *Høydedata*. <https://hoydedata.no/LaserInnsyn2/>
- Kjøllmoen, B. (2001). *Glaciological investigations in Norway 2000* (2/2001). NVE.
https://publikasjoner.nve.no/report/2001/report2001_02.pdf
- Kjøllmoen, B. (2016). *Glaciological investigations in Norway 2011-2015* (88–2016). Norwegian Water Resources and Energy Directorate.
- Kjøllmoen, B., Andreassen, L. M., & Elvehøy, H. (2023). *Glaciological investigations in Norway 2022* (23/2023). NVE.
https://publikasjoner.nve.no/rapport/2023/rapport2023_23.pdf
- Kjøllmoen, B., Andreassen, L. M., Elvehøy, H., & Jackson, M. (2018). *Glaciological investigations in Norway 2017* (82–2018). NVE.
https://publikasjoner.nve.no/rapport/2018/rapport2018_82.pdf
- Kjøllmoen, B., Andreassen, L. M., Elvehøy, H., & Jackson, M. (2019). *Glaciological investigations in Norway 2018* (46/2019). NVE.
https://publikasjoner.nve.no/rapport/2019/rapport2019_46.pdf
- Kjøllmoen, B., Andreassen, L. M., Elvehøy, H., & Jackson, M. (2020). *Glaciological investigations in Norway 2019* (34/2020). NVE.
https://publikasjoner.nve.no/rapport/2021/rapport2021_31.pdf
- Kjøllmoen, B., Andreassen, L. M., Elvehøy, H., Jackson, M., Kjøllmoen, B., & Melvold, K. (2017). *Glaciological investigations in Norway 2016* (76–2017). NVE.
https://publikasjoner.nve.no/rapport/2017/rapport2017_76.pdf
- Kjøllmoen, B., Andreassen, L. M., Elvehøy, H., & Melvold, K. (2021). *Glaciological investigations in Norway 2020* (31/2021). NVE.
https://publikasjoner.nve.no/rapport/2021/rapport2021_31.pdf
- Kjøllmoen, B., Andreassen, L. M., Elvehøy, H., & Storheil, S. (2022). *Glaciological investigations in Norway 2021* (27/2022). NVE.
https://publikasjoner.nve.no/rapport/2022/rapport2022_27.pdf
- Kjøllmoen, B. & Norges vassdrags- og energidirektorat. (2000). *Glasiologiske undersøkelser i Norge 1999 = Glaciological investigations in Norway 1999*. Norges vassdrags- og energidirektorat.
- Kjøllmoen, B., & Østrem, G. (1997). Storsteinsfjellbreen: Variations in mass balance from the 1960s to the 1990s. *Geografiska Annaler: Series A, Physical Geography*, 79(3), 195–200. <https://doi.org/10.1111/j.0435-3676.1997.00016.x>
- Knudsen, N. T., & Theakstone, W. H. (1988). Drainage of the Austre Okstindbreen Ice-dammed Lake, Okstindan, Norway. *Journal of Glaciology*, 34(116), 87–94. <https://doi.org/10.3189/S0022143000009102>
- Kolltveit, O. (1962). *Odda, Ullensvang og Kinsarvik i gamal og ny tid: Bygdesoga*. Odda, Ullensvang og Kinsarvik bygdeboknemnd. <https://books.google.no/books?id=b-UnAQAAMAAJ>
- Kondo, K., Sugiyama, S., Sakakibara, D., & Fukumoto, S. (2021). Flood events caused by discharge from Qaanaaq Glacier, northwestern Greenland. *Journal of Glaciology*, 67(263), 500–510. <https://doi.org/10.1017/jog.2021.3>

- Konstali, K., & Sorteberg, A. (2022). Why has Precipitation Increased in the Last 120 Years in Norway? *Journal of Geophysical Research: Atmospheres*, 127(15), e2021JD036234. <https://doi.org/10.1029/2021JD036234>
- Krøgli, I. K., Devoli, G., Colleuille, H., Boje, S., Sund, M., & Engen, I. K. (2018). The Norwegian forecasting and warning service for rainfall- and snowmelt-induced landslides. *Natural Hazards and Earth System Sciences*, 18(5), 1427–1450. <https://doi.org/10.5194/nhess-18-1427-2018>
- Lacasse, S. (2022a). *Handbook—Risk assessment and risk management for dams*. Norwegian Geotechnical Institute.
- Lacasse, S. (2022b). *Handbook—Risk assessment and risk management for dams*.
- Laumann, T., & Wold, B. (1992). Reactions of a calving glacier to large changes in water level. *Annals of Glaciology*, 16, 158–162. <https://doi.org/10.3189/1992AoG16-1-158-162>
- Lia, L. (1998). *Snow and ice blocking of tunnels*. NTNU. <https://www.osti.gov/etdeweb/servlets/purl/353157>
- Lied, K., Palmström, A., Schieldrop, B., & Torblaa, I. (1976). Dam Tunsbergdalsvatn. A dam subjected to waves generated by avalanches, and to extreme floods from a glacier lake. 861-875. <https://ngi.brage.unit.no/ngi-xmlui/handle/11250/3100050>
- Liestøl, O. (1956). Glacier Dammed Lakes in Norway. *Norsk Geografisk Tidsskrift - Norwegian Journal of Geography*, 15(3–4), 122–149. <https://doi.org/10.1080/00291955608542772>
- Liestøl, O., & Thorsnæs, G. (2024). Svartisen. In *Store norske leksikon*. <https://snl.no/Svartisen>
- Liu, J., Tang, C., & Cheng, Z. (2013). The two main mechanisms of Glacier Lake Outburst Flood in Tibet, China. *Journal of Mountain Science*, 10(2), 239–248. <https://doi.org/10.1007/s11629-013-2517-8>
- Lukas, S. (2011). Ice-Cored Moraines. In V. P. Singh, P. Singh, & U. K. Haritashya (Eds.), *Encyclopedia of Snow, Ice and Glaciers* (pp. 616–619). Springer Netherlands. https://doi.org/10.1007/978-90-481-2642-2_666
- Lützow, N., & Veh, G. (2023). *Glacier Lake Outburst Flood Database* (3.1) [dataset]. [object Object]. <https://doi.org/10.5281/ZENODO.7330344>
- Lützow, N., Veh, G., & Korup, O. (2023). A global database of historic glacier lake outburst floods. *Earth System Science Data*, 15(7), 2983–3000. <https://doi.org/10.5194/essd-15-2983-2023>
- Malczyk, G., Gourmelen, N., Goldberg, D., Wuite, J., & Nagler, T. (2020). Repeat Subglacial Lake Drainage and Filling Beneath Thwaites Glacier. *Geophysical Research Letters*, 47(23), e2020GL089658. <https://doi.org/10.1029/2020GL089658>
- Midttømme, G. H. (2002). *Flood Handling and Emergency Action Planning for Dams* [Doctoral thesis, Fakultet for ingeniørvitenskap og teknologi]. <https://ntnuopen.ntnu.no/ntnu-xmlui/handle/11250/242086>
- Midttømme, G. H. (2022, November 9). *Dam Safety Seminar NTNU*.
- Midttømme, G. H., & Pettersson, L. E. (2011). *Retningslinjer for flomberegninger* (Guidelines 4/2011). https://publikasjoner.nve.no/retningslinjer/2011/retningslinjer2011_04.pdf
- Mool, P. K., Wangda, D., Bajracharya, S. R., Joshi, S. P., Kunzang, K., & Gurung, D. R. (n.d.). *Inventory of Glaciers, Glacial Lakes and Glacial Lake Outburst Floods: Monitoring and Early Warning Systems in the Hindu Kush Himalayan Region Bhutan*. <https://doi.org/10.53055/ICIMOD.373>

- Morris, M., West, M., & Hassan, M. (2018). A Guide to Breach Prediction. *Dams and Reservoirs*, 28(4), 150–152. <https://doi.org/10.1680/jdare.18.00031>
- Mottershead, D. N., & Collin, R. L. (1976). A Study of Glacier-dammed Lakes Over 75 Years Brimkjelen, Southern Norway. *Journal of Glaciology*, 17(77), 491–505. <https://doi.org/10.3189/S0022143000013769>
- Multiconsult. (2016). *Revurdering Dam Storglomvatn og Dam Holmvatn* [Confidential Report].
- Multiconsult. (2021). *Flomberegning Dam Styggevatn* [Confidential Report].
- Multiconsult. (2022a). *Revurdering Tunsbergdalsdammen* [Confidential Report].
- Multiconsult. (2022b). *Teknisk Plan—Dam Mysevatn* [Confidential Report].
- Multiconsult. (2023). *Revurdering dam Styggevatn* [Confidential Report].
- National Snow and Ice Data Center. (n.d.-a). *Ice Sheets*. National Snow and Ice Data Center. Retrieved May 30, 2024, from <https://nsidc.org/learn/parts-cryosphere/ice-sheets/ice-sheet-quick-facts>
- National Snow and Ice Data Center. (n.d.-b). *Polar glacier*. National Snow and Ice Data Center. Retrieved June 2, 2024, from <https://nsidc.org/learn/cryosphere-glossary/polar-glacier>
- Nesje, A. (2023). Future state of Norwegian glaciers: Estimating glacier mass balance and equilibrium line responses to projected 21st century climate change. *The Holocene*, 33(10), 1257–1271. <https://doi.org/10.1177/09596836231183069>
- NGI. (2016). *RISIKOVURDERING FOR DAM DRAVLADALEN* (Damsikkerhet i et helhetlig perspektiv) [Confidential Report].
- Norconsult. (2019). *Rembesdalsdammen Revurdering* [Confidential Report].
- Norconsult. (2020). *Sysen dam og ventiler Revurdering* [Confidential Report].
- Norge digitalt. (2024). *Norge i Bilder*. <https://www.norgebilder.no/>
- NVE. (n.d.-a). *Breatlas / Glacier Inventories—NVE*. Retrieved May 26, 2024, from <https://www.nve.no/vann-og-vassdrag/vannets-kretsloep/bre/publikasjoner-publications/breatlas-glacier-inventories/>
- NVE. (n.d.-b). *NVE Temakart*. Retrieved May 26, 2024, from <https://temakart.nve.no/>
- NVE. (2015, September 9). *Storglomvatn*. <https://www.nve.no/om-nve/nves-listefoerte-kulturminner/dammer/storglomvatn/>
- NVE. (2018, March 5). *PQRUT-flommodell*. <https://www.nve.no/vann-og-vassdrag/vannets-kretsloep/analysemetoder-og-modeller/pqrut-flommodell/>
- NVE. (2024). *Sildre* [Hydrological databank]. <https://sildre.nve.no/map>
- O'Connor, J. E., Hardison, J. H., & Costa, J. E. (2001). *Debris flows from failures of neoglacial-age moraine dams in the Three Sisters and Mount Jefferson Wilderness areas, Oregon* (1606). U.S. Geological Survey. <https://doi.org/10.3133/pp1606>
- Om nasjonalparken*. (n.d.). Folgefonna Nasjonalpark. Retrieved May 13, 2024, from <https://folgefonna.info/om-nasjonalparken/>
- O'Neel, S., Pfeffer, W. T., Krimmel, R., & Meier, M. (2005). Evolving force balance at Columbia Glacier, Alaska, during its rapid retreat. *Journal of Geophysical Research: Earth Surface*, 110(F3), 2005JF000292. <https://doi.org/10.1029/2005JF000292>
- Otto, J.-C. (2019). Proglacial Lakes in High Mountain Environments. In T. Heckmann & D. Morche (Eds.), *Geomorphology of Proglacial Systems* (pp. 231–247). Springer International Publishing. https://doi.org/10.1007/978-3-319-94184-4_14
- Palmer, S. J., Dowdeswell, J. A., Christoffersen, P., Young, D. A., Blankenship, D. D., Greenbaum, J. S., Benham, T., Bamber, J., & Siegert, M. J. (2013). Greenland subglacial lakes detected by radar. *Geophysical Research Letters*, 40(23), 6154–6159. <https://doi.org/10.1002/2013GL058383>

- Richardson, S. D., & Reynolds, J. M. (2000). An overview of glacial hazards in the Himalayas. *Quaternary International*, 65–66, 31–47. [https://doi.org/10.1016/S1040-6182\(99\)00035-X](https://doi.org/10.1016/S1040-6182(99)00035-X)
- Robson, B. A. (2012). *A Remote Sensing Investigation into the evolution of Folgefonna Glacier over the last 150 years* [Master thesis, The University of Bergen]. <https://bora.uib.no/bora-xmlui/handle/1956/6191>
- Russell, A. J., Tweed, F. S., Roberts, M. J., Harris, T. D., Gudmundsson, M. T., Knudsen, Ó., & Marren, P. M. (2010). An unusual jökulhlaup resulting from subglacial volcanism, Sólheimajökull, Iceland. *Quaternary Science Reviews*, 29(11), 1363–1381. <https://doi.org/10.1016/j.quascirev.2010.02.023>
- Saetrang, A. C., & Wold, B. (1986). Results from the Radio Echo-Sounding on Parts of the Jostedalbreen Ice Cap, Norway. *Annals of Glaciology*, 8, 156–158. <https://doi.org/10.3189/S026030550000135X>
- Sicart, J. E., Hock, R., & Six, D. (2008). Glacier melt, air temperature, and energy balance in different climates: The Bolivian Tropics, the French Alps, and northern Sweden. *Journal of Geophysical Research: Atmospheres*, 113(D24), 2008JD010406. <https://doi.org/10.1029/2008JD010406>
- Sigtryggssdóttir, F. G. (2022). *Loads on dams* [Classroom lecture].
- Sjoen forsvann på ei natt. (2009, September 22). *Bergens Tidende*.
- Snorrason, A., Finnsdóttir, H. P., Moss, M. E., & International Association of Hydrological Sciences (Eds.). (2002). *The extremes of the extremes: Proceedings of an international symposium on extraordinary floods held at Reykjavík, Iceland, in July 2000*. International Association of Hydrological Sciences.
- SSB. (2023, September 22). *Families and households*. SSB. <https://www.ssb.no/en/befolkning/barn-familier-og-husholdninger/statistikk/familier-og-husholdninger>
- Statkraft. (n.d.). *Svartisen vannkraftverk*. Retrieved June 3, 2024, from <https://www.statkraft.com/om-statkraft/hvor-vi-har-virksomhet/norge/svartisen-vannkraftverk/>
- Statkraft AS. (n.d.). *Mauranger hydropower plant*. Retrieved May 22, 2024, from <https://www.statkraft.com/about-statkraft/where-we-operate/norway/mauranger-hydropower-plant/>
- Strandberg, G., Brandefelt, J., Kjellström, E., & Smith, B. (2012). High-resolution regional simulation of last glacial maximum climate in Europe. *Tellus A: Dynamic Meteorology and Oceanography*, 63(1), 107. <https://doi.org/10.1111/j.1600-0870.2010.00485.x>
- SWECO Norge. (2009). *Dam Slæddovagjavri Revurdering 2006* [Confidential Report].
- SWECO Norge. (2011). *Flomberegninger for Kvanngrøvatn, Juklavatn og Svartadalsvatn* [Confidential Report]. SWECO Norge AS.
- SWECO Norge. (2017). *Dam Gressvatn Revurdering 2014-2016* [Confidential Report].
- SWECO Norge. (2018). *Teknisk plan for fornying av dam Svartadalsvatn* [Confidential Report].
- SWECO Norge. (2023). *Revurdering Norddalsdammen, 2021* [Confidential Report].
- Theakstone, W. H. (1978). The 1977 drainage of the Austre Okstindbreen ice-dammed lake, its cause and consequences. *Norsk Geografisk Tidsskrift - Norwegian Journal of Geography*, 32(4), 159–171. <https://doi.org/10.1080/00291957808552038>
- USGS. (n.d.-a). *How old is glacier ice?* | U.S. Geological Survey. Retrieved May 14, 2024, from <https://www.usgs.gov/faqs/how-old-glacier-ice>

- USGS. (n.d.-b). *Where on Earth are temperate glaciers located?* | U.S. Geological Survey. Retrieved May 30, 2024, from [https://www.usgs.gov/faqs/where-earth-are-temperate-glaciers-located#:~:text=A%20temperate%20glacier%20\(as%20opposed,melting%2C%20area%2C%20and%20volume](https://www.usgs.gov/faqs/where-earth-are-temperate-glaciers-located#:~:text=A%20temperate%20glacier%20(as%20opposed,melting%2C%20area%2C%20and%20volume).
- Vuichard, D., & Zimmermann, M. (1987). The 1985 catastrophic drainage of a moraine-dammed lake, Khumbu Himal, Nepal: Cause and consequences. *Mountain Research and Development*, 91–110.
- Walder, J. S., Trabant, D. C., Cunico, M., Fountain, A. G., Anderson, S. P., Anderson, R. S., & Malm, A. (2006). Local response of a glacier to annual filling and drainage of an ice-marginal lake. *Journal of Glaciology*, 52(178), 440–450. <https://doi.org/10.3189/172756506781828610>
- Westoby, M. J., Glasser, N. F., Brasington, J., Hambrey, M. J., Quincey, D. J., & Reynolds, J. M. (2014). Modelling outburst floods from moraine-dammed glacial lakes. *Earth-Science Reviews*, 134, 137–159. <https://doi.org/10.1016/j.earscirev.2014.03.009>
- Wood, J. L., Harrison, S., Wilson, R., Emmer, A., Kargel, J. S., Cook, S. J., Glasser, N. F., Reynolds, J. M., Shugar, D. H., & Yarleque, C. (2024). Shaking up Assumptions: Earthquakes Have Rarely Triggered Andean Glacier Lake Outburst Floods. *Geophysical Research Letters*, 51(7), e2023GL105578. <https://doi.org/10.1029/2023GL105578>
- Woods Hole Oceanographic Institution. (2015, June 3). *Sudden draining of glacial lakes explained*. ScienceDaily. <https://www.sciencedaily.com/releases/2015/06/150603132250.htm>
- Xu, M., Bogen, J., Ragulina, G., & Read, A. (2015). Early and late Holocene sediment yield of Austdalsbreen glacier, southwest Norway. *Geomorphology*, 246, 277–289. <https://doi.org/10.1016/j.geomorph.2015.06.021>
- Yao, X., Liu, S., Han, L., Sun, M., & Zhao, L. (2018). Definition and classification system of glacial lake for inventory and hazards study. *Journal of Geographical Sciences*, 28(2), 193–205. <https://doi.org/10.1007/s11442-018-1467-z>
- Zhang, G., Carrivick, J. L., Emmer, A., Shugar, D. H., Veh, G., Wang, X., Labedz, C., Mergili, M., Mölg, N., Huss, M., Allen, S., Sugiyama, S., & Lützow, N. (2024). Characteristics and changes of glacial lakes and outburst floods. *Nature Reviews Earth & Environment*. <https://doi.org/10.1038/s43017-024-00554-w>
- Zhongguo ke xue yuan. Lanzhou bing chuan dong tu yan jiu suo, Nepal. Water and Energy Commission Secretariat, & Nepal Electricity Authority. (1988). *Report on First Expedition to Glaciers and Glacier Lakes in the Pumqu (Arun) and Poiqu (Bhotensun Kosi) River Basins, Xizang (Tibet), China: Sino-Nepalese Investigation of Glacier Lake Outburst Floods in the Himalayas*. Science Press. <https://books.google.no/books?id=pAGnAAAACAAJ>

Appendix A

Event Tree Analyses for H1 Hazard Condition

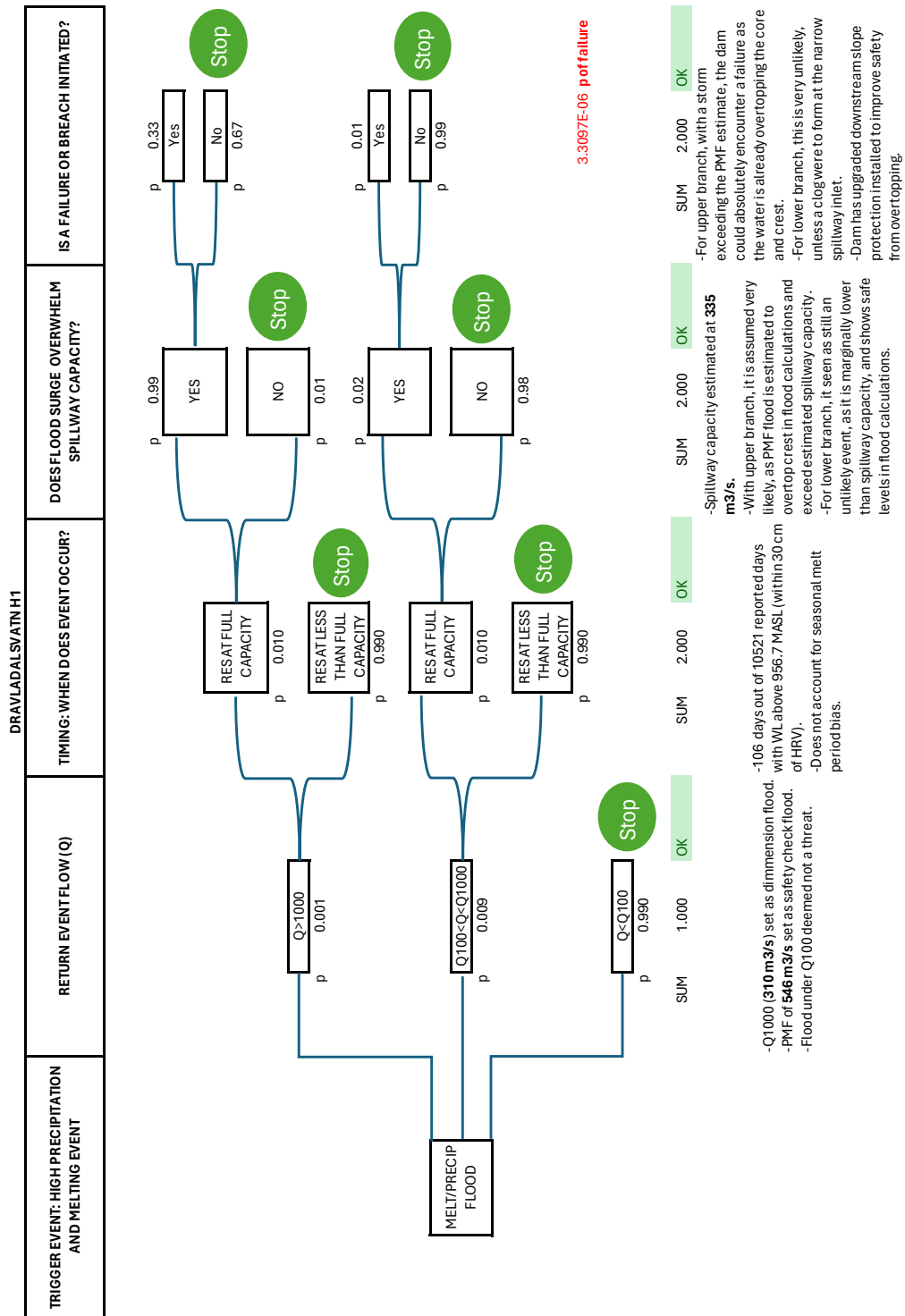


Figure 0.1 H1 Event tree analysis for Dravladalsvatn dam.

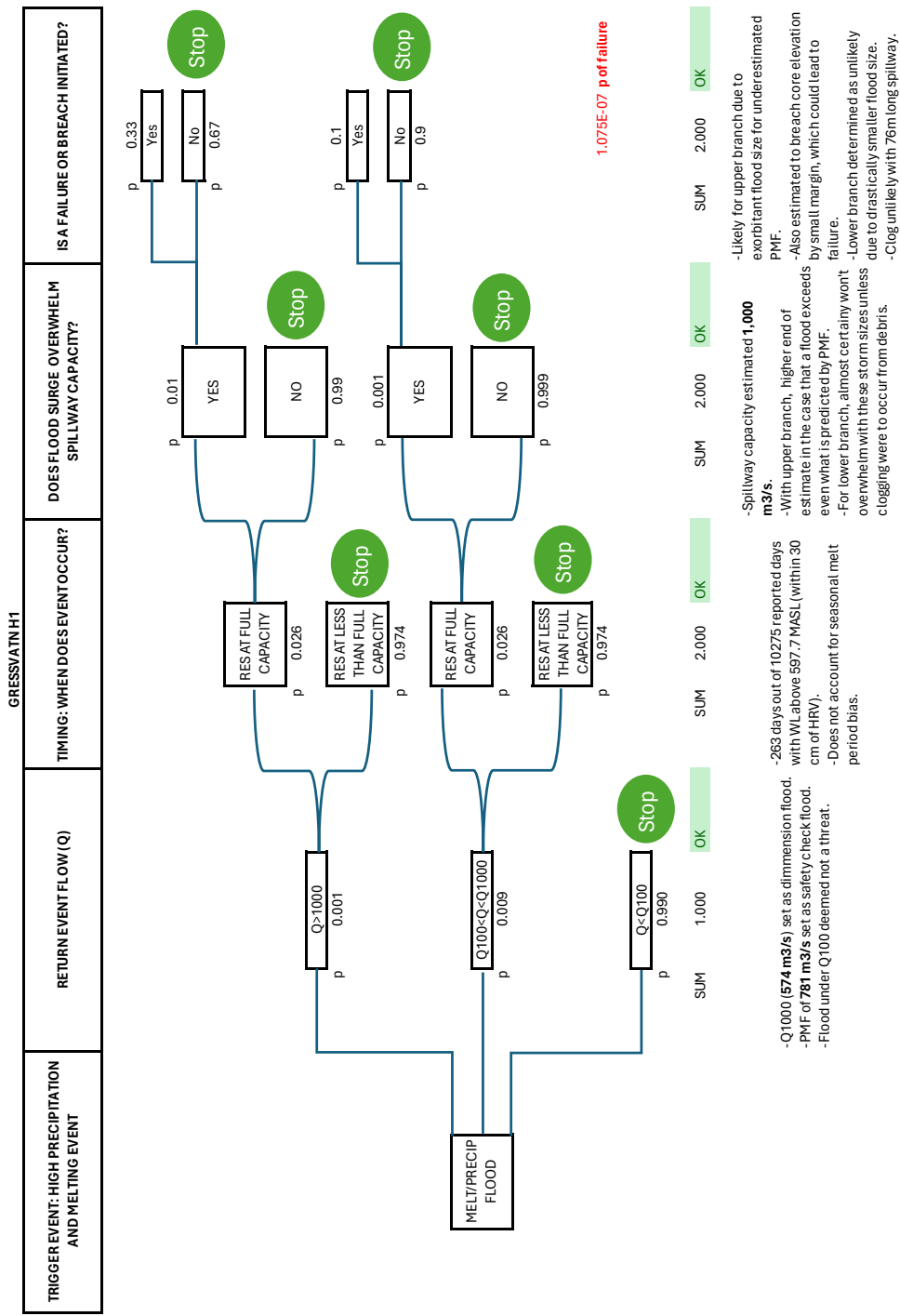


Figure 0.2 H1 Event tree analysis for Gressvatn dam.

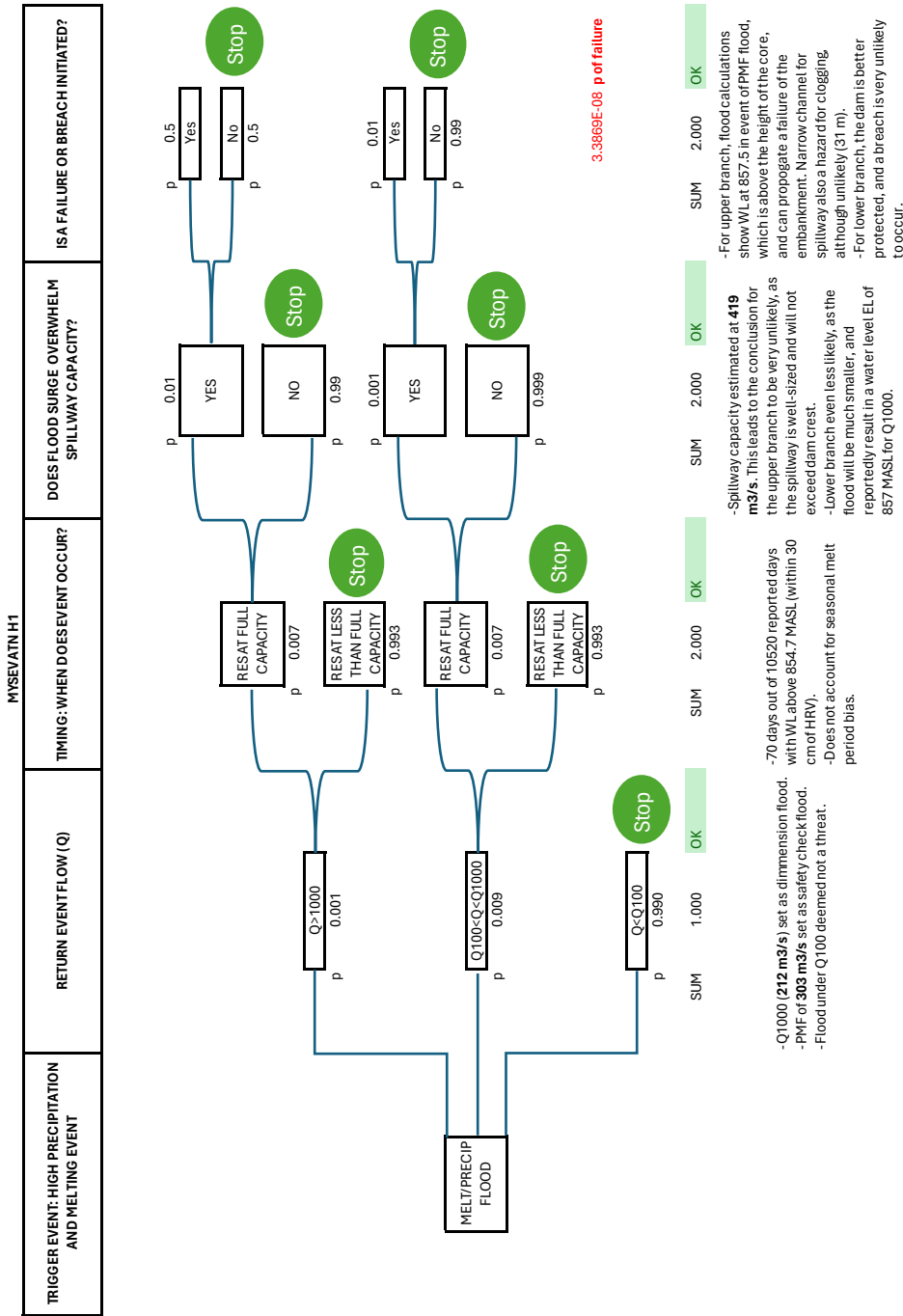


Figure 0.4 H1 Event tree analysis for Mysevatn dam.

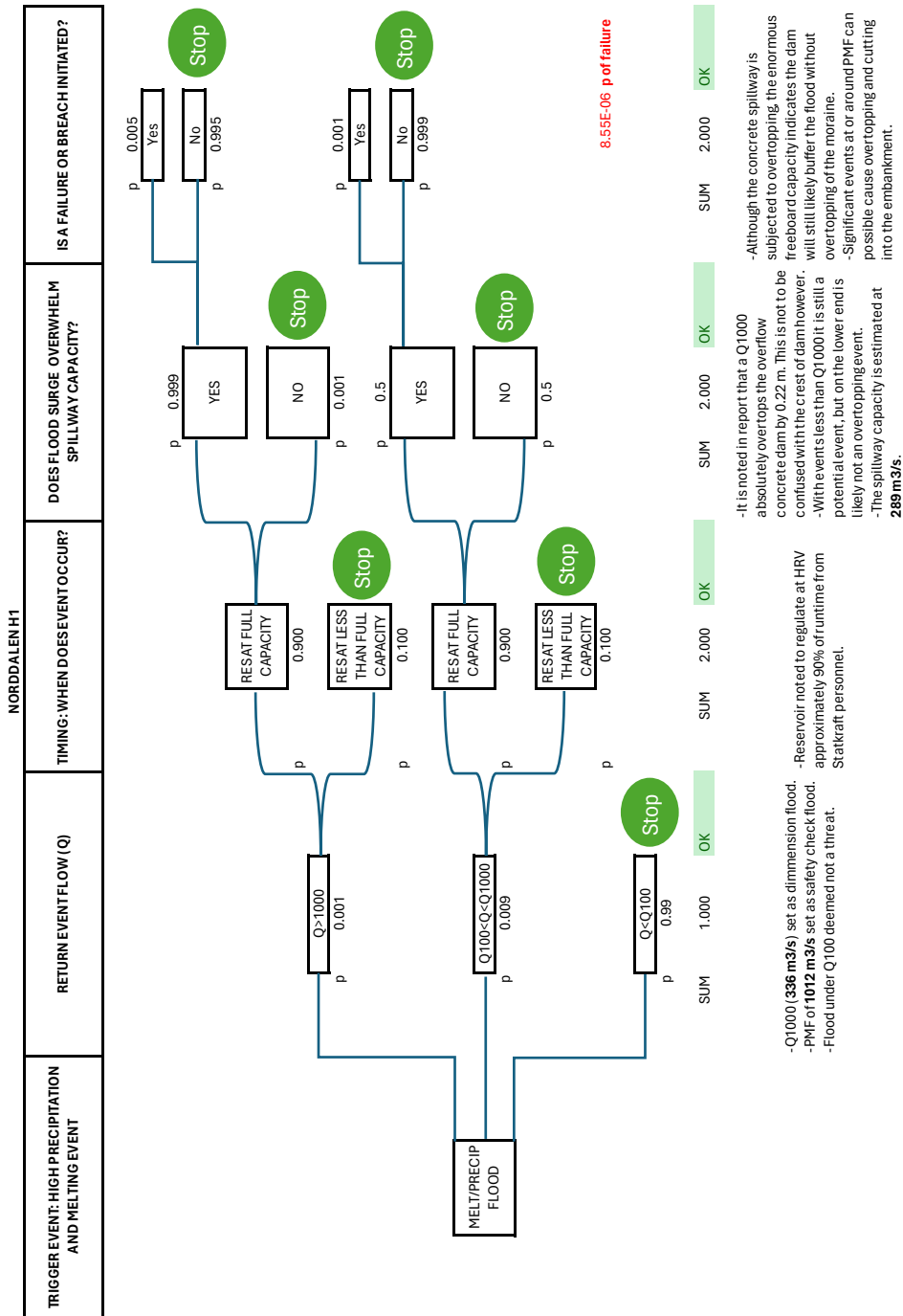


Figure 0.5 H1 Event tree analysis for Norddalen dam.

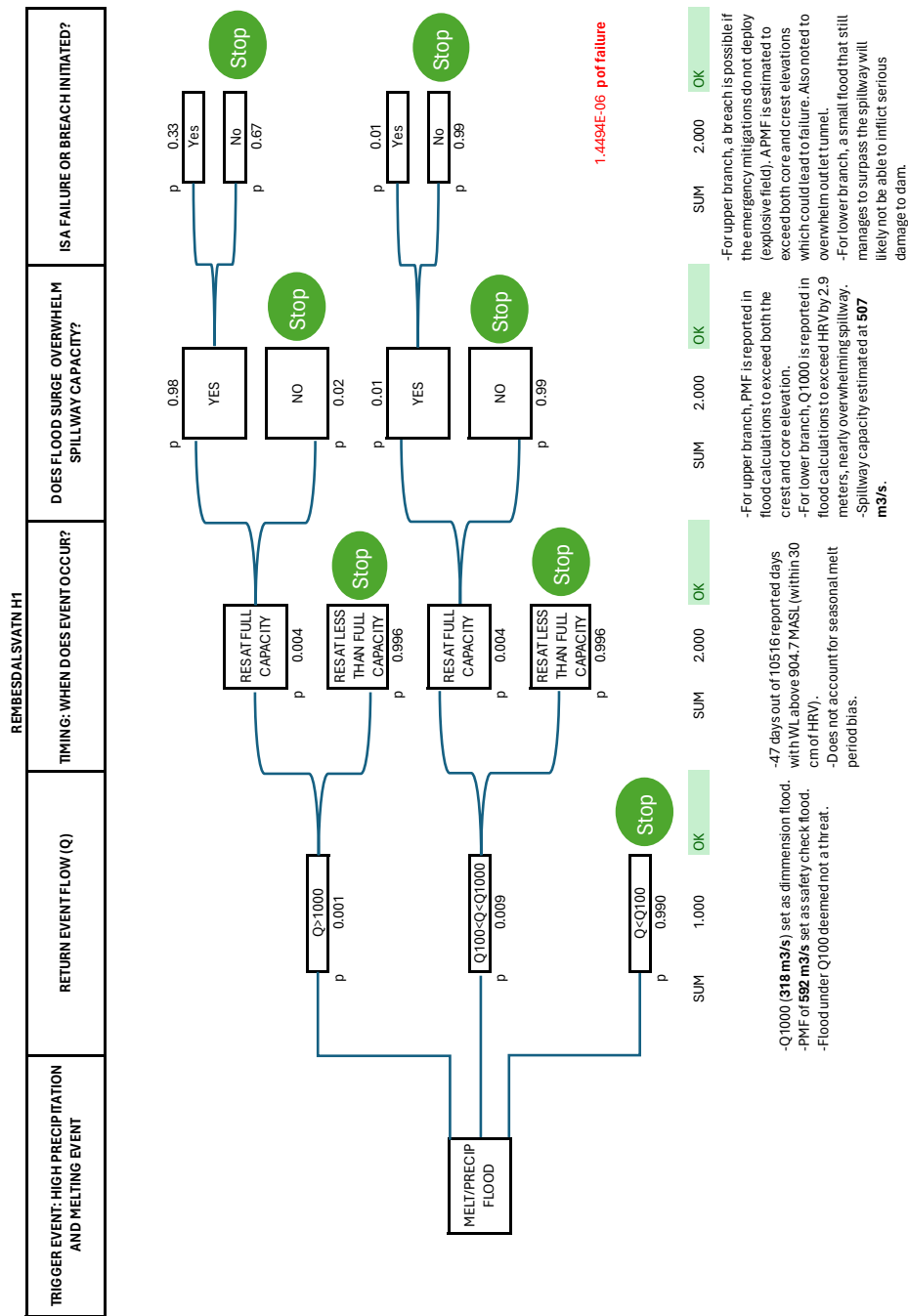


Figure 0.6 H1 Event tree analysis for Rembesdalsvatn dam.

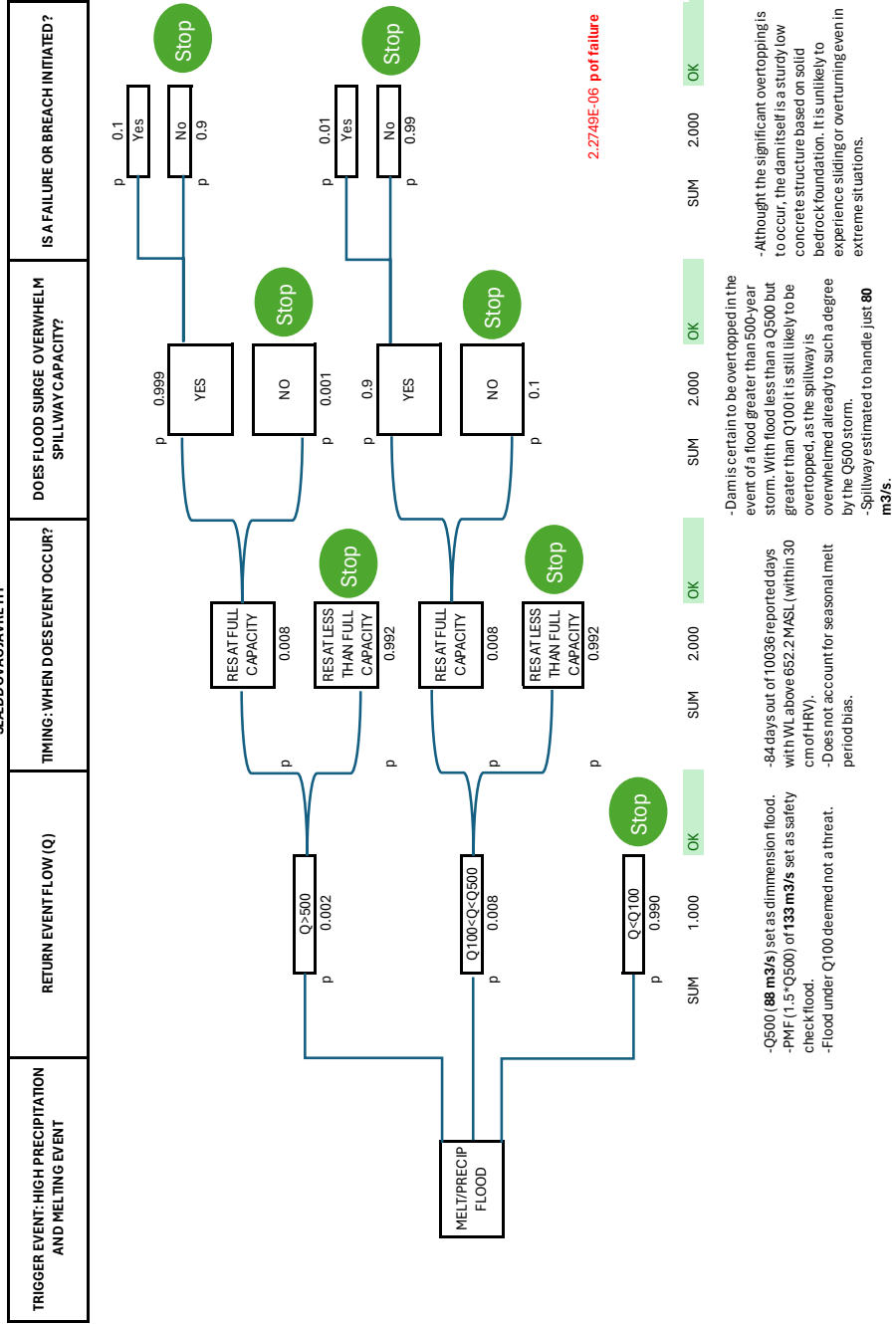


Figure 0.7 H1 Event tree analysis for Slæddovagjavre dam.

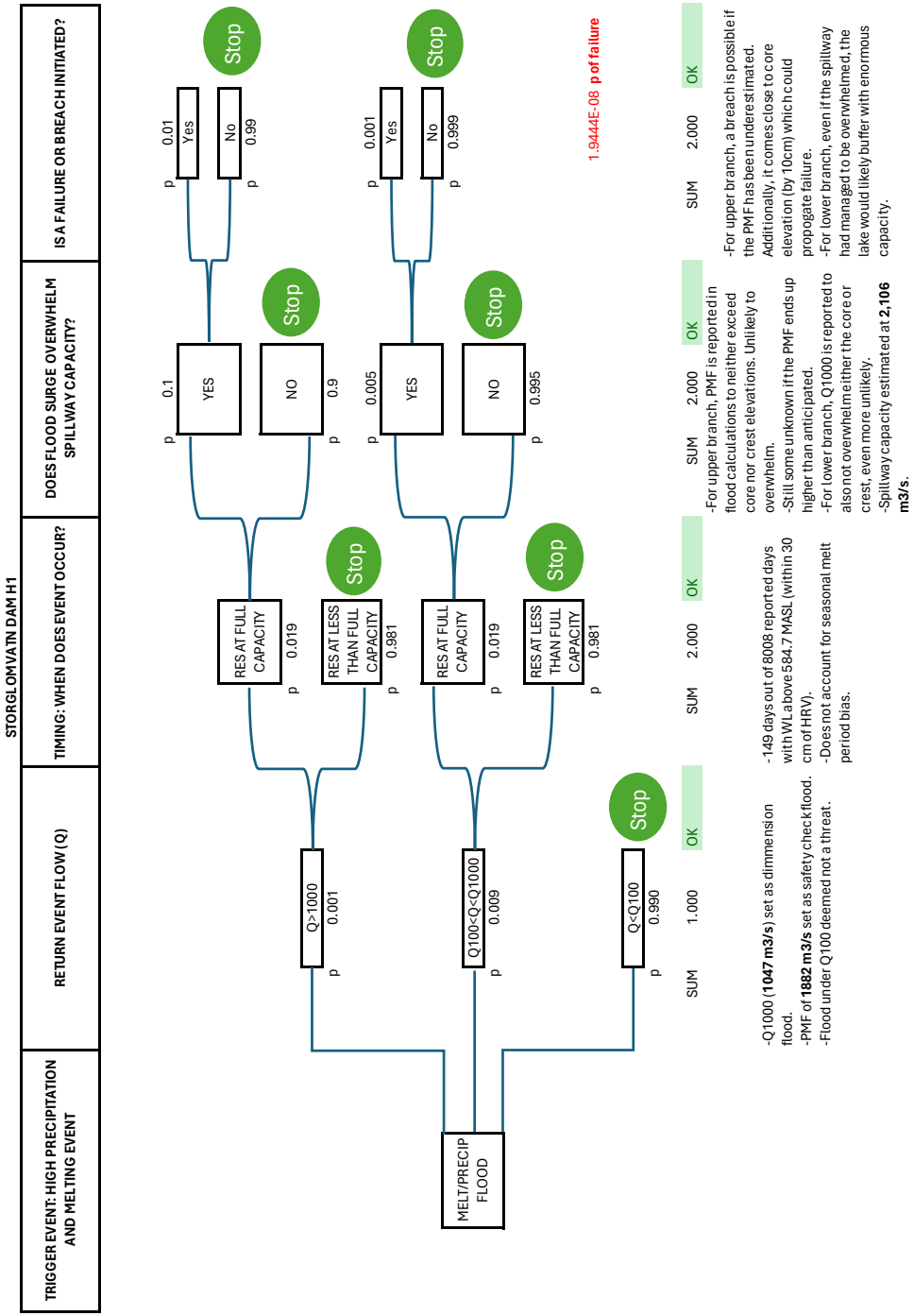


Figure 0.8 H1 Event tree analysis for Storglomvatn and Holmvatn dams.

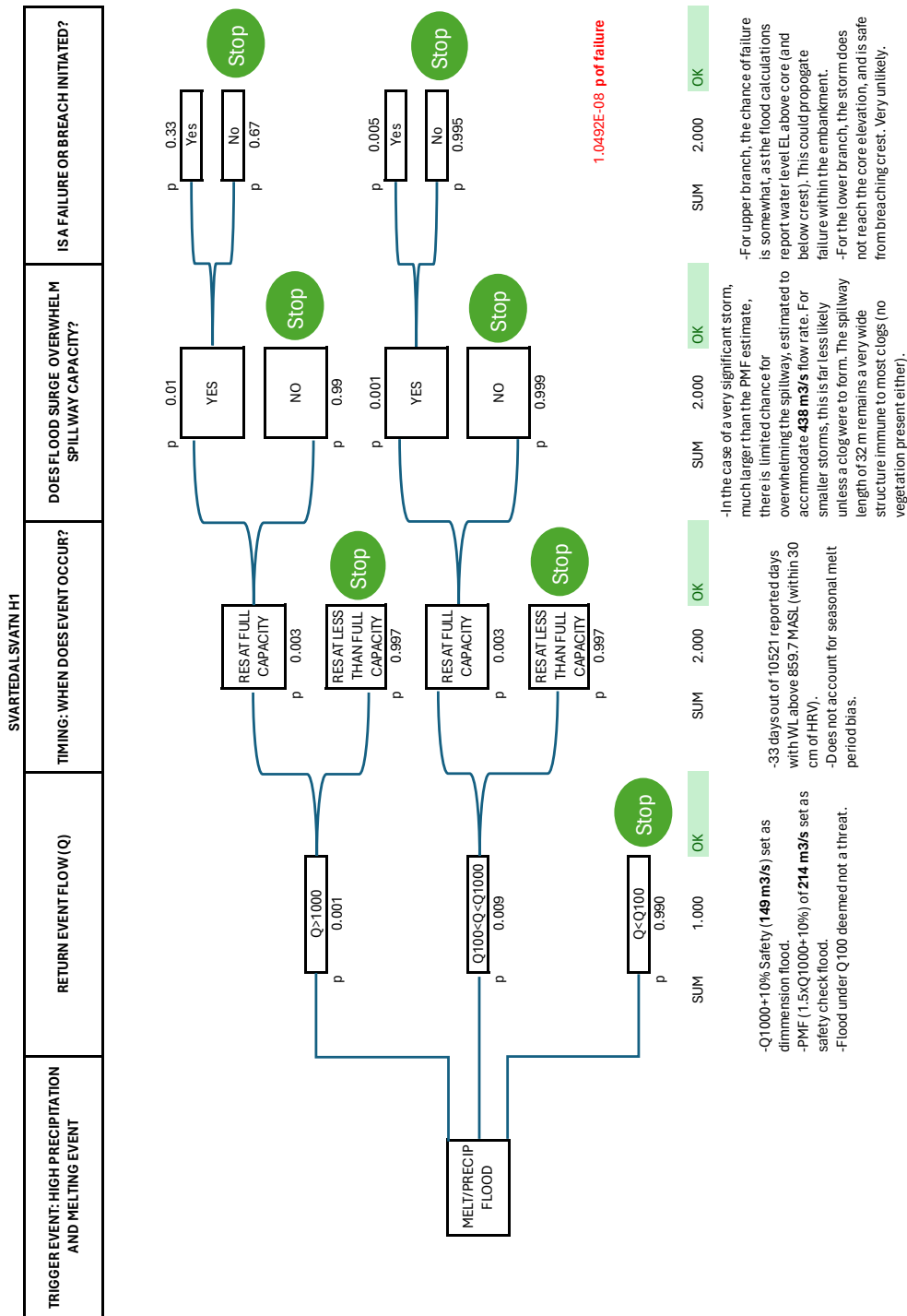


Figure 0.10 H1 Event tree analysis for Svartadalsvatn dam.

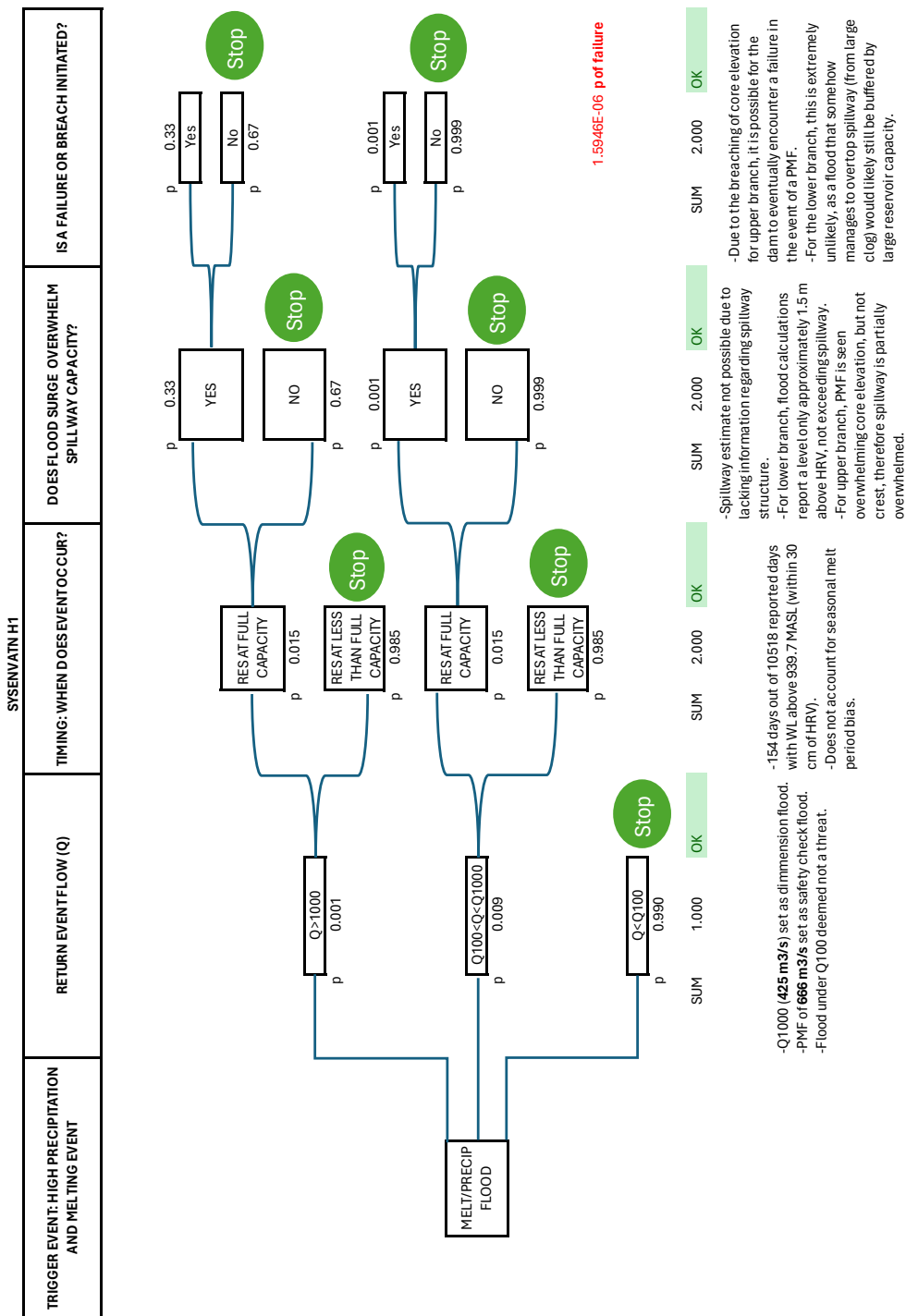


Figure 0.11 H1 Event tree analysis for Sysenvatn dam.

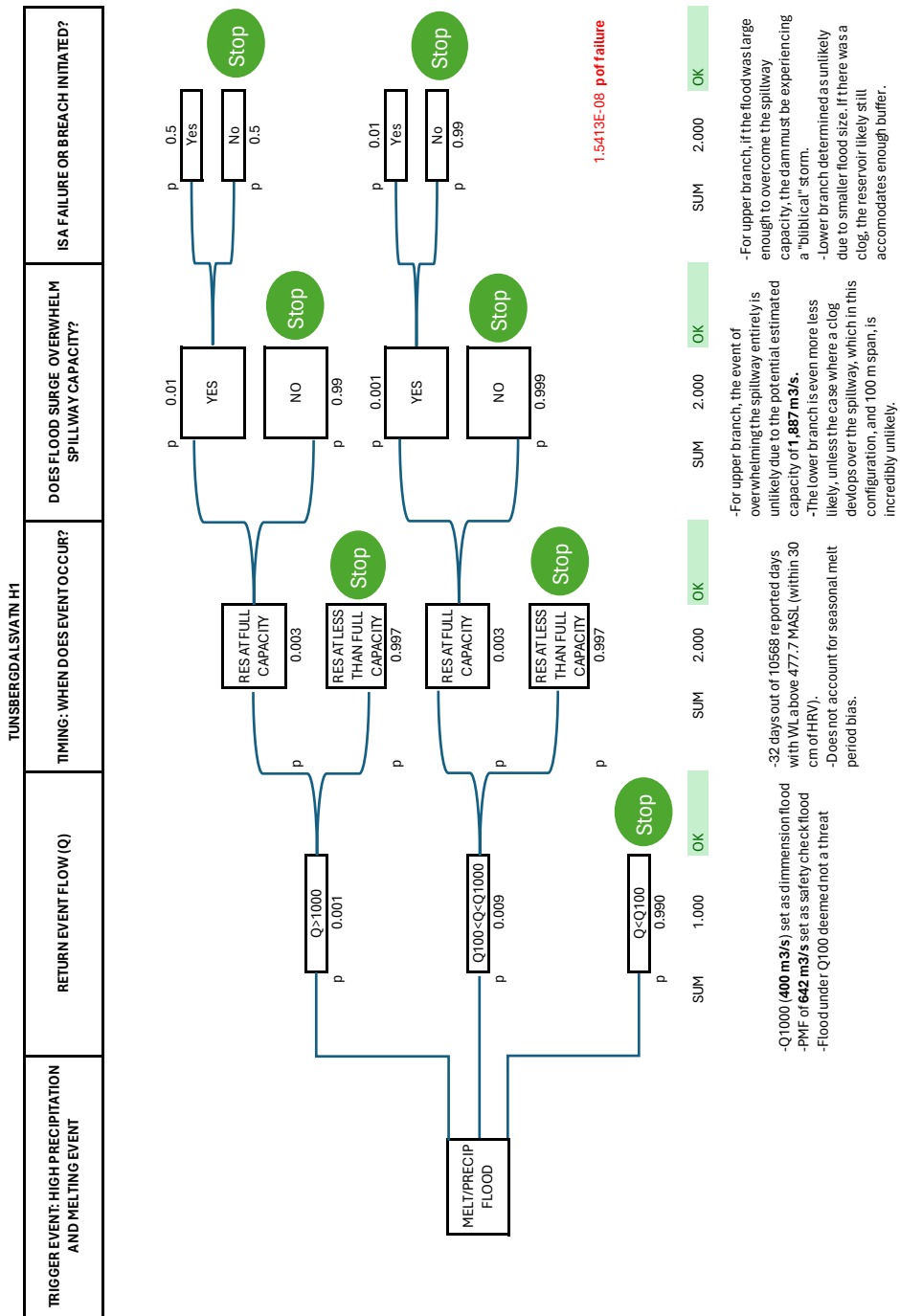


Figure 0.12 H1 Event tree analysis for Tunsbergdalsvatn dam.

Appendix B

Event Tree Analyses for H2 Hazard Condition

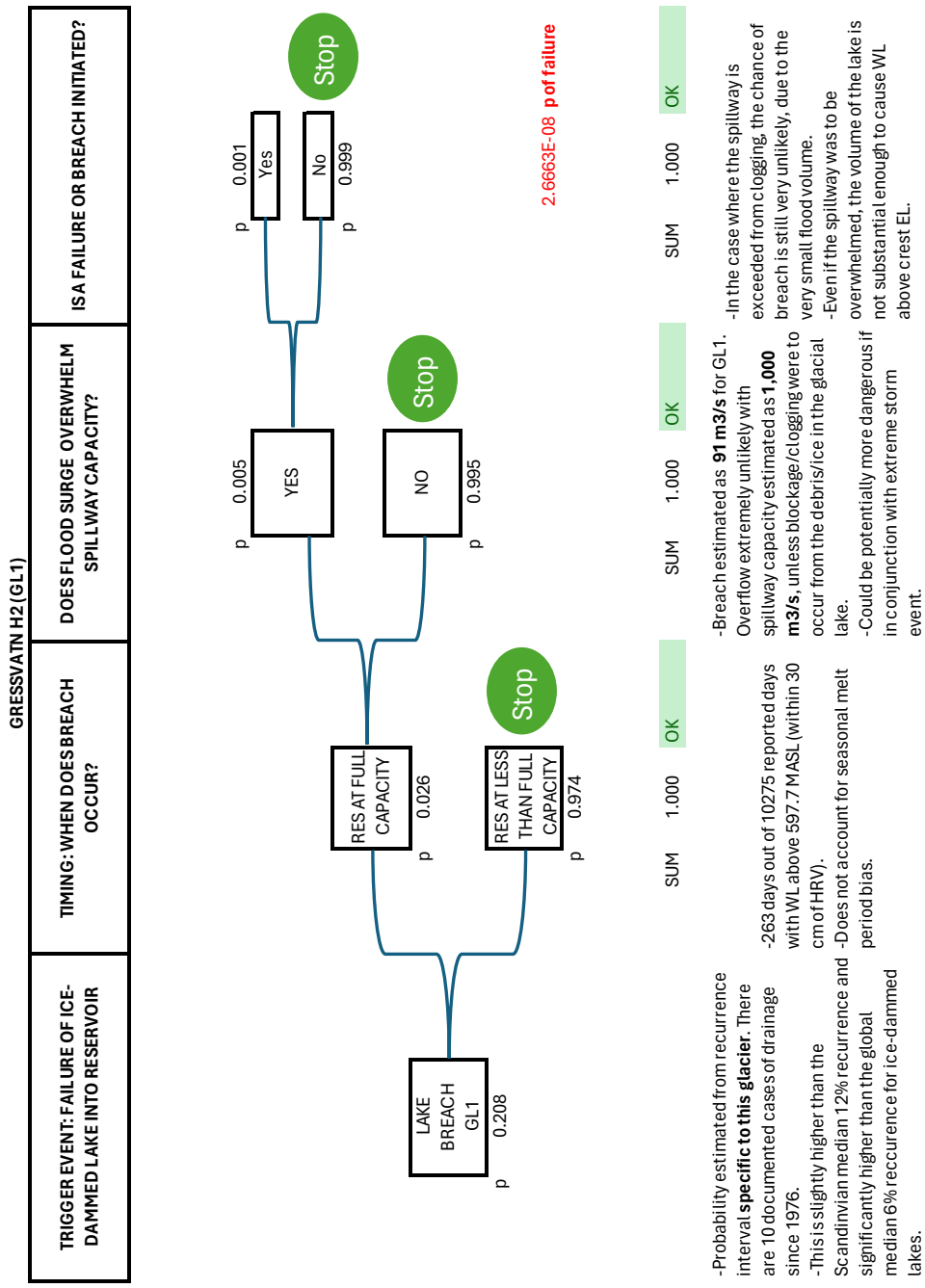
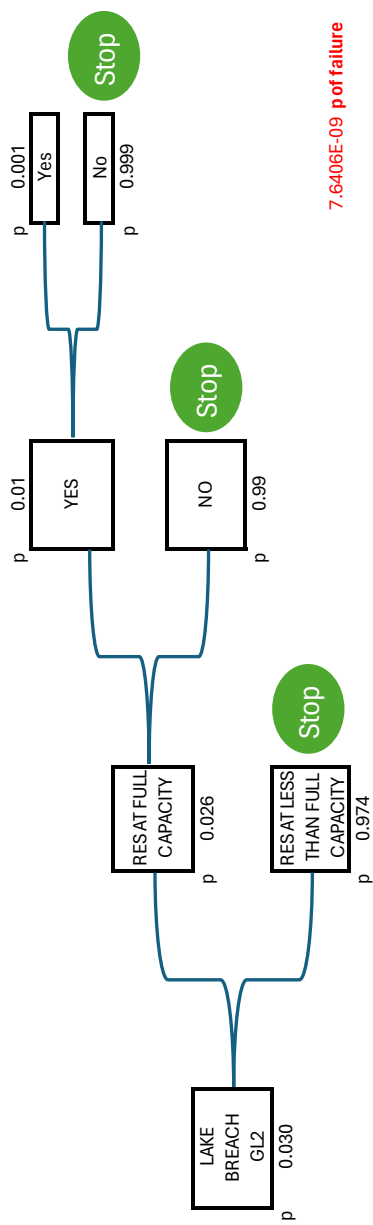
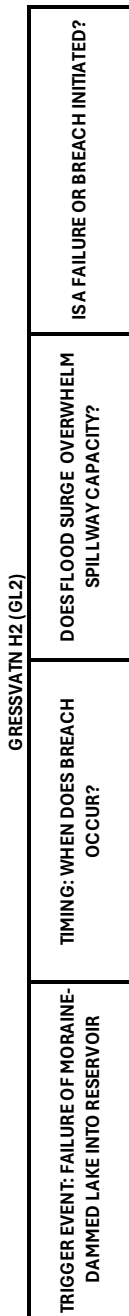


Figure 0.13 H2 Event tree analysis for Gressvatn dam (GL1).



7.6406E-09 p of failure

TRIGGER EVENT: FAILURE OF MORaine-DAMMED LAKE INTO RESERVOIR	TIMING: WHEN DOES BREACH OCCUR?	DOES FLOOD SURGE OVERWHELM SPILLWAY CAPACITY?	ISA FAILURE OR BREACH INITIATED?
SUM 1.000	SUM 1.000	SUM 1.000	SUM 1.000
OK	OK	OK	OK

-Probability for moraine failure sourced from global recurrence interval statistics for moraine-dammed glacial lakes (median of all data).
 -No record of incidents with this particular lake.
 -263 days out of 10275 reported days with WL above 597.7 MASL (within 30 cm of HRV).
 -Does not account for seasonal melt period bias.
 -Breach estimated as **97 m³/s** for GL2.
 -Overflow very unlikely with spillway capacity estimated as **1,000 m³/s**, unless blockage/clogging were to occur from the debris/ice in the glacial lake.
 -Moraine breach more violent than ice, potentially more dangerous than **GL 1**.
 -Could be potentially more dangerous if in conjunction with extreme storm event.
 -Wave forces are also not a concern due to wave protection on crest.
 -In the case where the spillway is exceeded from clogging, the chance of breach is still very unlikely, due to the very small flood volume.
 -Even if the spillway was to be overwhelmed, the volume of the lake is not substantial enough to cause WL above crest EL.

Figure 0.14 H2 Event tree analysis for Gressvatn dam (GL2).

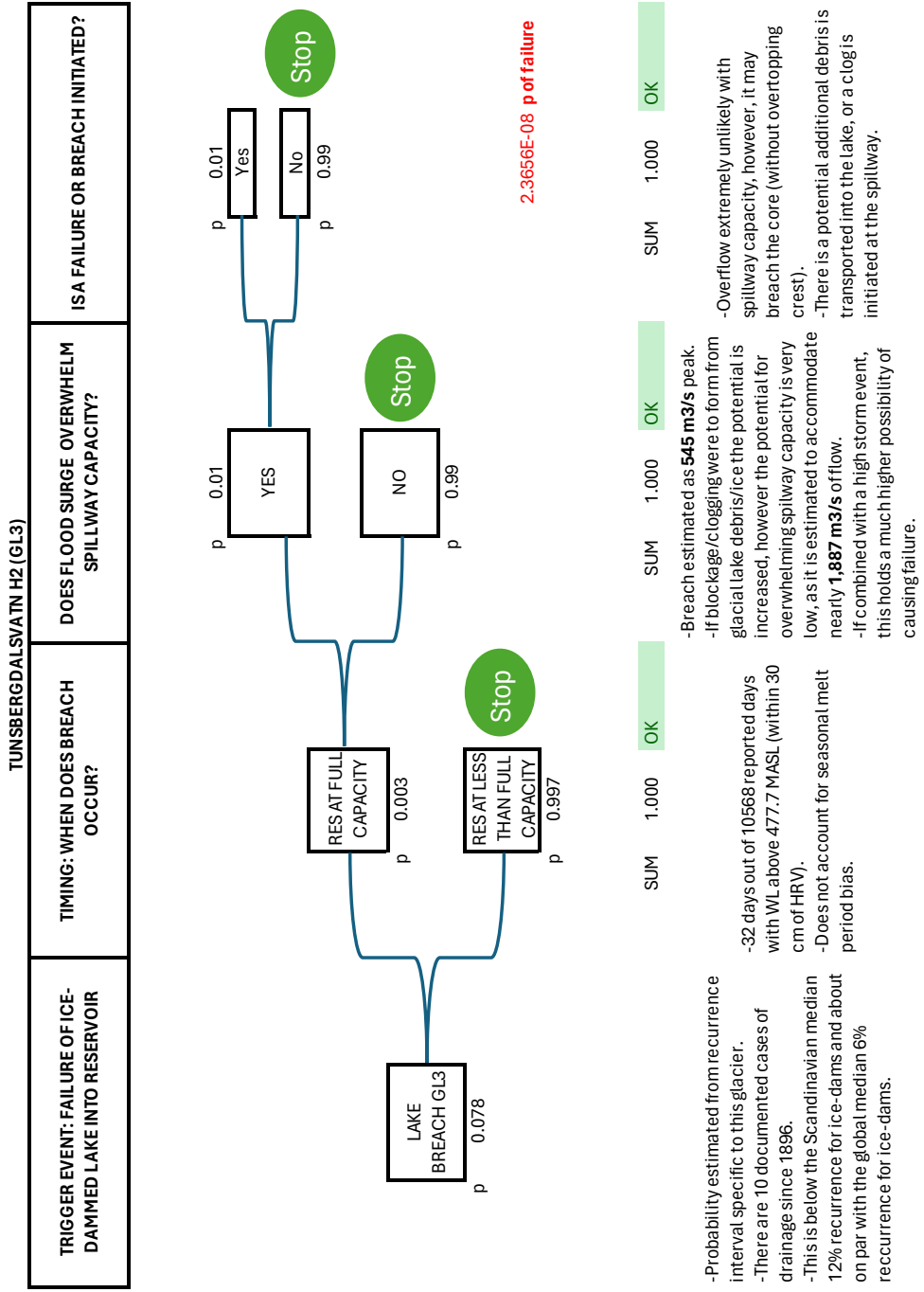


Figure 0.15 H2 Event tree analysis for Tunsbergdalsvatn dam (GL3).

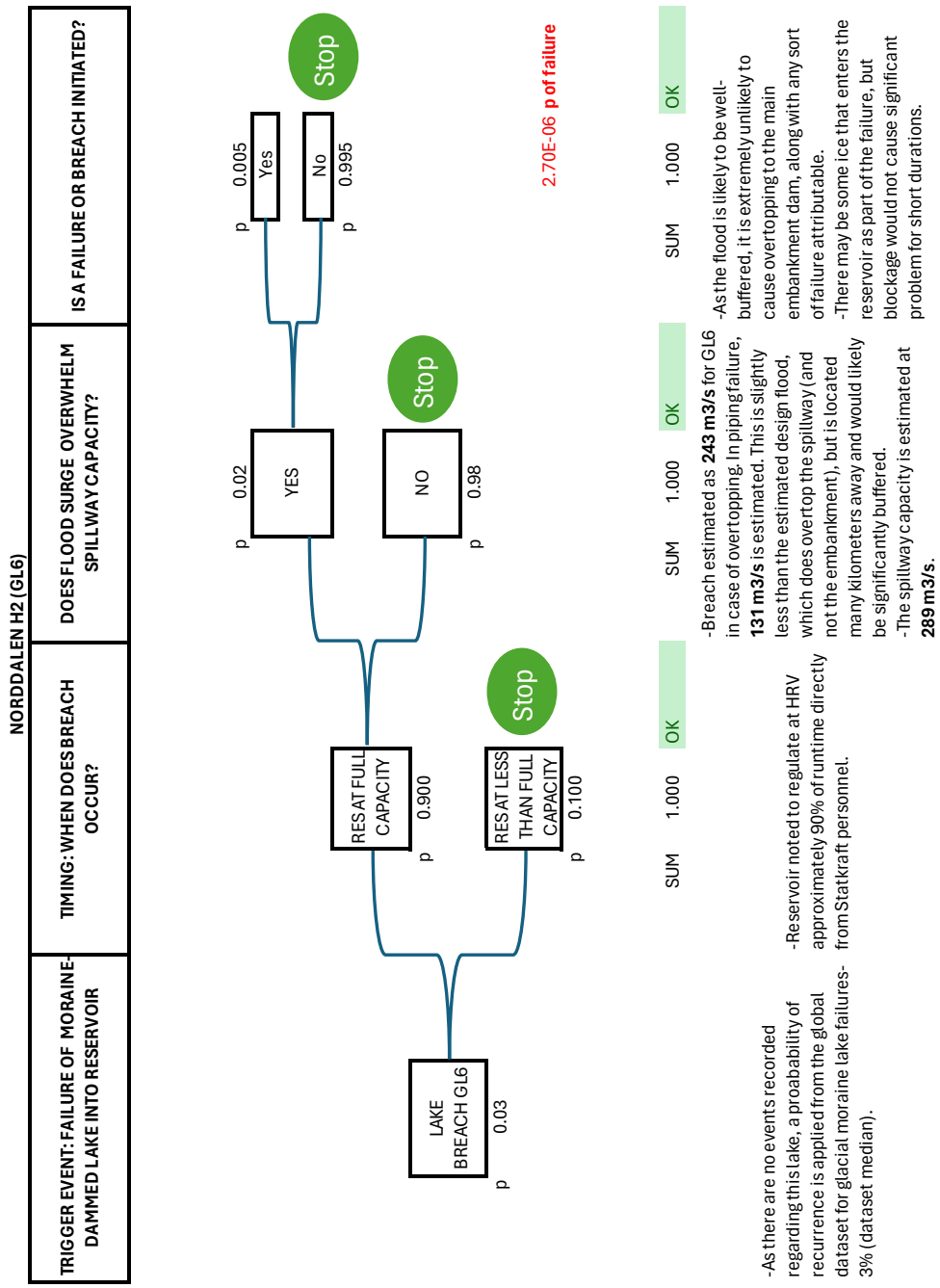


Figure 0.17 H2 Event tree analysis for Norddalen dam (GL6).

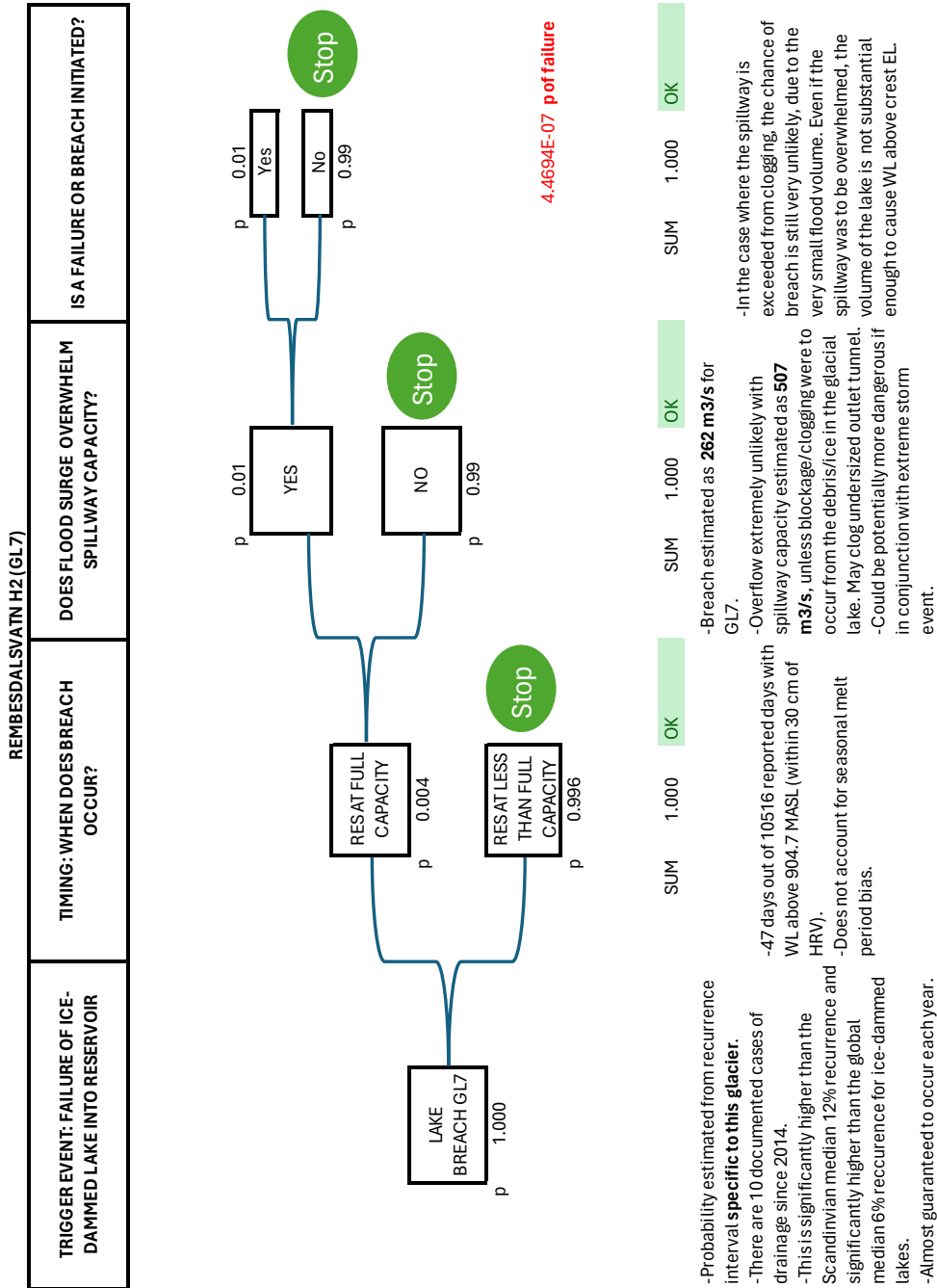


Figure 0.18 H2 Event tree analysis for Rembesdalsvatn dam (GL7).

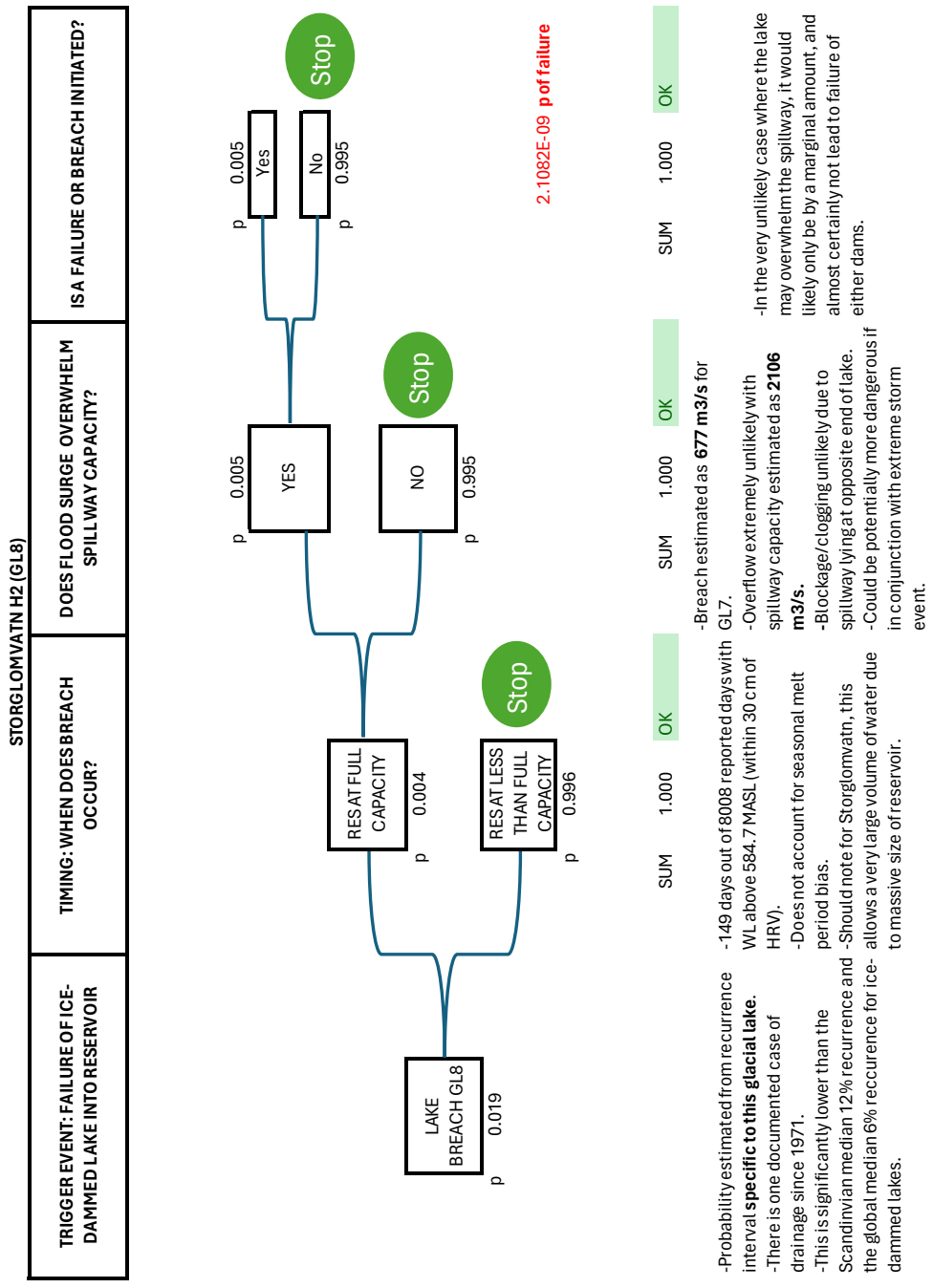


Figure 0.19 H2 Event tree analysis for Storglomvatn and Holmvatn dams (GL8).

Appendix C

Event Tree Analysis for H3 Hazard Condition

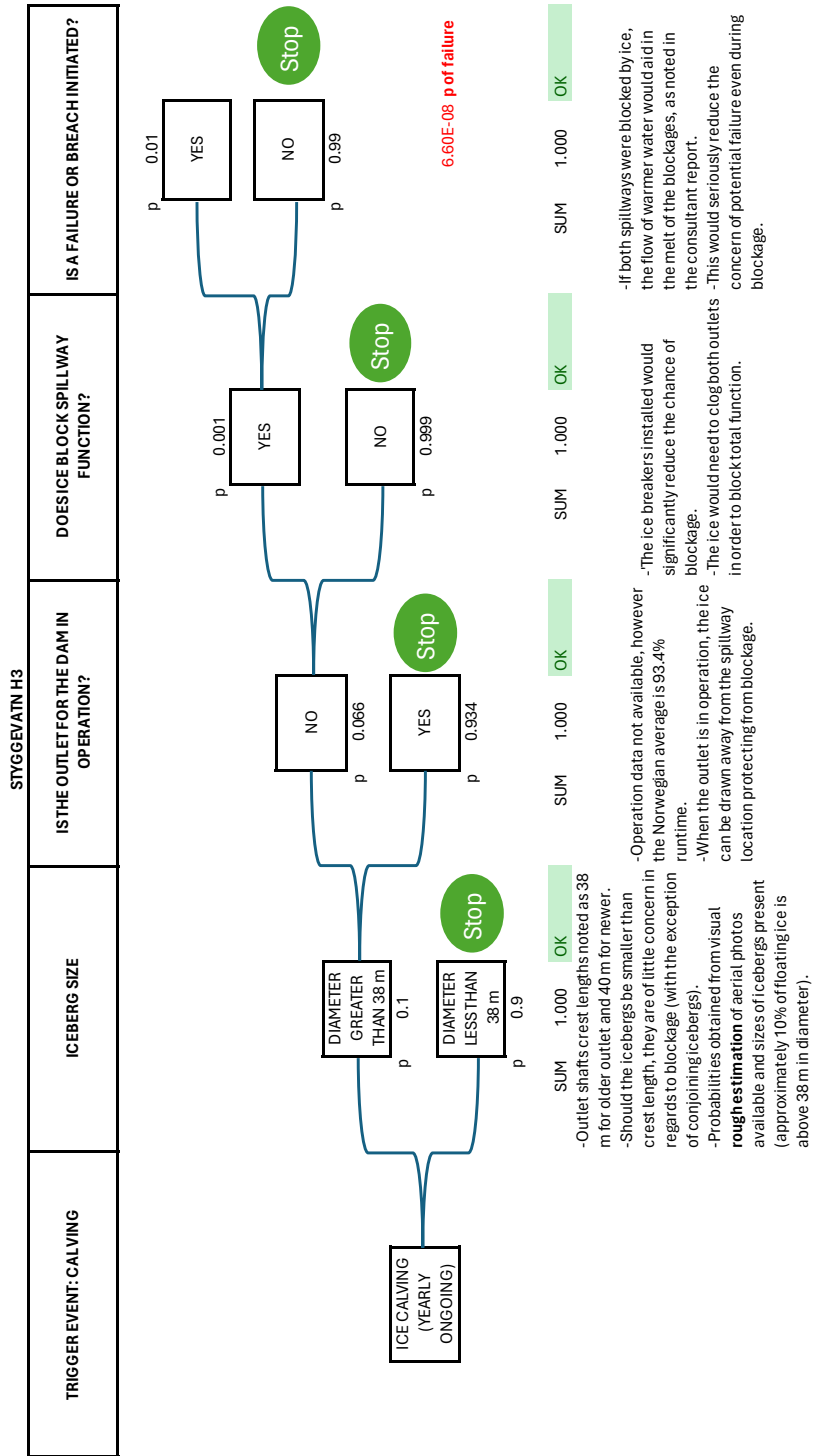


Figure 0.20 H3 Event tree analysis for Styggevatn dam.

Appendix D

Glacial Lake Estimation Calculations

Gressvatn

Leirskardalen glacial lake (GL1)

Ice-dammed lake
Full-Drainage Condition

Ice/Glacier Dam: Estimate for Maximum Flood Rate		
V*	0.35	Volume of water drained, million m3
Qmax (emp)	91.4	Max flow rate, m3/s
Qavg (24hr)	4.1	Average flow rate over 24hr, m3/s
2Qavg	8.1	Low end estimate flow peak, m3/s
6Qavg	24.3	Higher end estimate flow peak, m3/s

Comments

*Average of two reported volume estimates from literature used

Oksskottbreen glacial lake (GL2)

Glacial Lake Volume and Depth Estimate			
Lake	Surface Area	Cook Quincey	Cook Depth
	m2	m3	m
GL2	15,410	99,916	6.5

Comments

Estimated depth appears to be in line with ICIMOD statistics for cirque lakes.
Decision to use median value, in efforts to avoid over-estimating or underestimating.
Volume not reported in available literature

Moraine-dammed lake
Full-Drainage Condition
Piping Failure

Froehlich 2016a		
k0	1	(1.0 piping, 1.5 for overtopping failure)
Vw	99,916	Reservoir volume at time of failure, m3
hb	6.5	Height of final breach, m
Bavg	10.7	Average breach width, m
tf	0.26	Breach formation time, hr
Average side slopes: 1.0H:1V Overtopping 0.6H:1V Others (piping/seepage)		

Moraine Dam: Froehlich 2016b		
k0	1	(1.0 piping, 1.85 overtopping)
kH	1.0	Coefficient, see below
Vw	99,916	Reservoir volume at time of failure, m3
hw	6.5	H of water above breach bottom, m
hb	6.5	Height of final breach, m
W	30	Average embankment width
Q	52.6	Peak breach outflow, m3/s

Moraine-dammed Lake
Full-Drainage Condition
Overtopping Failure

Froehlich 2016a		
k0	1.5	(1.0 piping, 1.5 for overtopping failure)
Vw	99,916	Reservoir volume at time of failure, m3
hb	6.5	Height of final breach, m
Bavg	16.0	Average breach width, m
tf	0.26	Breach formation time, hr
Average side slopes: 1.0H:1V Overtopping 0.6H:1V Others (piping/seepage)		

Moraine Dam: Froehlich 2016b		
k0	1.85	(1.0 piping, 1.85 overtopping)
kH	1.0	Coefficient, see below
Vw	99916	Reservoir volume at time of failure, m3
hw	6.48	H of water above breach bottom, m
hb	6.48	Height of final breach, m
W	30	Average embankment width
Q	97.4	Peak breach outflow, m3/s

Tunsbergdals dammen ice-dammed lake (GL3)

Ice-dammed lake
Full-Drainage Condition

Ice/Glacier Dam: Estimate for Maximum Flood Rate		
V*	5.7	Volume of water drained, million m3
Qmax (emp)	545.3	Max flow rate, m3/s
Qavg (24hr)	66.0	Average flow rate over 24hr, m3/s
2Qavg	131.9	Low end estimate flow peak, m3/s
6Qavg	395.8	Higher end estimate flow peak, m3/s

*Previous reports indicate the largest flood volume could have been up to 30 million m3
The last reported volume of outburst is used in this calculation, from 1970
This is likely over-estimated, as the ice dam has receded

Svartadalavatn glacial lake (GL4)				
Ice-dammed glacial lake				
Glacial Lake Volume and Depth Estimate				
Lake	Surface Area	Cook	Quincey	Cook Depth
	m ²	m ³		m
GL4	7,808	39,158		5.0
Comments				
Lake determined not to be of significant impact to reservoir if drainage were to occur Volume estimated to be very minute				

Slæddovagjavre glacial lake (GL5)				
Glacial Lake Volume and Depth Estimate				
Lake	Surface Area	Cook	Quincey	Cook Depth
	m ²	m ³		m
GL5	110,000	1,498,693		13.6
Comments				
Estimated embankment width of 79m from aerial photos				

Froehlich 2016a					Moraine Dam: Froehlich 2016b				
Moraine-dammed lake					Full-Drainage Condition				
Piping Failure									
k0	1	(1.0 piping, 1.5 for overtopping failure)			k0	1	(1.0 piping, 1.85 overtopping)		
Vw	1,498,693	Reservoir volume at time of failure, m ³			kH	1.1	Coefficient, see below		
hb	13.6	Height of final breach, m			Vw	1,498,693	Reservoir volume at time of failure, m ³		
Bavg	26.3	Average breach width, m			hw	13.6	H of water above breach bottom, m		
tf	0.48	Breach formation time, hr			hb	13.6	Height of final breach, m		
Average side slopes:					W	79	Average embankment width		
1.0H:1V Overtopping					Q	419.8	Peak breach outflow, m ³ /s		
0.6H:1V Others (piping/seepage)									

Froehlich 2016a					Moraine Dam: Froehlich 2016b				
Moraine-dammed lake					Full-Drainage Condition				
Overtopping Failure									
k0	1.5	(1.0 piping, 1.5 for overtopping failure)			k0	1.85	(1.0 piping, 1.85 overtopping)		
Vw	1,498,693	Reservoir volume at time of failure, m ³			kH	1.1	Coefficient, see below		
hb	13.6	Height of final breach, m			Vw	1,498,693	Reservoir volume at time of failure, m ³		
Bavg	39.5	Average breach width, m			hw	13.6	H of water above breach bottom, m		
tf	0.48	Breach formation time, hr			hb	13.6	Height of final breach, m		
Average side slopes:					W	79	Average embankment width		
1.0H:1V Overtopping					Q	776.6	Peak breach outflow, m ³ /s		
0.6H:1V Others (piping/seepage)									

Norddalen glacial lake (GL6)

Glacial Lake Volume and Depth Estimate			
Lake	Surface Area m ²	Cook Quincey m ³	Cook Depth m
GL6	58,404	626,450	10.7

Comments
Wide moraine embankment lake

Moraine-dammed lake
Full-Drainage Condition
Piping Failure

Moraine Dam: Froehlich 2016a	
k0	1 (1.0 piping, 1.5 for overtopping failure)
Vw	626,450 Reservoir volume at time of failure, m ³
hb	10.7 Height of final breach, m
Bavg	19.68 Average breach width, m
tf	0.39 Breach formation time, hr
Average side slopes: 1.0H:1V Overtopping 0.6H:1V Others (piping/seepage)	

Moraine Dam: Froehlich 2016b	
k0	1 (1.0 piping, 1.85 overtopping)
kH	1.1 Coefficient, see below
Vw	626,450 Reservoir volume at time of failure, m ³
hw	10.7 H of water above breach bottom, m
hb	10.7 Height of final breach, m
W	155 Average embankment width
Q	131.4 Peak breach outflow, m ³ /s

Moraine-dammed lake
Full-Drainage Condition
Overtopping Failure

Moraine Dam: Froehlich 2016a	
k0	1.5 (1.0 piping, 1.5 for overtopping failure)
Vw	626,450 Reservoir volume at time of failure, m ³
hb	10.7 Height of final breach, m
Bavg	29.52 Average breach width, m
tf	0.39 Breach formation time, hr
Average side slopes: 1.0H:1V Overtopping 0.6H:1V Others (piping/seepage)	

Moraine Dam: Froehlich 2016b	
k0	1.85 (1.0 piping, 1.85 overtopping)
kH	1.1 Coefficient, see below
Vw	626,450 Reservoir volume at time of failure, m ³
hw	10.7 H of water above breach bottom, m
hb	10.7 Height of final breach, m
W	155 Average embankment width
Q	243.0 Peak breach outflow, m ³ /s

Rembesdalsvatn glacial lake (GL7)

Ice-dammed lake
Full-Drainage Condition

Ice/Glacier Dam: Estimate for Maximum Flood Rate	
V*	1.82 Volume of water drained, million m ³
Qmax (emp)	262.4 Max flow rate, m ³ /s
Qavg (24hr)	21.0 Average flow rate over 24hr, m ³ /s
2Qavg	42.1 Low end estimate flow peak, m ³ /s
6Qavg	126.2 Higher end estimate flow peak, m ³ /s

Average of last 10 years reported volumes*
This is likely over-estimated, as the ice dam has receded.

Holmvassdammen glacial lake (GL8)

Glacial Lake Volume and Depth Estimate			
Lake	Surface Area m ²	Cook Quincey m ³	Cook Depth m
GL8	950,000	29,227,349	30.8

Comments

Ice-dammed lake
Full-Drainage Condition

Ice/Glacier Dam: Estimate for Maximum Flood Rate		
V*	8	Volume of water drained, million m ³
Qmax (emp)	677.4	Max flow rate, m ³ /s
Qavg (24hr)	92.6	Average flow rate over 24hr, m ³ /s
2Qavg	185.2	Low end estimate flow peak, m ³ /s
6Qavg	555.6	Higher end estimate flow peak, m ³ /s

NVE reports that they estimate lake to hold only 8 million m³
 Lake volume estimate above results in a much higher estimate (29.2 million)
 Difference likely to do with lake being more shallow than normal

Appendix E

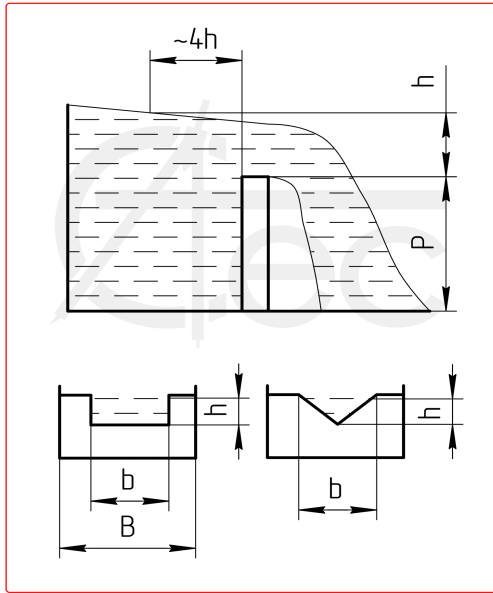
Dam Spillway Capacity Estimation Calculations

Weir Capacity Calculation

GRESSVATN

Rectangular Spillway

Fluid height (h)	m	4
Weir height (P)	m	6
Dam width (B)	m	445
Spillway width (b)	m	74
Flow Ratio Coefficient		0.3830
Flow Rate	m ³ /s	1,004

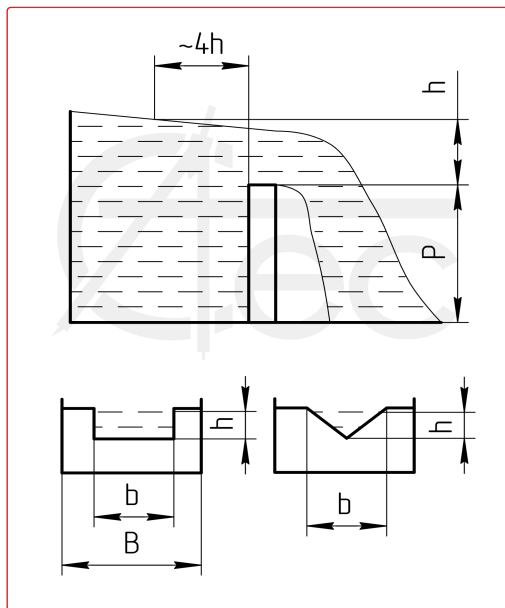


Weir Capacity Calculation

DRAVLADALSVATN

Rectangular Spillway

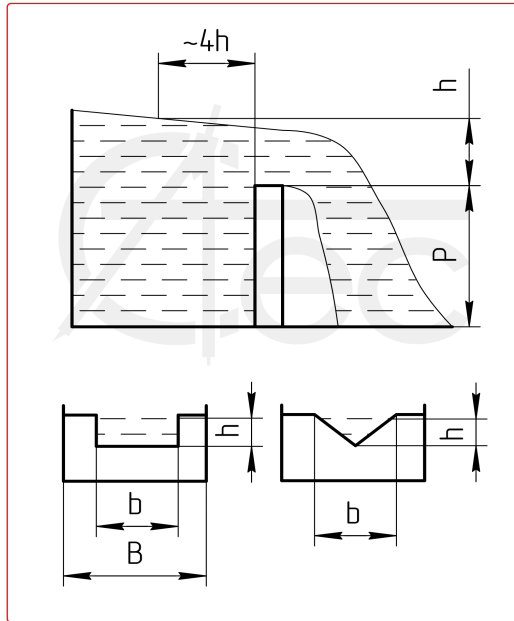
Fluid height (h)	m	4
Weir height (P)	m	3
Dam width (B)	m	340
Spillway width (b)	m	25
Flow Ratio Coefficient		0.37852298
Flow Rate	m ³ /s	335



Weir Capacity Calculation
[MYSEVATN](#)

Rectangular Spillway

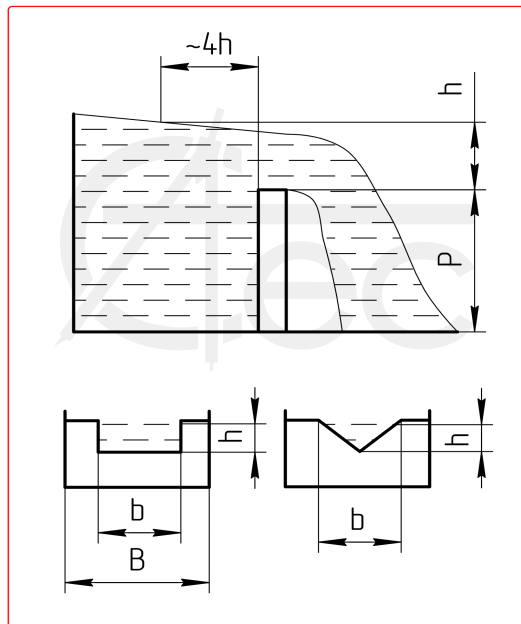
Fluid height (h)	m	4
Weir height (P)	m	4
Dam width (B)	m	250
Spillway width (b)	m	31
Flow Ratio Coefficient		0.38099923
Flow Rate	m ³ /s	419



Weir Capacity Calculation
[NORDDALEN](#)

Rectangular Spillway

Fluid height (h)	m	4.5
Weir height (P)	m	11
Dam width (B)	m	145
Spillway width (b)	m	18
Flow Ratio Coefficient		0.38025753
Flow Rate	m ³ /s	289

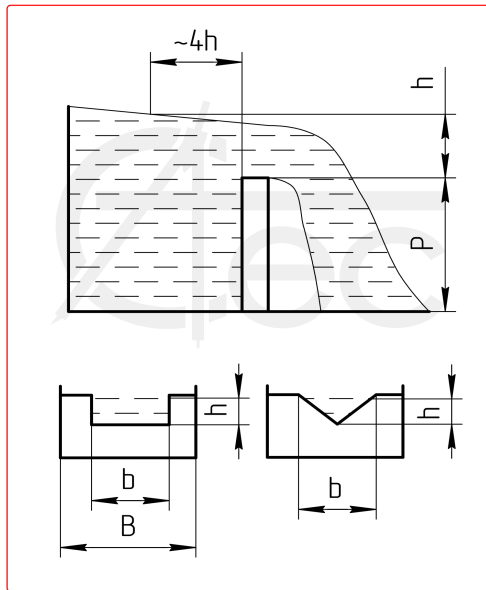


Weir Capacity Calculation

STORGLØMVAATN

Rectangular Spillway

Fluid height (h)	m	5.5
Weir height (P)	m	6.7
Dam width (B)	m	80
Spillway width (b)	m	75
Flow Ratio Coefficient		0.49157412
Flow Rate	m ³ /s	2,106

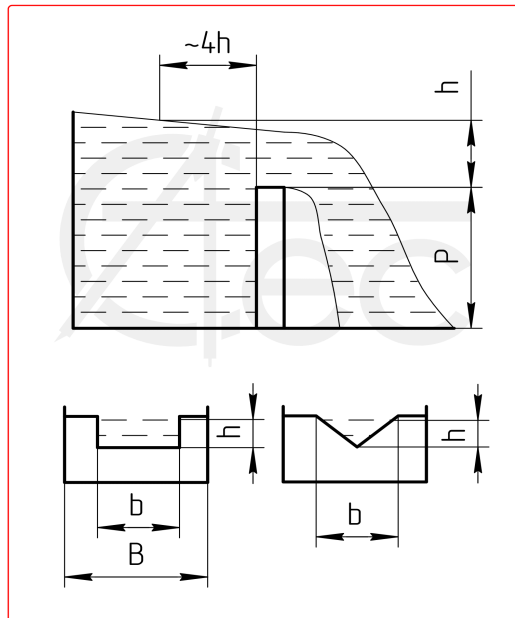


Weir Capacity Calculation

REMBESDALSVATN

Rectangular Spillway

Fluid height (h)	m	5.5
Weir height (P)	m	5.5
Dam width (B)	m	385
Spillway width (b)	m	23.5
Flow Ratio Coefficient		0.37770868
Flow Rate	m ³ /s	507



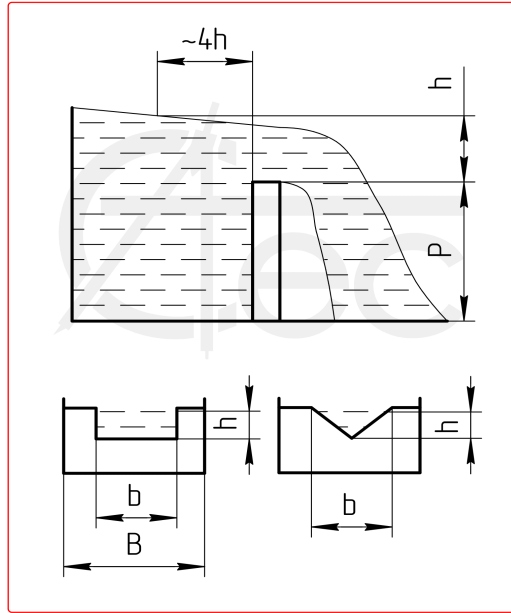
Weir Capacity Calculation

[SVARTADALSVATN](#)

Rectangular Spillway

Fluid height (h)	m	4
Weir height (P)	m	3
Dam width (B)	m	160
Spillway width (b)	m	32
Flow Ratio Coefficient		0.3864732

Flow Rate m³/s **438**



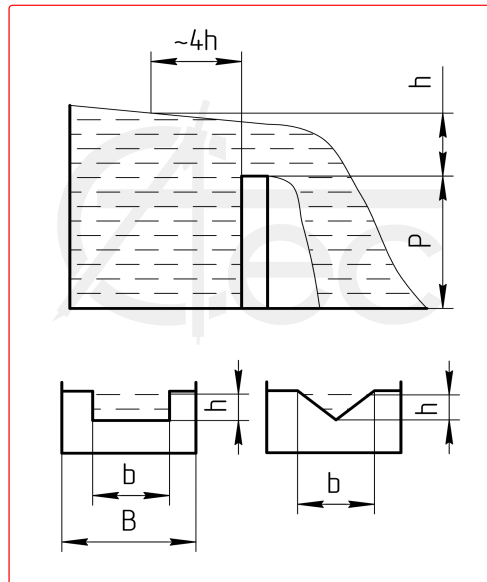
Weir Capacity Calculation

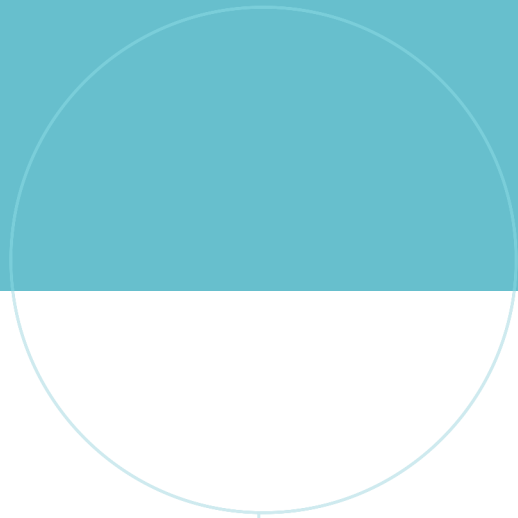
[TUNSBERGDALSVATN](#)

Rectangular Spillway

Fluid height (h)	m	6
Weir height (P)	m	4
Dam width (B)	m	870
Spillway width (b)	m	100
Flow Ratio Coefficient		0.38055023

Flow Rate m³/s **2,477**





 **NTNU**

Norwegian University of
Science and Technology